

**THE INFLUENCE OF CONTAMINATION ON THE FATIGUE
PERFORMANCE OF ELECTROFUSION JOINTS**

by

Pedrom Tayefi

A thesis submitted for the degree of Engineering Doctorate of the
University of Sheffield

Department of Mechanical Engineering

December 2014

For my father...

Abstract

For decades, polyethylene pipes have been used for potable water distribution in the United Kingdom (UK). Electrofusion welding is a common jointing method for polyethylene (PE) pipe. Here, electricity is used to heat a coil that melts the fitting and the host pipe of the same material. When the joint cools a strong bond is formed. Contamination of the jointing interface has been linked as a cause of premature failure and research has shown that brittle failures occur when fine particulate contaminants are present. Current literature fails to link failures associated with fatigue if the jointing system is installed incorrectly. Therefore, an experiment was designed with the aim of observing the performance of contaminated joints under dynamic load.

A novel experimental rig was used to cyclically pressurise PE tapping tee fittings that have been created with a controlled element of contamination. Low-cycle fatigue testing regimes were created using an industry standard test as the foundation for the methodologies. The pressure ranges used in the fatigue tests aimed to mimic variations in pressure that may be observed in water distribution networks in events such as surges.

Extensive testing has shown the fatigue performance of contaminated electrofusion tapping tees under fixed and variable mean pressure loading conditions. In high loading conditions, pressure ranges between 12.5 - 22.5 bar, failure occurred in less than 500 cycles with mean pressure equal to 12.5 bar. Importantly, electrofusion joints made to best practice and tested under dynamic load did not fail when subject to 1000 cycles at 22.5 bar pressure range and 12.5 bar mean pressure. This illustrates the detrimental effect that contamination has on asset integrity.

Destructive tests using industry standard methods were performed post-fatigue failure to better understand the failure mechanism of contaminated tapping tees. Here, fractography of a specimen was analysed using a Scanning Electron Microscope. Ductility was observed at the thresholds of 'U-valleys', previously housing the heating coil, at a microscopic level; indicating the source of a contaminated joint's strength.

Additionally, bespoke ultrasonic rigs were designed and built to monitor crack propagation of selected fittings during live dynamic tests in an attempt to confirm the mode of failure. These rigs proved unsuccessful due to design limitations and the complexity of the jointing interface. However, a change in signal intensity was observed in the initial pressurisation of the specimen

(prior to dynamic loading) which may be an influencing factor to the fatigue-life of contaminated tapping tees.

Acknowledgments

I feel that there have been many people that have helped me over the duration of this project, most of which will not be named in this section. However, I would firstly like to thank all those who aided me through this project that are not mentioned below.

I would like to thank Prof. Stephen Beck and Dr. Rachel Tomlinson for their consistent guidance and support over the last four years. My sponsors to this project: the Engineering and Physical Science Research Council (EPSRC), Severn Trent Water (STW) and WRc PLC - specifically, Julie Hart (STW), Peter Henley (WRc PLC) and Mike Smith (STW). Mike was essentially my industrial mentor for the majority of the project; his knowledge and experience was very beneficial to me as a young Research Engineer.

I'd like to thank Kia Yan Siaw and Naomi Shipway who worked very hard on their Masters dissertations at the University of Sheffield which also aided my research in the area of ultrasonic analyses.

I'd also like to thank Mike Rennison, Tom Howard and Jack Naumman for the many discussions we shared which ensured that the rigs I implemented in the project were of high quality. Furthermore, developing my skills in design, manufacture, instrumentation, data acquisition and processing.

I'd like to thank Hossein Rezaei, for his useful inputs on surges within water distribution networks. Fusion Provida and Control Point LLP for the demonstrations that have aided my knowledge and understanding of manufacturing and testing.

Finally, all my family of whom I am eternally grateful; and of which has changed so much over the course of this project. I'd like to thank my brother, Hootan for his support and my fiancé, Alanna, for her love and encourage throughout the project.

Contents

Abstract	i
Acknowledgments	iii
Contents.....	iv
List of Figures	ix
List of Tables.....	xiv
Nomenclature	xv
Chapter 1 Introduction	1
1.1. Piping: Progression of materials.....	1
1.1.1. Manufacturing PE pipes and fittings	2
1.1.2. A history of PE in the UK Water Industry	2
1.1.3. Terminology for water distribution	3
1.2. Common jointing methods of PE pipe	4
1.2.1. Mechanical jointing	5
1.2.2. Buttfusion welding	6
1.2.3. Electrofusion welding.....	7
1.2.5. Welding Mechanisms	13
1.3. Project scope.....	14
1.4. Joint failures in the UK Water Industry	15
1.4.1. Electrofusion Failures.....	15
1.4.2. The UK National Sewers and Water Mains Failure Database	19
1.5. Dynamic pressures in water distribution networks	19
1.5.1. Observing pressure variations in an existing network.....	20
1.6. Conclusions	23
Chapter 2 Literature Review: Testing of PE Electrofusion joints.....	24
2.1. Polyethylene as an applied engineering material	24

2.2.	An introduction to fatigue testing	26
2.2.1.	Fatigue of PE electrofusion fittings	27
2.3.	Basic fracture mechanics	29
2.4.	Destructive testing and electrofusion	31
2.4.1.	Crushing decohesion test	32
2.4.2.	Tolerance of electrofusion welds to contamination	34
2.5.	Understanding contamination	36
2.6.	Conclusions.....	37
Chapter 3	Fatigue performance of contaminated EF tapping tees.....	39
3.1.	Experimental procedure	39
3.1.1.	Short term burst test	39
3.1.2.	Dynamic load (fatigue) test.....	40
3.2.	Experimental rig design	40
3.2.1.	Preparing the test specimens	40
3.2.2.	Controlling contamination	42
3.2.3.	Designing the experimental hydraulic rig	43
3.2.4.	Plumbing the rig.....	46
3.2.5.	Controlling the rig.....	48
3.3.	Fatigue test variables.....	49
3.3.1.	Fixed mean pressure.....	49
3.3.2.	Variable mean pressure (constant amplitude)	53
3.4.	Concluding remarks	54
Chapter 4	Results from the fatigue testing programmes.....	56
4.1.	Fixed mean approach	56
4.2.	Fixed pressure range	60
4.3.	Influencing the welding parameters	65
4.3.1.	Lateral shift investigation.....	68
4.3.2.	Lateral shift – an influence on the performance of contaminated joints?	71
4.4.	Principal findings	74

4.4.1.	A critique of the research experiments	74
4.4.2.	Fixed mean approach.....	75
4.4.3.	Variable mean approach.....	75
4.4.4.	Influencing the welding parameters	76
Chapter 5	Understanding the failure mechanism - Destructive testing.....	78
5.1.	Imperfect vs. Perfect joints.....	79
5.2.	Adhesion with respect to fatigue tested specimens	81
5.3.	Specimen X	87
5.4.	Scanning Electron Microscopy	90
5.4.1.	SEM observations.....	92
5.5.	Conclusions	105
Chapter 6	Confirming the failure mechanism - Non-destructive testing	107
6.1.	An introduction to Non-destructive testing	107
6.1.1.	What is ultrasound?.....	108
6.2.	Static analysis	109
6.2.1.	Overcoming obstacles	110
6.2.2.	Preliminary results – proof of concept	111
6.2.3.	Leak path investigation with respect to fatigue pressure range.....	113
6.3.	Real-time analysis	116
6.3.1.	Rig concept – overcoming obstacles	117
6.3.2.	Ultrasonic sensor array design.....	119
6.3.3.	Mechanical component design	122
6.3.4.	Controlling and automating the processes.....	128
6.3.5.	Signal acquisition and data processing.....	132
6.3.6.	Benchmarking the apparatus	134
6.3.7.	Results from real-time ultrasound analysis	137
6.3.8.	Redesigning the apparatus.....	147
6.3.9.	Results as a consequence of the redesigned rig.....	149
6.4.	Conclusion.....	156

6.4.1.	Static analysis.....	156
6.4.2.	Real-time analysis.....	157
Chapter 7	Discussion.....	158
7.1.	Joint preparation.....	158
7.2.	Fatigue performance of contaminated electrofusion tapping tees.....	160
7.2.1.	The experimental hydraulic rig	160
7.2.2.	The fixed mean approach.....	161
7.2.3.	The variable mean approach	164
7.2.4.	Influencing factors	165
7.3.	Assessing the failure mechanism	166
7.3.1.	Destructive testing.....	166
7.3.2.	Non-destructive testing	172
Chapter 8	Conclusions.....	177
8.1.	Current literature	179
8.2.	The fatigue performance of electrofusion tapping tees.....	179
8.3.	Destructive tests	180
8.4.	Non-destructive tests.....	181
8.5.	Application to industry.....	182
8.5.1.	Operation and installation	182
8.5.2.	Experimental research approach	183
8.6.	Future directions	184
8.6.1.	On-site testing methodology	184
8.6.2.	Confirm the failure mechanism – non-destructive testing	185
8.6.3.	Influencing welding parameters.....	185
8.6.4.	Further investigation of specimens that did not fail.....	186
8.6.5.	Development of quantitative destructive test methodology for electrofusion tapping tees	186
References	188

Appendix A	Contamination Experiment.....	195
Appendix B	Equipment used	201
Appendix C	Experimental hydraulic rig & Ultrasonic rig Drawings	202

List of Figures

Figure 1-1 Example property with independent water supply	4
Figure 1-2 Mechanical 25 mm end cap.....	5
Figure 1-3 Fully-automatic buttfusion welding machine.....	6
Figure 1-4 Typical electrofusion coupler.....	8
Figure 1-5 Typical electrofusion tapping tee	8
Figure 1-6 Underside of a typical electrofusion tapping tee	9
Figure 1-7 Diagram of a typical electrofusion coupler	10
Figure 1-8 Diagram of a typical tapping tee	10
Figure 1-9 Electrofusion tapping tee with strap and tightening bolts	11
Figure 1-10 Electrofusion tapping tee and top-loading clamp.....	12
Figure 1-11 A 25mm PE 80 pipe mechanically scraped.....	16
Figure 1-12 Cross-section sample of electrofusion coupler.....	16
Figure 1-13 Ovality on a Ø180 mm PE pipe	17
Figure 1-14 Tapping-tee failure causing leak to mains pipe.....	18
Figure 1-15 Failed tapping-tee (underside).....	18
Figure 1-16 A pressure transient [31]	21
Figure 1-17 Pressure variations [31].....	22
Figure 2-1 Ethylene (C ₂ H ₄) – Monomer	25
Figure 2-2 Polyethylene – Polymer	25
Figure 2-3 Fatigue parameters with regards to stress loading.....	27
Figure 2-4 Three modes of loading.....	30
Figure 2-5 Indicative sketch of crushing decohesion test (tapping tees) – example methodology	33
Figure 2-6 Cross-section schematic of short term burst test.....	35
Figure 3-1 Diagram showing stem and service pipe outlet for an electrofusion tapping tee .	42

Figure 3-2 Schematic showing all components.....	44
Figure 3-3 Cross-section of hydraulic piston assembly	45
Figure 3-4 Cross section of piston head showing seal profiles and air bleed.....	45
Figure 3-5 3D representation of hydraulic piston.....	46
Figure 3-6 Test specimen general arrangement.....	47
Figure 3-7 Trapezoidal loading patterns for dynamic (fatigue) test showing 1 cycle	52
Figure 3-8 Examples of variable mean loading patterns showing 1 cycle	54
Figure 4-1 Pressure Range vs. Number of cycles to failure for the fixed mean low-cycle fatigue test	57
Figure 4-2 Pressure Range vs. Log Number of cycles to failure.....	59
Figure 4-3 Log Pressure Range vs. Log Number of cycles to failure	60
Figure 4-4 Mean pressure Vs. No. of cycles to failure.....	61
Figure 4-5 Mean pressure Vs. Log No. of cycles to failure	63
Figure 4-6 Log Mean pressure vs. Log No. of cycles to failure.....	64
Figure 4-7 Mean pressure Vs. No. of cycles to failure highlighting data gaps	65
Figure 4-8 Electrofusion tapping without lateral shift (top view)	67
Figure 4-9 Electrofusion tapping tee with lateral shift (top view)	67
Figure 4-10 Fixed mean fatigue testing results including lateral shifted joints.....	68
Figure 4-11 Top-loading G-clamp	69
Figure 4-12 Drawing of tapping tees on 530 mm PE pipe	70
Figure 4-13 Schematic of tapping tee welding with dead-weights	72
Figure 4-14 Fatigue-life of contaminated joints containing lateral shift during weld process.....	73
Figure 5-1 Aerial view of specimen post-crush test.....	79
Figure 5-2 Talced specimen removed from crushing device	80
Figure 5-3 Post-crush of ‘perfect’ specimen	81
Figure 5-4 Failing tapping tee showing ‘major’ leak path	83
Figure 5-5 Specimen H (90% $P_{MAT, MAX}$).....	83
Figure 5-6 Specimen W (80% $P_{MAT, MAX}$).....	84

Figure 5-7 Specimen BW (70% $P_{MAT, MAX}$).....	84
Figure 5-8 Specimen P (60% $P_{MAT, MAX}$).....	85
Figure 5-9 Specimen AP (50% $P_{MAT, MAX}$).....	85
Figure 5-10 Specimen CS (40% $P_{MAT, MAX}$)	86
Figure 5-11 Specimen ‘X’ prior to crush test	87
Figure 5-12 Specimen X during crush test.....	88
Figure 5-13 Specimen X parent pipe	89
Figure 5-14 Specimen X tapping tee (removed).....	89
Figure 5-15 Fusion zones on parent pipe of specimen L (a) and specimen X (b)	90
Figure 5-16 Approximate location of SEM samples – specimen X.....	91
Figure 5-17 Specimen X samples for SEM	92
Figure 5-18 Sample 1 (x100 magnification)	93
Figure 5-19 Sample 1 (x300 magnification)	94
Figure 5-20 Sample 1 (x902 magnification)	94
Figure 5-21 Sample 1 (x2000 magnification)	95
Figure 5-22 Sample 1 (x1500 magnification)	96
Figure 5-23 Sample 1 (x1000 magnification)	97
Figure 5-24 Sample 1 (x1000 magnification)	97
Figure 5-25 Sample 2 (x60 magnification)	98
Figure 5-26 Sample 2 (x150 magnification)	99
Figure 5-27 sample 3 (x70 magnification).....	100
Figure 5-28 Sample 3 (x1000 magnification)	100
Figure 5-29 Sample 3 (x1500 magnification)	101
Figure 5-30 Sample 3 (x2000 magnification)	102
Figure 5-31 Sample 3 (x2500 magnification)	103
Figure 5-32 Sample 4 (x150 magnification)	104
Figure 5-33 Sample 4 (x355 magnification)	104
Figure 6-1 Ultrasound static scanning rig	110

Figure 6-2 Approximate transducer locations with respect to PE bump	111
Figure 6-3 Preliminary line scan results showing leak path (a) and scan direction (b) [74]	112
Figure 6-4 Hand pump and fitting (attached)	113
Figure 6-5 Static ultrasonic scan of perfect joint [67]	114
Figure 6-6 Ultrasonic scan of Joint H [67]	115
Figure 6-7 Ultrasonic scan of Joint BW [67]	116
Figure 6-8 Ultrasonic analysis of Joint AP [67]	116
Figure 6-9 Circular piezoelectric transducers.....	119
Figure 6-10 Sensor cutting device.....	120
Figure 6-11 Aluminium ultrasound sensor array holder	120
Figure 6-12 Sensor array holder with sensors	121
Figure 6-13 Sensor holder showing damaged sensors	122
Figure 6-14 Aluminium fork design (a) & aluminium thrust block (b)	123
Figure 6-15 Photograph of aluminium fork, spring and thrust block.....	123
Figure 6-16 Sensor holder, forks roller bearings and fasteners (a) & X-section without fasteners (b)	124
Figure 6-17 Driving shaft and aluminium coupler	124
Figure 6-18 Design of column platform and drive shaft bearing	125
Figure 6-19 Stepper motor, platforms and columns.....	126
Figure 6-20 Stainless steel end cap	126
Figure 6-21 Live ultrasound testing rig assembly (model).....	127
Figure 6-22 Live Ultrasound rig in PE pipe clamps.....	128
Figure 6-23 Micro-processing unit and stepper motor driver (unwired).....	129
Figure 6-24 Computer representation of pipe, fitting and probe (aerial view).....	129
Figure 6-25 Diagram showing 1 scan of ultrasonic rig	130
Figure 6-26 Graph showing cycle with trigger and cycle rest period	131
Figure 6-27 Schematic of real-time ultrasound testing rig.....	132
Figure 6-28 Typical initial reading of a single sensor on parent PE pipe	133

Figure 6-29 Ø110 mm pipe with holes drilled	134
Figure 6-30 Data from ultrasound scan of holes in pipe	135
Figure 6-31 Scan of a perfect joint.....	136
Figure 6-32 Initial scan – No pressure – specimen ES	137
Figure 6-33 Initial scan – 12.5 bar pressure – specimen ES	138
Figure 6-34 Difference in results with respect to starting pressure – specimen ES.....	138
Figure 6-35 First cycle of fatigue test – specimen ES	139
Figure 6-36 Cycle 2 – showing difference from first cycle – specimen ES.....	140
Figure 6-37 Cycle 5 – showing difference from first cycle – specimen ES.....	141
Figure 6-38 Cycle 6 – showing difference from first cycle – specimen ES.....	141
Figure 6-39 Final (7 th) cycle – showing difference from first cycle and approximate leak path – specimen ES	142
Figure 6-40 Specimen ES showing major leak path	142
Figure 6-41 First cycle – specimen ET	143
Figure 6-42 Cycle 2 – showing difference from first cycle – specimen ET	143
Figure 6-43 Cycle 3 – showing difference from first cycle – specimen ET	144
Figure 6-44 Cycle 4 – showing difference from first cycle – specimen ET	144
Figure 6-45 Cycle 5 – showing difference from first cycle – specimen ET	145
Figure 6-46 Cycle 6 – showing difference from first cycle and approximate leak path – specimen ET.....	145
Figure 6-47 Specimen ET showing major leak path.....	146
Figure 6-48 Individual ultrasound sensors.....	147
Figure 6-49 Individual sensors in circular arrangement on bore of PE pipe.....	148
Figure 6-50 Sketch showing sensor numbers with respect to pipe and fusion zone	148
Figure 6-51 Initial scan – no pressure present	149
Figure 6-52 Pre-test scan: Pressure = 12.5 bar.....	150
Figure 6-53 Difference at starting pressure – 12.5 bar.....	151
Figure 6-54 First cycle scan (benchmark scan).....	152

Figure 6-55 Cycle 2 (a) and cycle 3 (b).....	152
Figure 6-56 Cycle 4 (a) and cycle 5 (b).....	153
Figure 6-57 Cycle 6 (a) and cycle 7 (b).....	153
Figure 6-58 Cycle 8 (a) and cycle 9 (b).....	154
Figure 6-59 Cycles 10 (a) and cycle 11 (b)	154
Figure 6-60 Cycle 12 (failure cycle)	155
Figure 6-61 Specimen EU showing leak path area and direction.....	156

List of Tables

Table 1-1 Water service element responsibility	4
Table 3-1 Failure pressures at different ramp rates	50
Table 3-2 Fixed mean testing parameters.....	52
Table 3-3 Variable mean testing values	54
Table 4-1 Summary of specimens that did not fail during fatigue test.....	62
Table 5-1 Summary of tested joints	82
Table 5-2 Summary of observations for SEM samples	91
Table 6-1 Joints discussed in this section.....	115

Nomenclature

$\Delta P/\Delta t$	Pressure ramp rate (bar/min)
\emptyset	Diameter
μm	Micrometre (1 mm = 1 x 10 ⁻⁶ m)
2D	Two dimensional
3D	Three dimensional
A-CW	Anticlockwise
AWWA	American Water Works Association
BS	British Standard
CW	Clockwise
DAQ	Data Acquisition
d_p	Distance between each crushing device
EN	European Standard
FEA	Finite Element Analysis
HAZ	Heat Affected Zone
HDPE	High Density Polyethylene (or PE 100)
Hz	Hertz (1 Hz = 1 cycle/second)
ICI	Imperial Chemical Institute
IGN	Information and Guidance Note
ISO	International Organization for Standardisation
LDPE	Low Density Polyethylene
Ltd	Limited
LVDT	Linear Variable Differential transformer
MDPE	Medium Density Polyethylene (or PE 80)
MHz	Mega-Hertz
mm	Millimetre (1 mm = 1 x 10 ⁻³ m)
MPa	Mega Pascal (1 MPa = 10 bar)
MRS	Minimum Required Strength
NDT	Non-destructive Testing
NMFD	National Mains Failure Database
OfWAT	Water Services Regulation Authority
PC	Personal Computer
$P_{\text{CYCLE MAX}}$	Maximum pressure in fatigue cycle (bar)
PE	Polyethylene
PE 100	Polyethylene with 10 MPa MRS
PE 80	Polyethylene with 8 MPa MRS
$P_{\text{MAT, MAX}}$	Maximum pressure of material (bar)

P_{MEAN}	Mean pressure (bar)
PN	Nominal Pressure
PP	Polypropylene
P_{RANGE}	Pressure range (bar)
PS	Polystyrene
PTFE	Polytetrafluoroethylene
P_{TRIGGER}	Trigger pressure (bar)
PVC	Polyvinyl Chloride
PVCu	Unplasticized Polyvinyl Chloride
SDR	Standard Dimensional Ratio
SEM	Scanning Electron Microscopy
STW	Severn Trent Water
t_{RAMP}	Ramp time (s)
t_{REST}	Rest time (s)
TRR	Trapezoidal Ramp Ratio
t_{TOTAL}	Total time (s)
UK	United Kingdom
UKWIR	UK Water Industry Research Ltd
USB	Universal Serial Bus
WIS	Water Industry Specification

Chapter 1

Introduction

This chapter provides an overview of pipes used for water distribution purposes, specifically PE pipe. The history of the material in the UK water industry is given as well as the common methods of joining the pipe material. Here, electrofusion jointing is outlined as a common jointing practice. In-service failures with respect to electrofusion jointing are also discussed. Dynamic variations in water distribution systems are also introduced in this chapter.

1.1. Piping: Progression of materials

Piping water has been prolific in the majority of England and Wales since the late 18th century. Some parts of England and Wales have had piped water supplies since the 15th century [1]. Piping potable water has been the preferred method of water distribution for centuries, however the materials with which to achieve this have altered over the years.

Cast iron pipes originally began to be manufactured in the 19th century by casting molten iron in vertical moulds. In the 1930s, ‘spun’ cast iron pipes began to be manufactured whereby molten cast iron was poured into cylindrical moulds at high speeds so that the pipe walls were formed by centrifugal force [2].

Modern plastics date back to the early 20th century. The Imperial Chemical Institute (ICI) first invented PE in 1933 [3] and one of its first applications was cable protection for radar insulation during World War 2 [4].

The development of carbochemistry gave birth to our everyday plastics such as Polystyrene (PS), Polyvinyl Chloride (PVC), Polypropylene (PP) among others [5]. Today, plastics can be used to manufacture pipes whereby different types of plastic can hold specific performance benefits that can prove useful to the end user. PE is a common plastic used for many applications such as bottles and carrier bags, however, this plastic is also common in the manufacture of pipes and is currently used in the UK water industry for the distribution of potable water in the supply network.

1.1.1. Manufacturing PE pipes and fittings

Traditionally, PE pressure pipes are manufactured using a process known as extrusion. The following is a brief overview of the manufacture process, adapted from Rotheiser [6].

Pipes are created from PE resin that usually begins in the form of pellets. The pellets, that are stored in bulk, are transported to a hopper which feeds an extruder. The extruder consists of a barrel that contains a screw and heaters. As the screw turns, the pellets are heated until the resin meets a die. Here the pipe shape is formed. In general, beyond the die, cooling takes place. The newly formed pipe enters a series of cooling tanks until it is at the correct specification to be cut to length or wound into a wheel (depending on the product being manufactured).

PE pressure pipes can be joined together using fusion welding or mechanical fittings. These joining methodologies are discussed in more detail in Section 1.2. With regards to the manufacture of the plastic fittings [for fusion welding], these can be created using a process known as injection moulding. Here, precision engineered casting moulds are used to house the molten resin (commonly the same grade as the parent pipe – i.e. PE) whilst it sets to form the required shape.

1.1.2. A history of PE in the UK Water Industry

The use of plastic pipes within the UK water industry dates back to the 1950s [7]. Initially, PVC was predominant, but this has gradually been superseded by PE which has become a standard material for the water industry. The first blue High Density PE (HDPE) pressure pipe was introduced in the 1980's for potable water distribution [8]

Today, PE pipes can be divided into two main grades, PE 80 and PE 100. The grades are determined by the performance of the material over a 50 year lifespan. Testing in accordance to ISO 12162 [9] uses extrapolation of regression curves to achieve a 50 year design life; methodology specified in ISO 9080 [10]. The polymer grade is based on the Minimum Required Strength (MRS) over this design life. In general, MDPE pipes are referred to as PE 80 as they have an MRS of 8 MPa and HDPE pipes are referred to PE 100 pipes as they have an MRS of 10 MPa.

PE pipes undoubtedly have financial and environmental advantages over traditional pipe; for example [11]:

- Fusion jointing – leak-tight, end-load resistant;

- Trenchless technologies (installation benefits) – cost savings, reduced environmental impact;
- Flexibility – follow curves of trenches, fewer joints;
- Cheaper in comparison to other materials;
- Does not corrode;
- Recyclable material.

There are two main techniques used for the installation of PE pipe networks, trenched and trenchless excavations (mentioned above); the latter being extremely useful in built up areas and may hold certain cost saving advantages over traditional methods.

According to MacKellar *et al.* [12] PE pipe is chosen for up to 90% of all new water mains laid in the UK. Research by Hoang and Lowe [13] suggests that PE will exceed its expected design life of 50 years at operating temperatures of between 10 and 25 °C.

1.1.3. Terminology for water distribution

With regards to potable water distribution from source (i.e. the water treatment works) water will travel through pipes of various sizes and pressures before entering the end users' (customer) household or business premises. For the purpose of this project, the sizes have been grouped generically into 3 types and are explained here.

Trunk mains are the largest type of pipe for water distribution. They are usually large in diameter and are used to transfer large amounts of water around the network. Typically, households are not directly connected to trunk mains to maintain the integrity of the system.

For the purpose of this thesis, distribution mains are classed as medium sized pipes. These are usually connected to trunk mains and may branch out to supply a number of buildings (such as a housing estate) with potable water. This type of main can be buried under pathways and households can be connected to these pipes.

A communication pipe is usually the smallest diameter of the water network. This type of pipe connects the distribution main to a 'stopcock' (valve) that is usually located just next to the street boundary of the property (see Figure 1-1 and Table 1-1). The pipe connecting the stopcock to the property is known as the supply pipe. In general but not in all circumstances, all pipes up to and including the stopcock is the responsibility of (property of) the water company. Therefore, in this example (Figure 1-1), the supply pipe would be the responsibility of the consumer.

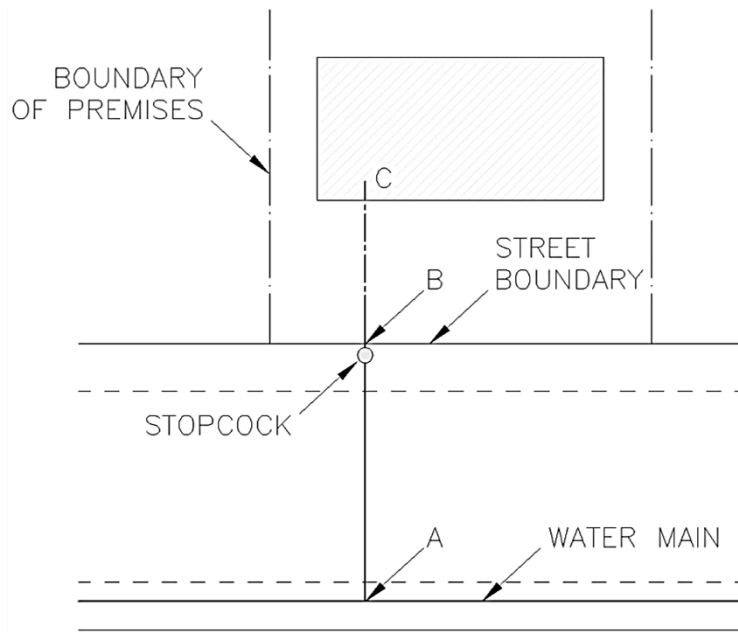


Figure 1-1 Example property with independent water supply

<i>Water service element</i>	<i>Responsibility/owner</i>
A – B Communication pipe	Water company
Stopcock	Water company
B – C Supply pipe	End user
Internal plumbing	End user

Table 1-1 Water service element responsibility

1.2. Common jointing methods of PE pipe

There are two common practices for jointing PE pipes; these are known as butt fusion and electrofusion welding. Both methods create a bond using heat to aid the adhesion process. Both methods are used widely in the UK water industry to join PE pipes. Each method has specific requirements with regards to the material properties pipes to be joined; these are further explored in this section.

With regards to the pipe requirements for welding to take place, it is important to note that butt fusion can only join PE pipes of the same diameter, thickness, Standard Dimensional Ratio¹ (SDR) and polymer grade (i.e. PE 100 to PE 100). In contrast, electrofusion jointing

¹ Standard Dimensional Ratio (SDR) is the dimensionless relationship between the diameter of the pipe and the thickness of the pipe (i.e. $SDR = \text{nominal outside diameter} / \text{minimum wall thickness}$)

can be used on pipes of different diameter, thickness and material as long as the correct coupler is used. Details of fusion jointing procedures, tolerances and equipment are outlined in Water Industry Specification (WIS) 4-32-08 [14] and are further explained in Sections 1.2.2 and 1.2.3.

An alternative to fusion welding is the use of mechanical fittings. This is explained in Section 1.2.1. A brief description of the welding mechanisms of buttfusion and electrofusion welding are given in Section 1.2.4.

1.2.1. Mechanical jointing

Mechanical joints are used when PE has to be connected to a different material such as steel or cast iron. For example, a mechanical connection is required when connecting to a hydrant or a service valve. Mechanical joints can also be used when electrofusion becomes impractical such as when water is still present within the pipe. They are also frequently used in repair scenarios [15].

Mechanical joints can be used as an alternative to fusion welding. They are also used in grounds that contain harmful (with respect to water quality) contaminants. These will be used in conjunction with PE pipes that contain a special barrier (known as barrier pipes) to ensure no contaminant such as petrochemicals can penetrate the pipe and therefore affect water quality.

Figure 1-2 shows a mechanical end cap fitted to a 25 mm diameter PE 80 pipe.



Figure 1-2 Mechanical 25 mm end cap

1.2.2. Buttfusion welding

In essence, buttfusion welding uses a heater plate to join two PE pipes of the same properties. The minimum equipment required for jointing will consist of a heater plate, mechanical pipe scraper, pipe clamps and control box. Figure 1-3 shows some of the typical equipment used for buttfusion welding. Buttfusion machines can be fully-automatic, whereby the appropriate drag forces are calculated by the control box. This type of machine may be preferred as it may eliminate any potential risk of variation in the welding procedure.

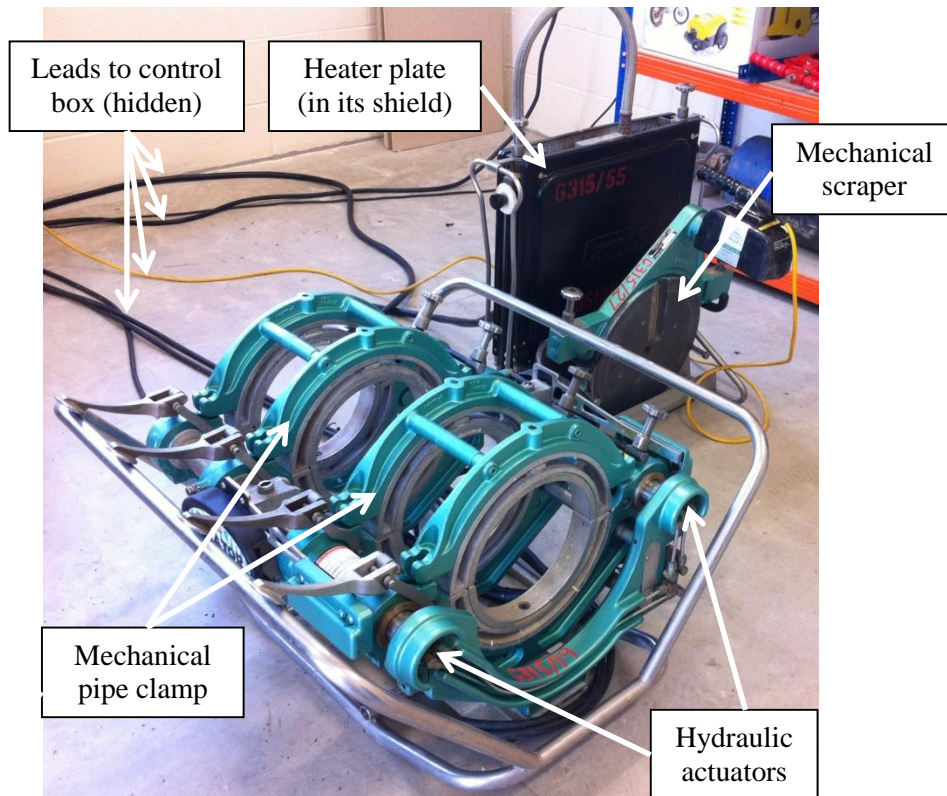


Figure 1-3 Fully-automatic buttfusion welding machine

(Note: Welding control box not visible)

Buttfusion machine types are of the preference of the installer; however, fully-automatic machines will automatically calculate the contact forces required, therefore potentially reducing the risk of error.

In general, buttfusion equipment is larger in comparison to electrofusion equipment. Therefore buttfusion welds are usually accomplished above ground.

1.2.3. Electrofusion welding

Electrofusion jointing is more dependent on the operator in comparison to buttfusion, as buttfusion can be accomplished using fully-automated machinery. Electrofusion jointing is somewhat a more ‘manual’ process whereby the operative needs to follow specific preparation procedures which are highlighted in WIS 4-32-08 [14]. This type of jointing requires only an electrofusion control box (or welding box) to achieve a successful weld. Once the control box leads are connected to the terminals of an electrofusion product, an electrical circuit is complete. Here, electricity is used to heat the filament wires in the electrofusion product for a given duration. This is how the polymer local to the fitting and pipe begin to melt and form a bond.

Electrofusion holds an advantage over buttfusion welding due to the size of the equipment needed to complete a successful joint. Furthermore, welds can be completed in smaller spaces such as trenches.

Electrofusion welding can join PE pipes of different SDR and material strength (i.e. PE 80 to PE 100). There is a wide range of electrofusion products available to ease design and installation. These include couplers, reducers, bends, stub flanges, tapping tees among others.

An electrofusion coupler (Figure 1-4) is used to join two pipes together. Communication pipes, previously mentioned in Section 1.1, can be joined to the mains pipe via electrofusion tapping tees (sometimes known as ‘tapping saddles’) (Figure 1-5). The stem of the tapping tee contains a cutting screw which is screwed locally into the host main to tap it post-weld. Once the cutting screw is unscrewed to its original position - flush with the top of the stem - water can freely flow from the host main and through the communication pipe. As noted previously in Figure 1-1 and Table 1-1, the communication pipe usually connects to the stopcock outside a property before reaching the end users’ household plumbing. In theory, if an area is being supplied water via a PE distribution main, every household will potentially be connected to the main via a tapping tee.

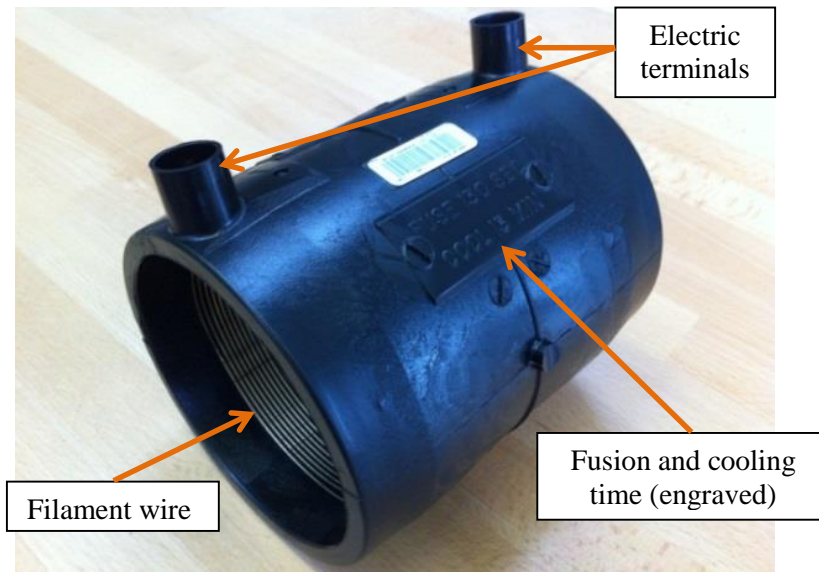


Figure 1-4 Typical electrofusion coupler

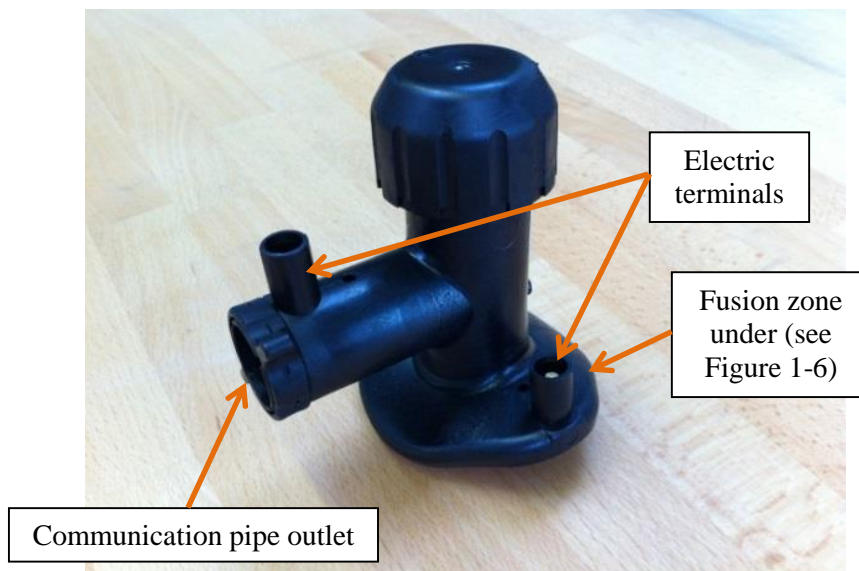


Figure 1-5 Typical electrofusion tapping tee

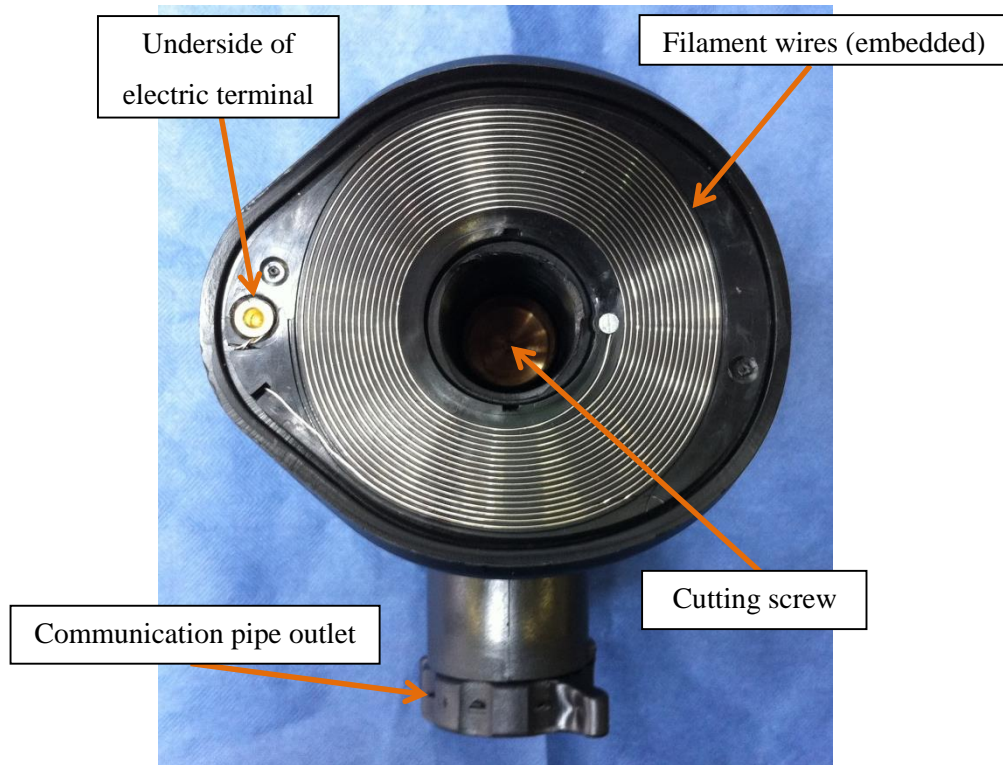
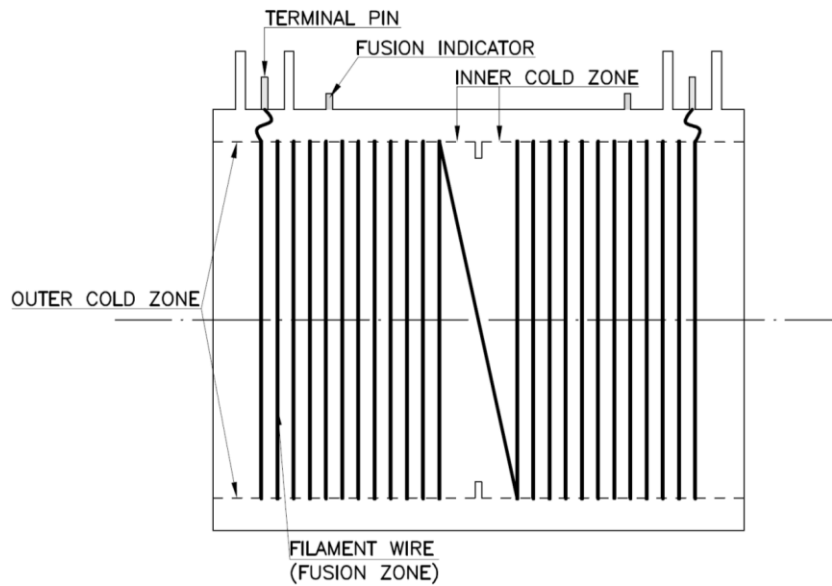
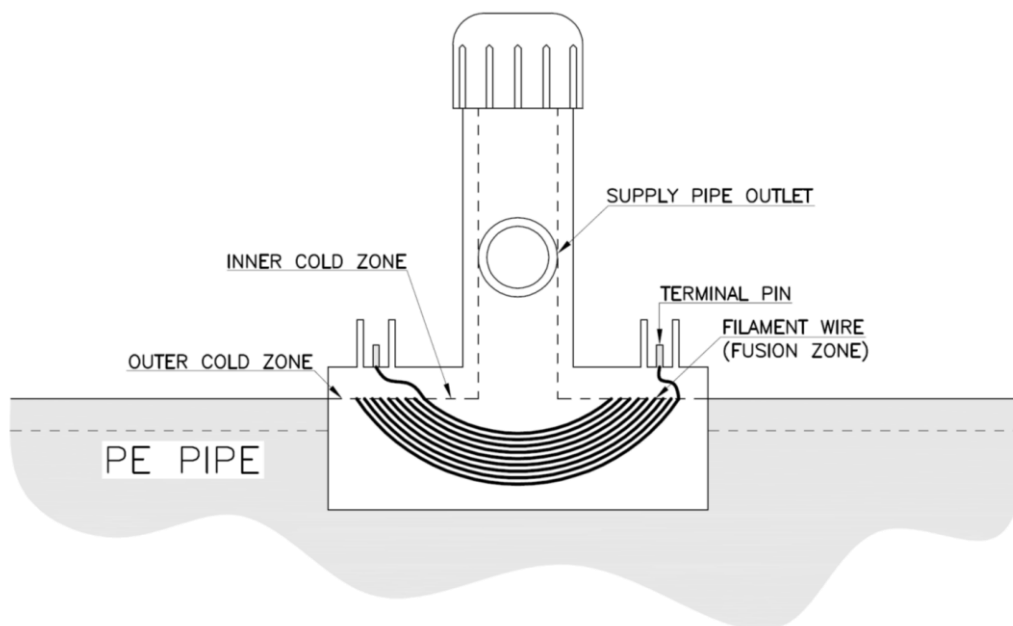


Figure 1-6 Underside of a typical electrofusion tapping tee

As mentioned previously, all electrofusion products contain a filament wire inset within the polymer carcass or (for tapping tees for example) situated on a pad that is attached to the fitting. In general, a coil is spun or attached in such a way that two terminal pins remain on the outside of the fitting; this is where the electrofusion control box connectors are inserted (see Figure 1-7 & Figure 1-8). The control box provides a stable power supply to the fitting [16].



*Figure 1-7 Diagram of a typical electrofusion coupler
(adapted from [16])*



*Figure 1-8 Diagram of a typical tapping tee
(adapted from [16])*

Summarising the weld process; an electrofusion welding control box uses electricity to heat the filament wire for a required time – fusion and cooling durations are usually marked on individual fittings to inform the operative of the appropriate times (see Figure 1-4). The localised heating of the pipe and coupler about the filament wires causes a combination of

melting and flow of the polymer at the welding interface; as the weld cools the bond is formed [17].

With regards to electrofusion tapping tees, these require a slightly different preparation procedure as the products are clamped onto the pipe. In general, there are three ways in which tapping tees are clamped to the host pipe in order to restrict movement during the welding process [14]: under-clamping, wrap-around systems and top-loading. Figure 1-9 shows a wrap-around type electrofusion tapping tee held on a pipe via a strap and tightening bolts.

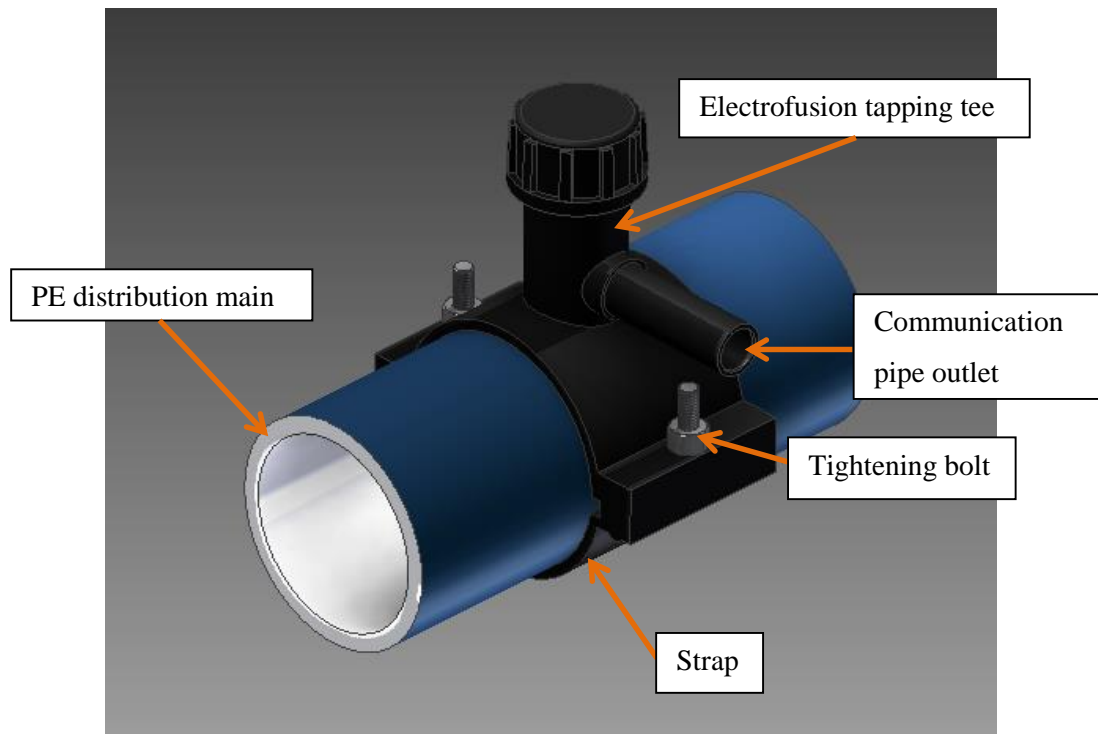


Figure 1-9 Electrofusion tapping tee with strap and tightening bolts

Clamping should eliminate localised movement of the tapping tee to secure a bond between pipe and fitting. For top-load clamping, a tapping tee is placed onto the pipe and the top-loading clamp is positioned in such a way that a compressive force is exerted onto the host pipe (see Figure 1-10).

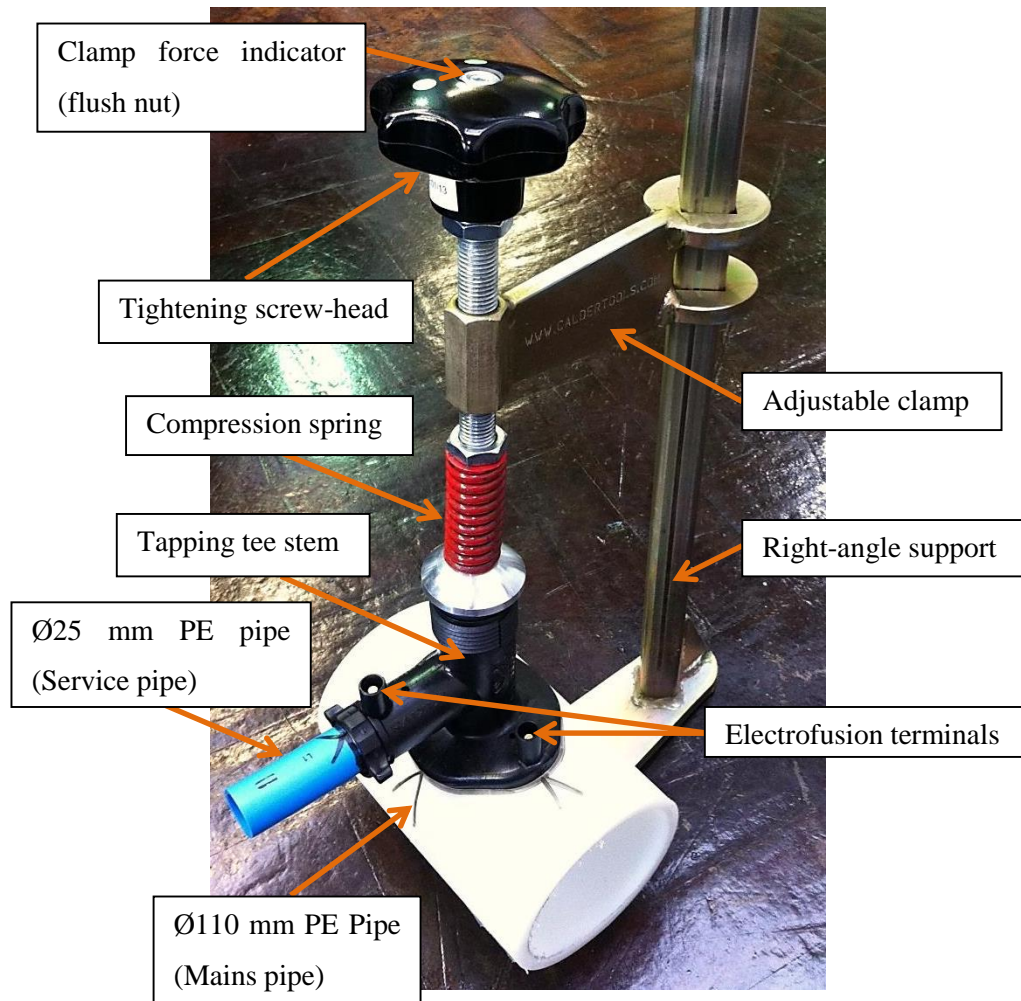


Figure 1-10 Electrofusion tapping tee and top-loading clamp

As illustrated in Figure 1-10, the adjustable part of the clamp locates the top of the tapping tee stem; then the tightening screw-head is wound until the clamp force indicator sits flush with the top of the head. This would indicate that the correct amount of compressive force is being applied by the compressive spring. It is important to note that the nut may recess by a small amount over time. This may be due to the localised compressive force being applied on the pipe. Furthermore, manufacturers may recommend different loading pressures for their fittings.

1.2.5. Welding Mechanisms

An adhesive can be described as:

“...any material that causes one body to stick or adhere to another.”

Parker & Taylor [18]

With regards to welding PE to PE the process that will take place is autohesion. This is a particular form of adhesion which involves the formation of a strong bond as a result of contact between two surfaces of the same substance [19].

Buttfusion and electrofusion welding both use heat to join pipes together. However, the way in which the bond is achieved on a molecular level may differ.

Cosgrove [19] finds the buttfusion weld obtains its strength from the melt shear that occurs at the bead roll over stage as previously mentioned in Section 1.2.2. The shear forces are therefore at their greatest when the two pipes are joined after the heater plate is removed and the pipes are forced together. It can be assumed that this degree of shear mixing is what gives the buttfusion joint its strength.

The electrofusion weld is more likely to be mechanisms such as adsorption and diffusion as the use of clamps restricts the mechanical displacement during the fusion cycle. Adsorption is the theory that adhesion results from molecular contact between two materials and the surface forces which develop [20]. Diffusion theory is where adhesion arises through interdiffusion of long-chained molecules that are capable of movement [20]. Bowman [16] also agrees that diffusion theory best describes the healing process of electrofusion. It can further be assumed that the heat applied during the fusion cycle will cause a localised expansion and aid the bonding process.

Plastics Design Library [17] describes electrofusion welding in 4 stages:

- i) Incubation. Heat is applied via the filament wires embedded into a coupler's carcass. The PE of the carcass (local to the filament wires) begins to expand, filling the gap between coupler and PE pipe. Temperatures between 120 – 135 °C cause the polymers to melt which leads to joint formation.
- ii) Joint formation. Here the melt from the coupler combines with that of the pipe and a melt pool is created. Joint strength at this stage is low due to limited intermolecular diffusion across the welding interface – resulting in brittle failures.

-
- iii) Consolidation stage. Here joint strength increases during the fusion time – moving from brittle to ductile failure modes. This is due to high molecular weight molecules beginning to diffuse across the welding interface.
 - iv) Cooling. Once the fusion time is complete the joint begins to cool. Macromolecular diffusion and polymer chain entanglements about the welding interface give the joint strength.

With regards to the welding mechanism of electrofusion tapping tees, previously mentioned in Section 1.2.3, Marshall *et al.* [21] comments on the performance of tapping tees in some experimental work noting: “...it is possible that the degree of melt movement generated by application of the top-loading [clamp] during welding causes some shear mixing of the interface by melt movement”.

1.3. Project scope

The products and the procedures used to install PE pipes and fittings are similar for both the water and gas industries. Therefore there is an argument that knowledge gained from this research could be transferred to the gas industry. With regards to the gas industry, there are also many similarities in the in standard methods of assessing the performance of PE pipes and fittings. However, it shall be noted that research performed during this project was purely focussed on the UK water industry. Therefore it can be assumed that the author holds no knowledge of the operation, maintenance and repair of PE assets for any other industry outside the UK water industry; including the gas industry.

Section 1.2 highlights the three methods for jointing PE pressure pipes. However, as Section 1.4 will explain, the focus of the research has been solely on electrofusion jointing. Therefore, electrofusion jointing will henceforth become predominant.

The main focus of this project was to observe the detrimental effect that contamination has on joint integrity. It has been previously highlighted that electrofusion joints are commonly made in trenches which may increase the risk of contamination about the welding interface. Although this may be the case, it is paramount to note that this does not mean that all electrofusion joints are at a ‘high’ risk of contamination. Furthermore, defining risk with regards to contamination is subjective and was considered to be out of the scope of this project.

1.4. Joint failures in the UK Water Industry

Leakage can be defined as the water lost between the Water Treatment Works and the customer's home or business [22]. A burst (fail in-service) would undoubtedly cause leakage – this may be seen when it comes to the surface or found using leakage detection methods. Background leakage can be described as the accumulation of smaller leaks that may be more difficult to detect [23]. One of the main concerns for all water companies, with regards to potable water, is leakage from the distribution system as the economic regulator for England and Wales, OfWAT, uses 'leakage' as a performance indicator for regulated companies.

There are many variables which are considered when dealing with the improvement, repair or rehabilitation of distribution systems, the majority of which may be reasoned economically. For example, a water company may accept an economic level of leakage, meaning that it is more economically viable that a certain part of its distribution system is leaking water as opposed to locating and repairing that section of the system; as the direct and indirect costs associated with the repair may outweigh the benefit (i.e. financial risk).

1.4.1. Electrofusion Failures

Premature electrofusion failures can occur in water distribution systems if pre-welding preparation methodologies are not followed on site. The common causes have been highlighted as: poor scraping, misalignment (including problems associated with ovality) and contamination [24, 25, 26, 7]. As electrofusion jointing is more dependent on the operator, the variables which could cause failure are arguably a lot less controlled.

Two of the three aforementioned workmanship issues can potentially be overcome by the implementation of training and tooling provided to the operative. However, contamination is an environmental issue that may be harder to overcome. As electrofusion jointing can take place in trenches, introducing contamination – such dirt, dust and water - from the immediate surrounding may be seen as an increased risk. Therefore, it is important that extra care be taken to ensure the assembly is clean. If the pipe were to become contaminated then it is recommended that an appropriate 'wet wipe' be used to clean the jointing surface prior to welding. However, in essence a wet wipe is a semi-permeable membrane which can be used incorrectly. If the rubbing element (a hand for instance) holding the wet wipe were to be dirty, some dirt may transfer through the wet wipe and onto the proposed cleaning surface; thus defeating the object of using the wet wipe as a cleaning utensil. This may be avoided by scrunching the wet wipe to create a pad, then apply the pad onto the area to be cleaned.

Testing by Marshall *et al.* [24] proved scraping to be an essential practice and can have an improved effect on joints that are pre-contaminated using talcum powder upon testing. Thus, inadequate scraping of PE pipes can affect the integrity of an electrofusion welded system. The purpose of scraping the pipe prior to welding is to remove the anti-oxidised layer on the surface of the pipe to allow mixing of melt from the pipe and fitting during the welding process [17]. This can be achieved with either a mechanical (see Figure 1-11) or hand scraper. Mechanical scrapers are generally preferred as they can produce a consistent prepared surface that is potentially transferable from operator to operator – in theory.

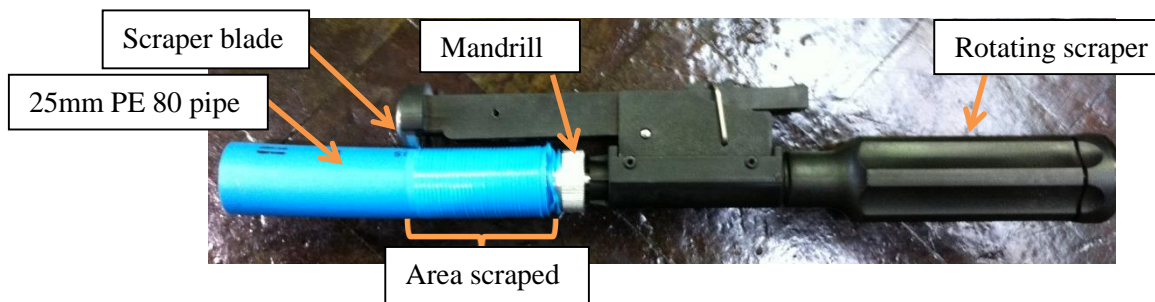


Figure 1-11 A 25mm PE 80 pipe mechanically scraped

The misalignment of pipes is avoided when clamps are used in the preparation procedure to ensure the assembly remains true throughout the welding process. When pipes are misaligned, grouping of filament wires may occur which can lead to short circuiting and gaps may be introduced inside the coupler with respect to the pipe [27]. Figure 1-12 is a cross-sectional sample taken from an electrofusion coupler, provided by a manufacturer, where it is believed that the grouping of wires and visible gap in the fusion zone is a result of misalignment of pipes with respect to the coupler.

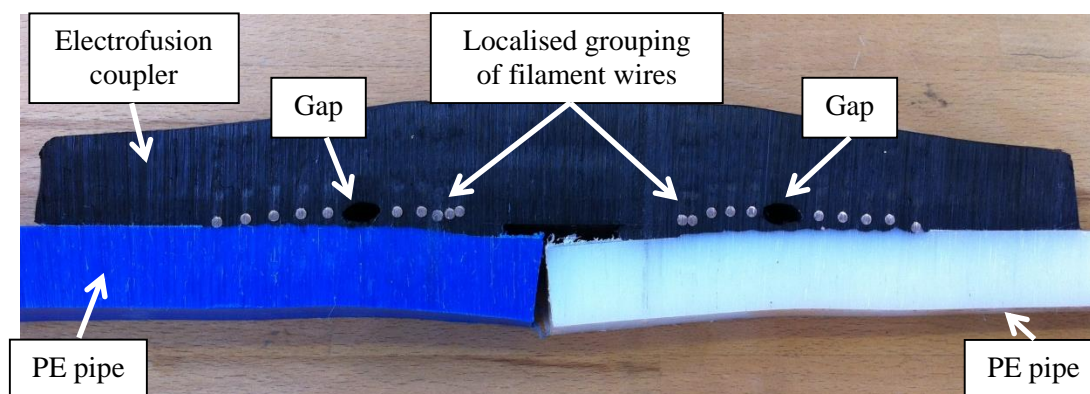


Figure 1-12 Cross-section sample of electrofusion coupler

PE pipes can be manufactured in such a way that they are wound to a drum – these are known as ‘coiled pipes’. A coiled pipe has installation advantages as it will reduce the number of

joints leaving a large array of pipe. They are commonly used in no-dig installations as they have economic benefits to the installer and can dramatically reduce road disruptions. However, coiled pipes have a tendency to be oval as a consequence of being wound into a drum. Figure 1-13 illustrates the severity of ovality on a 180 mm diameter PE coiled pipe which was cut at random from the coil drum. In situations like this, re-rounding clamps can be used to ensure the ovality tolerances are within specification before and during the welding processes.



Figure 1-13 Ovality on a Ø180 mm PE pipe

Figure 1-14 shows a failed tapping tee being repaired by the operative (left in Figure 1-14). It shall be noted that this example depicts a repair scenario and therefore not a new installation. The purpose of this example is to show the potential conditions that operatives may be required to work in. Specific attention should be paid to the depth as well as the overall size of the excavation. In this particular case, the failed electrofusion tapping tee (Figure 1-15) was replaced using a mechanical fitting.



Figure 1-14 Tapping-tee failure causing leak to mains pipe

From observing Figure 1-15, small marks of the black top-tee are visible on the white pipe; which suggest that the failure was of a brittle nature as there are no remnants of the white pipe on the underside of the tapping tee.

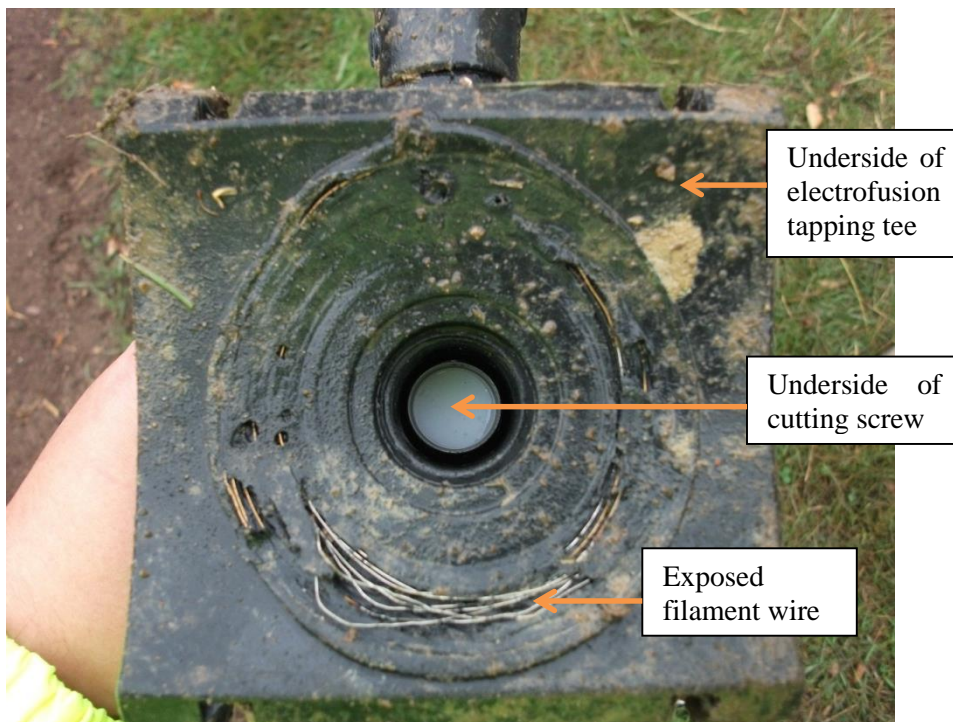


Figure 1-15 Failed tapping-tee (underside)

1.4.2. The UK National Sewers and Water Mains Failure Database

A report written by UKWIR [7] states there may be a lack of consistency in operative competency resulting in the high amount of electrofusion failures in the industry. The report describes findings from an analysis of the UK National Sewers and Water Mains Failure Database (NMFD). The NMFD is a record of all the failures that occur in UK water industry. The data is vast and interesting conclusions from the analysed data have been made which may become a driving force to implement improvements in the industry. The NMFD can offer perspective and is without question a powerful tool in obtaining information on failures on both a company and national level.

From the NMFD records between 2005 – 2007, 3 to 4 failures per year per 100 km for PE water mains [7] were recorded. However, it is fundamental to note that PE was the best performing material with respect to failure rates observed in this data set. Therefore, despite issues discussed in this chapter, PE shows strong performance in comparison to other pipe materials. Several years have passed since the publication which may warrant another investigation to observe any difference in material performance with regards to in-service failures.

1.5. Dynamic pressures in water distribution networks

Water pipes will vary in size depending on their design. The pipe designer should ensure that the pipes have sufficient capacity to fulfil demand within its design life. Water companies usually regulate pressure within the distribution network to ensure that it is neither too high nor too low when it reaches the end user.

Due to a topographical variation of pipelines, air-valves are strategically placed in distribution systems to bleed air from the network. In general, [service] valves are used to control the flow of water in the network. However, as a valve is closed, the pressure may increase upstream, which may have an effect on the system. If a valve were to be closed and opened too quickly, this may cause a pressure transient ('surge') in the system.

A surge can be defined as a sudden change in pressure [28]. The effect of a surge event is the generation of pressure waves which can be in the excess of the rated pressure of the system [29]. The pressure range can be quite large but generally occurs over a very short space of time. According to Headford *et al.* [30] the effects of surge on PE water distribution networks have been well researched and documented since the late 1990's. Beech *et al.* [29] found that all pumping mains are subject to surge pressures throughout their lifetime. The common causes

of surge were highlighted as the shutdown and start-up of pumping stations and the re-closure of air valves.

1.5.1. Observing pressure variations in an existing network

Water companies can monitor the water pressures in their network by using pressure sensors and loggers. Many logging systems in the distribution network work at low frequencies with regards to the acquisition of data; this may give a ‘steady state’ impression of the pressure within the network. These low frequency loggers may struggle to capture surge events as they may happen within the capture rate of the pressure logger. This can be overcome by the use of high frequency loggers; due to the high frequency sample rate, these loggers are able to capture sudden increases/decreases in pressure in such events as surges.

In 2013, high frequency pressure loggers were installed in a water distribution network with the aim of observing dynamic variations in pressure [31]. Most loggers were able to capture and store data at a sample rate of 128 Hz (128 samples per second) for approximately one month. This section will illustrate real-life data taken from a distribution network showing any variations in pressure. It is important to note that this section purely adds value for explanatory purposes. The observations of which are not necessarily common in all data observed by high frequency loggers in any given month. For a greater understanding of any area of network, a detailed surge analysis should take place; this may include the addition of high frequency pressure loggers.

The sites chosen have no geographical or demographical significance. Furthermore, no analyses were conducted in this section to investigate the cause of the variation in pressures as well as the pipe material it relates to; as this was deemed outside the scope of the project. The following examples show data sampled at 64 Hz.

Figure 1-16 shows a pressure transient captured using a high frequency pressure logger in a real network. In this example, the sudden increase in pressure, peak-to-peak, occurred in just under 0.5 seconds. The range in pressure with regards to this increase is 1.8 bar (0.18 MPa) – a relatively small change in pressure. Data was recorded for one month, however, the timescale of the data represented in Figure 1-16 is approximately 3 minutes.

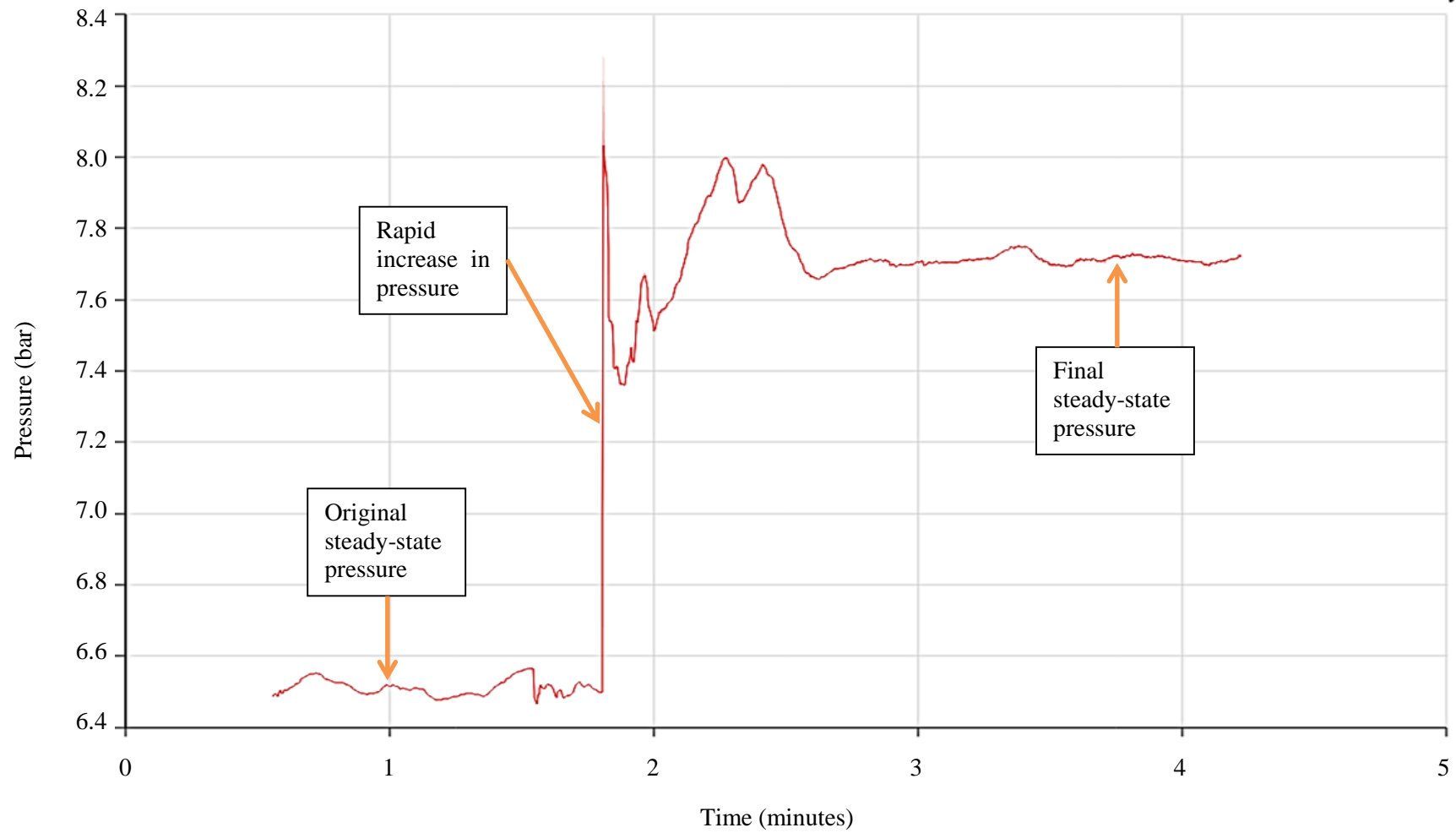


Figure 1-16 A pressure transient [31]

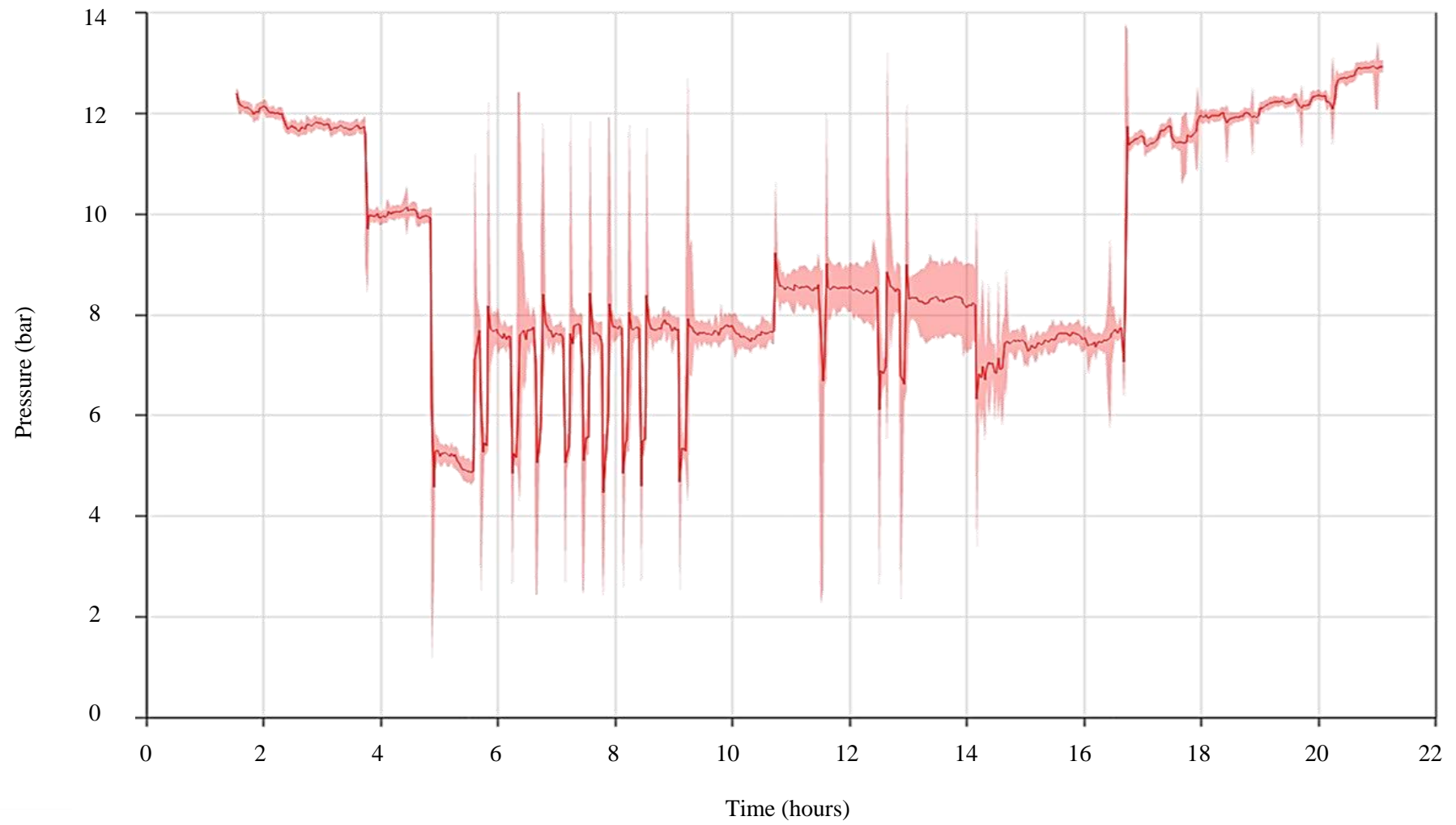


Figure 1-17 Pressure variations [31]

Figure 1-17 shows a number of sudden variations in pressure on a particular pipe in a distribution network. The data is a representation of approximately 18 hours. It shows a number of surge events that occurred within this timeframe. The minimum pressure within the data set is approximately 1 bar (0.01 MPa) and the maximum pressure is approximately 14 bar (0.14 MPa) – although there are periods of steady-state pressure between the minimum and maximum.

It is clear that variations in pressure in water distribution networks will undoubtedly differ in magnitude from network to network (or analysis to analysis). It is also important to note that the examples given in this section are not necessarily common for all networks.

1.6. Conclusions

A background to the manufacture and history of PE pipe in the UK water industry has been illustrated. The common methods of jointing have also been highlighted of which, failures with regards to electrofusion jointing was discussed. Literature suggests that three causes of premature electrofusion failures are: misalignments, poor scraping and contamination. Two out of the three issues (misalignment and poor scraping) can arguably be overcome through further operator training and awareness and potentially the implementation of good tooling. However, issues surrounding contamination may be harder to overcome with regards to electrofusion jointing. This may be because it is an environmental issue and operatives can be faced with difficult working conditions when welding. With regards to jointing, it shall be noted that if best practice is followed to WIS 4-32-08 [14] then acceptable performance of the joint will be achieved [32].

The complexity of distribution systems should be appreciated with regards to their design, installation and maintenance. Variations of pressure in water distribution networks was also discussed and some examples were presented.

Joints play a fundamental role in a distribution network. With the aforementioned points in mind, Chapter 2 will focus on research that surround these areas; specifically looking at dynamic testing of PE pipes and fittings.

Chapter 2

Literature Review: Testing of PE Electrofusion joints

This chapter will give a brief explanation of the chemistry of PE followed by a review of fatigue testing techniques; finally focussing on the fatigue response of electrofusion fittings. The use of fracture mechanics to analyse electrofusion joints will be explained giving reference to current standards and test methodologies. Finally, ‘contamination’ is discussed with respect to its performance on electrofusion assets.

2.1. Polyethylene as an applied engineering material

Polymers are often referred to as ‘plastics’, but in fact, polymers encompass a large variety of compounds of various properties and can be natural or synthetic [33]. In essence, polymers are the basic ingredient of plastics. Polymers are large molecules formed by polymerisation (chemical linking) of repeating small molecular units, fundamentally making a chain [3].

Polyethylene is a polymer that is formed through polymerisation of ethylene gas. Ethylene gas consists of two double bonded carbon atoms and four hydrogen atoms (see Figure 2-1). During the chemical reaction, the double bond between carbon atoms is broken which allows for a single carbon atom to be added. The result is a single chain of PE being created (see Figure 2-2). The polymerisation of ethylene is temperature and pressure dependant and various catalysts can be used to engineer different properties of material.

True PE is classed as a homopolymer as it is derived from one species of monomer [33]. A monomer is a molecule that can bind chemically to other monomers to form a polymer.

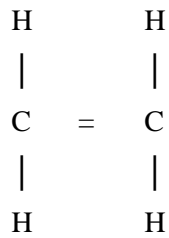


Figure 2-1 Ethylene (C₂H₄) – Monomer

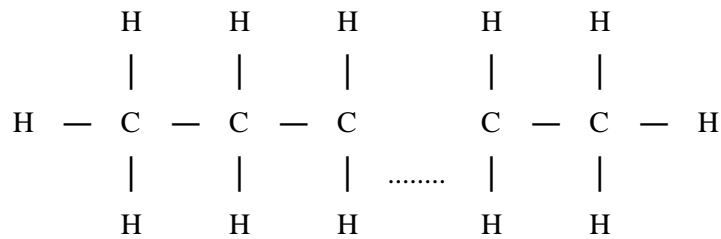


Figure 2-2 Polyethylene – Polymer

Polymers are commonly separated into three groups which are purely based on the molecular structure of the polymers: thermoplastics, elastomers and thermosets [34]. Thermoplastics can be further sub-divided into crystalline and non-crystalline (more commonly known as amorphous). The balance of amorphous and crystalline parts manages the performance and resistance of the material [5]. PE is characterised as a semi-crystalline polymer, made up of crystalline regions and amorphous regions [35]. Crystalline regions are densely packed and layered in parallel, whereas amorphous regions are the less dense regions.

2.2. An introduction to fatigue testing

Fatigue can be described as:

“...the loss of strength or other important property as a result of stressing over a period of time.”

Hertzberg & Manson [36]

Repetition of loading can induce one or more tiny cracks in a material. These cracks may grow over time and load until failure occurs. Therefore fatigue can be a common cause of fracture [34]. The prevention of fatigue fracture is an integral part of the design process if an element were to be subject to dynamic loading or vibration.

Fatigue tests are classically exemplified in polymers and metals by S-N curves [36]. This is usually in the form of stress range vs. the number of cycles to failure and can appear on logarithmic scales (axes).

If ‘stress’ (as opposed to strain) is the focus of testing under fatigue, then the following basic parameters are usually considered [34]:

$$\Delta\sigma = \sigma_{max} - \sigma_{min} \quad (2-1)$$

$$\sigma_m = \frac{\sigma_{max} + \sigma_{min}}{2} \quad (2-2)$$

$$\sigma_a = \frac{\Delta\sigma}{2} \quad (2-3)$$

where $\Delta\sigma$ is the stress range, σ_m is the mean stress, σ_a is the stress amplitude and σ_{max} and σ_{min} are the stress maximum and minimum respectively. These are further illustrated in Figure 2-3 which shows a sinusoidal loading pattern; here the mean stress is the dotted line through the centre of the waves on the longitudinal axis.

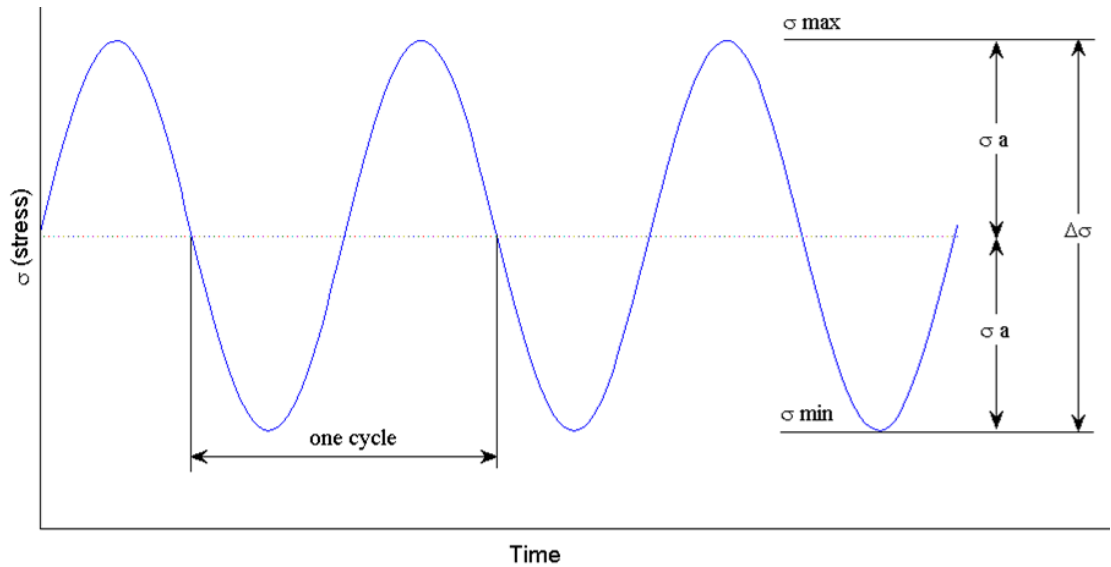


Figure 2-3 Fatigue parameters with regards to stress loading

A Stress Ratio, R , is sometimes used where;

$$R = \frac{\sigma_{min}}{\sigma_{max}} \quad (2-4)$$

If tensile stresses are regarded as positive viz. compressive stresses negative; and compressive stresses are present, then $R < 0$. With regards to fatigue testing of pipe, pressures are usually positive, thereby $R > 0$ [37].

For the fatigue testing of pipes, the hoop stress range in the pipe is commonly used as the stress range when presenting data. The hoop stress range is dependent on the pressure range inside the pipe with respect to the thickness and diameter of the pipe. The calculation will vary slightly depending if the pipe has a 'thick' or 'thin' wall.

2.2.1. Fatigue of PE electrofusion fittings

This section will focus ultimately on the fatigue response of PE electrofusion fittings. However, a brief overview of fatigue testing with regards to PE pipe will be presented in order to further understand the literature spectrum. It is important to note that PE can hold advantages over metallic materials as it has a lower elastic modulus; therefore the pressure wave speed and the pressure rise intensity is greatly reduced in comparison to metallic materials [29].

There is a wide range of information available on the fatigue performance of MDPE and HDPE of which the research has been undertaken using various techniques and on either pipes or samples. Research observing creep and fatigue in sections of MDPE [38, 39, 40, 41] and round and square bar sections [42] all use MDPE pipe as the source material for test specimens. Some fatigue research on HDPE uses specimens cut from compression moulded sheets [43, 44]. Whereas, Phua *et al.* [45] performed sinusoidal fatigue tests on notched HDPE pipe at 80 °C at 0.4 Hz; with pressure mean and amplitude 5.5 ± 4 bar (0.55 ± 0.4 MPa) respectively. A fractographic study took place including the use of SEM analysis to observe the fracture surfaces.

In general, fatigue tests can be long in duration which can arguably give the possibility of long test times required for worthy data generation. It is common for PE fatigue tests to be performed at elevated temperatures. Sandilands [46] explains how the test temperature of PE pipes can significantly affect the stress rupture times – showing that testing at 80 °C identifies brittle failure in pipes and reduced test times.

Section 1.5 gives examples of variations in pressure in water distribution networks. Here, ‘surge’ is defined as a sudden change in pressure. Although, the reoccurrence of surges can be described as a fatigue mechanism, Marshall *et al.* [47] describes that surge and fatigue are two distinctively different loading conditions that can be treated separately, with regards to pipe systems.

For pipe systems used in day-to-day operation, Bowman [37] explains that they may be subject to two different types of fatigue: firstly, a diurnal fatigue by which the demand on the network causes fluctuations in pressure (≤ 4 bar [0.4 MPa]), ranging between 3.7×10^4 cycles and 9.0×10^4 cycles in a 50 year design life; secondly, the operation of pumps and valves in the distribution network (> 6 bar [0.6 MPa]). It is important to note that during either event, the material will experience periods of constant (‘steady-state’) pressure in addition to fluctuations.

The UK water industry’s Information and Guidance Note (IGN) 4-37-02 [48] – *Design against surge and fatigue conditions for thermoplastic pipes* – gives guidance on the pipe rating criteria to cope with surge and fatigue conditions for thermoplastic pipes. In brief it states that for high toughness PE materials, de-rating of the pipe may not be required to cope for repeated cyclic events. The report further explains that there is no reported history of service problems caused by long term failure due to fatigue in PE pipes.

Bowman [37] also summaries some fatigue research on HDPE pipes; one piece of research suggesting that there was evidence that pulsations increase the strength of PE pipe. These tests

were conducted at 20 °C using high stress to induce failures in reasonable timeframes. There was no evidence of a fatigue weakness according the research. Testing by Beech *et al.* [29] on V-notched pipe used a saw-tooth cycle with a ramp rate of 9 (± 1) bar/sec; of which no failures occurred after 1.6×10^6 cycles. The testing temperature was 10 °C. Similarly, Beech *et al.* [29] conducted two other independent tests under the regime described previously but with electrofusion couplers on PE pipe. These were subject to 2.0×10^6 cycles of which no failure occurred.

Bowman [49] tested electrofusion couplers under dynamic trapezoidal loading cycles (frequency ≈ 0.067 Hz) at 80 °C to failure. Brittle failure always occurred in the coupler and not the pipe; crack propagation through the body of the carcass in the circumferential plane with fatigue-life ranging from 4.60×10^4 to 7.26×10^4 . Interestingly, the findings show that the fatigue response of couplers are not independent of their design, however, the resin in which they are manufactured can affect the performance under dynamic load.

2.3. Basic fracture mechanics

Fracture mechanics refers to the study of crack growth originating from flaws that may exist within a material or structure [50]. All materials contain flaws, cracks or inhomogeneities which can propagate to cause failure [51]. These flaws can be caused by an infinite number of things which may occur during a materials' manufacture, transport, installation or service.

There are three basic modes of loading which describe the separation of the crack surfaces; these are depicted in Figure 2-4:

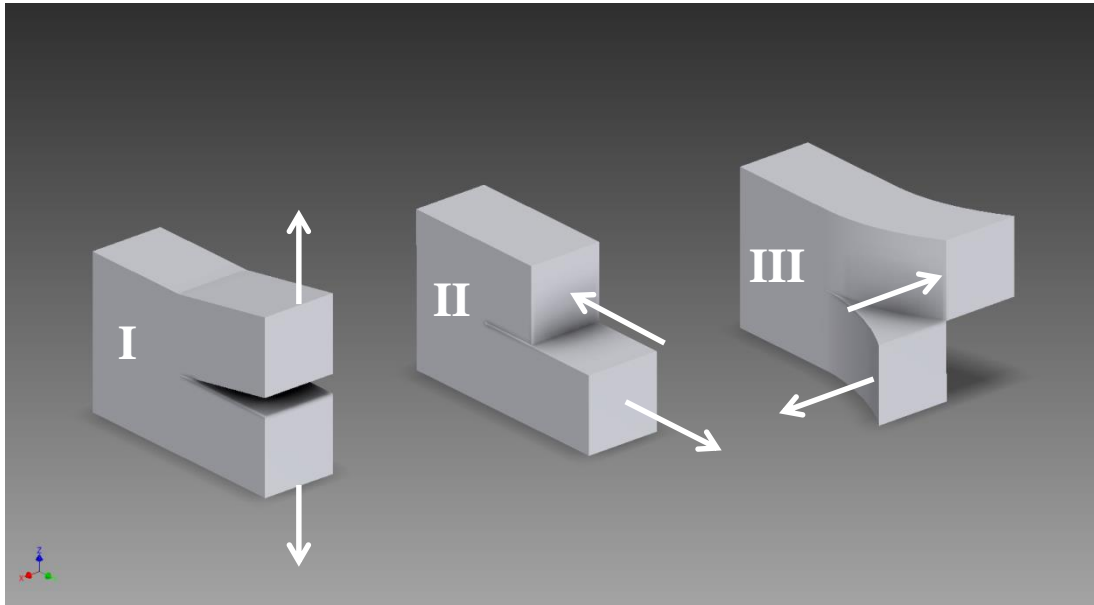


*Figure 2-4 Three modes of loading
(adapted from [52])*

From Figure 2-4 the three failure modes can be explained thus [52]:

- Mode I (Left) – tensile opening mode;
- Mode II (middle) – in-plane sliding mode;
- Mode III (right) – tearing or anti-plane shear mode.

In general, testing electrofusion joints can be performed on the entire assembly or samples (coupons). Section 1.1.2 explained how internal pressure tests are used to extrapolate the lifetime of PE pipe over 50 years. Bowman [16] combines current research to explain that using this method to assess the strength of the fusion joint interface is not ideal for three reasons [assuming the joint has been made correctly]. Firstly, electrofusion joints do not fail along the fusion interface; applicable to 20 °C (ductile) and 80 °C (brittle) test regimes. Secondly, slow crack growth (SCG)² through the body of the fitting is the failure mechanism for electrofusion joints tested at 80 °C. Thirdly, the brittle 80 °C failures are at a lifetime of over one year. Therefore internal pressure loading is not common for assessing the joint strength of electrofusion joints. The creation of coupons from electrofusion joints and testing using basic fracture mechanics is generally used to assess joint strength. Furthermore, UKWIR

² “Slow crack growth (SCG) – the slow extension of the crack with time.” [3]

[53] comments “...that fracture mechanics forms the best framework for considering both the design and assessment of products...” with regards to electrofusion joints.

2.4. Destructive testing and electrofusion

For decades, the UK has implemented the use of PE pipe for water distribution networks. However, the grade of PE resin used to manufacture the pipe has changed through its service. This was widely due to the improvement of standards as well as the demand to improve engineering properties of the resin itself to resist known failures like SCG and rapid crack propagation (RCP)³ [11]. In short, this was the transition from LDPE to MDPE (PE 80). Furthermore, HDPE (PE 100) is the more common pipe used within the industry today.

In the UK, PE pipes have to conform to current standards and specifications: British Standard (BS), European Standard (EN), International Standard (ISO) and Water Industry Specification (WIS) where applicable. According to the Civil Engineering Specification for the Water Industry (CESWI) [54], PE pipe systems for water supply should conform to BS EN 12201-1 [55] - Plastic Piping Systems for water supply - Polyethylene (PE) - Part 1: General and BS EN 12201-2 [56] - Part 2: Pipes. Furthermore, electrofusion fittings should conform to BS EN 12201-3 [57] - Part 3: Fittings. BS EN 12201-5 [58] illustrates the fitness for purpose of the system and highlights testing criteria for joints.

With regards to the manufacture of PE fittings, PD CEN/TS 12201-7 [59] explains that type tests are performed to prove that a product will meet the requirements given in the relevant standard. Whereas batch release tests are performed by or on the behalf of the manufacturer before a batch can be released.

In this section, two tests will be discussed. The former destructive test promotes fracture to observe the decohesion about the jointing interface. The latter is a short term burst test used to assess the resistance of electrofusion assemblies to contamination; contamination was previously highlighted in Section 1.4.1 as an influence on premature failures in electrofusion assets.

³ “Rapid Crack Propagation (RCP) – A running-crack failure associated with lower temperatures and gas media, initiated by a significant impact. Cracks, once initiated, run at high speed and result in cracks many feet in length.” [3]

2.4.1. Crushing decohesion test

The crushing decohesion test is outlined in ISO 13955 [60] and can be used for both electrofusion couplers and tapping tees. The purpose of the test is to observe the nature of failure as well as calculate the amount of decohesion about the jointing interface. This is calculated as a percentage.

For couplers, the specimen is welded and left for a 6 hour conditioning period before being sawn in half longitudinally. The specimen is left for a further 6 hours before being inserted into a device of undefined size but able to crush the specimen at a rate of 100 mm/min (1.67 mm/s) until double the wall thickness of the pipe is achieved. If the specimen does not yield away from the host pipe after the crushing exercise, a lever can be used to prise the specimen away from the pipe - no impact forces are allowed.

The brittle failure is observed and measured in the fusion plane. The percentage of brittle failure decohesion, C_C , is calculated thus:

$$C_C = \left(\frac{S_F}{S_T} \times 100 \right) \quad (2-5)$$

where S_F is the brittle failure area and S_T is the area of the fusion plane.

For electrofusion tapping tees, the same principle is followed. However, the fitting will not be disturbed when the pipe is cut in half longitudinally. Thus, the entire fusion zone of the fitting is tested. Figure 2-5 illustrates an example of the principle of the testing apparatus for electrofusion tapping tees; where d_p is the distance between each crushing device.

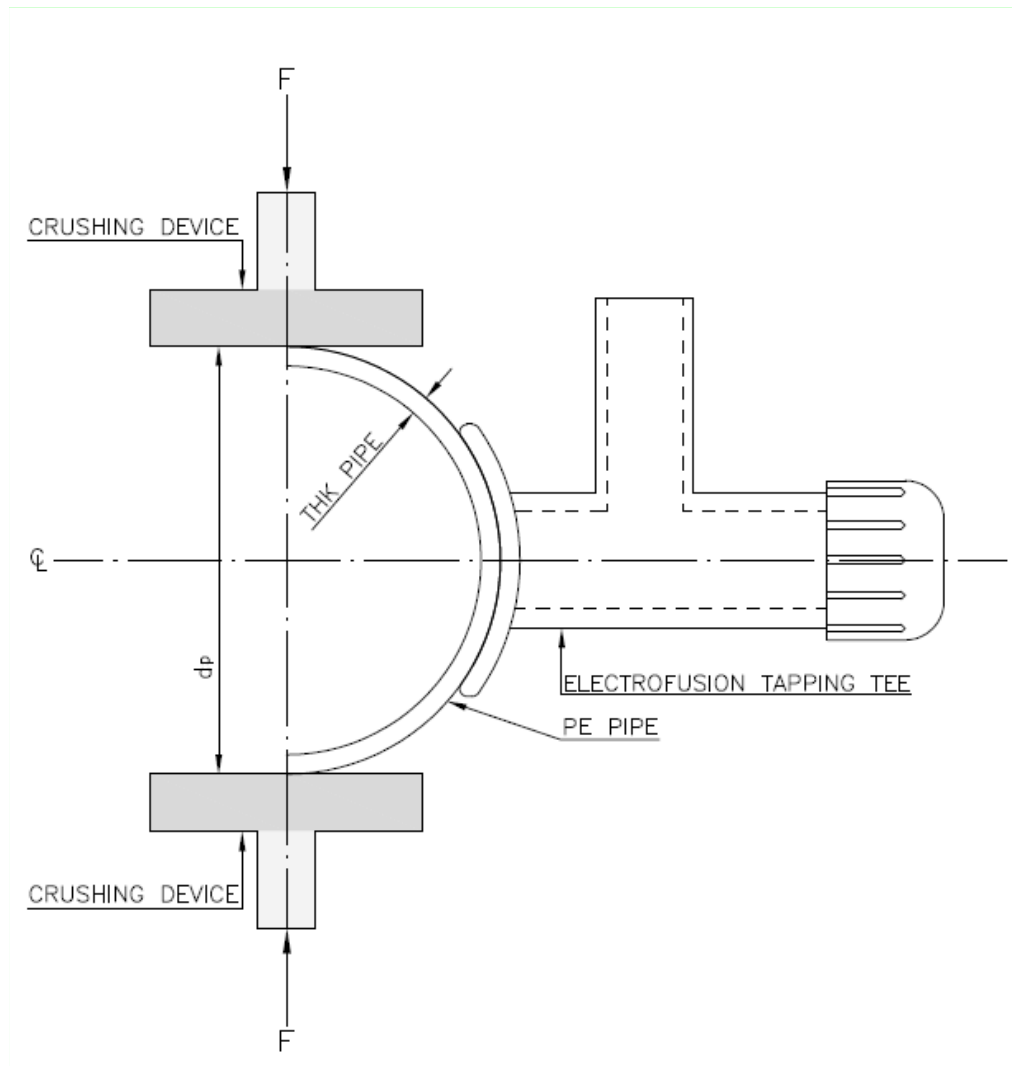


Figure 2-5 Indicative sketch of crushing decohesion test (tapping tees) – example methodology

As can be seen in Figure 2-5, as d_p decreases during the crush test, the forces present should induce failure about the jointing interface by producing a crack that propagates as the crush test is performed.

Even though the percentage of decohesion is estimated, the test arguably holds no bearing on the long term performance of the joint. No strength characteristics (i.e. fracture toughness) are calculated. Therefore this test may be seen as a qualitative procedure. However, the test holds advantages in that it can quickly assess the quality of a weld – more importantly easily identifying poor welds.

2.4.2. Tolerance of electrofusion welds to contamination

WIS 4-32-08 [14] – *Appendix A: Method of assessing tolerance of electrofusion welds to contamination – short term burst test*, highlights a test procedure for assessing the resistance of electrofusion joints to contamination. The contamination used is fine china talc with particle size of $0.63\ \mu\text{m}$ – $63\mu\text{m}$; which according to research by Marshall *et al.* [24] has the worst effect on the fracture toughness of electrofusion joints in comparison to particle sizes greater than the talc. This is explained more detail in Section 2.5.

For this test, the pipe is scraped and cleaned prior to the application of the fine china talc. The electrofusion fitting is assembled and welded; end caps are fitted to the pipe and the joint is then attached to hydraulic rig capable of increasing the internal pressure at a constant rate of 5 bar/min (8.33 KPa/s) until failure or to at least 2.5 x nominal pressure (PN). A cross-sectional schematic of the test can be found in Figure 2-6.

The amount of pipe used in the test assembly is restricted to less than one pipe diameter exposed between the end of the fitting and the testing end caps. This inevitably reduces hoop stress effects in the pipe and high forces are present on the end constraints. The fitting fails when a critical shear stress acting on the joint [interface] is reached [24].

According to WIS 4-32-08 [14] for pipe sizes less than 180 mm in diameter, a short term burst pressure in excess of 40 bar (4 MPa) is required to ensure that long term operation at 16 bar (1.6 MPa) will be secure. For electrofusion tapping tee assemblies, a pressure of at least 18 bar (1.8 MPa) must be attained.

An assembly that meets the requirements of this test does show that it has some resistance to contamination - thus passing the test. However, if best practice principles are not followed on site the joint *may* still fail in service even though the joint has passed this test during the manufacturing approval stage (type testing).

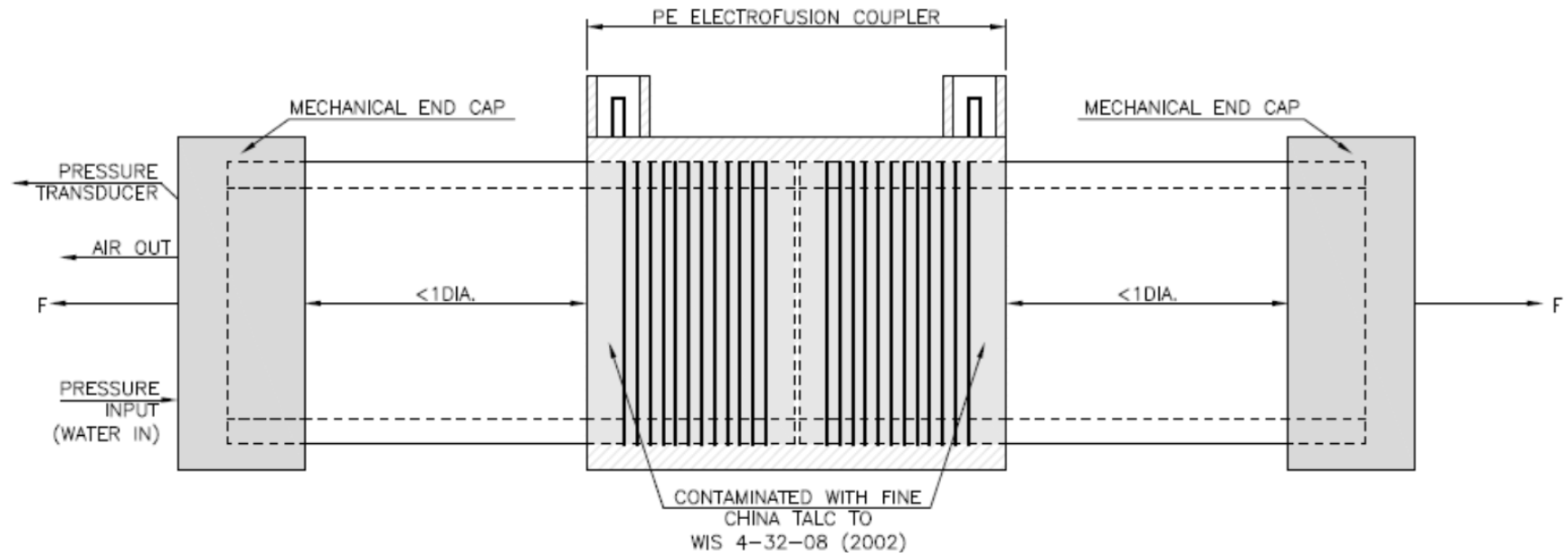


Figure 2-6 Cross-section schematic of short term burst test

The WIS highlights a methodology that offers consistent results with regards to the application of talc onto the pipe prior to assembly of the fitting. The standard illustrates this apparatus which uses a 31 g/m² textile mesh screen with 34 µm threads and 53 µm apertures, held with a tensile force of 140 kN/m². However, with regards to assemblies that have a limited area to be contaminated, for example tapping tees, it is acceptable practice to use a brush to apply the contaminant [61].

To exercise good experimental procedures, the application of the talc by apparatus capable of producing a consistent result would prove beneficial. However, regardless of the consistency of the size and distribution of talc on the pipe surface, there is no guarantee that the contaminated surface remains undisturbed when the coupler is inserted onto the pipe (or vice versa). It is interesting to note therefore that regardless of the talc application method [apparatus or brush], the short term burst test may be seen as subjective for this reason. No research was found by the author comparing the particle distribution of the two talc application methods despite both application methods being mentioned by UKWIR [53, 61]. However, for reasons mentioned previously regarding consistency, the need for a device to apply the contaminant would reduce preparation variations across an industry.

An experiment was conducted by the author to compare the application of contamination using a brush versus the apparatus method that is specified in WIS 4-32-08 [14], specifically observing the particle distribution for each method. The outcomes of this experiment are highlighted in Appendix A.

2.5. Understanding contamination

A contaminant is:

“Any physical, chemical, biological or radiological substance or matter that has an adverse effect on air, water, soil etc.”

New Dictionary of Civil Engineering [62]

In this section contamination is referred to the context of its effects on the mechanical performance of electrofusion assets. As the quotation above suggests, in the correct context, a contaminant could quite literally be anything! Electrofusion welding is usually accomplished in trench-like conditions that may be far from ideal; therefore any contaminants are likely to be those found in on site conditions such as dust, soil and sand.

Scholten [63] illustrates different contaminants including silicones, silicates (sand, clay) and calcium carbonate (cement dust) in observations on several field joints that had previously failed the peel decohesion test specified in ISO 13954 [64]. The chemical information was extracted using one of three techniques which included Scanning Electron Microscopy (SEM). It was believed that the finer dust-like particles may have been attracted to the pipe via an electrostatic charge created as a result of scraping the pipe using a mechanical scraper to remove the anti-oxidised layer.

A contaminant will vary in particle size which is an important factor with regards to adhesion during the electrofusion process. With regards to electrofusion jointing, both Cosgrove [19] and Marshall *et al.* [24] express that for larger foreign particles [at the welding interface], the melt is able to flow around the particles to create some bond between pipe and fitting. However, this is likely to lead to crack propagation about the welding interface which may affect the long term performance of the joint. Nishimura [65] finds in the presence of sand contamination, electrofusion joints decrease in ductility and peel load with the increase in the degree of sand (weight/area) at the welding interface. Again, peel tests on electrofusion coupons were used in the research.

For finer dust particulates, there is an even distribution across the weld interface; reducing the pipe-to-fitting contact [24], viz. less bonding and reduced strength. A fine particulate contamination may promote a brittle failure along the welding interface [19]. Troughton *et al.* [66] also experienced brittle failure about the welding interface for talc contaminated electrofusion joints subject to the peel decohesion test of ISO 13954 [64].

Research conducted on the performance of contaminated electrofusion joints using destructive methods of assessment, led to the development of the ‘tolerance of electrofusion welds to contamination’ test previously specified in Section 2.4.2.

2.6. Conclusions

This chapter has illustrated that there is a wide range of research on the fatigue response of PE pipe. Some of the research has influenced the creation of the IGN for the water industry. Interestingly, in comparison to the volume of research conducted on the fatigue response of PE pipe; very little research has been conducted on electrofusion joints with regards to fatigue.

This chapter has illustrated that contamination can have a negative influence on the mechanical performance of electrofusion joints – causing brittle failure at the welding interface.

Contamination was also highlighted in Chapter 1 as a cause of premature failures in electrofusion assets. Destructive testing, specifically the resistance to contamination – short term burst test, explained in this chapter has shown that standards exist to ensure that electrofusion products hold a degree of resistance to contamination and are designed suitably for use in the industry. However, short term tests such as these can prove difficult in relating to the long term performance of an asset.

Research has shown that PE pipe has good short term response to pulses in pressure – showing an increase in strength. However, the effect that variations in pressure can have on the long term performance of electrofusion assets that may hold defects from installation is yet to be addressed.

Chapter 1 also highlighted the importance of electrofusion tapping tees within the distribution network – linking distribution mains to the end user (customer). To the author's knowledge, no research has been conducted on the fatigue response of electrofusion tapping tees. Furthermore, it is in the remit of this project to explore the effects that contamination has on the performance of electrofusion tapping tees when they are subject to dynamic loading.

Chapter 3

Fatigue performance of contaminated EF tapping tees

It was important to make a decision as to what type of electrofusion fitting would be the subject of the testing programme. The majority of fatigue research highlighted in Chapter 2 was focussed on PE pipe with little research on electrofusion couplers in comparison. Couplers are undoubtedly a fundamental part of the distribution system as this is the electrofusion method of joining two pipes together. In comparison, electrofusion tapping tees have no research conducted on them with regards to their fatigue response. If a PE distribution main were to be laid in an area with the intention of providing water to domestic users; a tapping tee would usually be welded to the pipe for each domestic user. Therefore, the potential for long term problems as a consequence of poor installation is huge. With regards to experimental testing, the advantage of selecting tapping tees is that there is a smaller fusion area in comparison to couplers which may be easier to analyse with regards to post-failure analyses.

3.1. Experimental procedure

The aim of the testing programme was to test destructively and analyse the failure mechanisms associated with contaminated electrofusion tapping tees when subject to dynamic loading. Two separate tests had to be developed and furthermore a rig needed to be designed, built and validated to perform these tests.

The design criterion for the rig needed to encompass the following tests: (i) a short term burst test and (ii) a dynamic load (fatigue) test.

3.1.1. Short term burst test

In order to continue with the dynamic load (fatigue) testing programme, a benchmark value needed to be achieved for the maximum failure pressure of contaminated electrofusion tapping tees. A short term burst test could achieve this whereby repetition of the experiment would establish an average failure pressure for the fitting (i.e. $P_{MAT,MAX}$). Furthermore, the average

failure pressure would be used as a starting value for calculating the pressure ranges in the dynamic test.

The tolerance of electrofusion fittings to contamination, explained in Section 2.4.2, highlights how electrofusion fittings need to have a degree of resistance to contamination in order to be satisfactory for the UK water industry. This test best suited the rig design criterion and furthermore, the use of an industry standard test as a starting point can add uniformity to the research.

3.1.2. Dynamic load (fatigue) test

Once an average failure pressure, $P_{MAT,MAX}$, is achieved from the short term burst test, the dynamic load testing variables can be calculated. For clarity, specimens would still have to be created to the identical procedure as in the aforementioned short term burst test.

There are two main variables with regards to the parameters of the dynamic load experiment: the mean pressure (P_{MEAN}) and the pressure range (P_{RANGE}). Both of these will be explored in this research and shall follow a trapezoidal loading pattern.

In brief, contaminated joints will be created as if to be tested in the short term burst test specified in WIS 4-32-08 [14] and will be pressurised cyclically until failure. The number of cycles to failure will be recorded and plotted in the form of a typical fatigue-life curve, the S-N curve. However, due to the irregular geometry of the electrofusion tapping tee, the stress will not be calculated. Therefore results will be expressed graphically as pressure (range or mean - depending on test variable) versus number of cycles to failure.

3.2. Experimental rig design

In order to achieve the testing goals, careful planning, research and design needed to be done to reduce the number of variables and ensure that the testing objectives would be reached in the timeframe given.

3.2.1. Preparing the test specimens

All the pipes and fittings used in this research were created to the European specification series EN 12201 [55] and were from a single UK manufacturer. The PE pipe was 110 mm diameter pipe of grade PE100 with SDR 17. The pipe product used in the experiment had a protective

‘skin’ that covers the outer surface of the pipe of the pipe. During the manufacture of the pipe, a secondary layer of polymer is extruded to surround the already extruded PE pipe. The skin was made from polypropylene and the pipe manufacturing method for this particular product is known as co-extrusion. It is important to note that the skin and pipe are not the same material; the skin is simply there as a protective layer mainly for installation purposes. The skin was removed from the pipe locally about the required fitting area as recommended by the manufacturer using a specially designed cutting tool. This revealed a smooth surface for jointing, of which no further preparation (i.e. scraping) was required. It is important to note that once the skin was removed, jointing took place immediately. The average density of the PE pipes was 950.1 kg/m^3 . This information was provided by the manufacturer on request.

The tapping tees used were injection moulded PE100 grade fittings; the same type of product was used consistently through the test programme and all tapping tees were supplied off-the-shelf. The product used required the use of a top-loading G-clamp and were welded to the procedure highlighted in WIS 4-32-08 [14]. For the particular electrofusion tapping tee product used in the experiment, a clamping (compressive) force of between 1.0 - 1.5 kN needed to be maintained before and during the heating and cooling cycles of the weld. This was achieved using an industry standard top-loading G-clamp (see Chapter 1 - Figure 1-10). Furthermore, the clamping apparatus was checked in-house every 3 months using a calibrated 5 kN load cell. The specimens were created in a laboratory environment with an ambient temperature of $21 (\pm 1.5) ^\circ\text{C}$ and once welded, were conditioned at ambient temperature for a minimum of 24 hours before testing.

All specimens were created by the author using industry standard welding equipment and tooling. The choice of equipment and tooling used was selected with the aid of a water industry contractor to try and replicate on-site workmanship through the implementation of identical tooling products. A list of equipment used can be found in Appendix B.

According to the short term burst test highlighted in WIS 4-32-08 [14], tapping tees should fail at pressures above 18 bar [1.8 MPa] ($1.5 \times \text{PN}$). It is stated that the tapping tee is welded onto a pipe as if it were to be back-pressurised⁴. The pressure is then increased via the service pipe outlet at a constant rate of 5 bar/minute (8.33 KPa/s) until failure occurs. The same methodology was adapted for this experiment; however, instead of increasing the pressure from the service pipe outlet, the pressure was increased from the stem of the tapping tee (see Figure 3-1).

⁴ The purpose of the back-pressurised test is to assess the fusion weld prior to the pipe being tapped through to the host pipe. Furthermore, if the joint fails, i.e. leaks, the operative knows not to use the fitting.

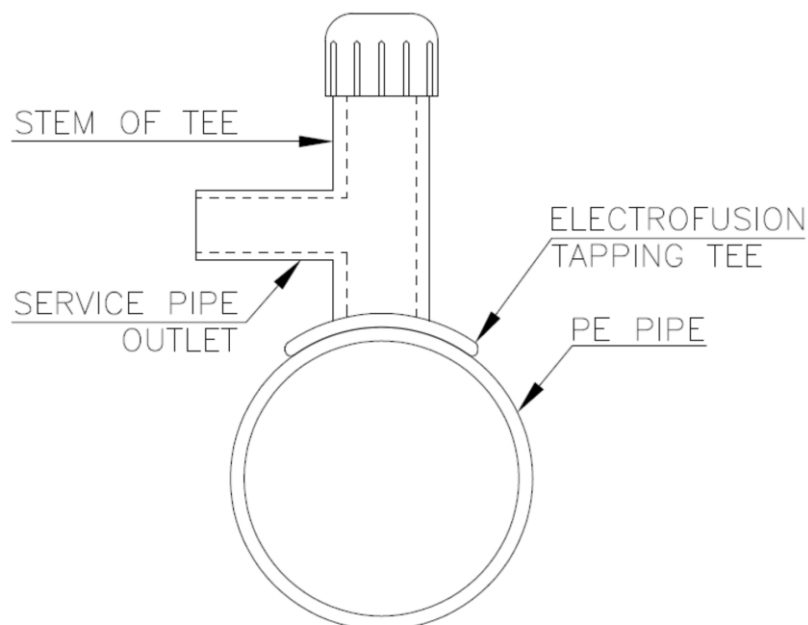


Figure 3-1 Diagram showing stem and service pipe outlet for an electrofusion tapping tee

Due to the design of the particular tapping tee, the service pipe and the mains pipe are fused simultaneously. Therefore, for all test specimens, a length of approximately 125 mm of 25 mm diameter PE80 pipe with SDR 11 was welded at the same time as the main fusion to the host (PE100) pipe. Furthermore, a 25 mm diameter electrofusion end cap was welded to the exposed 25 mm diameter pipe. Later, a mechanical end cap was used as a cheaper alternative as it could be reused (see Figure 1-2).

All equipment was checked before use for cleanliness and damage. The electrofusion control box was calibrated every 6 months by the manufacturer and showed no problems or variation throughout the duration of the project.

3.2.2. Controlling contamination

Defining contamination is important with regards to being able to reproduce contaminated specimens consistently. The most important factors are the particle size and distribution of the particulate.

As mentioned previously in Section 2.4.2, WIS 4-32-08 [14] specifies a fine china talc to be used with a particle size between 0.63 – 6.3 μm . A fine china talc was provided by a local manufacturer of PE pipe and fittings, who use this talc themselves to implement the tolerance to contamination test.

To ensure that the contaminant was applied in a consistent manner and according to the standard, an experiment took place to ensure the particle size and distribution was to specification. A thorough methodology of the experiment can be found in Appendix A. This experiment concluded that the fine china talc would be adequately applied by a soft bristled paint brush to achieve the required distribution of the specification. However, the limitation of the brush application was that the same operative applied the contaminant for the experiment (in this case the author). Furthermore, all joints in this project were created by the author in the same laboratory using the same equipment and tooling.

3.2.3. Designing the experimental hydraulic rig

To obtain results for the experimental goals discussed in Section 3.1, a rig would need to be built. The initial design ideas for an experimental rig aimed to utilise water as the desired testing medium as this would be consistent with the short term burst test previously mentioned in section 3.1.1. It would therefore be logical to use water as the host medium for the dynamic test to be consistent with the short term burst test. To achieve this, a hydraulic piston was designed and built to be retrofitted to an existing four-post servo-hydraulic fatigue testing machine manufactured by ESH. The machine usually houses small specimen material tests but, through careful planning and detailed design, the machine hosted a hydraulic piston to perform the dynamic tests in this project.

A schematic showing the set-up of the rig can be found in Figure 3-2.

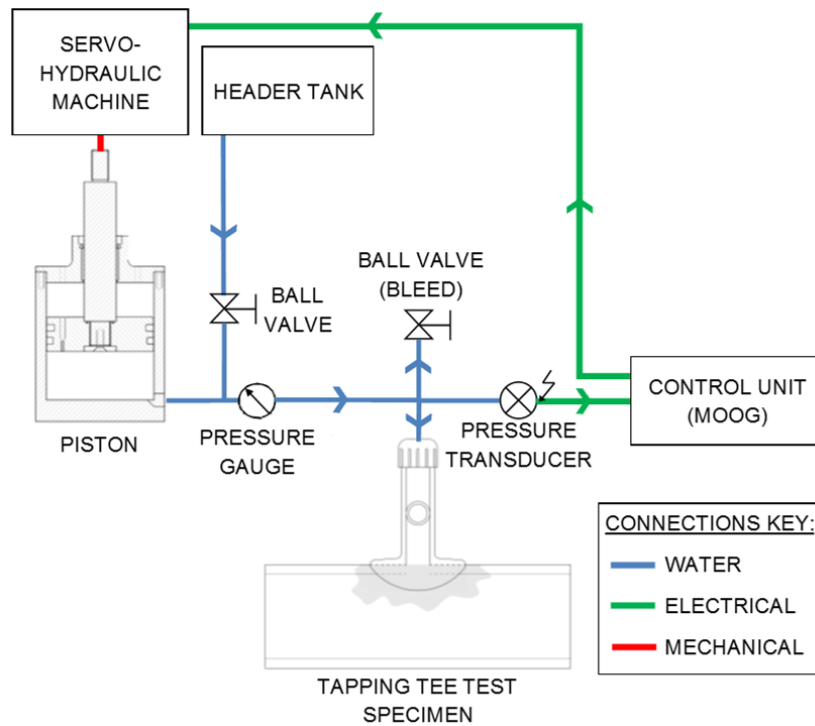


Figure 3-2 Schematic showing all components

For the initial design of the hydraulic piston, research into the short term burst test was conducted in order to gauge the maximum failure pressures expected. Forward planning with regards to future testing and development was considered to avoid under-designing the rig. UKWIR [61] found failure pressures of electrofusion joints (couplers) of around 65 bar (6.5 MPa) in the short term burst test. Therefore a maximum operating pressure of 80 bar (8.0 MPa) was considered for the purpose of the design.

Assumptions were made to ease the design of the piston:

- i) There would be no flow through the system as the movement of the piston would increase/decrease the pressure, and;
- ii) No air would be present as this will be bled from a high point in the system.

By using the maximum design pressure in combination with an assumption that the specimen would increase in volume by only 1%, a maximum stroke length of the piston rod could be calculated. This in turn gave the required depth of the cylinder that housed the piston head.

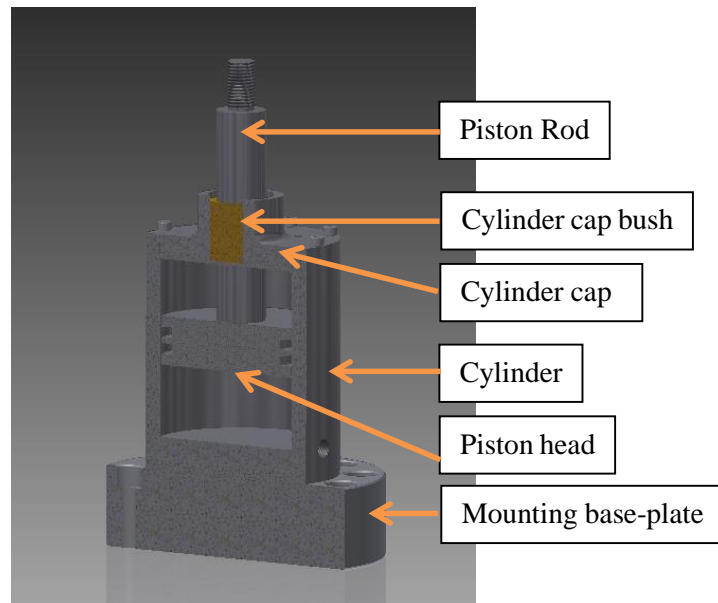
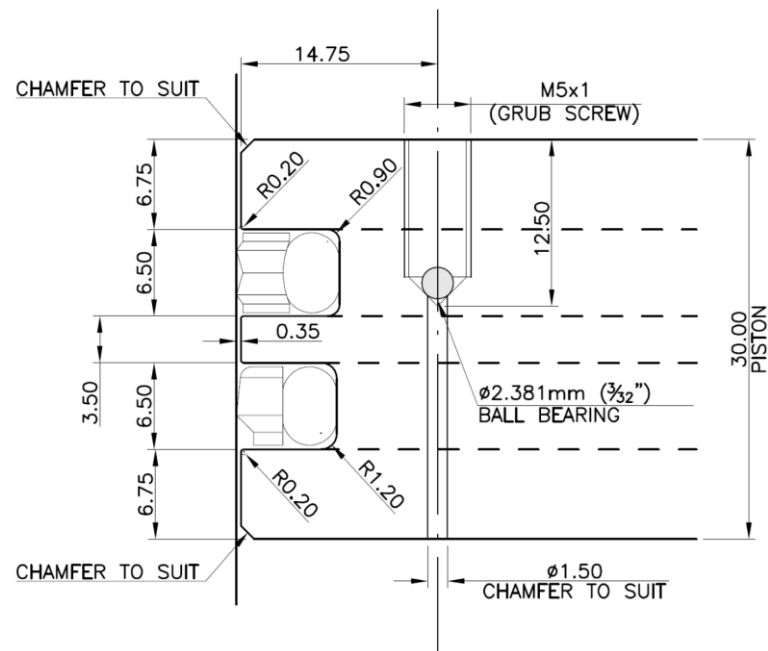


Figure 3-3 Cross-section of hydraulic piston assembly

Fatigue tests can be long in duration therefore all aspects of the rig needed to be durable in order to mitigate wear and tear and ensure the results were consistent. Specially engineered piston seals were used to ensure that the piston would remain water tight in long duration fatigue tests (see Figure 3-4). These seals governed the design of the piston head and influenced the surface finish of the cylinder's bore (sliding surface).



*Figure 3-4 Cross section of piston head showing seal profiles and air bleed
(Note: Drawing not to scale - All dimensions in 'mm' unless stated otherwise)*

A full set of design drawings can be found in Appendix C.

It is important to note that the initial piston was created using mild steel. The piston began to corrode in a matter of days. Furthermore, the bore of the piston was ‘turned’ with regards to the method in which it was machined. The finish was too ‘rough’ and caused a small amount of constant leakage when the rig was subject to increases in pressure. A second piston was machined out of stainless steel and the bore was ‘ground’ to a near mirror finish (a required tolerance $\leq 2.5 \mu\text{m}$). This ensured that the piston seals performed to their full potential – providing a rust and leak-free system.

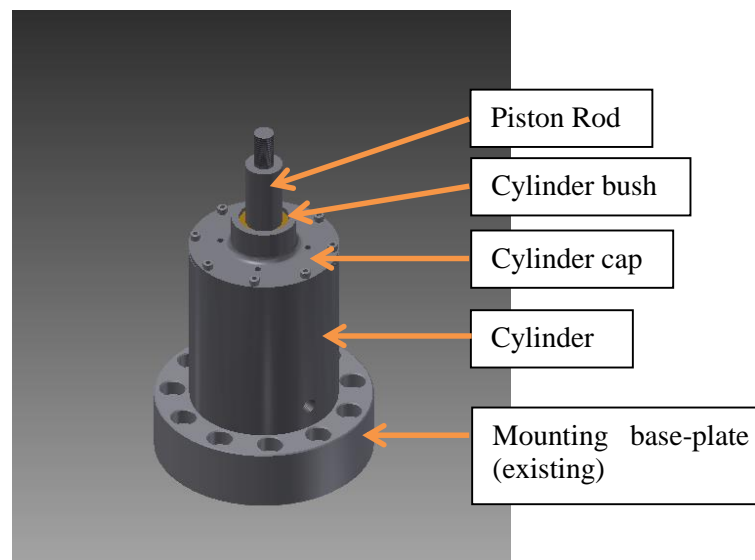


Figure 3-5 3D representation of hydraulic piston

3.2.4. Plumbing the rig

Once the testing specimens were created and the hydraulic piston was secured to the servo-hydraulic testing machine, the specimens needed to be plumbed to the piston. It is important to note that air should not be present in the system as both a safety mechanism and to ensure consistent results. A hole was drilled and tapped through the piston head and a grub screw fitted so that the cylinder could be bled of air (see Figure 3-4. Note: a full set of design drawings can be found in Appendix C). As the piston was the high point of the test i.e. the specimens to be tested would be below the piston. However, during fatigue tests, it was observed that water would seep between the valleys of the threads of the bleed hole. This was mitigated by dropping a ball bearing that was large enough to sit on the smaller orifice of the bleed hole; the grub screw would bear onto the ball bearing, closing the smaller orifice to ensuring it was water tight. This avoided the use of ordinary plumbing (PTFE) tape being

applied around the grub screw before each test as this would make the threads awkward to clean after every test.

Specimens were contained in a large plastic container with a transparent lid to contain the water once the specimen had failed. Furthermore, the specimens were not tested in a temperature controlled/monitored water bath as this was not a requirement of the short term burst test in WIS 4-32-08 [14]. All tests were conducted at ambient temperature in the large container but temperature within the test environment was monitored and recorded manually to ensure consistency; ranging between $21 (\pm 1.5) ^\circ\text{C}$.

A hydraulic hose from the piston to a four-way cross connection was used to connect the test specimen, pressure transducer and bleed valve (see Figure 3-6). By opening the bleed on the piston head and all the ball valves, gravity-fed water can fill the rig. Closing the valves allowed the bleeding of air from the piston head. The grub screw was then installed and tightened to seal the system.

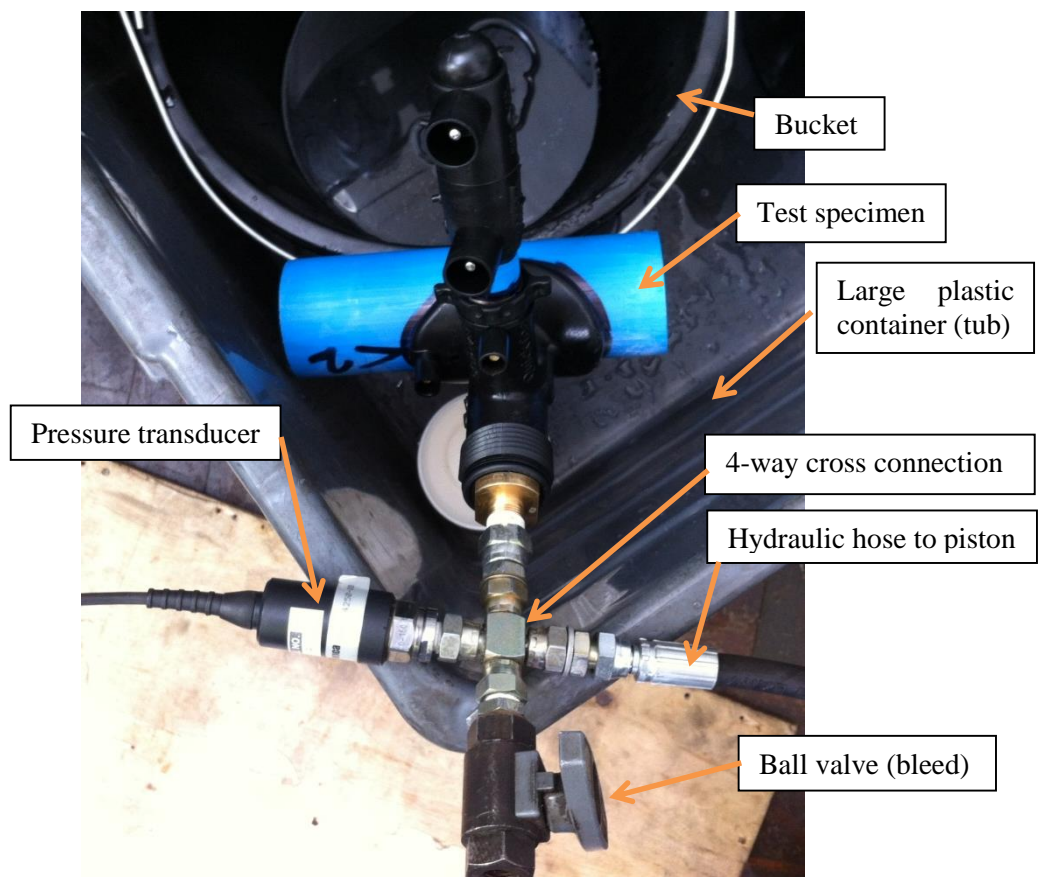


Figure 3-6 Test specimen general arrangement

A header tank attached to a ball valve and tee was situated at a high point above the piston and was used to fill the rig with water. Ordinary tap water was used but was left standing for over 12 hours to aid the removal of air.

PTFE tape was used prolifically on threaded connections to remove the possibility of leakage. Furthermore, gasket sealant was used on a custom-made washer that bears on the threaded connection between the piston rod and piston head. This, as well as the use of PTFE tape on the piston rod thread, prevented any leakage through the aforementioned threaded connections.

Some parts of the rig were subject to wear and tear such as a ball valve that needed to be replaced as leakage was observed during a fatigue test. Some washers and male-to-male connections were also replaced if a visual inspection showed any sign of damage, wear or corrosion.

3.2.5. Controlling the rig

A test controller manufactured by MOOG (the ‘MOOG Portable Test Controller’) was connected to the servo-hydraulic testing machine. A pressure transducer was attached to the control unit and a calibration table was created manually by connecting a hand-pump to the transducer. Two pressure gauges were used in line with the hand-pump to confirm the absolute values for the calibration table. Once created, the table was further checked for linearity.

It is important to note that the control unit is used primarily to control the main actuator (load cell) of the testing machine. However, for the purpose of this testing programme both software and hardware alterations of the control unit needed to take place in order for the pressure transducer to be the governing feedback source of the proposed testing regime.

Once the system was filled with water and bled of air, the piston was able to drop in an attempt to compress the water thus increasing the pressure. It was soon discovered that the closed-loop system was extremely sensitive to even the smallest amounts of air present in the system. The MOOG controller operated on a proportional, integral and differential (PID) control system which was tuned manually in order to gain control of the system. Although the system was extremely sensitive, the system was reliable with regards to achieving target pressures (amplitude matching). Minor tuning of the PID values were made manually on occasions to ensure the stability and accuracy of the long duration fatigue test. Furthermore, several specimens were ‘lost’ due to the initial instability of the control unit. These tests were not included in any of the results or analysis of data in the project but are mentioned here to observe the initial problems with rig design. It was later thought that the instability of the rig may have been caused by the specimen beginning to fail or pockets of air that were trapped in the system.

In hindsight, with regards to the rig design, creating a smaller piston (i.e. decreasing the bore size) may have mitigated the aforementioned ‘teething problems’ of the system. As water is near-incompressible, once a small pressure increase is observed due to the lowering of the piston head, further minor displacements would see greater increases in pressure; as:

$$Pressure = \frac{Force}{Area} \quad (3-1)$$

Therefore, reducing the bore size (thus cross-sectional area) would increase the stroke length therefore increasing the response potential for the control-loop. Furthermore, the dynamic nature of servo-hydraulic testing machines allow for high frequency fatigue tests to be conducted; in hindsight, the piston rig may have been better suited on an electric motor driven testing machine as the proposed frequencies for this testing programme are very slow in contrast to high frequency fatigue tests.

3.3. Fatigue test variables

As mentioned in Section 3.1.2, the fatigue test followed a trapezoidal loading regime. The following section will explain how the variables were defined prior to the implementation of the testing programme.

3.3.1. Fixed mean pressure

With regards to the fixed mean approach, the varying parameter was the pressure range (P_{RANGE}). In order to establish the different pressure ranges, two main parameters were established. The first is the ultimate (failure) pressure of the material ($P_{MAT,MAX}$) the second is the mean pressure (P_{MEAN}).

$P_{MAT,MAX}$ was established from the short term burst test explained in Section 3.1.1. WIS 4-32-08 [14] recommends a ramp rate of 5 bar/min (8.33 KPa/s) but this was deemed too slow for reasonable test durations in the fatigue programme. Therefore, the ramp rate was increased from 5 bar/min (8.33 KPa/s) to 25 bar/min (41.67 KPa/s). The short term burst test was carried out four times per ramp rate. The results from this are shown in Table 3-1. The results show that there was negligible difference in the average failure pressures of approximately 25 bar [2.5 MPa] ($= P_{MAT,MAX}$). In addition to these tests, several identically-made specimens were

tested at a third party test house comparing results with those observed with the experimental rig to benchmark the apparatus.

Test No.	<i>Failure pressure (bar) at 5 bar/min ramp rate</i>	<i>Failure pressure (bar) at 25 bar/min ramp rate</i>	<i>Third party testing at 5 bar/min (bar)</i>
1	24.6	22.3	21.1
2	25.8	26.5	23.4
3	25.7	25.4	-
4	23.2	23.6	-
<i>Average failure pressure (bar)</i>	24.8	24.5	22.3
<i>Median failure pressure (bar)</i>	25.2	24.5	

Table 3-1 Failure pressures at different ramp rates

For this testing regime the mean pressure was taken as half of the maximum pressure of the material; i.e.:

$$P_{MEAN} = \frac{1}{2} \times P_{MAT,MAX} \quad (3-2)$$

A total of six pressure ranges were taken as percentage decrements from 90% – 40% of $P_{MAT,MAX}$. i.e. for; $n \in \{90, 80, \dots, 40\}$:

$$P_{RANGE} = n\% \times P_{MAT,MAX} \quad (3-3)$$

With regards to a trapezoidal loading pattern, there will inevitably be an associated rest time, t_{REST} , at the top and bottom of each cycle. It was decided that the ramp rate, $\frac{\Delta P}{\Delta t}$, of each cycle should be identical to the recommended ramp rate of the WIS (5 bar/min). However, this would have led to prolonged test times. The ramp rate was therefore increased to 25 bar/min (41.67 KPa/s) as the results from Table 3-1 indicates little difference in the average failure pressure with regards to $\frac{\Delta P}{\Delta t}$.

As the fatigue regime would be based on a fixed ramp rate, the rest time was calculated as a proportion ($2/3$) of the total time it would take to ramp to the required pressure from the mean

pressure. The time from which the pressure would start at the mean pressure to the target pressure was noted as: t_{RAMP} . Thus;

$$t_{REST} = \frac{2}{3} \times t_{RAMP} \quad (3-4)$$

It is key to note that this meant that each rest time varied thus influencing the frequency of loading. Once t_{REST} and t_{RAMP} have been specified, the loading frequency (in *Hertz*) was calculated, thus:

$$Frequency = \frac{1}{(2 \times (t_{REST} + 2t_{RAMP}))} \quad (3-5)$$

The testing parameters are summarised in Table 3-2 and are illustrated in Figure 3-7 showing one cycle.

% Failure Pressure	P_{RANGE} (bar)	Maximum Pressure (bar)	Minimum Pressure (bar)	t_{REST} (s)	t_{RAMP} (s)	Frequency (Hz)
90	22.50	23.75	1.250	18.0	27.0	0.00694
80	20.00	22.50	2.500	16.0	24.0	0.00781
70	17.50	21.25	3.750	14.0	21.0	0.00893
60	15.00	20.00	5.000	12.0	18.0	0.01042
50	12.50	18.75	6.250	10.0	15.0	0.01250
40	10.00	17.50	7.500	8.0	12.0	0.01563

Table 3-2 Fixed mean testing parameters

For; $P_{MAT,MAX} = 25 \text{ bar}$, $P_{MEAN} = 12.5 \text{ bar}$, $\frac{\Delta P}{\Delta t} = 25 \text{ bar/min}$

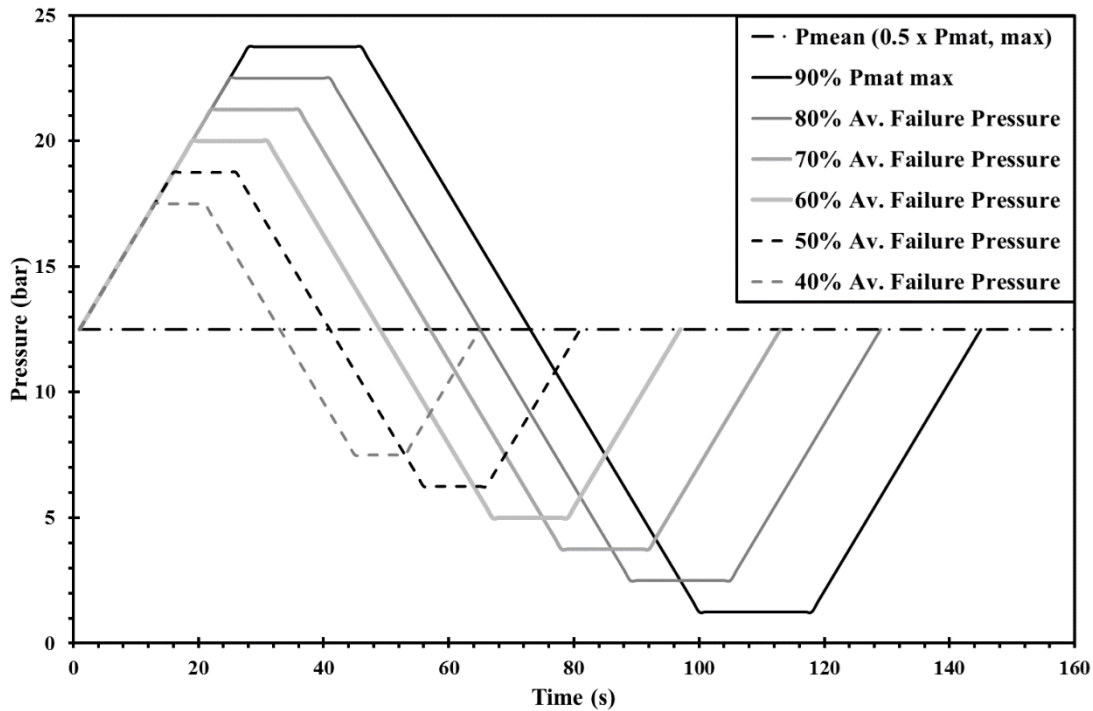


Figure 3-7 Trapezoidal loading patterns for dynamic (fatigue) test showing 1 cycle

For $P_{MAT,MAX} = 25 \text{ bar}$, $P_{MEAN} = 12.5 \text{ bar}$, $\frac{\Delta P}{\Delta t} = 25 \text{ bar/min}$,

$$P_{RANGE} = n\% \times P_{MAT,MAX}$$

To summarise, a fixed ramp rate was chosen to fatigue test tapping tees, subject to a talc contamination, to destruction. The mean pressure was fixed at 12.5 bar (1.25 MPa) and the pressure range varied. The pressure range was defined as a percentage of the maximum failure

pressure of tapping tees under a short term burst test at a 25 bar/min (41.67 KPa/s) ramp rate. Tapping tees were loaded dynamically until failure in each pressure range. The ramp rate (increase/decrease in pressure) of each cycle was fixed to replicate the ramp rate of the short term burst test (at 25 bar/min) and a minimum of 6 tests per pressure range were conducted.

3.3.2. Variable mean pressure (constant amplitude)

If the mean pressure is to be the variable in the fatigue testing regime, a constant P_{RANGE} needs to be decided. For this testing regime, P_{RANGE} was fixed at 15 bar [1.5 MPa] ($= 60\% \times P_{MAT,MAX}$). This was chosen as test times were reasonable with regards to fatigue failure at $P_{RANGE} = 12.5$ bar (1.25 MPa) and therefore if the pressure ranges were to reduce, test times should not increase dramatically thus not affecting the flow of data generation.

For $P_{RANGE} = 15$ bar; $t_{REST} = 12$ seconds and $t_{RAMP} = 18$ seconds (from Table 3-2).

As in the previous test programme, tapping tees were loaded cyclically until failure. A minimum of 8 tests were completed for each variation in mean pressure. The mean pressure was increased by 0.75 bar (0.08 MPa) increments from 9.50 - 15.50 bar (0.95 – 1.55 MPa) mean pressure. Therefore, for $m \in \{9.50, 10.25, \dots, 15.50\}$;

$$P_{MEAN} = m \quad (3-6)$$

As per Equation (3-6), the mean pressures that were tested and their respective maximum and minimum pressures are displayed in Table 3-3 and graphically illustrated by example in Figure 3-8.

<i>Mean Pressure (bar)</i>	<i>Max. Pressure (bar)</i>	<i>Min. Pressure (bar)</i>
15.50	23.00	8.00
14.00	21.50	6.50
13.25	20.75	5.75
12.50	20.00	5.00
11.75	19.25	4.25
11.00	18.50	3.50
10.25	17.75	2.75
9.50	17.00	2.00

Table 3-3 Variable mean testing values

Where; $P_{\text{RANGE}} = 15 \text{ bar}$, $\frac{\Delta P}{\Delta t} = 25 \text{ bar/min}$, Freq. = 0.01042 Hz

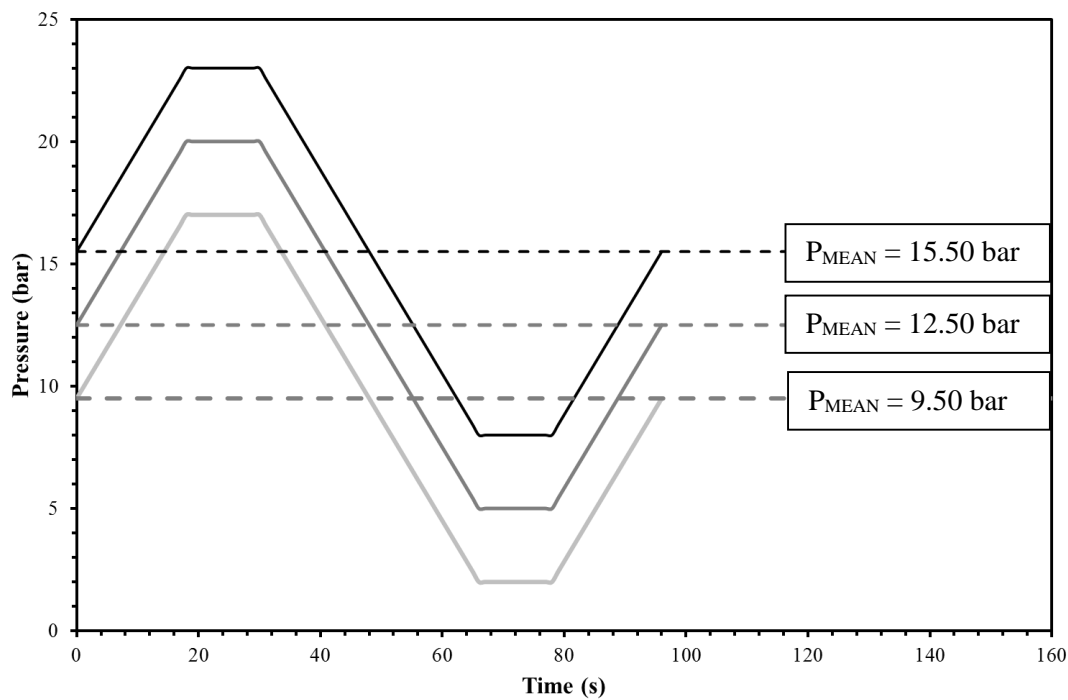


Figure 3-8 Examples of variable mean loading patterns showing 1 cycle

3.4. Concluding remarks

This chapter has illustrated methodologies for testing the fatigue-life of contaminated tapping tees based on the concluding remarks of Chapter 1 and Chapter 2 . The testing regimes are built on the foundation of the short term burst test for contaminated assemblies stated in WIS

4-32-08 [14]. The methodologies used for this project focus on a fixed mean (variable range) and a fixed amplitude (variable mean) with an aim to initially observe the fatigue response of contaminated electrofusion tapping tees (under a fixed mean approach), with a notion to reduce the mean pressure (fixed amplitude approach) to observe the performance at operational pressures that may be expected in water distribution systems; whereby the mean pressure may be representative of the steady-state pressure in the system.

An experimental hydraulic rig was designed, built and retrofitted to an existing servo-hydraulic test machine. The rig was designed to accommodate all the aforementioned testing programmes and acquire the data needed for interpretation of results and quality assurance. The results from the testing programmes are given in Chapter 4

Chapter 4

Results from the fatigue testing programmes

Extensive fatigue testing has taken place to observe the relationships between pressure range and mean pressure with respect to fatigue life. To reiterate, the test specimens were electrofusion tapping tees that were subject to a talc contaminant prior to welding to the parent pipe. Both pipe and fitting were PE100 grade and created by the same UK manufacturer. Without tapping through into the main pipe, the tee specimen was filled with water and subjected to cyclic pressure until it failed. A failure is described as a joint (specimen) not being able to maintain pressure. This was usually when the delamination of the bonding surface was such to create a clear leak path.

Two test regimes were explored: (i) constant mean pressure, variable pressure range and (ii) constant pressure range, variable mean pressure. Both regimes followed a trapezoidal loading pattern with a fixed rate in the increase/decrease in pressure (≈ 25 bar/min [41.67 KPa/s]). The fixed pressure rate was consistent with current industry standards.

In general, the results from both testing regimes are expressed in a form similar to a stress-life (S-N) curve. However, due to the complex geometry of the tapping tee the ‘stress’ was not calculated as there will be varying stress concentrations as the geometry changes throughout the fitting. Therefore, the results are expressed as pressure range vs. number of cycles to failure.

4.1. Fixed mean approach

A number of tests were accomplished when the mean pressure was equal to 12.5 bar (1.25 MPa). Figure 4-1 shows the results for the fatigue test represented as pressure range vs. number of cycles to failure.

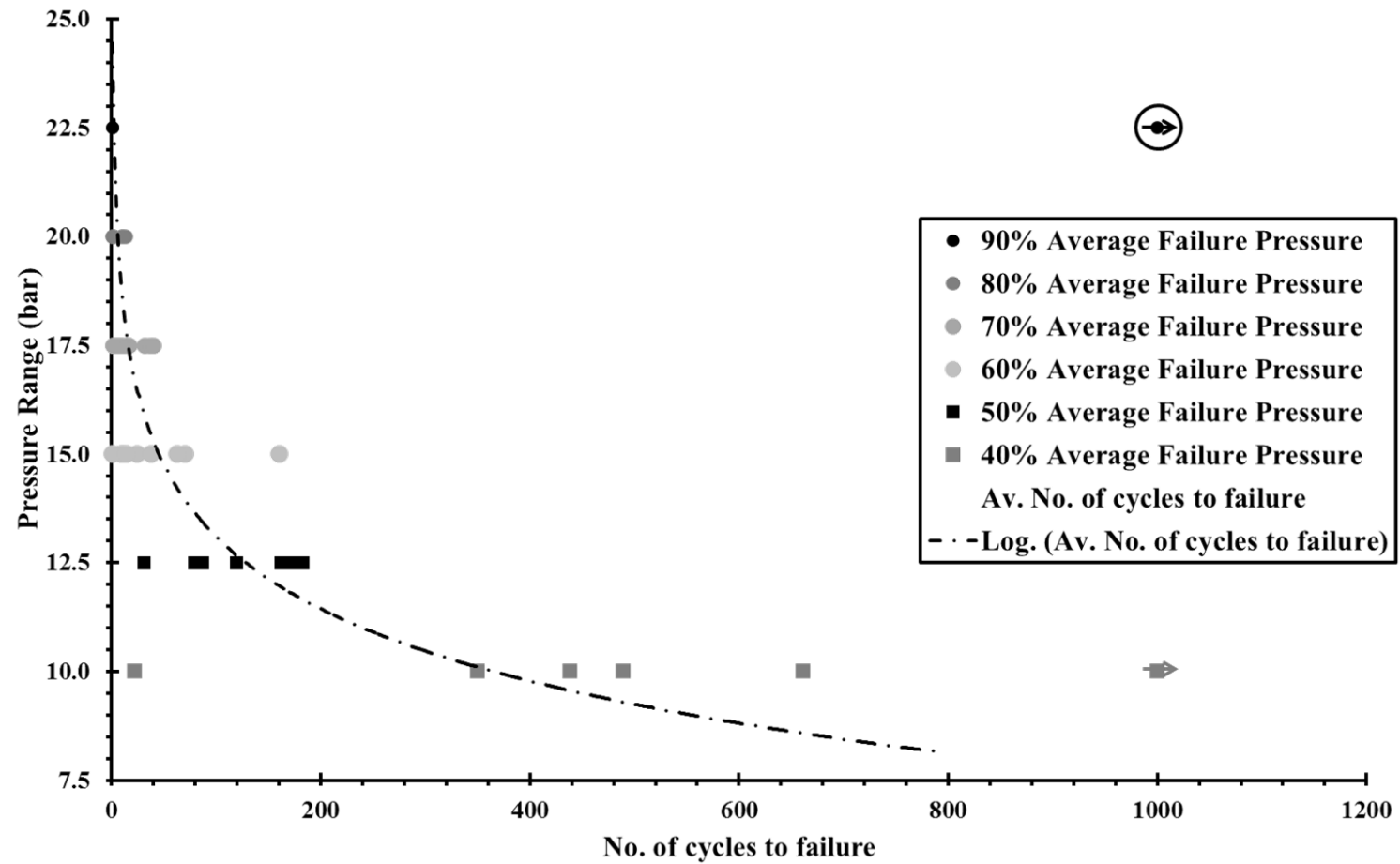


Figure 4-1 Pressure Range vs. Number of cycles to failure for the fixed mean low-cycle fatigue test

where; $P_{MEAN} = 12.5$ bar

It is important to note that the fatigue test was stopped if a specimen did not fail after 1000 cycles therefore this testing programme is classed as low-cycle fatigue [34]. A minimum of 8 tests was conducted for each pressure range with the exception of the 90% $P_{MAT,MAX}$ pressure range where three specimens failed to reach one cycle. The maximum pressure to be expected in this pressure range is 23.75 bar (2.38 MPa) which is 5% from the average maximum pressure of a contaminated tapping tee ($P_{MAT,MAX}$). Considering there is a rest time (t_{REST}) at the top of each cycle, it is considered that the pressure and the respective time sustained at this pressure is beyond the integrity limits of contaminated tapping tee joints.

As a comparison, two tests were conducted within this pressure range (90% $P_{MAT,MAX}$) using two specimens made to best practice principles – i.e. no contamination. This specimen, circled in Figure 4-1, did not fail after 1000 cycles. This shows the detrimental effect that contamination can have on electrofusion tapping tees and proves that joints made to best practice principles do not fail under this testing regime.

It can be observed (in Figure 4-1) that as the pressure range decreases, the distribution of failure time increases. In the 40% $P_{MAT,MAX}$ pressure range, five tests were successful in that they failed within 1000 cycles, however, four tests did not fail (i.e. exceeded 1000 cycles). It can be argued that the fixed mean low-cycle fatigue testing approach is only fit for purpose for pressure ranges greater than 12.5 bar (1.25 MPa); here failure of contaminated joints seems certain for this product according to these results.

Based on the indicative logarithmic line, based on the trend in data, plotted against the mean number of cycles to failure (Figure 4-1), it can be said that if the pressure range were to be dropped further, there is a likelihood that most specimens would successfully reach 1000 cycles without failure. Hence lowering the pressure has no benefit as failure is likely to occur in an unrealistic timescale.

Using the experimental data in Figure 4-1, a regression analysis was performed and the 95% confidence limits obtained. Figure 4-2 indicates the average number of cycles to failure with the 95% confidence limits on pressure range vs. Log number of cycles to failure. The limits show two results that clearly lie well below the lower boundary at 15 and 10 bar (1.5 and 1.0 MPa) pressure range as highlighted in Figure 4-2 (circled).

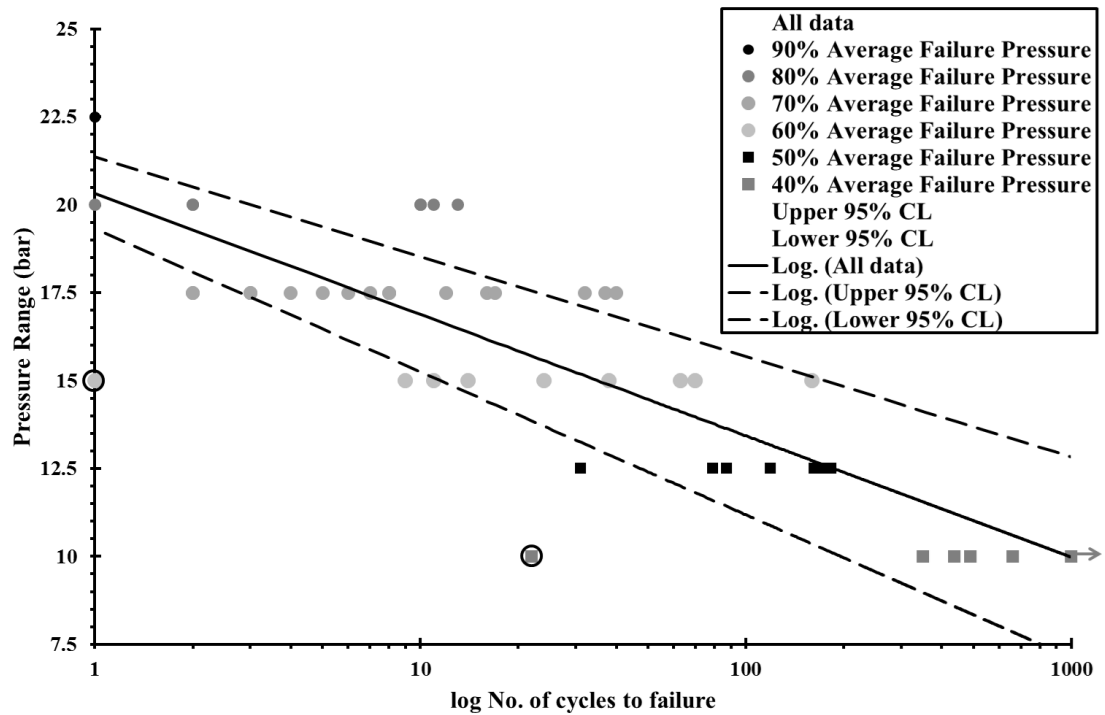


Figure 4-2 Pressure Range vs. Log Number of cycles to failure

The majority of data sits within the upper and lower 95% confidence boundaries. However, it can be seen that the boundaries become wider as the pressure range is reduced. Therefore, the analysis of the data reinforces that the predictability of failure becomes more difficult as the pressure range is decreased.

Figure 4-3 illustrate the same dataset but in the traditional log-log format.

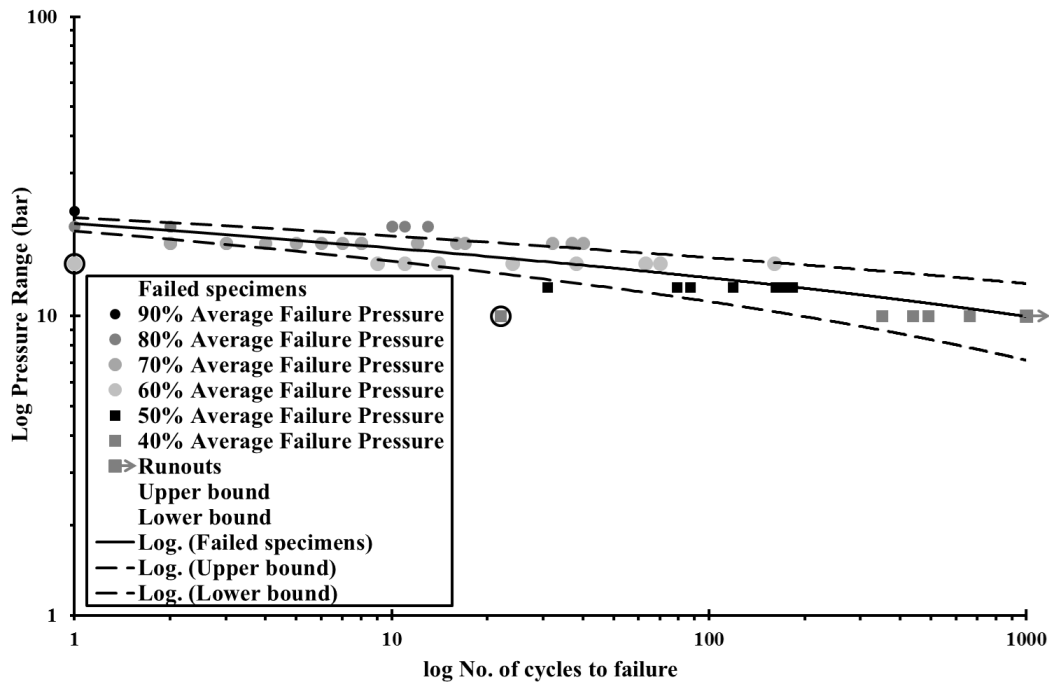


Figure 4-3 Log Pressure Range vs. Log Number of cycles to failure

4.2. Fixed pressure range

After analysis of the results obtained from the fixed mean approach, highlighted in Section 4.1, a secondary test regime was undertaken to observe the impact of the change in mean pressure with respect to fatigue-life.

For the previous fatigue testing programme, a fixed mean pressure of 12.5 bar (1.25 MPa) was used. This value is comparable to the operating pressure of a distribution main and thereby the cycles relate to the increase/decrease in pressure that may be expected in a water distribution network. The mean pressure (12.5 bar [1.25 MPa]) would arguably be too ‘high’ for distribution mains of 110 mm diameter and water suppliers may prefer to operate at much lower pressures. The second testing programme would increase as well as decrease the mean pressure and observe the fatigue-life. The lower mean pressures would be more ‘realistic’ with regards to typical operating pressures that are experienced in water distribution networks; giving the testing programme validity to water network operations.

Figure 4-4 shows the results from the fixed range testing regime.

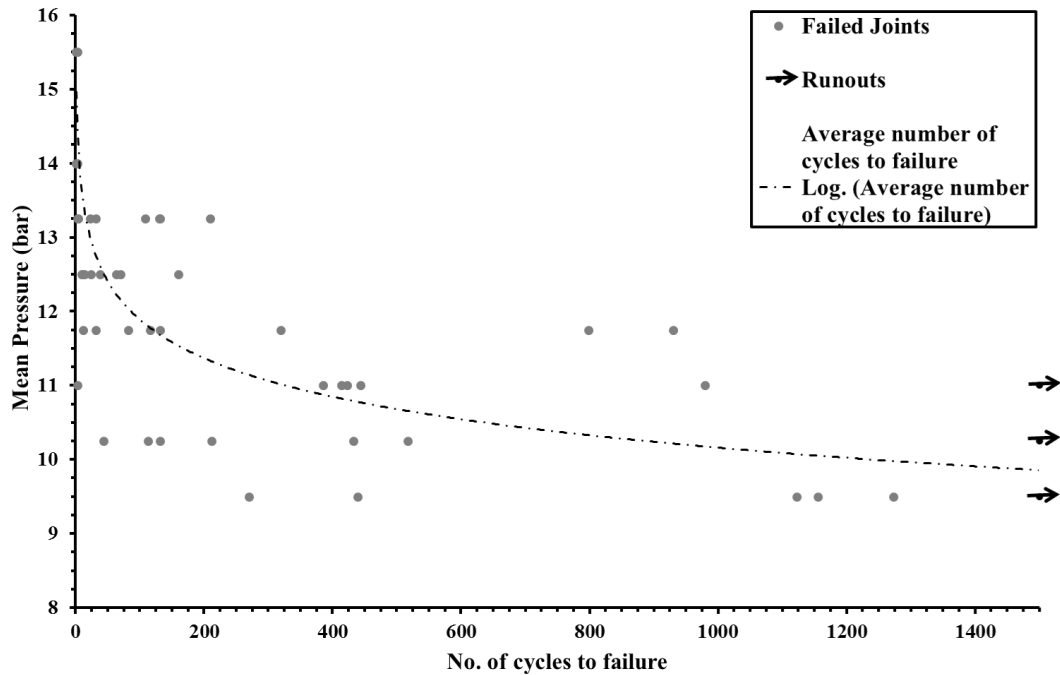


Figure 4-4 Mean pressure Vs. No. of cycles to failure

when $P_{\text{RANGE}} = 15 \text{ bar}$, $\text{Freq.} = 0.01042 \text{ Hz}$

The results depicted in Figure 4-4 shows an increase in ‘scatter’ in comparison to the results obtained in the fixed mean approach in Section 4.1. Dowling [34] explains that scatter can be expected if multiple tests are run at one stress level. However, there is over a factor of 10 difference in results in some cases – specifically when the $P_{\text{MEAN}} = 11.00$, 10.25 and 9.50 bar (1.10 , 1.03 and 0.95 MPa) where there were failures below 300 cycles and run outs that exceeded 1500 cycles without failure.

A total of 8 tests were conducted for each mean pressure with the exception of 14.0 bar (1.4 MPa) and 15.50 bar (1.55 MPa) whereby 6 specimens (3 at each mean pressure) failed to complete a single cycle successfully. The maximum pressures in these cycles were 21.50 bar (2.15 MPa) and 23.00 bar (2.30 MPa) respectively. This is 14% and 8% respectively from the average maximum failure pressure ($P_{\text{MAT,MAX}}$) of a contaminated joint. This, in combination with the associated rest times of the cycle was enough to cause failure of the specimens. Therefore continuing to repeat tests at these mean pressures at this fatigue regime was seen as an unrewarding task.

The logarithmic line in Figure 4-4 is based on the average number of cycles to best fit the failure for each mean pressure. It is interesting to note that failures at the lower mean pressures (10.25 bar and 9.50 bar [1.03 and 0.95 MPa]) sit below the indicative line which may suggest

there is a significant shift in the results which make the line difficult to interpret statistically. For this testing programme, a cut-off value of 1500 cycles was drawn for all specimens. Therefore, like the fixed mean testing regime mentioned in Section 4.1, this testing regime can again be classed as a low-cycle fatigue testing programme. In the three lowest mean pressures tested (11.00, 10.25, 9.50 bar [1.10, 1.03, 0.95 MPa]), there were several joints that did not fail within 1500 cycles. It is important to note that it is neither possible nor accurate to say that these joints would never fail if they continued cycling. Again, a line needed to be drawn to aid the momentum of data generation to achieve a quantity of data worthy for discussion in the project timeframe. Table 4-1 summarises the joints that did not fail with their respective mean pressures.

<i>Mean Pressure (bar)</i>	<i>No. of failed specimens</i>	<i>Average No. of cycles to failure</i>	<i>No. of specimens that DID NOT fail</i>	<i>Cycle count when test stopped</i>
11.00	6	442	1	2500
10.25	6	242	2	2501, 2644
9.50	5	852	3	1765, 2026, 2500

Table 4-1 Summary of specimens that did not fail during fatigue test

The joints that did not fail are extremely significant as they can suggest several things:

- The scatter increases exponentially as the mean pressure is reduced. This was also witnessed in the fixed mean testing regime in Section 4.1.
- There may be a variation in fatigue performance due to different batches of pipe and fittings.

Bowman [49] explains that changing the material used manufacture electrofusion couplers significantly influenced the fatigue response of the joint. The fittings used in this experiment were purchased off-the-shelf and therefore no history of the fitting's manufacture was obtained. This may have influenced the results of the testing programme giving increased scatter. However, the same product was used throughout and the pipe and fittings were of the same grade (PE100) which makes this highly unlikely.

- Possibility of variation in the welding procedure: e.g. providing a variable amount of talc distribution on the pipe prior to welding. This may result in a larger than normal amount of scatter.

This is unlikely as the specimens were created by the same operative using the identical preparation schedule as the previous testing programme.

As with the results obtained for the fixed mean approach in Section 4.1, a regression analysis was performed on the results obtained for the variable mean approach (i.e. from Figure 4-4). The results from the regression analysis can be found in Figure 4-5 which also shows the 95% confidence limits with respect to the average number of cycles to failure.

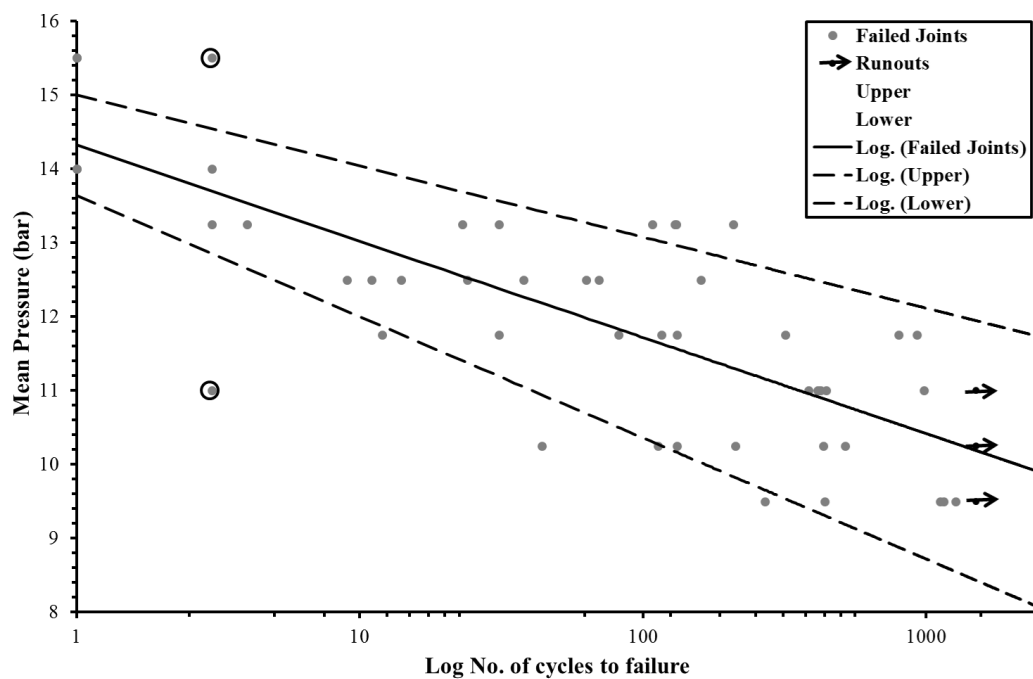


Figure 4-5 Mean pressure Vs. Log No. of cycles to failure

From the analysis in Figure 4-5, it can be said that, like the results from the fixed mean approach, as the mean pressure is reduced, the predictability of failure becomes more difficult; to the extent that some specimens may not fail at lower mean pressures in below 1500 cycles. Again, this is not to say that they will never fail; implying there may be limitations to this testing regime.

Two results have been circled in Figure 4-5 as outliers as they sit well outside the range of the confidence limits. Interestingly (but most likely coincidentally) there were also 2 outlying results in the fixed mean testing regime highlighted in Figure 4-2 of section 4.1. The outlying result at $P_{MEAN} = 15.50$ bar (1.55 MPa) failed after 3 cycles; although this is not far from '1' cycle,

it is far enough away from the confidence limits to be disregarded statistically. As was discussed in the previous section (4.1), it is not clear why some results are outliers from the confidence limits and therefore it is possible that these specimens had significantly less joint strength. However, in fatigue testing there will undoubtedly be a degree of ‘scatter’ in the results but for some mean pressures in this testing regime there is greater than a factor of 10.

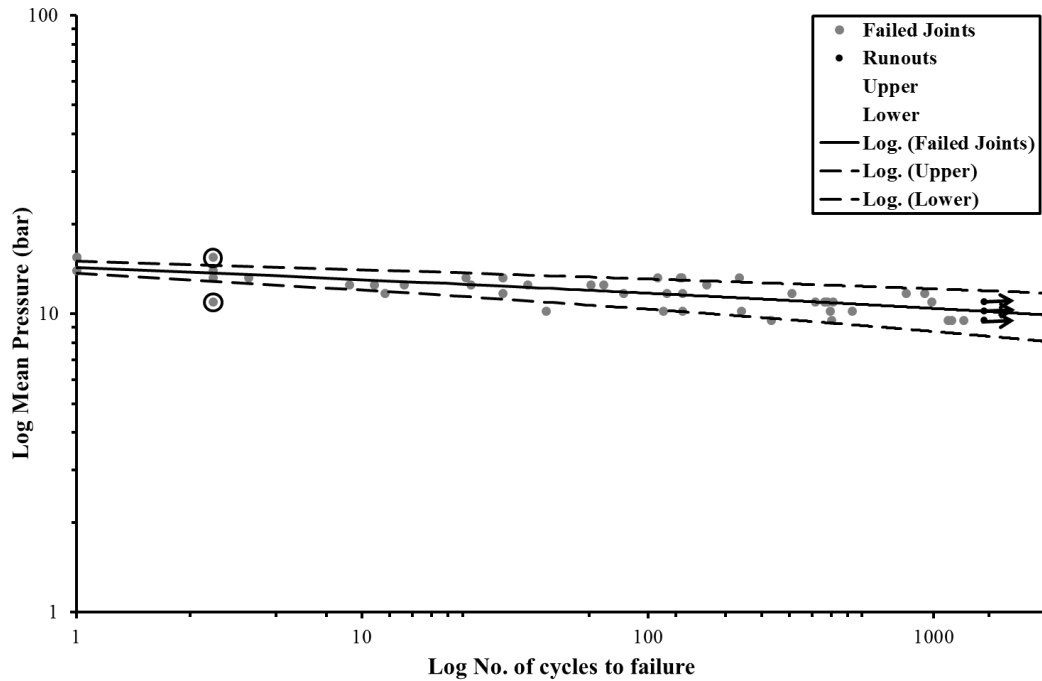


Figure 4-6 Log Mean pressure vs. Log No. of cycles to failure

Figure 4-6 shows the same dataset as Figure 4-5 but in traditional log-log form. The same two results that were circled in Figure 4-5 are also circled here. It can be seen that the result where $P_{MEAN} = 15.50$ bar (1.55 MPa) appears to just fall outside the range of the 95% confidence limit. This appears to be exaggerated in Figure 4-5.

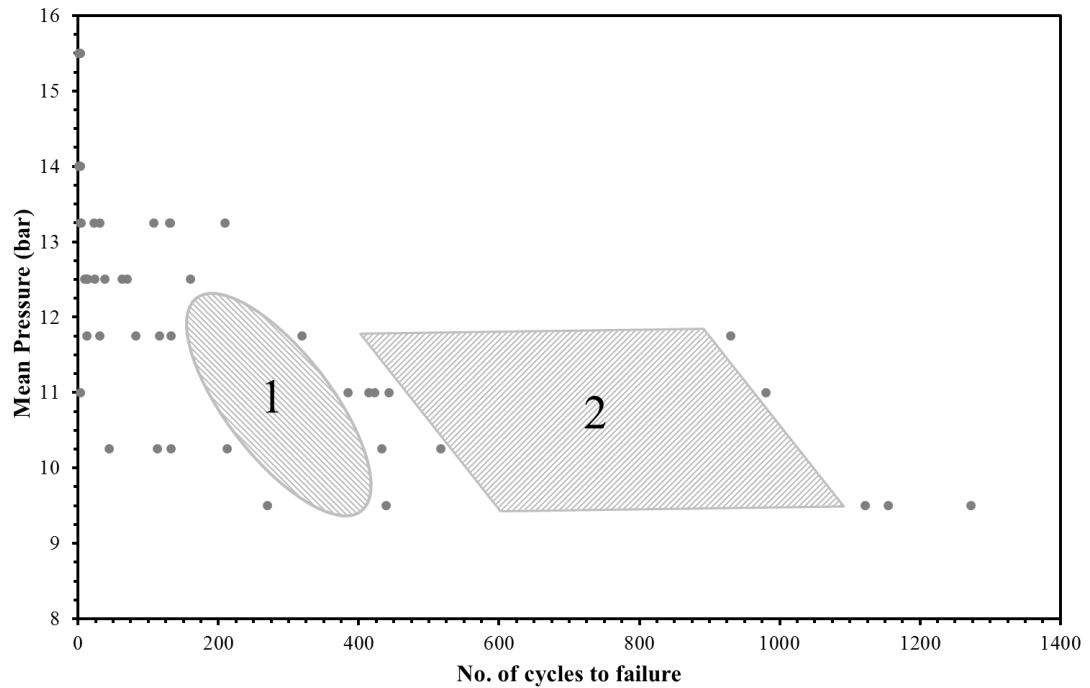


Figure 4-7 Mean pressure Vs. No. of cycles to failure highlighting data gaps

Figure 4-7 shows the results from the variable mean approach as per Figure 4-4 however, the specimens that did not fail after 1500 cycles have been removed from the dataset. The figure also illustrates 2 areas where significant ‘gaps’ appear within the dataset. Although scatter is expected in fatigue testing, as previously mentioned, the areas show visual trends where data is grouped either side of the gaps. These areas are harder to find, and therefore may have been missed, when the data was plotted on a logarithmic scale. The oval-shaped area marked ‘1’ may be mitigated through further testing as the gap between results appear relatively small. However, the trapezoidal area marked ‘2’ is a larger area showing a noticeable difference in failure time with respect to mean pressure. For example at $P_{MEAN} = 11.75$ bar (1.18 MPa) there is a factor of almost 3 difference with respect to the shaded area. This may suggest that there is a bimodal distribution in this testing regime. This may explain why some joints exceeded 1500 cycles without failing. However, further testing may rule out this hypothesis as it may fill in the gaps.

4.3. Influencing the welding parameters

As results from the first testing programme were obtained, the data were collated into Microsoft Excel for graphical outputs. This aided in monitoring the progress of the testing

programme and allowed for early interpretation/hypotheses of the results to be made by observing trends in the failure data.

Towards completion of the first testing programme, seven outlying results were observed which appeared to sit beyond the cluster of scatter from the fatigue test. Although a degree of scatter can be expected in fatigue testing, these outlying results were severe enough to skew the average number of cycles to failure for respective pressure ranges. Upon further investigation, it was clear that this small number of outlying results all had a similar trait in common; the tapping tee appeared to have moved laterally along the pipe during the welding process. This was noticed by the offset of the tapping tee with respect to the permanent pen markings added during the preparation stage of the electrofusion weld. A marker pen can be used to indicate where the joint was fused with respect to the pipe and the clamps. This is not a fundamental requirement to accomplish a successful electrofusion weld. However, it is recommended practice as it shows that extra care has been taken during the preparation process. For an electrofusion coupler for example, if a failure were to occur in service, the investigator will be able to recognise and appreciate that the pipe had been inserted to the correct depth with respect to the coupler – once the joint had been sectioned in half. With regards to this project, pen markings were primarily used to reference the tapping tee to the pipe so that if destructive testing were to take place post-fatigue failure, the orientation of the tapping tee with respect to the pipe would be known. Furthermore, it was apparent that the tapping tee had shifted laterally during the welding process as the marker pen is used prior to the heating process of the electrofusion weld – whilst the joint is in the top-loading G-clamp.

Figure 4-8 and Figure 4-9 show electrofusion tapping tees without and with a lateral shift respectively. The lateral shift (in Figure 4-9) was 2.36 mm, measured by eye using a Vernier Caliper to a resolution of 0.02 mm.



Figure 4-8 Electrofusion tapping without lateral shift (top view)

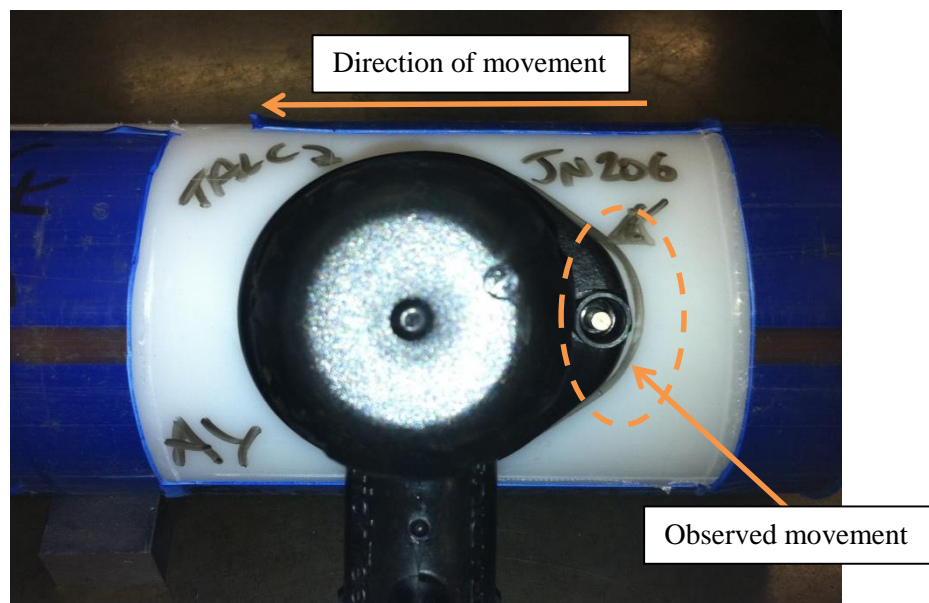


Figure 4-9 Electrofusion tapping tee with lateral shift (top view)

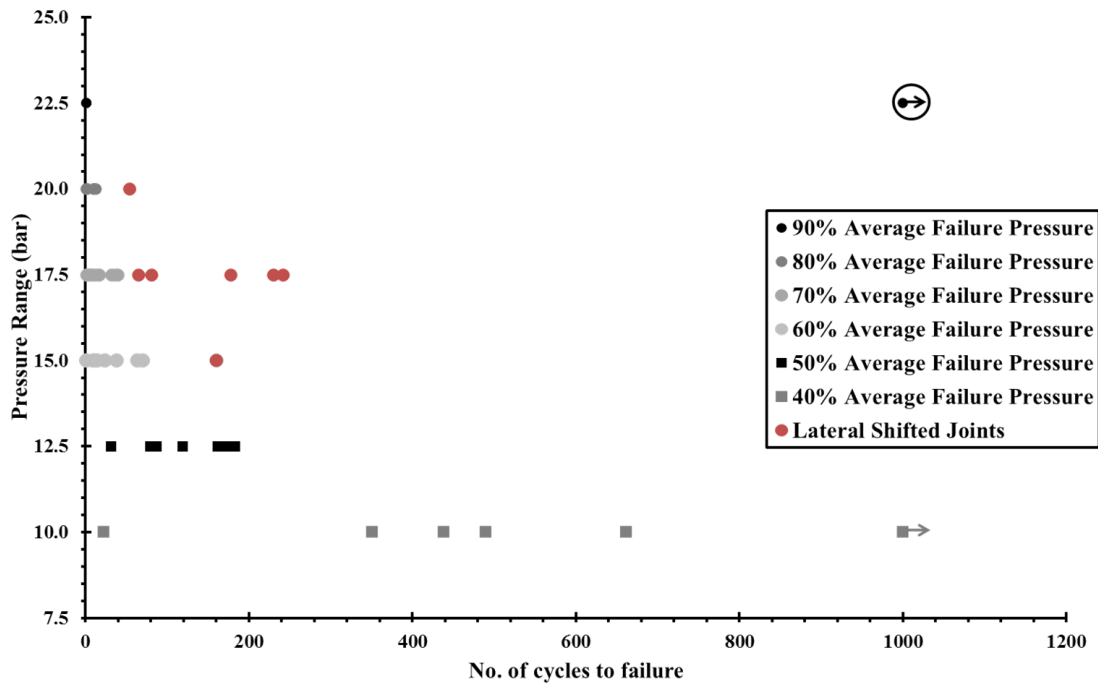


Figure 4-10 Fixed mean fatigue testing results including lateral shifted joints

Figure 4-10 shows the variation in results from the fixed mean approach testing programme. Note that the joints that shifted laterally during the welding process are coloured red.

The results coloured **red** in Figure 4-10 were not included in the previous set of fatigue testing results (i.e. Figure 4-1 of Section 4.1), as including the results would be an unfair representation of the fatigue performance of contaminated electrofusion tapping tees. The results however are included here as the phenomena can be explained.

Further observations of the joints that had shifted showed that they all moved in the same direction with respect to the pipe, fitting and clamp. For explanatory purposes, this would be in the 'left' direction of Figure 4-9.

4.3.1. Lateral shift investigation

An investigation was carried out to find the cause of the lateral shift of the tapping tees during the weld process. Firstly and quite simply, several joints were created with a notion of carefully observing the fitting during the heating and cooling process to see if there were any obvious overlooked issues in tooling or in the preparation process. After careful study, the probable cause of the phenomenon was reached.

It was believed that the cause of the shift was influenced by two variables:

- i) the top-loading G-clamp, in combination with;
- ii) the length of pipe the tapping tee is to be welded to.

The top-loading G-clamp is used to hold the tapping tee to the parent pipe and apply the appropriate compressive force to the tapping tee. For the tapping tees used in this project a compressive force between 1 to 1.5 kN must be maintained during the specified heating and cooling time – specified by the manufacturer. For clarity, the top-loading G-clamp was calibrated in-house every 3 months using a calibrated load cell to ensure the compressive force remained between these limits.

The top-loading clamp used for this project consisted of two separate parts: (a) the stand and (b) the adjustable clamp mechanism (see Figure 4-11).

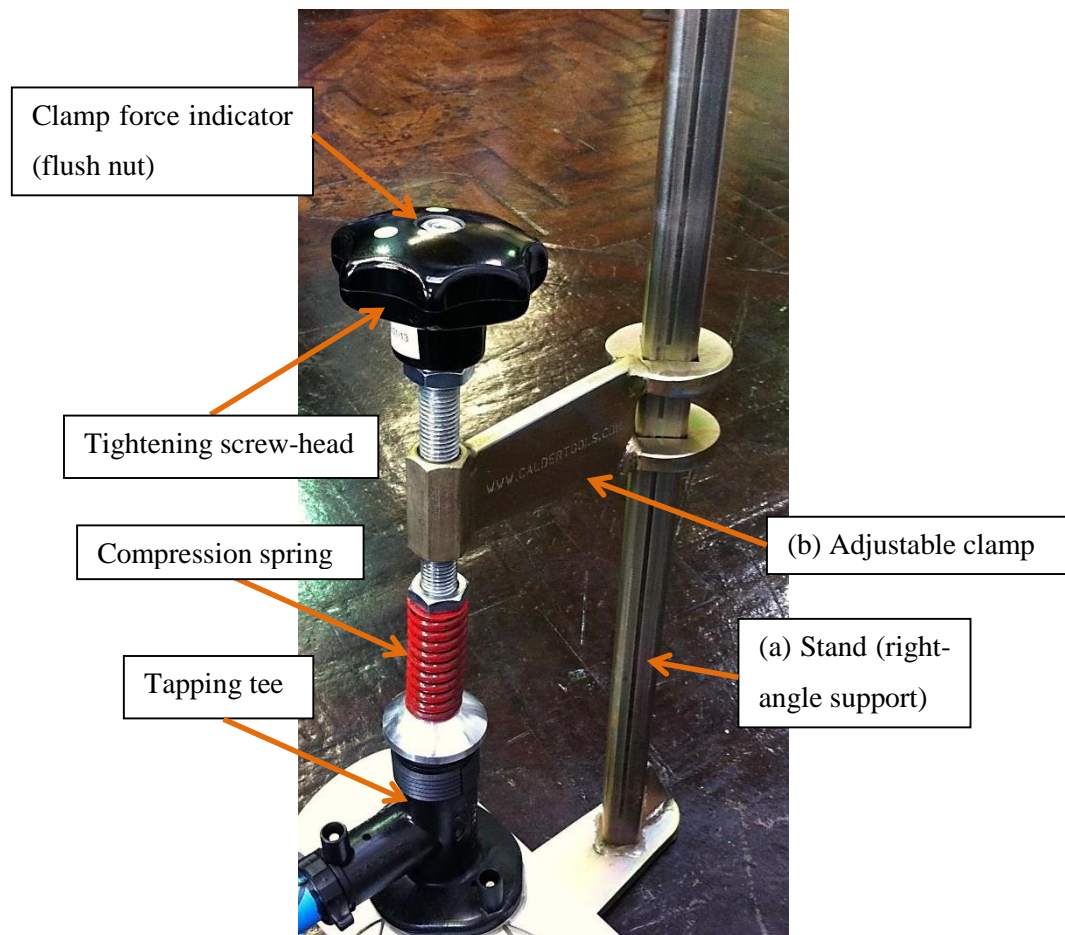


Figure 4-11 Top-loading G-clamp

The stand would sit on a solid surface, the pipe would be rested on the stand and the adjustable clamp would be lowered to ensure the tapping tee fitting rested securely on the pipe. Then the tightening screw was wound until the nut located on the top of the screw mechanism was flush

with the screw head. This would indicate that the screw had been wound enough to compress the spring and therefore provide the correct compressive force between pipe and fitting. In calibration, a flush nut would indicate approximately 1.4 kN of compressive force (checked manually using a calibrated load cell).

When the clamp was slid onto the stand, the hole in the adjustable clamp that allows for the clamp to freely slide up and down the stand, had enough 'play' within the mechanism to provide a slight angle that was off perpendicular to the base of the stand. Thus the resultant force at the jointing interface (between pipe and fitting) would consist of an expected large vertical force but also a small lateral force. The lateral force becomes evident when the heating cycle commences as the jointing interface begins to melt thus allowing the fitting to move as a result.

The second and arguably the most important variable that influenced the lateral shift to take place is how close the tapping tee fitting was to the end of the pipe. The force exerted by the top-loading G-clamp was enough to bend the pipe wall, causing a temporary ovality of the pipe. During the creation of contaminated joints, a pipe length of approximately 530 mm was always used to create 2 specimens (see Figure 4-12). It was decided that welding 2 specimens on the same pipe would save pipe material if a 110 mm (one pipe diameter) gap were to be left between the fitting and pipe.

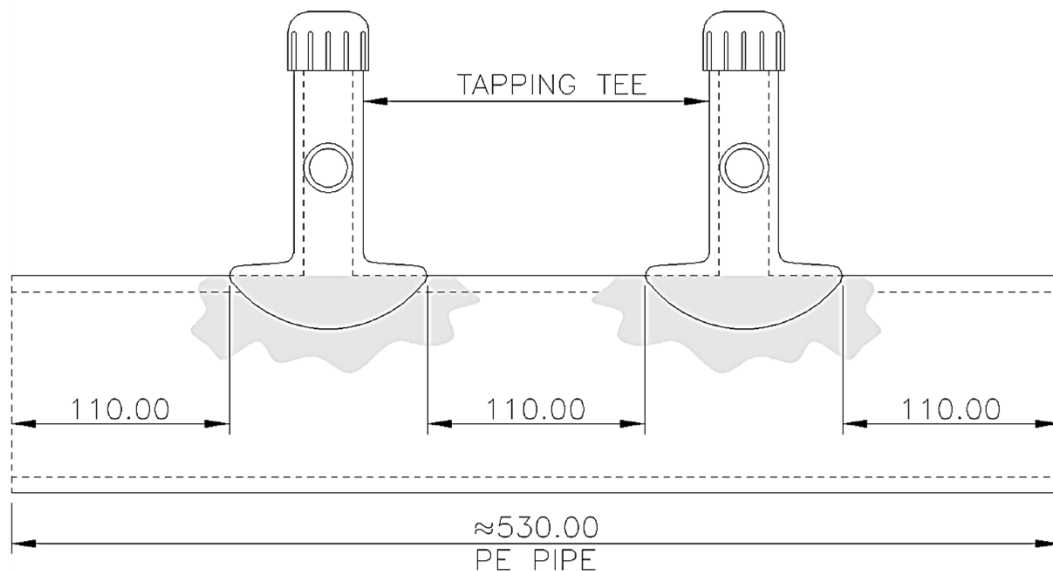


Figure 4-12 Drawing of tapping tees on 530 mm PE pipe

(Note: All dimensions are in 'mm')

It was noted that fittings welded on the left of the pipe (as per Figure 4-8) would not move during the welding process, however, some joints on right of the pipe (as per Figure 4-9) would move laterally.

It was believed that the closer the fitting were to the end of the pipe, the more likely the fitting would shift during the fusion cycle; as the severity of local deformation about the end of the pipe is likely to increase the closer the fitting (thus the vertical force) is to the end of the pipe. Retrospectively, this was not always the case as the severity of the offset angle of the loading clamp differed.

4.3.2. Lateral shift – an influence on the performance of contaminated joints?

Based on the hypothesis on the cause of the lateral movement of some joints during the welding process, explained in Section 4.3.1, several welds were completed and monitored with a digital Linear Variable Differential Transformer (LVDT) with 50 mm travel and accurate to 0.01 mm. Some joints had already been welded and appeared to have shifted laterally during the welding process. The severity of lateral displacement was measured using a Vernier Caliper post-weld. The lateral movement of tapping tees was not consistent in that it did not occur on each weld when expected.

Therefore, an experiment was performed with the aid of promoting lateral movement by applying dead-weights in the lateral plane of the assembly to promote movement. The dead-weights were specified as percentages of the compressive vertical force (1.4 kN) applied by the loading clamp when the joint is assembled; 50 N (3.57%), 70 N (5.00%) and 90 N (6.43%). Each experiment was recorded using a webcam that was focussed on the assembly, a stopwatch and the digital LVDT. The LVDT data was plotted against time and webcam ‘stills’ were used to confirm the data recorded – observing the LVDT and the stopwatch (see Figure 4-13 for experimental schematic).

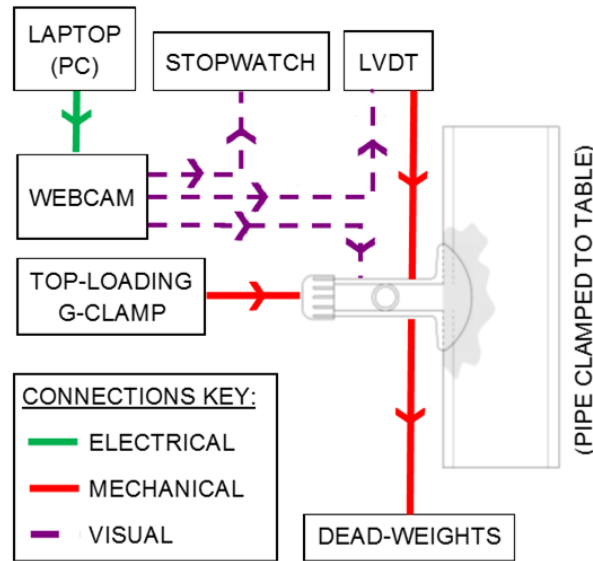


Figure 4-13 Schematic of tapping tee welding with dead-weights

It was decided that these welded joints, containing an element of lateral shift, would be subject to dynamic load using a predetermined loading pattern. The pressure range used for this test was 70% $P_{MAT,MAX}$ ($P_{RANGE} = 17.50 \text{ bar [1.75 MPa]}$) and the mean pressure was fixed at 12.5 bar [1.25 MPa] (i.e. $P_{MEAN} = 12.50 \text{ bar}$) as per the fixed mean fatigue testing regime highlighted in Section 3.3.1. This loading pattern was used as the results from pressure range and testing regime, highlighted in Section 4.1, indicated relatively short test times.

The results from the fatigue tests are depicted in Figure 4-14 and are expressed as lateral shift vs. number of cycles to failure.

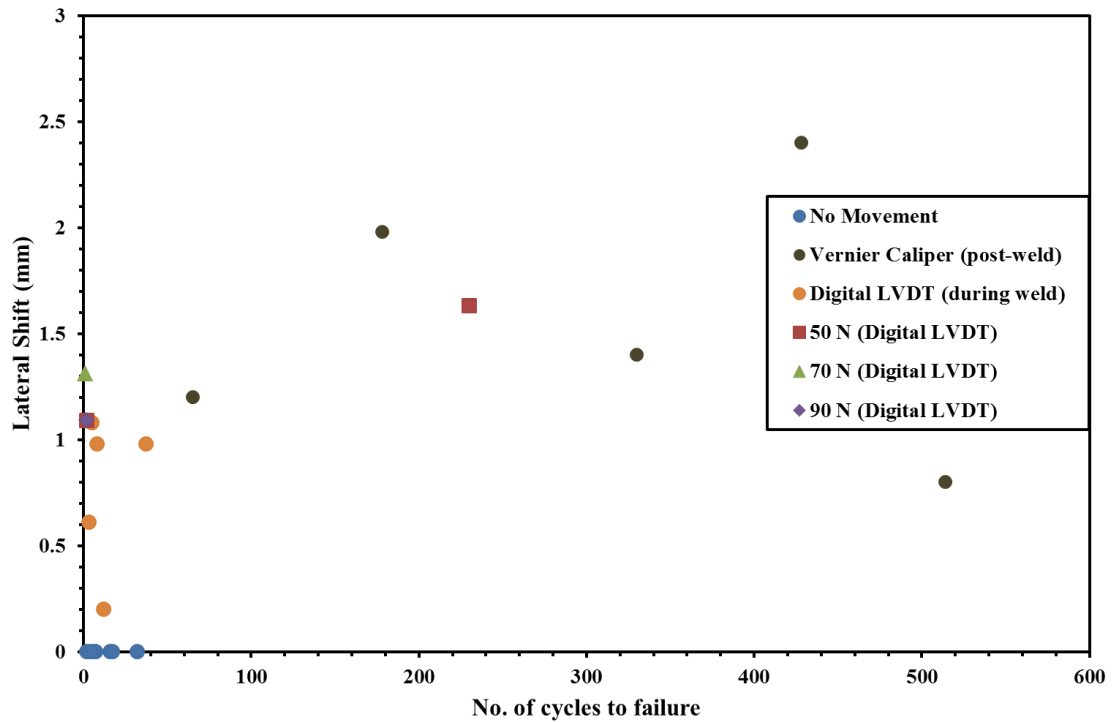


Figure 4-14 Fatigue-life of contaminated joints containing lateral shift during weld process when $P_{MEAN} = 12.50$ bar and $P_{RANGE} = 17.50$ bar

Figure 4-14 illustrates that if below 1.30 mm of lateral shift occurs, there is little or no change to the fatigue performance of a contaminated electrofusion tapping tee. However, there is a single instance whereby the joint moved by 0.80 mm (measured using a Vernier Caliper) and lasted 514 cycles. There was no obvious reason why this particular joint had an increase in fatigue performance.

There is an argument from this dataset that with a lateral shift greater than 1.30 mm, the fatigue performance of an electrofusion joint may increase. However, there is insufficient data to confirm this hypothesis; therefore further testing would be required to confirm or disprove this.

As mentioned in Section 4.3.1, the compressive force exerted by the top-loading G-clamp was 1.4 kN when the nut was flush with the top of the screw mechanism. This load reduces slightly during the welding process due to the heat that is applied and some local deformation. Comparing the side loading from the dead-weights to the initial compressive force (in brackets); 50 N (3.57%), 70 N (5.00%) and 90 N (6.43%) respectively, the load cases are low percentages of the initial compressive load and therefore heavier dead-weights may be required to promote larger lateral displacements – say 140 N (10% of initial compressive force).

4.4. Principal findings

A brief summary of the principal findings from the fatigue testing programmes is illustrated here. These findings include the fixed mean approach, the variable mean approach as well as the consequences of influencing the welding parameters by introducing lateral movement during the heating cycle of the weld.

Points discussed hereafter will be explained in further detail in the discussion and conclusion sections viz. Chapter 7 and Chapter 8 respectively.

4.4.1. A critique of the research experiments

Although the testing programmes described in this chapter have led to some interesting points for discussion, there are several aspects of this research that should be noted in order to highlight the context and value of this research.

- Only a single product from a single manufacturer was tested. Other products may vary in performance.
- All fatigue results are expressed graphically as pressure (mean/range) vs. number of cycles to failure. In general, fatigue-life curves are expressed as stress versus number of cycles to failure (S-N curves); stress was not calculated due to the complex geometry of the tapping tee. This holds an advantage as the test programme can be repeated simply by using a pressure gauge (or transducer) and device capable of producing dynamic loads. However, there is an argument that a genuine comparison of performance would require the calculation of stress at the fusion interface. This may require the use of finite element analysis (FEA) to achieve accurate results but may be time consuming when weighed against the potential benefits.
- The fusion interface was tested and therefore the fitting was not tapped through to the parent pipe as in a real-life situation. As a result, this eliminated hoop stress effects from the pipe and honed the research to the fusion interface alone; thus reducing test variables.
- The higher pressure ranges used in the fixed mean approach are arguably too large with respect to surge events and therefore are not an accurate representation of such events.
- The pressure gradient used for both testing programmes (25 bar/min [41.67 KPa/s]) is not representative of a surge event as these events tend to have rapid

increases/decreases in pressure. This pressure gradient was used to try to maintain some consistency with current industry standards.

- The use of talc as a contaminant can be seen as subjective as there may be some variation in the distribution of talc on the parent pipe between different applicants (technicians). However, without a thorough investigation into this, i.e. across various test houses, there is little evidence to support this.

4.4.2. Fixed mean approach

- Fatigue failure is possible for contaminated electrofusion tapping tees using a low-cycle fatigue testing regime.
- Joints made to best practice principles (i.e. ‘perfect joints’) did not fail under this testing regime.
- Higher pressure ranges dramatically reduce the fatigue-life of contaminated electrofusion tapping tees. This is most likely to be because the maximum pressures observed in the higher pressure ranges are close to the average failure pressure ($P_{MAT,MAX}$) of a contaminated electrofusion tapping tee.
- As the pressure range decreases, the predictability of failure decreases thus making it difficult to predict failure with a reasonable degree of confidence.
- Some joints at the lowest pressure range in this testing regime ($P_{RANGE} = 10 \text{ bar}$ [1.0 MPa]) did not fail after 1000 cycles which may indicate that the scatter in results is so great that it exceeds the 1000 cycle marker set by the author. For clarity, that is not to say that these joints would not fail if the dynamic test continued.
- The mean pressure selected for this testing regime is arguably a representation of the operating pressure of a water distribution main. However, this pressure (12.50 bar [1.25 MPa]) would arguably be too high for distribution mains – thus the reasoning behind implementing a secondary test regime whereby the mean pressure is reduced to pressures that resemble typical distribution main pressures.
- In general, the average number of cycles to failure increases at an almost exponential rate as the pressure range decreases.

4.4.3. Variable mean approach

- Much like the general trend for the fixed mean approach testing method, as the mean pressure decreases, the predictability of failure also decreases.

- Much like the previous testing regime, the general trend is that as the pressure is reduced, the fatigue-life of a contaminated tapping tee increases.
- In general, the scatter in results for nearly all pressure ranges increased as the mean pressure decreased; to the extent that some joints did not fail within the 1500 cycle limit set by the author. This may suggest that as the mean pressure decreases, the confidence of predicting a failure of a contaminated electrofusion tapping tee is extremely low. Again, with regards to the joints that did not fail, this is not to say they would not fail if the fatigue test were to continue. It is important to note that tests needed to be stopped in order to maintain momentum in data generation for the project.
- Following on from the previous point, there is an argument that decreasing the mean pressure may prolong the longevity of a contaminated electrofusion tapping tee. However, this research also suggests that quantifying the impact of such actions will prove difficult in that the predictability of a contaminated joint becomes more difficult as the mean pressure is reduced.

4.4.4. Influencing the welding parameters

With regards to introducing a lateral shift during the welding cycle to improve the performance of a contaminated electrofusion tapping tee, the research is still in its infancy. However, even with a small number of successful data points, allowing the joint to move during the welding cycle appeared to give an increase in performance with regards to the fatigue-life of a contaminated electrofusion tapping tee; potentially worthy of further investigation.

It is paramount to note that this ‘phenomenon’ is likely to be a freak occurrence that was observed in laboratory conditions and was quickly overcome in order to ensure that the results obtained for fatigue testing were fair and consistent. It is also important to note that this phenomena is highly unlikely to occur on site as tapping tees are usually welded to completed mains and not short pieces of pipe. It shall also be noted that there are no design flaws with the top-loading G-clamp and this phenomena only occurred due to the nature of how the joints were prepared for this project. However, local deformation (ovality) of the pipe may be expected due to the compressive force of the top-loading G-clamp. However, this should slowly dissipate once the clamp is removed, allowing the pipe to return to its original shape.

It is important to note that there is a potential flaw in the acquisition of data for this experiment in that the amount of lateral shift was measured by different means therefore there is potential for inconsistency in the results. There lies doubt in the hypothesis and therefore it is recommended that the experiment be repeated using more controlled measures. Furthermore,

there is scope for post-failure investigation of the joints by means of destructive testing to examine and compare the fracture surface of the jointing interface.

Chapter 5

Understanding the failure mechanism - Destructive testing

Discussion from extensive fatigue testing in Chapter 4 states the likely failure mechanism for electrofusion joints subject to fatigue would be the development of cracks in the jointing interface, i.e. crack propagation. However, as there is no published research on the fatigue performance of contaminated electrofusion tapping tee joints, a series of destructive tests were conducted in order to better understand the failure mechanism(s).

In brief, destructive tests were performed on joints that had previously failed during the fatigue testing programme, highlighted in Chapter 4, to current industry standard test methodologies. These destructive tests were also conducted on ‘perfect’ joints (i.e. joints made to best practice principles) so a direct comparison could take place.

As mentioned in Section 2.4.1, the crushing decohesion test observes and quantifies (as a percentage) the amount of ductile decohesion present at the jointing interface – post-crushing of the surrounding pipe to the fitting. The requirements and methodology of this test are highlighted in ISO 13955 [60]. This test has been used in this section, however, after repetition of this test on many contaminated joints, the areas that appeared to show bonding on the fracture surface of the parent pipes were similar therefore, for the purpose of this project, the amount of ductile decohesion was not quantified and thus not compared from joint to joint. As will be explained and illustrated in this section, the amount of ‘bonding’ that took place when a pipe was subject to the talc contaminant was minimal but crucial in aiding to understand the failure mechanism.

Initially, a comparison was made between a joint that had been subject to the talc contaminant and a joint that had been made to best practice principles. The crush test was further performed on specimens that had failed under the fatigue testing regime as highlighted in Chapter 4. A final specimen was subject to the crush test and further investigated using a Scanning Electron Microscope (SEM). The outcomes of the SEM analysis are highlighted in Section 5.4.

5.1. Imperfect vs. Perfect joints

Specimen L was contaminated with talc and subject to the crush decohesion test specified in ISO 13955 [60]. Figure 5-1 shows an aerial view of the pipe and fitting when the crushing device reached its maximum distance. As can be seen in Figure 5-1, very little bonding took place between pipe and fitting. Many of the filament wires were embedded into the pipe and it was assumed initially that these wires were offering some structural strength to the joint assembly despite being contaminated with talc.

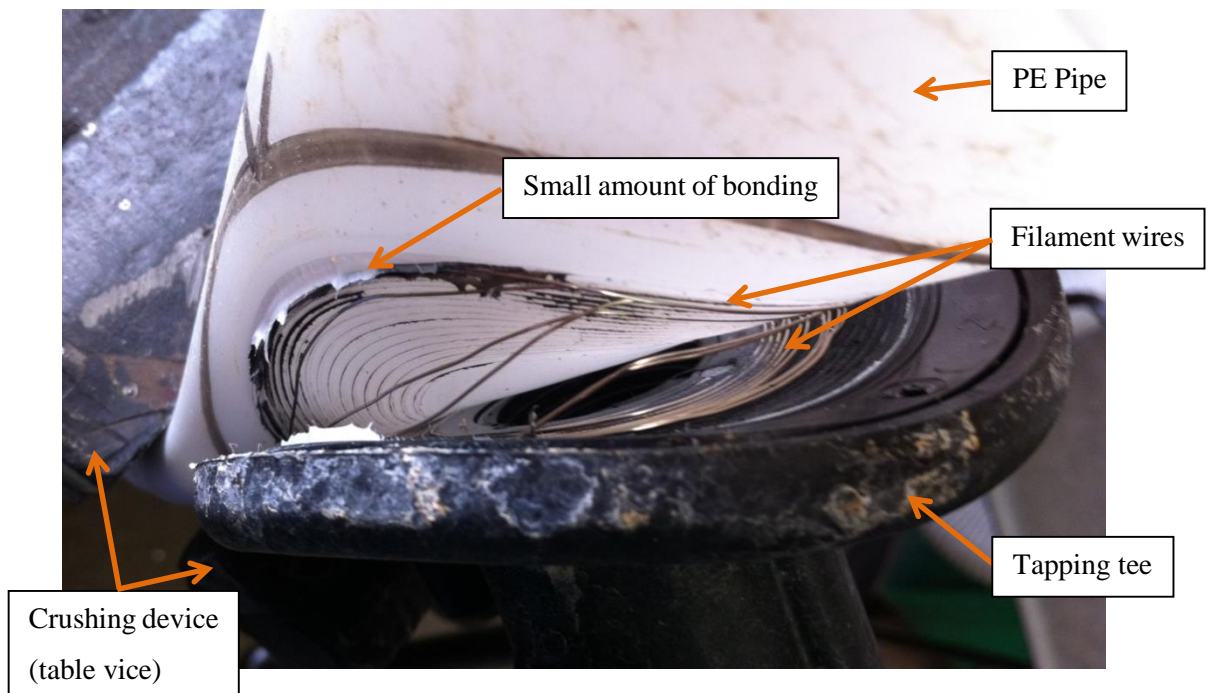


Figure 5-1 Aerial view of specimen post-crush test

Once the maximum displacement was reached in the crushing test, the fitting was further removed from the host pipe by using a relatively small amount of force which was applied by hand; using the stem of the tapping tee, moving away from the crushing device. Figure 5-2 shows the joint after it has been removed from the crushing device. It can be observed that there was very little bonding between the fitting and the host pipe. There were small black marks on the pipe where it appears a small amount of bonding had taken place. However, indentations on the surface of the pipe from where the filament wires were embedded into the pipe further emphasise that they may have been offering structural support to the assembly.

Small amounts of ductility are visible to the naked eye about the outer circumference of the fusion zone. Note that this area was where the filament wires were mostly embedded into the parent pipe. It is important to note that the failure of the joint when subject to this test should be classed as a brittle failure. However, the ductility observed is very small and localised about

the outer circumference of the fusion interface; more specifically, either side of the indentations on the parent pipe created by the filament wires during the welding process.

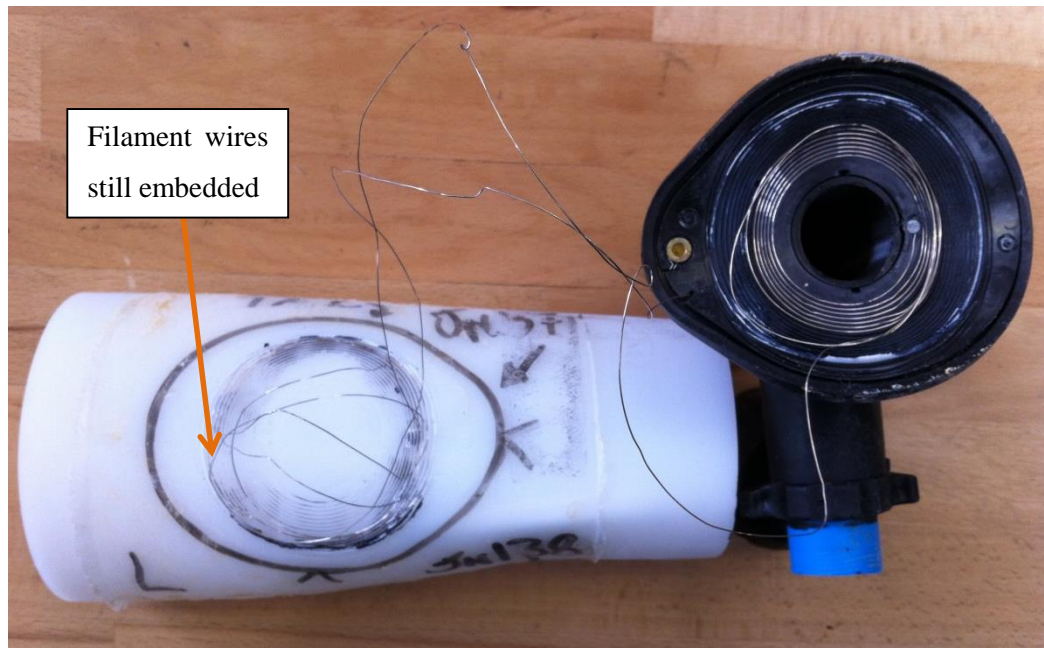


Figure 5-2 Talced specimen removed from crushing device

As a comparison, the crush test was conducted on a specimen that was welded to best practice. Figure 5-3 shows the specimen after it has been subject to the full extent of the crushing device. As can be seen, the specimen was just beginning to fail on the outer part of the fusion zone but still remains fully adhered to the PE pipe when the maximum crushing distance is reached; suggesting that a ductile failure would occur.



Figure 5-3 Post-crush of 'perfect' specimen

The assembly was further crushed on the opposing side of the fitting assembly in an attempt to yield the specimen but with no success. It can also be seen (in Figure 5-3) that there is very little opportunity to insert a lever to persuade the specimen away from the pipe. ISO 13955 [60] states that no impact forces shall be used to yield the fitting from the pipe, therefore using only a lever to remove the fitting from the pipe was a next to impossible task. It was therefore concluded that the specimen would fail in a fully ductile manner. This further enforces the detrimental nature that contamination has on joint integrity.

5.2. Adhesion with respect to fatigue tested specimens

A project, fully supervised by the author, was conducted as part of an MEng final year assignment [67] with the aim of observing any trends in leak paths of specimens that had failed

under the fatigue testing regime highlighted in Section 4.1. Initially, non-destructive ultrasonic techniques were used to attempt to observe the leak paths at the jointing interface – the results, interpreted with the aid of the author, will be discussed in Section 6.1. The potential leak paths observed from the ultrasonic analysis were confirmed using a basic hand pump to produce a flow of water through the fittings. The bonded areas were then observed after the fittings were subject to the crush decohesion test.

A total of six joints were analysed from the fatigue testing regime that used the fixed mean pressure approach, where $P_{MEAN} = 12.50 \text{ bar}$ (see Section 4.1). Each joint represented a pressure range from the fatigue test; a summary of the joints is given in Table 5-1:

<i>Joint Reference</i>	<i>Pressure Range</i>	<i>Pressure Range (bar)</i>	<i>No. of cycles to failure</i>
H	90% $P_{MAT, MAX}$	22.50	1
W	80% $P_{MAT, MAX}$	20.00	2
BW	70% $P_{MAT, MAX}$	17.50	3
P	60% $P_{MAT, MAX}$	15.00	38
AP	50% $P_{MAT, MAX}$	12.50	119
CS	40% $P_{MAT, MAX}$	10.00	350

Table 5-1 Summary of tested joints

Specimens (as per Table 5-1) were selected as the fatigue-life (number of cycles to failure) was the closest to the average number of cycles to failure for each pressure range tested to the fixed mean approach. This was assumed to be a logical selection and a fair representation of each pressure range considering the time associated with data acquisition and analysis was limited for this project.

Figure 5-5 to Figure 5-10 (captions by Shipway [67]) show the pipe of each joint specified in Table 5-1. The approximate leak paths are illustrated in each figure. The leak paths were obtained post-failure whereby a hand pump was used to generate a flow of water through the already failed specimen; thus showing the leak path(s). Visual inspection of the leak paths were quantified into two categories: major and minor leaks. These are illustrated in Figure 5-5 to Figure 5-10 using turquoise and purple dashed arrows respectively. A major leak can be described as the primary flow of water; whereas a minor leak would be almost a trickle of water that is subsidiary to the major leak. Figure 5-4 shows a tapping tee that has been subject to a short term burst test as specified in Section 2.4.2; showing a major leak path for example purposes.

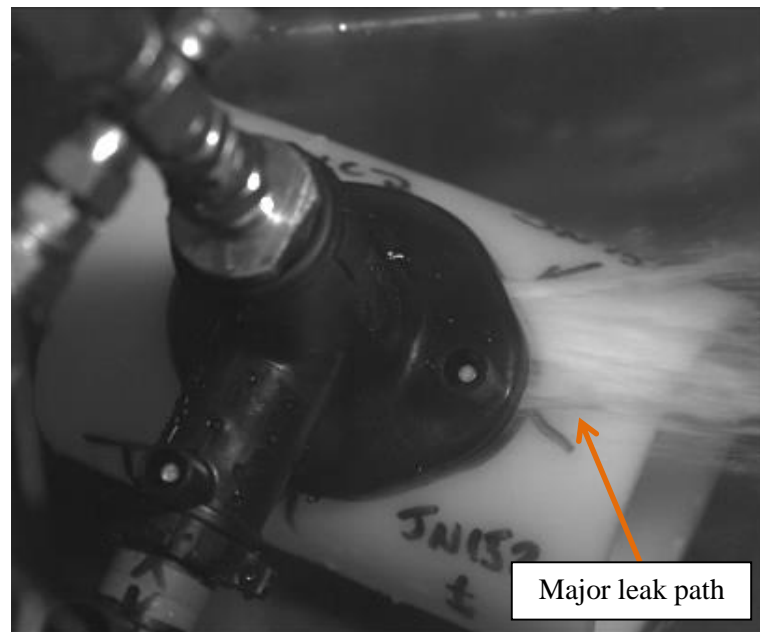


Figure 5-4 Failing tapping tee showing 'major' leak path

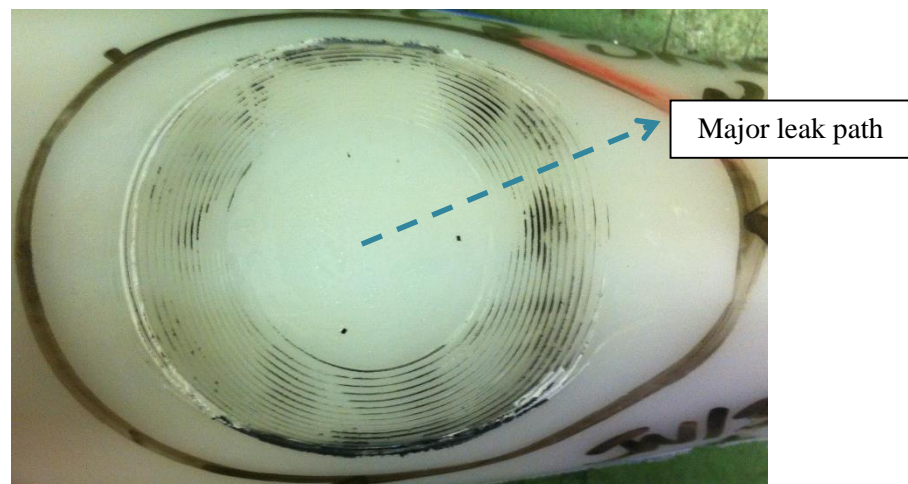


Figure 5-5 Specimen H (90% $P_{MAT, MAX}$)

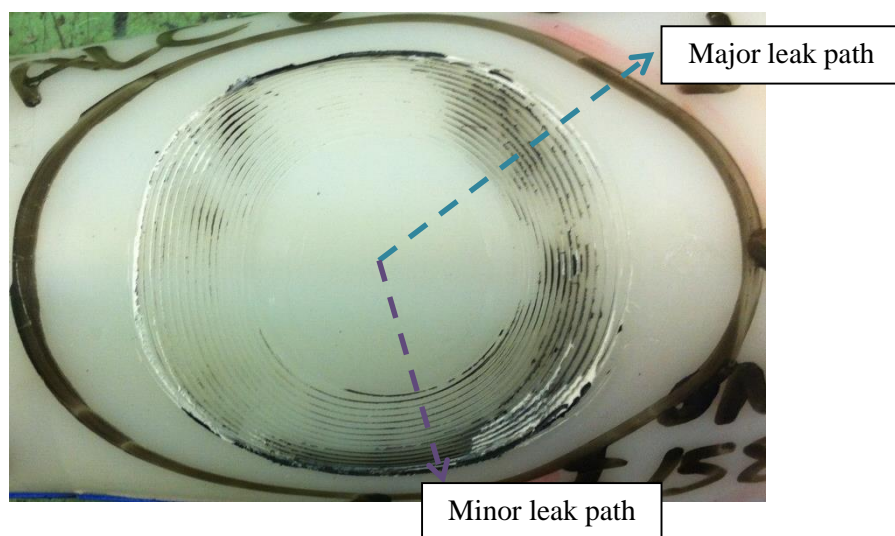


Figure 5-6 Specimen W ($80\% P_{MAT, MAX}$)

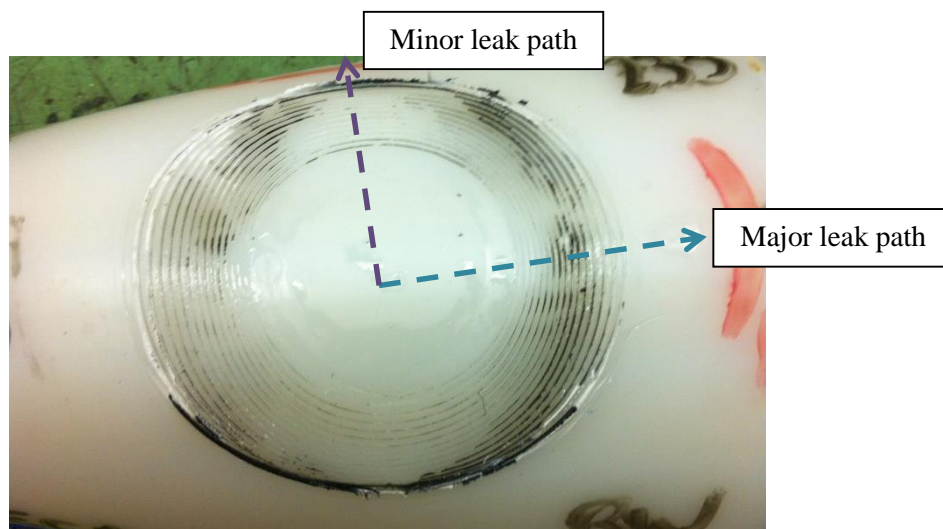


Figure 5-7 Specimen BW ($70\% P_{MAT, MAX}$)

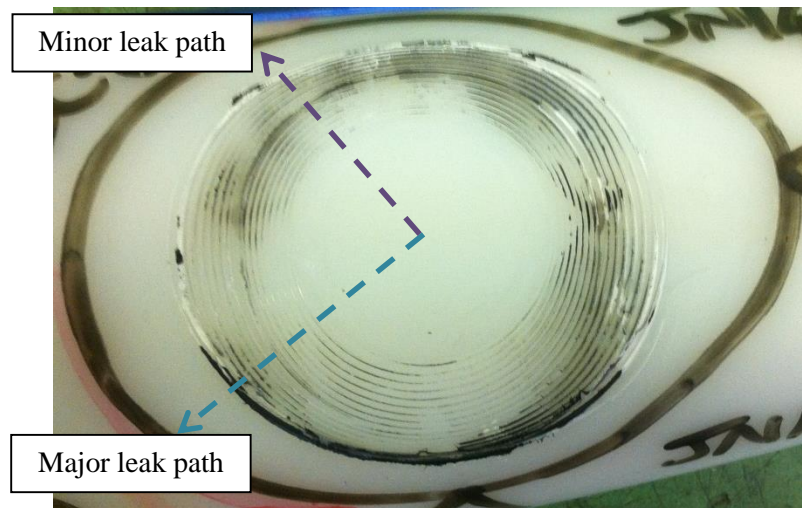


Figure 5-8 Specimen P (60% $P_{MAT, MAX}$)

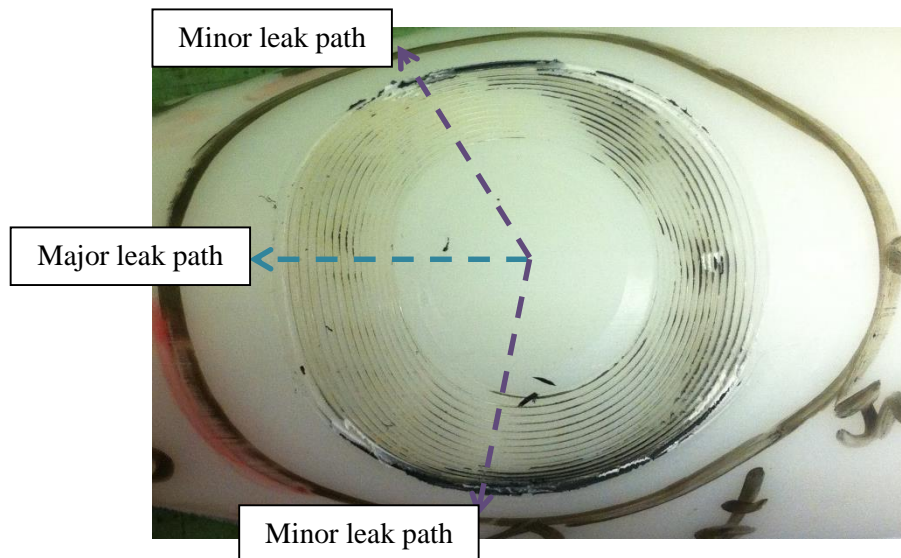


Figure 5-9 Specimen AP (50% $P_{MAT, MAX}$)

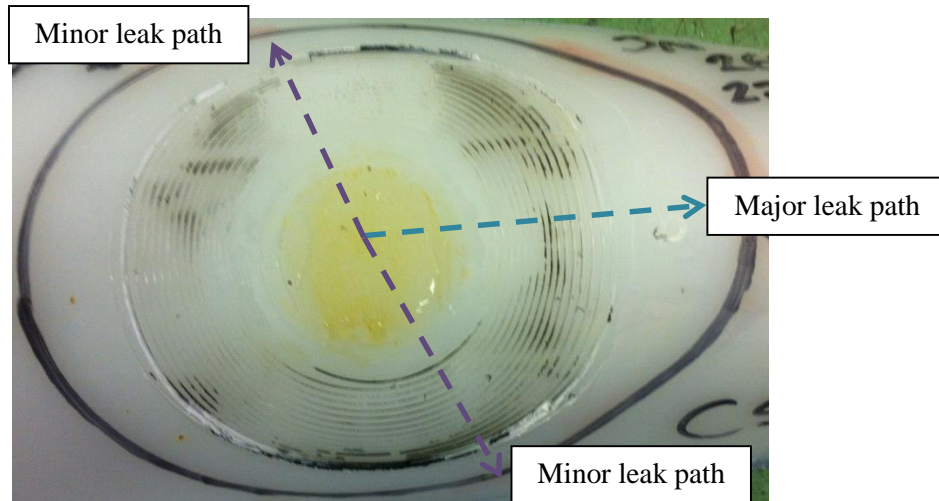


Figure 5-10 Specimen CS (40% $P_{MAT, MAX}$)

In general, the observations of the analysis are highlighted thus;

- The effects that contamination has on the adhesion of the fitting to the parent pipe are clear in that there is very little signs of ductility once the fitting is removed from the pipe.
- To the naked eye, bonding appears to be the best at the outer circumference of the fusion zone. Here, a very small amount of ductility can be seen and it is believed that this bonding is located either side of the indentations caused by the filament wires during the welding process.
- Some of the filament wires were still present on the parent pipe once the fitting was fully removed on all specimens – post crush test.
- Major and minor leak paths appear at random locations which may strengthen the case that the fittings were created without bias by the author.
- Minor leak paths become more predominant as the pressure range is decreased in the fatigue testing regime i.e. Specimen H (90% $P_{MAT, MAX}$) (Figure 5-5) has one clear major leak path that is coincidentally somewhat identical to that shown in Figure 5-4, whereas Specimen CS (40% $P_{MAT, MAX}$) (Figure 5-10) has one major leak path and two minor leak paths. This may suggest that the lower pressure ranges promote crack growth under dynamic loading; potentially in a circular manner.

5.3. Specimen X

Specimen 'X' is a contaminated joint that had previously failed under dynamic load from the fixed mean approach – results shown in Section 4.1. The specimen was tested with parameters $P_{\text{RANGE}} = 20 \text{ bar}$ (2.0 MPa), $P_{\text{MEAN}} = 12.5 \text{ bar}$ (1.25 MPa) and held a fatigue-life of 2 cycles. An aerial perspective of the specimen is illustrated in Figure 5-11.

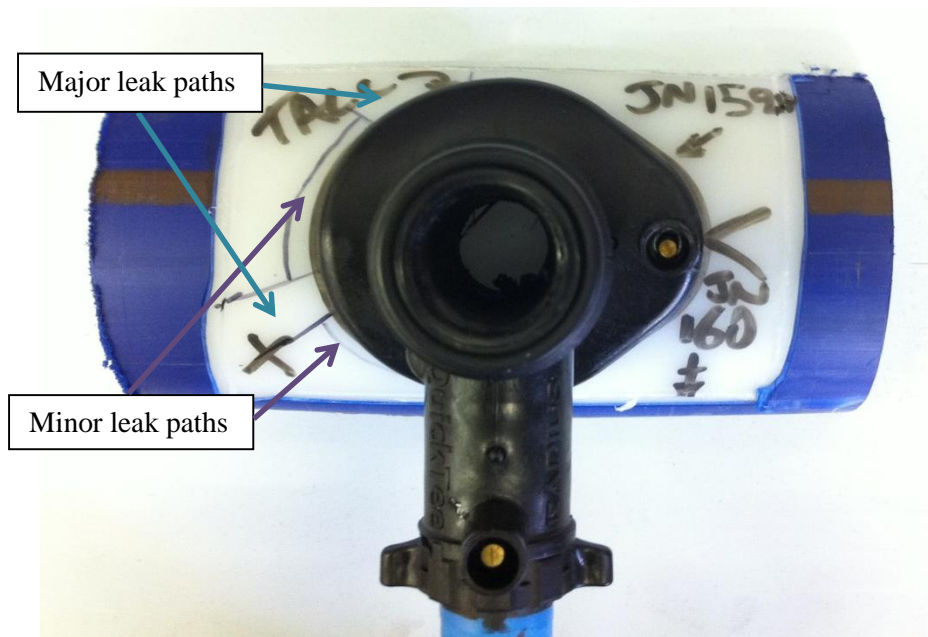


Figure 5-11 Specimen 'X' prior to crush test

Prior to the destructive test of specimen X, a hand pump was used to produce a flow of water through the fitting in order to observe the leak path(s) – it was thought it may be visually clear where some 'good' adhesion took place if the leak path was known. The leak paths are illustrated as to their severity. There was a large and obvious (major) leak path at the top of the Figure 5-11 as well as a large but narrow leak path at the bottom-left of the photo. Smaller leak paths are also noted in Figure 5-11 at the left and bottom of the photograph.

Similarly to Figure 5-1, specimen X quickly came away from the host pipe when it was subject to the crushing device (see Figure 5-12). Once the maximum crushing distance was achieved, the fitting was completely removed from the parent pipe by forcing the tapping tee away from the pipe by hand. Again, very little physical force was required to achieve this.

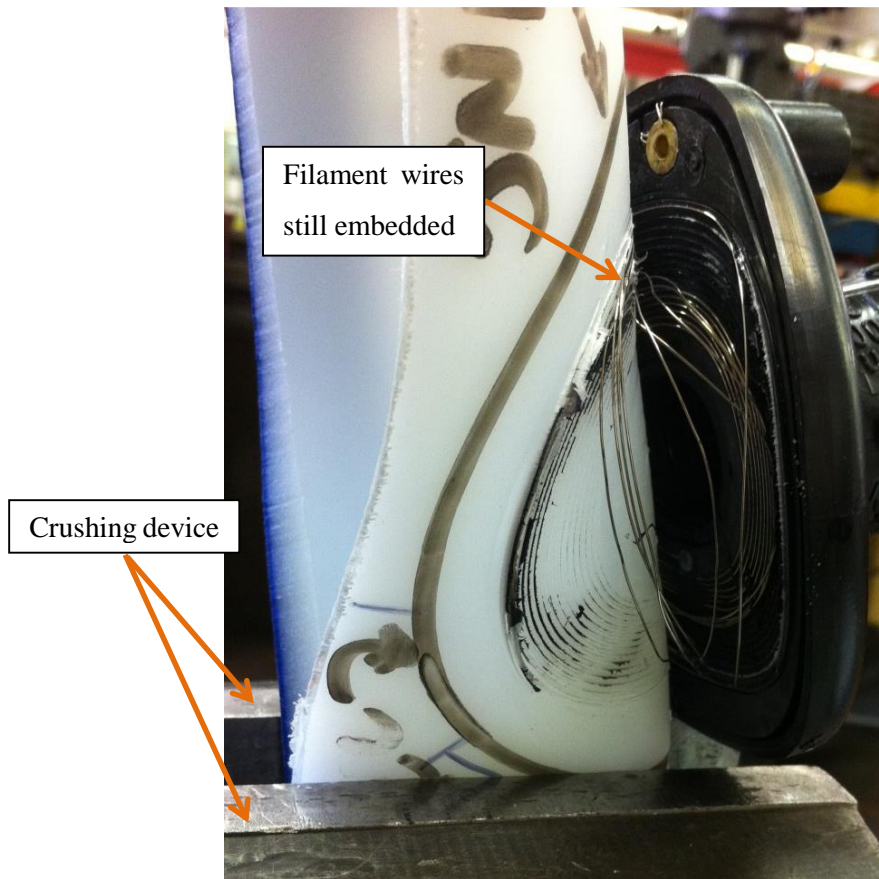


Figure 5-12 Specimen X during crush test

Much like Figure 5-1, many of the filament wires were still embedded into the parent pipe.

Figure 5-13 and Figure 5-14 show the parent pipe and the fitting respectively. It can be seen that there is little or no bonding at the bottom-left of the fusion zone which corresponds to the leak path observation defined in Figure 5-11. However, specimen X was subject to a dynamic load (fatigue) and then was further analysed using destructive methods, i.e. the crush test. Therefore, observing the fusion zone on the parent pipe as well as the tapping tee after the crush test does not give an indication of the mechanism of failure of the fitting when it is under dynamic load. However, it does give an idea of the quantity (and quality) of adhesion that took place during the welding process.

Figure 5-14 shows the underside of the electrofusion tapping tee of specimen X. It is also key to note that the filament wires were carefully removed from both the parent pipe and the fitting once they were separated from one another.

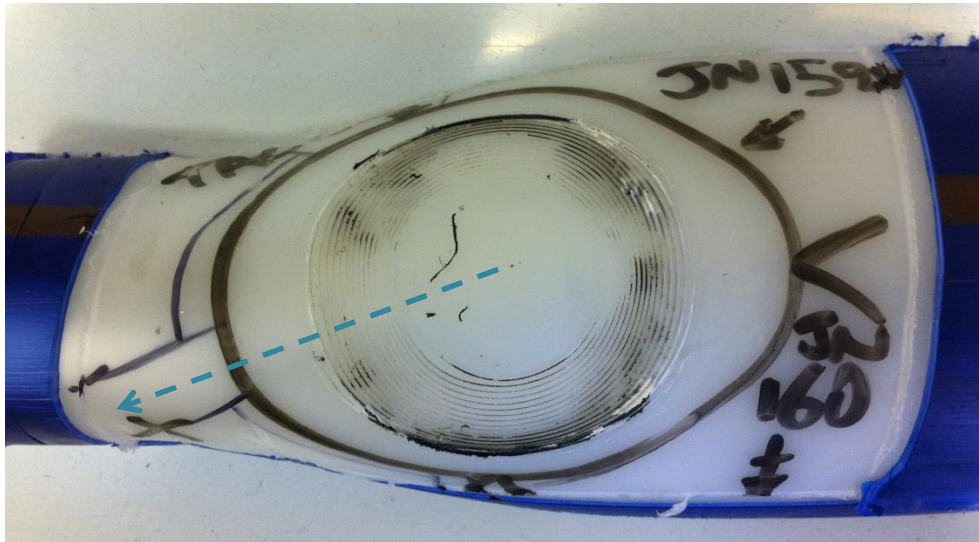


Figure 5-13 Specimen X parent pipe



Figure 5-14 Specimen X tapping tee (removed)

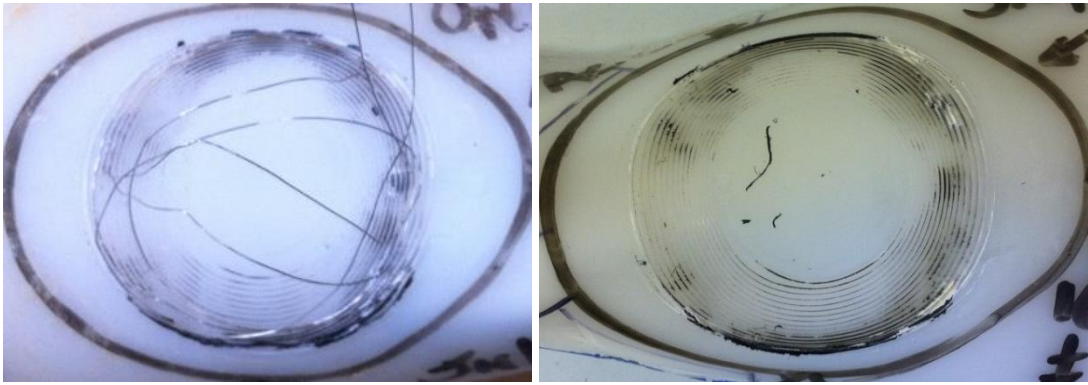


Figure 5-15 Fusion zones on parent pipe of specimen L (a) and specimen X (b)

By observing the fusion zone of specimen L (from Section 5.1) and specimen X (see Figure 5-15), similarities become more evident. Both specimens appear to have some remains of the tapping tee (black polymer) on the surface of the pipe. Both specimens show a very small amount of ductility to the bottom right and top right of each specimen. This is also consistent with the findings of the comparison of adhesion with respect to the fatigue testing pressure range stated in Section 5.2 whereby a small amount of localised ductility is observed either side of the indentations made when the filament wires are heated during the welding process.

5.4. Scanning Electron Microscopy

Many fractographic studies have been conducted on PE pipes that were failed under loading conditions such as creep and fatigue [41, 68, 45]. These were undertaken using Scanning Electron Microscopy (SEM) analyses to observe the fracture surface.

Further investigation into the failure surface of Specimen X (from Section 5.3) was undertaken using the SEM analysis. The aim of the SEM analysis was to observe any obvious differences in the failure surface between areas on the parent pipe that appeared to have a small amount of bonding and those that appeared to have none; these areas were dictated via a visual inspection. A small amount of black polymer (belonging to the tapping tee) remaining on the pipe would be classified as a partially bonded area. Therefore, an area that lacked this would be known as an area without bonding.

Four pieces approximately 15 x 15 mm were carefully cut from the parent pipe using a junior hack saw. Figure 5-16 shows the approximate locations of samples 1 to 4. A summary of the observations made can be found in Table 5-2.

<i>Sample</i>	<i>Visual observations/comments</i>
1	There appeared to be a small amount of ductile failure throughout the area on close inspection (to the naked-eye); located where the filament wires were embedded into the parent pipe.
2	Same as sample 1 except to a greater extent but only in an area approximately 2 mm ² .
3	Very little bonding. Some black polymer remained on the outer section of the fusion zone. Again, located where the filament wires appeared to have sat.
4	Almost no black polymer remains on the parent pipe. Note: area is in line with the observed leak path.

Table 5-2 Summary of observations for SEM samples

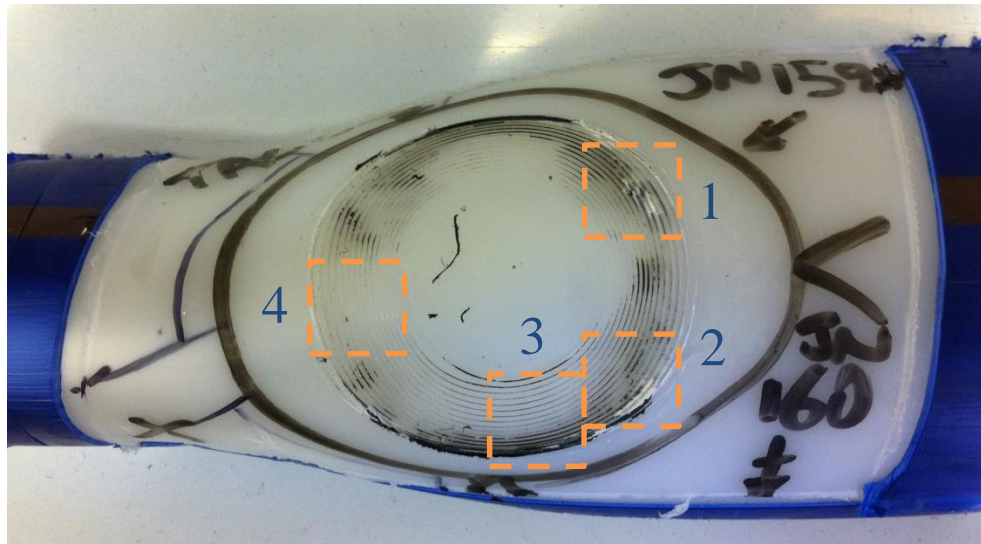


Figure 5-16 Approximate location of SEM samples – specimen X

Prior to the SEM analysis the samples were cleaned using an isopropanol solution and carbon-coated. Figure 5-17 shows the four samples cut and ready for preparation prior to the SEM analysis.



Figure 5-17 Specimen X samples for SEM

5.4.1. SEM observations

It is important to note that in general, specimens that are contaminated with talc prior to the welding process fail in a brittle manner. However, the SEM analysis will show microscopic regions of ductility that will be referred to as ‘ductile’. For clarity, when ductility is discussed, it is not referring to the specimen as a whole, but to an observed microscopic region under SEM analysis.

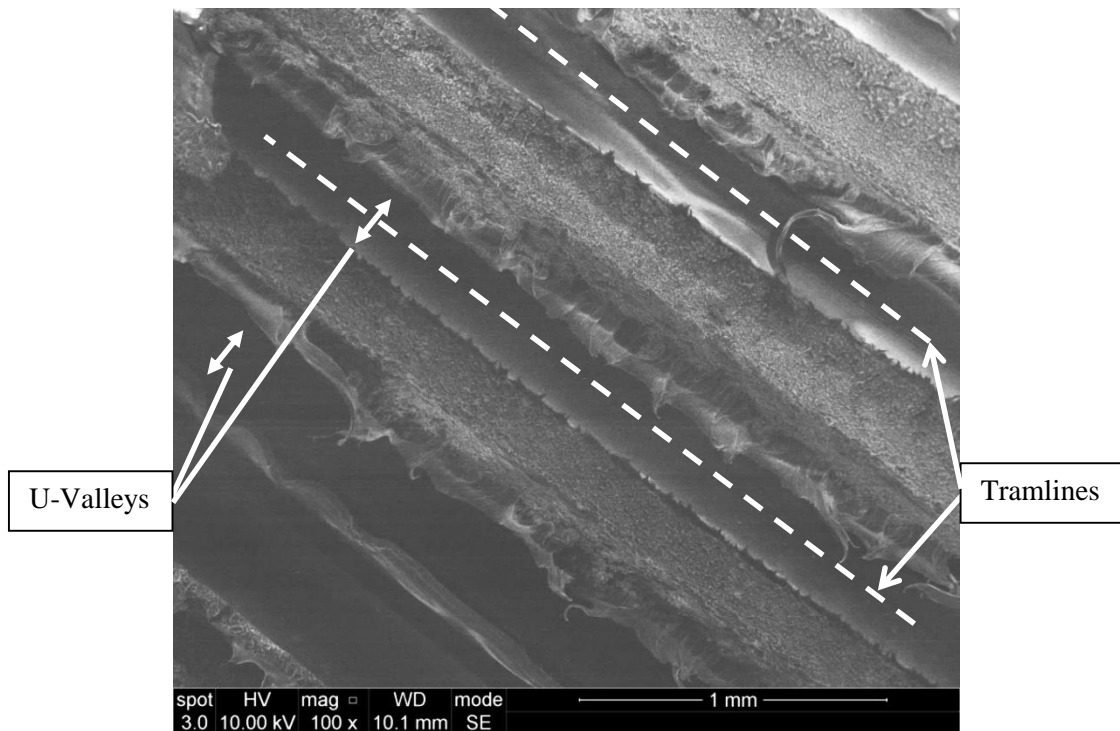
Sample 1

Figure 5-18 Sample 1 (x100 magnification)

Figure 5-18 shows Sample 1 at x100 magnification. There are three very distinct ‘tram lines’ moving from the top-left to the bottom-right of Figure 5-18. These are the indentations caused by the filament wire during the heating process of the electrofusion welding cycle. It would appear that the heat produced by the filament wires, in combination with the vertical force applied as a result of the top-loading clamp, forces the filament wires to embed into the parent pipe during the heating cycle, thus leaving indentations in the form of ‘U-shaped’ valleys on the parent pipe and perhaps giving the joint some structural strength.

A closer inspection of the area between the filament wire indentations can be seen in Figure 5-19. At the brink of the U-valleys there appears to be some elongation of polymer which suggests some ductility. In contrast, the centre of Figure 5-19 shows the failure-surface to be more brittle.

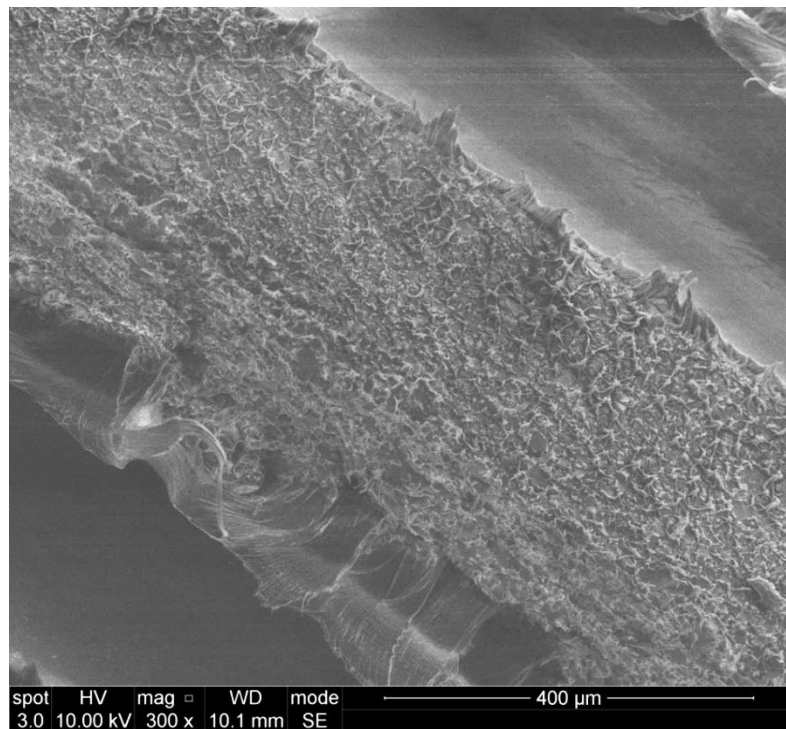


Figure 5-19 Sample 1 (x300 magnification)

Closer inspection of a ductile area at the threshold of the U-valley gives a clearer idea of the extent of ductility present in this region.

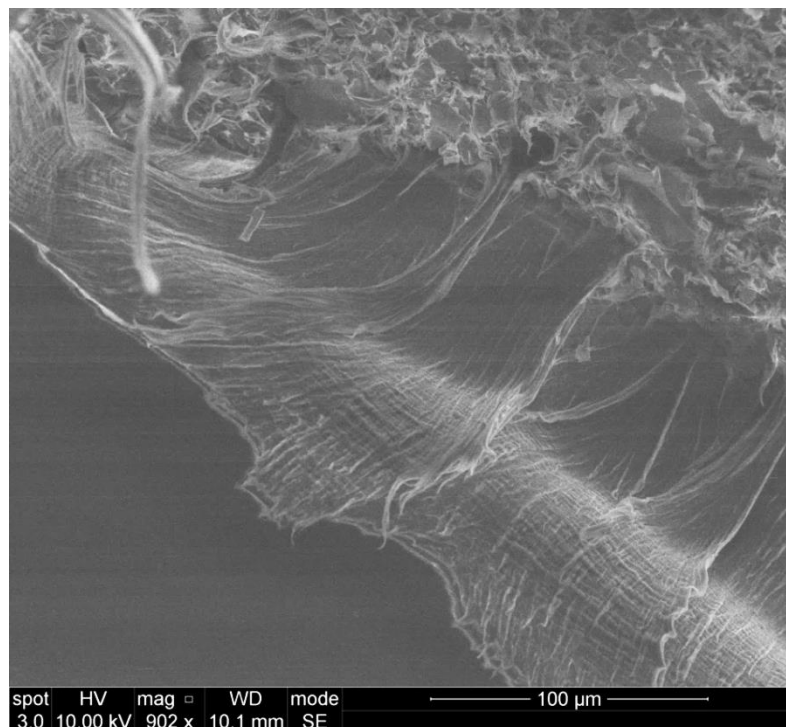


Figure 5-20 Sample 1 (x902 magnification)

Figure 5-21 shows a ripple effect on a ductile elongation evident at 2000 times magnification; likely to be caused by the opening effect of the crush test. If this small area of the joint was adhered post-weld then it is likely that this type of failure can be expected when the tapping tee is subject to the crushing decohesion test.

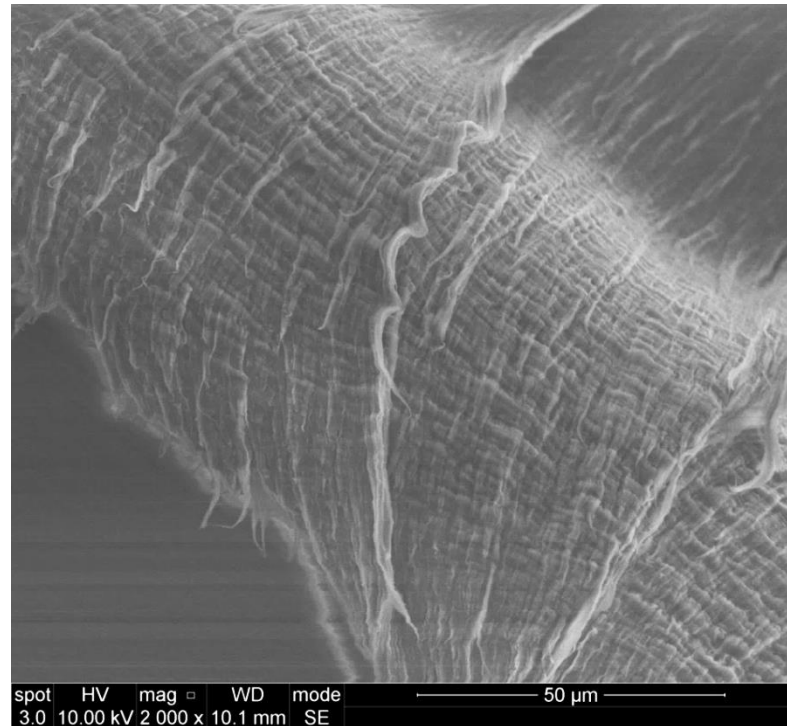


Figure 5-21 Sample 1 (x2000 magnification)

Moving away from the extreme end of the ductile failure (i.e. the threshold of the U-valley), to the start of the ductile elongation; a transition from brittle to ductile failure is observed. This is illustrated in Figure 5-22 at 1500 times magnification.

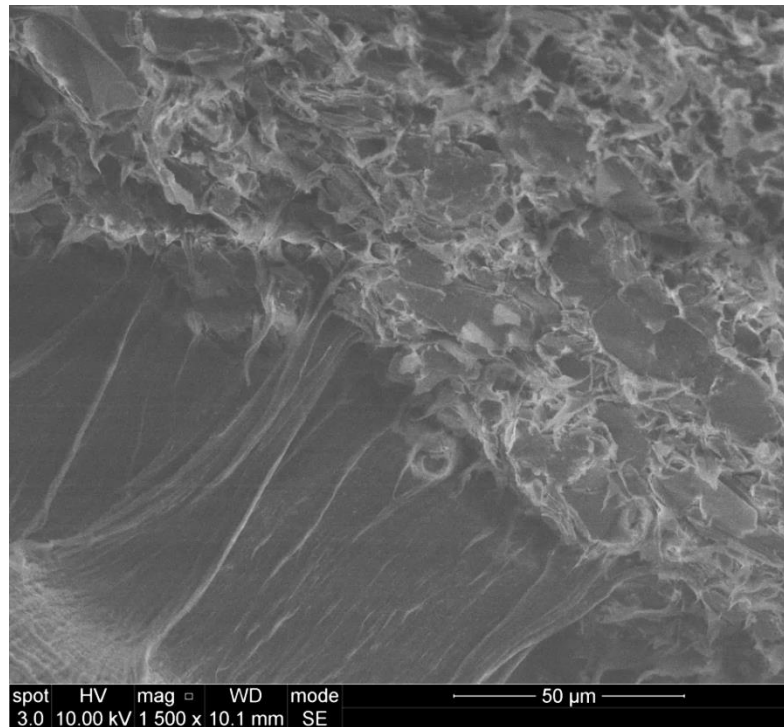


Figure 5-22 Sample 1 (x1500 magnification)

Figure 5-23 and Figure 5-24 both show the brink of two U-valleys at slightly different locations but on the same filament wire line at 1000 time magnification. Here, the failure surface shows some attempt at bonding to the fitting with some short polymer elongations throughout the surface. It is interesting to note that in the centre of each 'dark' region (between elongations on the pipe surface), there appears to be lighter coloured patches. This may be the remains of the talc contamination. However, this is only an assumption and would require a further chemical analysis of the failure surface to take place to determine the makeup of the fracture surface.

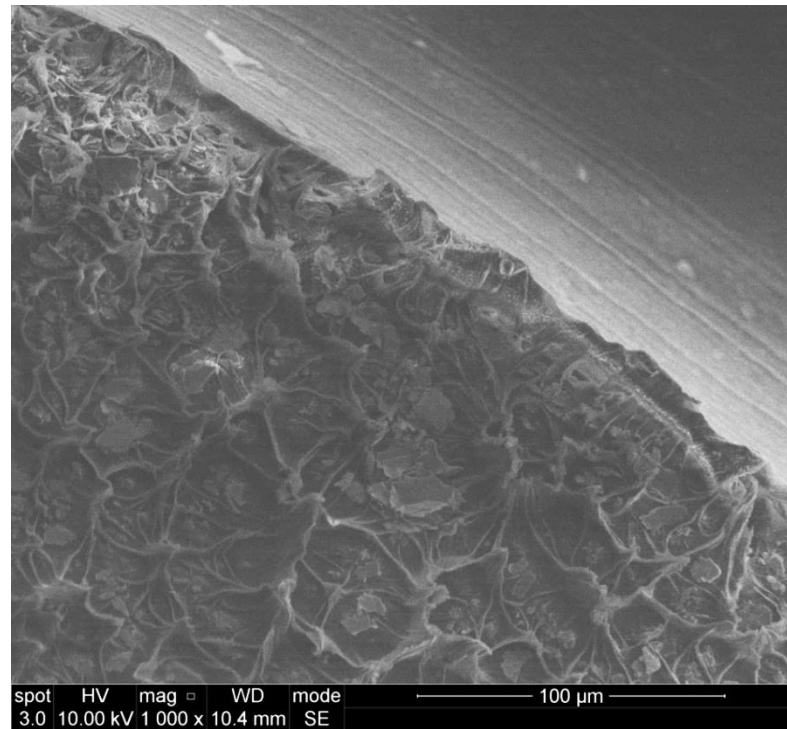


Figure 5-23 Sample 1 (x1000 magnification)

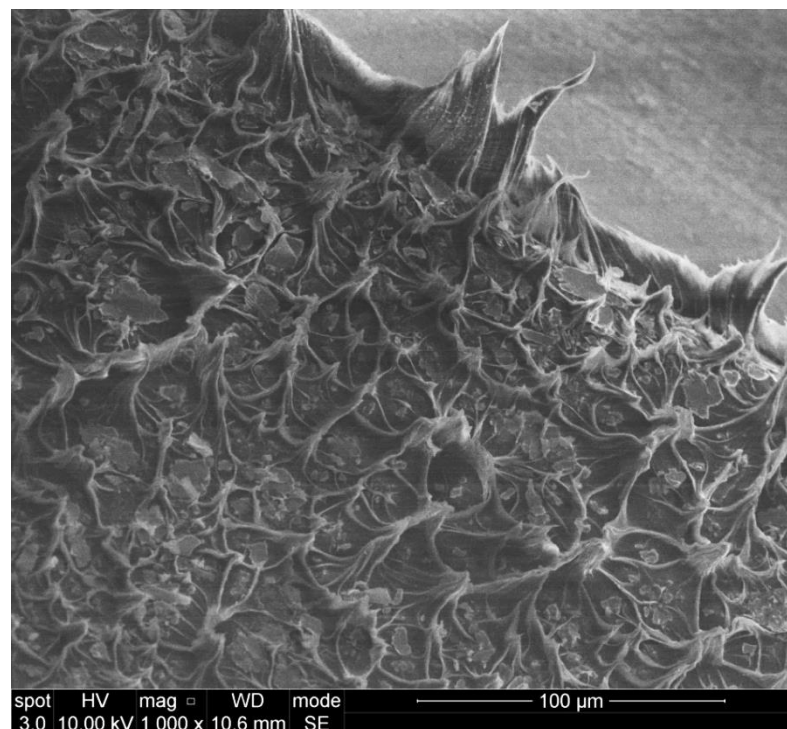


Figure 5-24 Sample 1 (x1000 magnification)

Sample 2

Figure 5-25 and Figure 5-26 show SEM analysis of U-valleys for sample 2 at 60 and 150 times magnification respectively. Like sample 1, there appears to be a difference in failure surface between the threshold of the U-valley in comparison to between the valleys themselves.

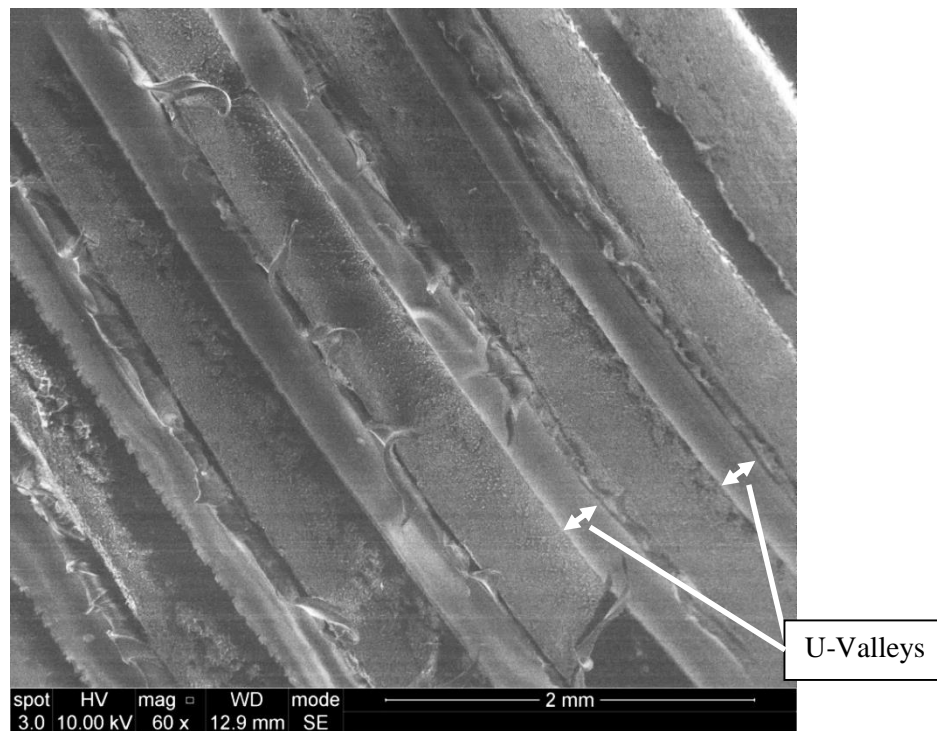


Figure 5-25 Sample 2 (x60 magnification)

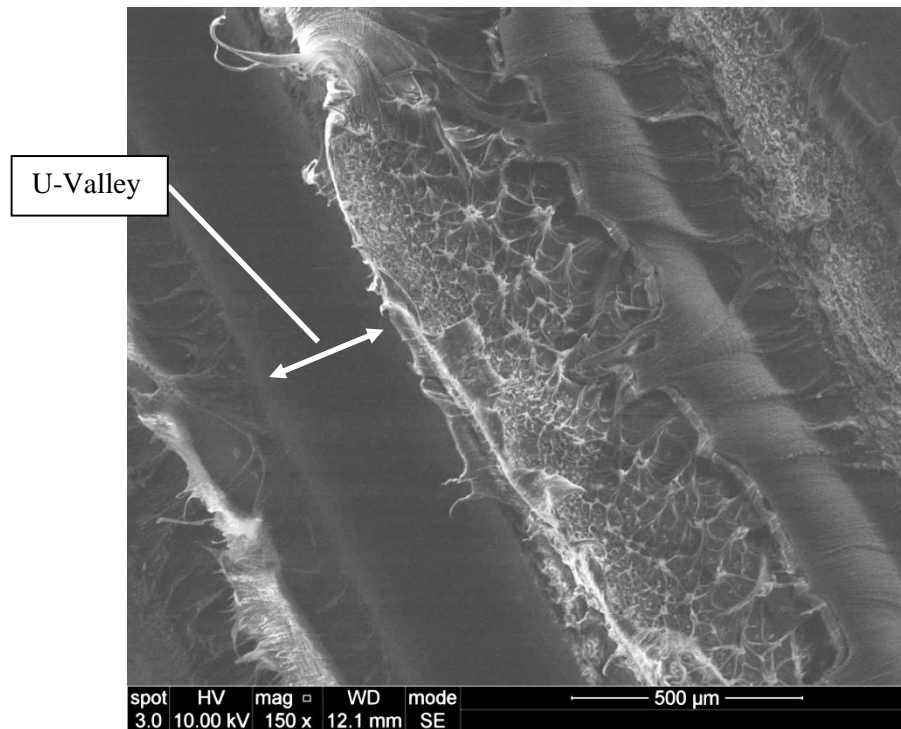


Figure 5-26 Sample 2 (x150 magnification)

Much like Sample 2, Figure 5-26 shows some ductile elongations are at the threshold of the U-valleys.

Sample 3

The third sample showed little bonding present via inspection by eye. Figure 5-27 shows the failure surface of sample 3 showing the U-valleys running left to right in the picture.

Figure 5-28 illustrates the failure surface of the parent pipe between the U-valleys. Much like the failure surface between valleys observed in sample 1 and 2, there appears to be a mainly brittle failure.

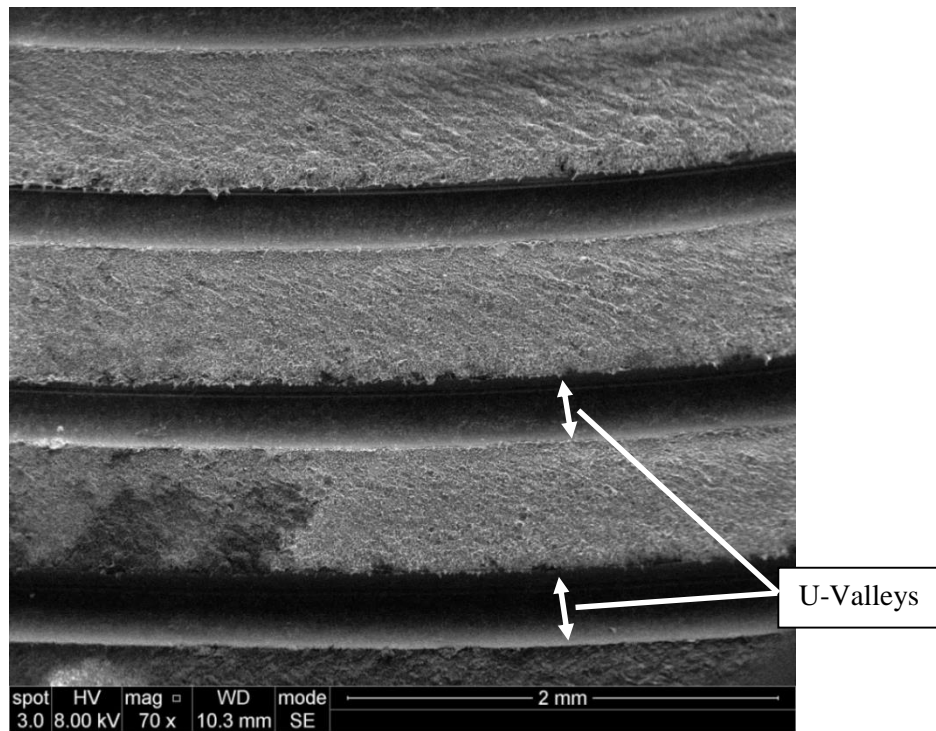


Figure 5-27 sample 3 (x70 magnification)

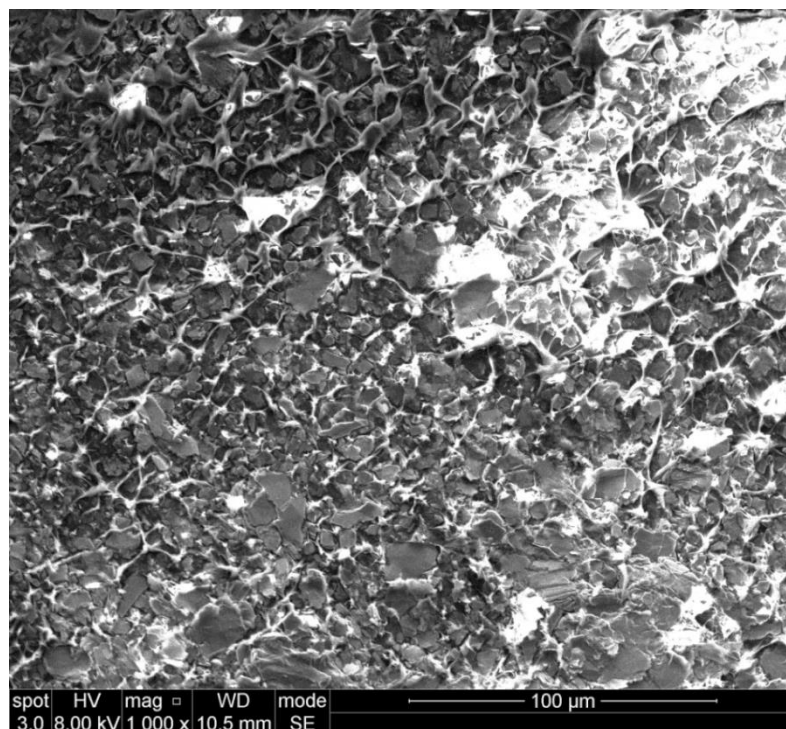


Figure 5-28 Sample 3 (x1000 magnification)

Figure 5-29 gives an indication of the brittle surface at 1500 time magnification.

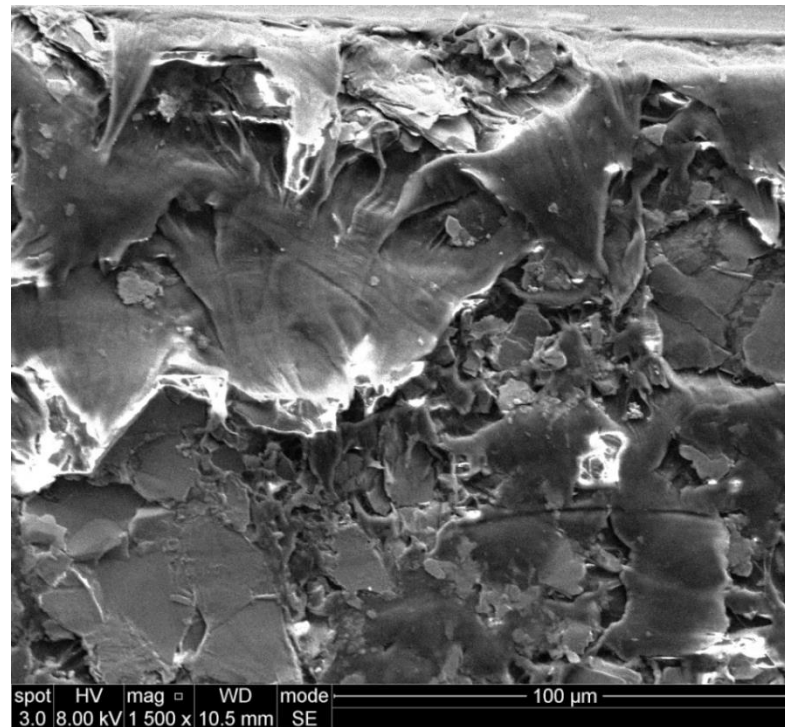


Figure 5-29 Sample 3 (x1500 magnification)

Figure 5-30 illustrates the U-valley at the top of the photograph and the brittle failure surface at the bottom. Note that in the middle of the photograph there are elongations that show a small amount of bonding has taken place.

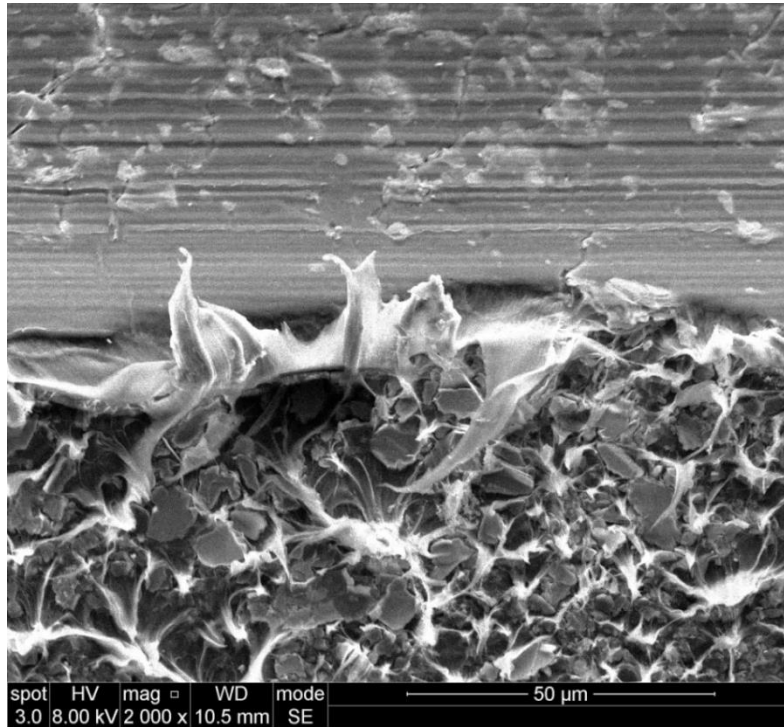


Figure 5-30 Sample 3 (x2000 magnification)

Figure 5-31 (below) shows the full extent of the U-valley. The channel appears to have small white particles that vary in size ranging from $\approx 0.5 \mu\text{m}$ to $\approx 6 \mu\text{m}$. Five particles were picked at random and the size was estimated using the '50 μm ' scale at the bottom of the photograph. These white particles (areas) correspond to the particle sizes and distribution that is expected from the talc contamination of the pipe surface prior to welding (see Appendix A for Contamination Experiment for distribution and size particulate contaminant using talcum powder). However, there is no evidence that upholds this without providing a chemical analysis of this surface. Unfortunately, the analysis was unable to be performed during the SEM analysis in this project.

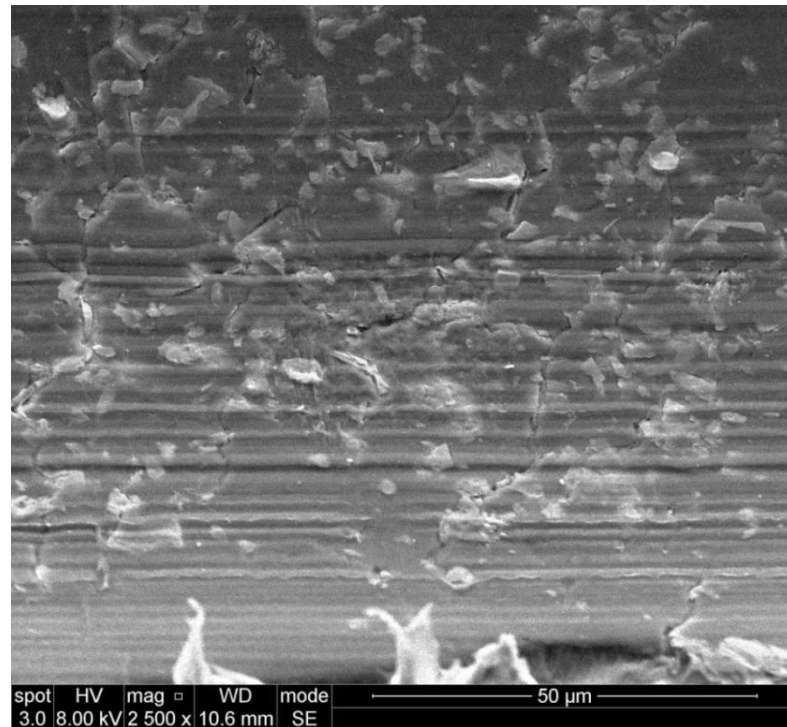


Figure 5-31 Sample 3 (x2500 magnification)

Sample 4

Sample 4 was observed visually to have no remains of black polymer from the fitting. It was also highlighted as this was the area that had the most prolific leak path when water flow was applied using a hand pump.

Under the SEM analysis, like the previous samples, there appeared to be a distinct difference in the failure surface at the threshold of the U-valley in comparison to between the valleys. This is further evident in Figure 5-32 and Figure 5-33.

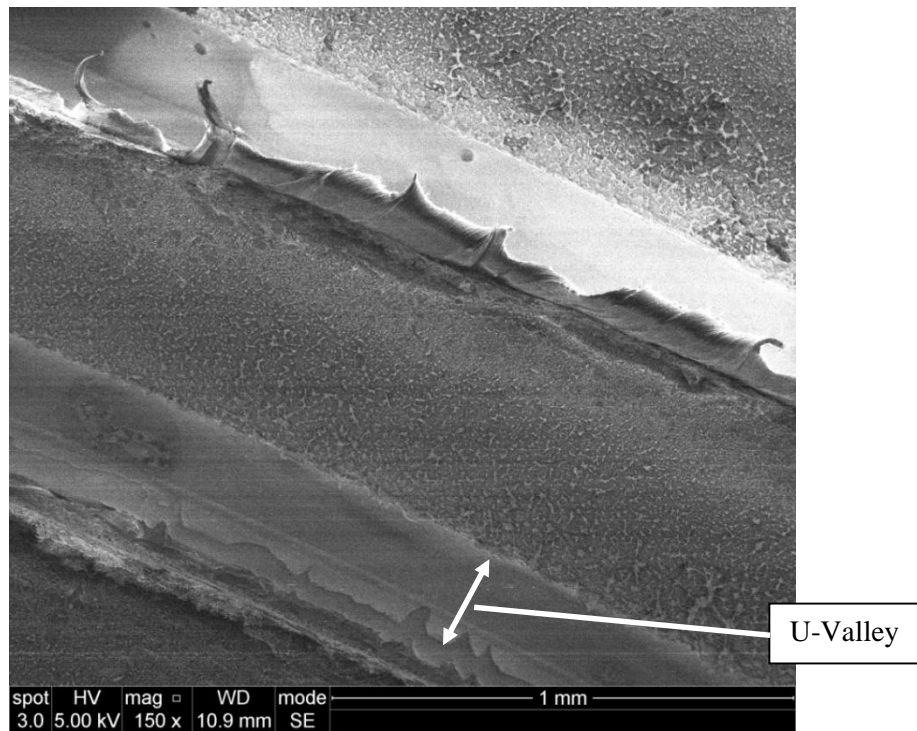


Figure 5-32 Sample 4 (x150 magnification)

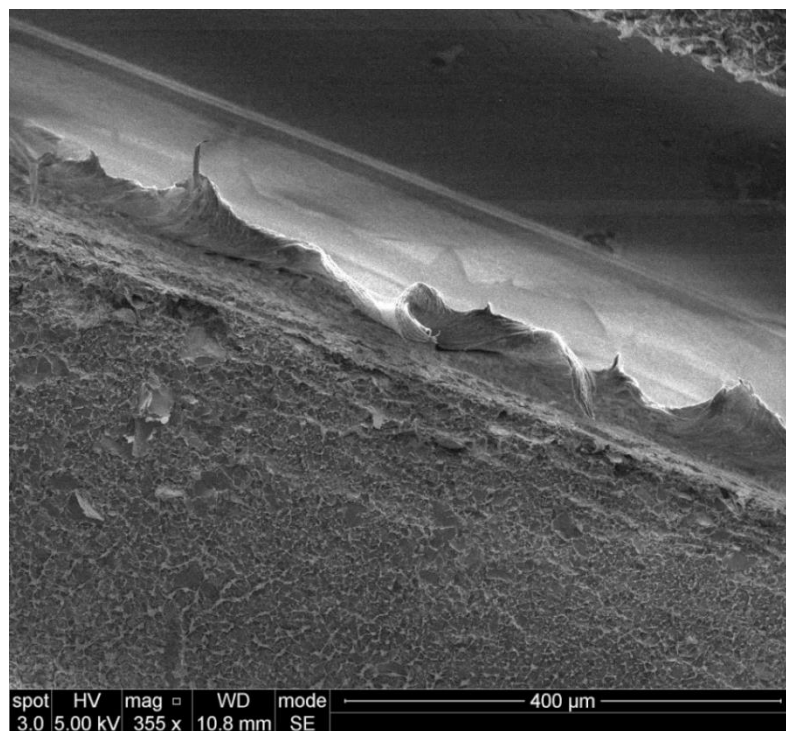


Figure 5-33 Sample 4 (x355 magnification)

5.5. Conclusions

In basic terms, the crushing decohesion test showed a major difference in failure mode between a contaminated joint and a joint that had been made to best practice. It is important to stress that the perfect joint did not fail during the implementation of this test which shows the significant capacity of strength of an electrofusion tapping tee. However, in comparison, the contaminated electrofusion tapping tee came away from the parent pipe showing a classic Mode I tensile failure about the fracture surface.

Adhesion with respect to fatigue testing confirmed the similarities in bonding with respect to the failure surface of a contaminated electrofusion tapping tees. It also confirmed that filament wires were always still embedded in some areas of the parent pipe which suggests that the wires may have been offering a degree of structural strength to the fitting under load. Major leak paths appeared to be random across the samples which may suggest that failure is spontaneous with respect to failure path and reinforces that the joints were welded without bias. However, minor leak paths became more predominant as the pressure range reduced. This may suggest that the entire fusion zone is subject to crack propagation (i.e. delamination) during long periods of dynamic load.

A generalised summary of the findings from the SEM analyses are given below:

- There was a distinct difference in the failure surface between the threshold of the U-valley (where the filament wire was held post-fusion) and in-between U-valleys.
- The failure surface at the threshold of the U-valley appeared to be of a ductile nature with some examples showing long elongations and even ripples of the polymer at high magnifications.
- The failure surface between the U-valleys was different to the threshold of the U-valleys. Here, the surface was peppered with very short elongations of polymer which suggest a very small amount of ductility. However, closer inspection between these elongations potentially shows a brittle surface
- The analysis suggests that some talc contamination may be embedded onto the failure surface. This is shown as a lighter colour in contrast to its surroundings. However, this assumption requires further research; potentially a chemical analysis will be required in order to confirm that the observed is actually due to the talc contaminant.

The specimen that was cut into samples for the SEM analysis, Specimen X, was subject to the fatigue testing regime as highlighted in Section 5.3. Post-failure of the fatigue test, the specimen was subject to the crushing decohesion test; it is at this point samples were created

for the SEM analysis. It is essential to note that the conclusions stated above are likely to be a result of the crushing decohesion test as opposed to the fatigue test. When a specimen fails during the fatigue test a leak path is formed such that the water housed within the system escapes via the leak path. Full delamination of the jointing surface does not occur and therefore it is difficult to assess the exact failure mechanism. The aim of the SEM analyses were to gauge a better understanding of the bonding between the two PE elements (pipe and fitting) when they are subject to the talc contamination. This would inevitably only be achieved by full delamination of the joint assembly and therefore the crushing decohesion test facilitated this.

To gain a better understanding of delamination and during a live fatigue test, non-destructive techniques are required. This in turn should confirm the failure mechanism of contaminated joints subject to a low-cycle fatigue testing regime. This will be explored and explained further in Chapter 6

Chapter 6

Confirming the failure mechanism - Non-destructive testing

Following analyses obtained from destructive tests to better understand the potential failure mechanism using industry standard testing methods, non-destructive ultrasonic methods of analyses were performed in two scenarios with two separate aims. Fundamentally, both methods aimed to better understand and potentially confirm the failure mechanism of contaminated electrofusion tapping tees. The methods are briefly explained thus:

- i. Static analysis: A rig was designed to observe leak paths in joints that had failed under dynamic load as per Section 4.1 to observe the leak path of the failed specimens to observe any similarities in the failure mode with relation to pressure range; viz. post-failure analysis.
- ii. Real-time analysis: Rigs were designed to observe the failure mechanism of contaminated electrofusion tapping tees during a live fatigue test. Here, it was hoped that delamination of the welding interface would be observed.

The following section will explain (i) and (ii) in further detail. It shall be noted that static analyses were performed in conjunction with this project, under the supervision of the author, by two separate MEng final year students in consecutive years. An outline of their methodology and outcomes will be explained to strengthen the discussion and conclusions of this research. However, for further details, the theses of the candidates should be referenced.

6.1. An introduction to Non-destructive testing

Destructive testing is an essential practice to assess and ensure that any product is fit for purpose. In general, non-destructive testing (NDT) can be used to assess the current state of an element, product or assembly without causing damage. NDT methods can be computational; whereby signals are sent and received from instrumentation that processes the

information into the required format, or visual; where a trained operative will assess the element.

With regards to NDT of PE pipes and fittings, there are several computational techniques that are used in the industry; ultrasonic testing is one of these. Further guidance of the use of ultrasonic testing for welded joints can be found in BS EN 13100-3 [69].

6.1.1. What is ultrasound?

Szilard [70] describes a ‘sound wave’ to be within an audible range with frequencies approximately between 20 and 20,000 Hz. Waves below this range are known as infrasound and waves higher than this range are known as ultrasound. The penetrative nature of ultrasound has led to its use in non-destructive testing methods for engineering applications. The efficiency in which energy can propagate through a given material will be dependent on the stiffness and damping properties of the host material [71].

There are several different methods and techniques of implementing ultrasonic technology for analytical purposes to plastic pipes and fittings. A method that can be used in detecting defects and voids in PE pipe and buttfusion welds is the use of Phased Array Ultrasonic Technology (PAUT) [72]. This method has also been transposed to assess defects in electrofusion welds [73]. Here, a ‘wedge’ was developed consisting of multiple sensor elements and normal linear (perpendicular to the surface) scans were – specifically focussing at the fusion zone. The initial results showed that the fusion wires and the heat affected zone (HAZ) were visible using the PAUT method.

6.2. Static analysis

A rig was designed and built (

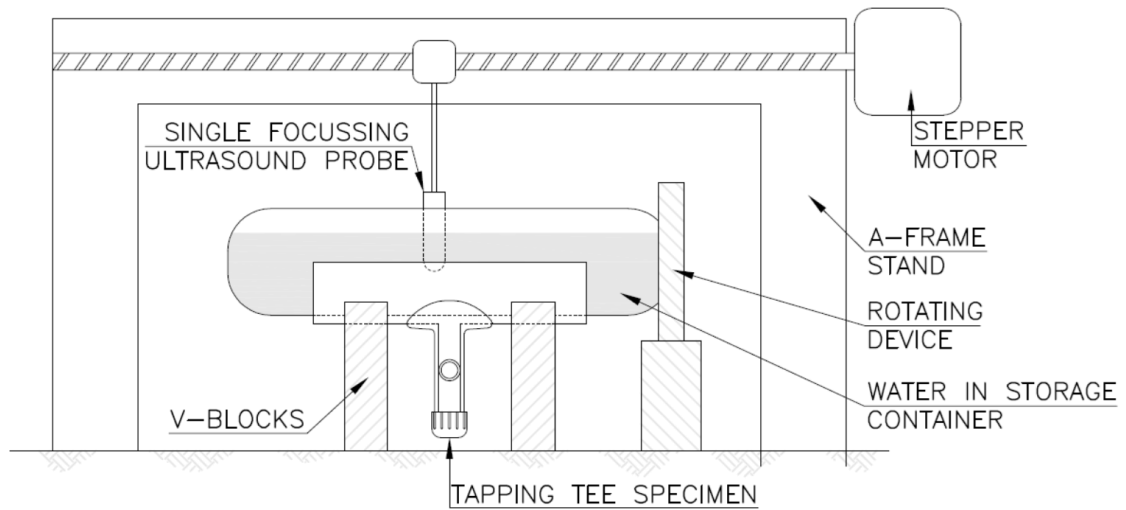


Figure 6-1) to observe the leak paths of contaminated electrofusion tapping tee joints failed in the fixed mean fatigue test previously mentioned in Section 4.1. The rig consisted of a single 10 MHz ultrasonic focussing transducer attached to a stepper motor and moveable stage; allowing individual line scans to be performed. Scans were executed on the bore of the pipe with an aim to identify leak paths (delamination of the jointing interface) by observing the fusion zone using a single ultrasonic transducer and post-processing the data obtained. The first MEng project [74] aimed to develop the rig and perform sample scans as a proof of concept. Three scans were performed using the rig. However, the specimens used in this experiment had previously failed in a ramp to burst test with a constant increase in pressure of 25 bar/min (see Section 3.1.1 for the outline methodology).

The previously failed joints were cut in half along the centre line of the pipe using a bandsaw. This left the bore and the underside of the tapping tee exposed so that the ultrasonic transducer could focus on the bore of the pipe. The focussing lens transmitted ultrasonic pulses perpendicular to the bore of the PE pipe and fitting assembly, thus observing the fusion zone.

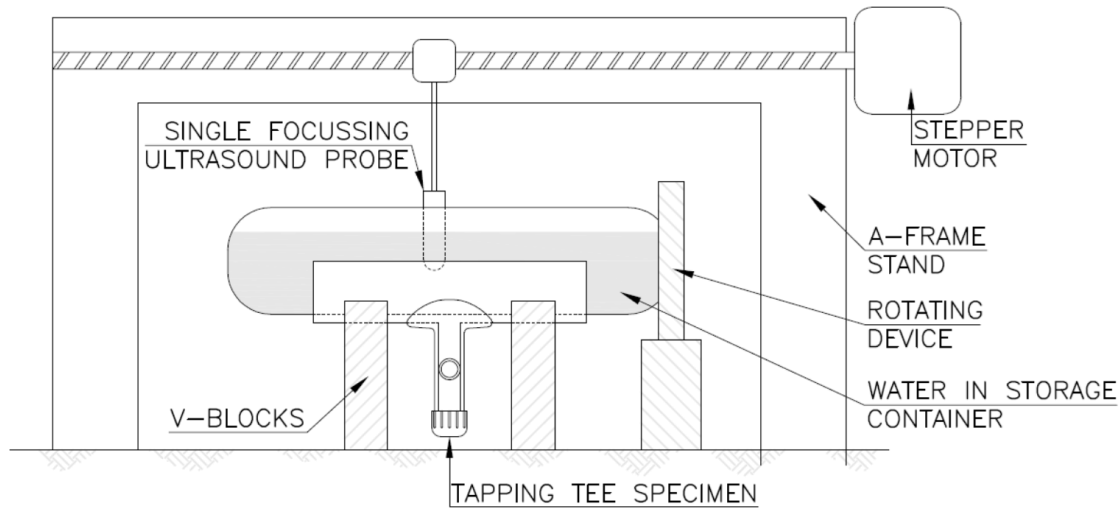


Figure 6-1 Ultrasound static scanning rig

A plastic container was secured to the tapping tee and filled with tap water which acted as the couplant medium for the transducer. A rotating mechanism with protractor was retrofitted to the container as an engineered solution for referencing the rotation of the specimen for individual scans. Once a line scan was performed, the specimen was rotated 2° and another line scan was performed. This was repeated until the entire fusion zone was scanned. All mechanical aspects of the rig were controlled using a bespoke program for this project co-written by the author and Howard [75]. This was achieved using a visual programming language, LabVIEW by National Instruments.

6.2.1. Overcoming obstacles

During the welding process of an electrofusion tapping tee, as mentioned in Section 1.2.3, there is a small degree of local deformation caused by the force applied by the top-loading clamp. The deformation temporarily causes the pipe to become slightly oval locally but more importantly, a small bump is formed that is usually the same diameter as the cutting screw hole of the tapping tee (see Figure 1-8). The local ovality and bump are difficult to see with the naked eye. However, the bump can be felt on the bore of the pipe when brushed over by hand. The deformation is small so it is therefore negligible with respect to affecting on the performance of the asset. However, with regards to ultrasonic analyses, signals are lost when the transducer passes over the bump as the pulse is not reflected parallel to the surface of the pipe. To overcome this issue, the transducer was locally rotated in order to pick up the lost signals and give a complete dataset of the scan. As the size and shape of each bump may have

varied, the rotated transducer's angle of attack may have been slightly different for each joint analysed.

The transducer was rotated using a fine pitch adjustable clamp until a strong signal was received about the bump of the bore of the pipe. The transducer was then removed from the clamp and replaced with a pointer manufactured from mild steel. The pointer was used to ensure the probe's starting position was consistent with scans conducted perpendicularly to the surface of the pipe. Once the probe was rotated, the angle was in the region of 45° to the surface of the pipe as per Figure 6-2. Note that Figure 6-2 is not to scale and therefore is indicative only.

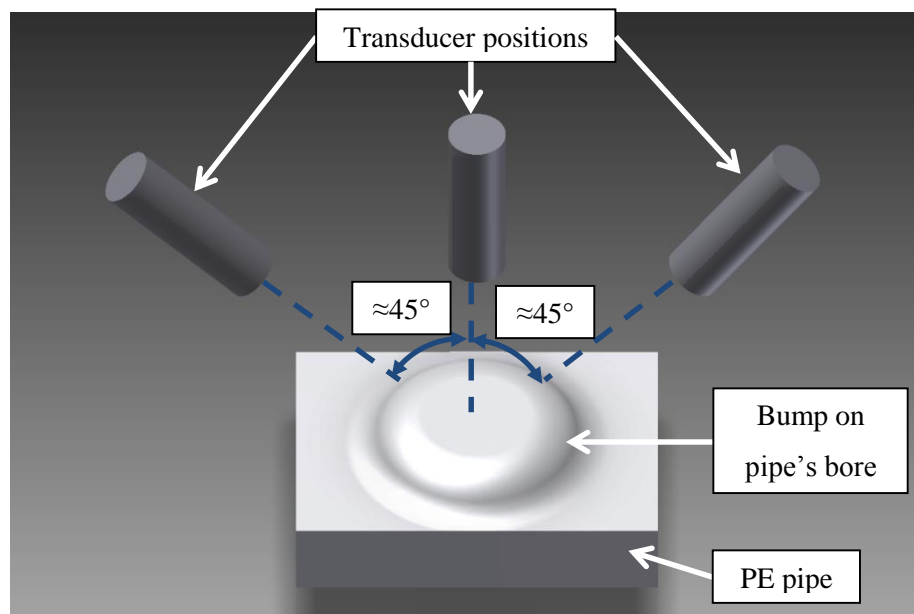


*Figure 6-2 Approximate transducer locations with respect to PE bump
(Note: Indicative sketch only – Not to scale)*

6.2.2. Preliminary results – proof of concept

Preliminary line scans were conducted on the bore of the pipe to observe any delamination about the fusion interface of three contaminated electrofusion tapping tees after they were previously failed via the ramp to burst test. The data obtained from the line scans were processed using MATLAB. The data were arranged to create an intensity map by knitting together the individual line scan data; thus showing the fusion zone. Intensity in this case is expressed as the magnitude of reflected signal received by the ultrasonic transducer. In theory, once intensity is plotted with respect to line scan position, a leak path should be observed. Figure 6-3 shows the intensity map (Figure 6-3a) and the specimen scanned (Figure 6-3b).

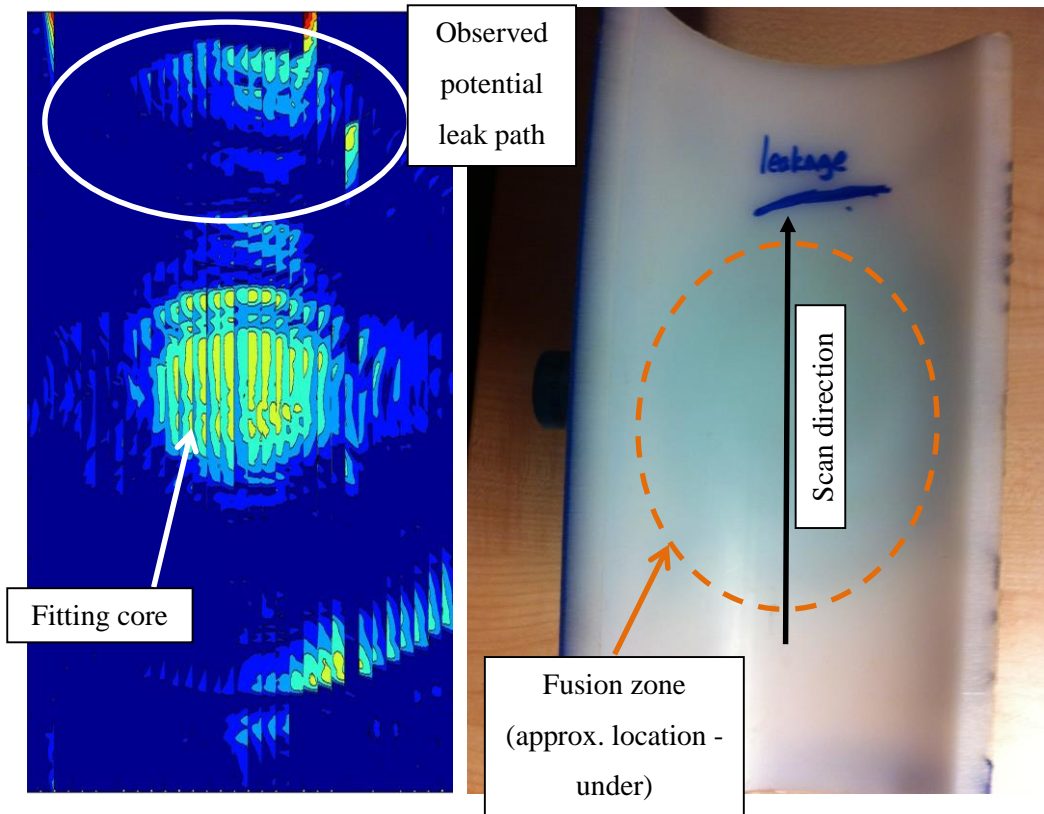


Figure 6-3 Preliminary line scan results showing leak path (a) and scan direction (b) [74]

Once the map was created and analysed, the leak path hypothesis could be confirmed by applying a flow of water through the tapping tee fitting. This was achieved using a basic hand pump that was attached to the stem of the fitting (Figure 6-4). For this particular specimen, the leak path has been highlighted to be at the same location as found from the ultrasonic line scan experiment.

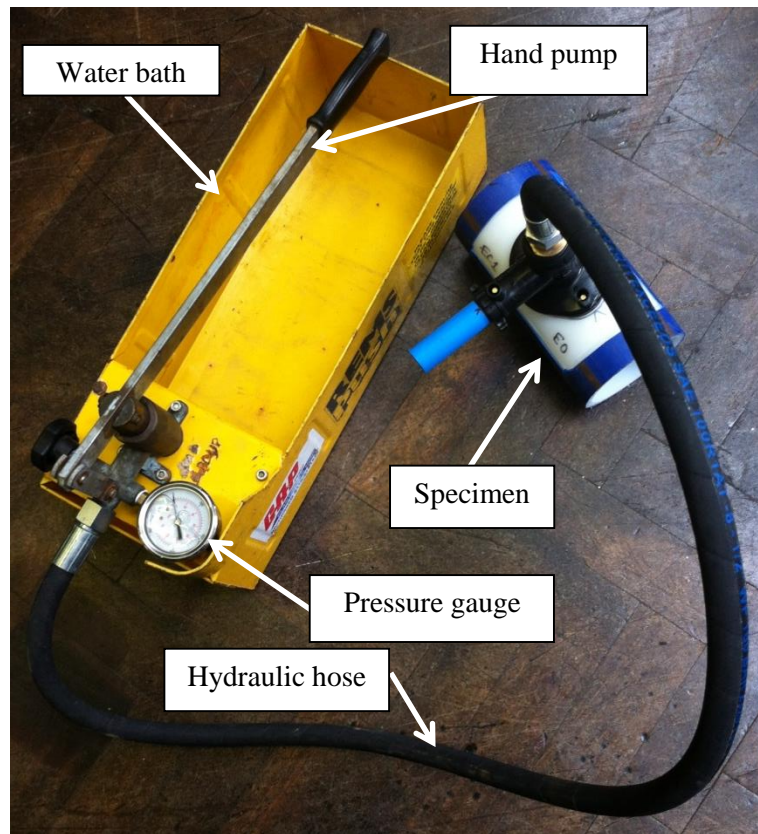


Figure 6-4 Hand pump and fitting (attached)

For the purpose of this thesis, the two other scans performed in this MEng project as a proof of concept will not be shown. In general, the results from the two scans appeared to show the major leak path of each specimen. However, the signal intensity maps appeared to highlight other parts of the fusion zone that could have been interpreted as leak paths. The aforementioned parts were not apparent when the results were verified using the hand pump. Therefore, a secondary MEng project was conducted the following year to further develop the data capture and analysis techniques – this is further explained in Section 6.2.3.

6.2.3. Leak path investigation with respect to fatigue pressure range

Specimens were further analysed as part of a second MEng project as previously mentioned in Section 5.2 - Adhesion with respect to fatigue test. This project, fully supervised by the author, used the existing static analysis rig and observed several joints that had failed at different pressure ranges as highlighted in Table 5-1. Like the previous project explained in Section 6.2.2, the data obtained from the scans was analysed using MATLAB.

Initially, a specimen that had been made to best practice principles was scanned to further benchmark the apparatus and data analysis methods post-scan; this can be observed in Figure

6-5. Here, the fitting core is clearly observed as is the outer area of the fusion zone. As the main features of the analysis are the fitting core and the outer regions of the fitting (beyond the fusion zone), it is evident that this fitting has no leak paths present, i.e. no obvious signs of delamination about the jointing interface. Note that the x-axis is in millimetres and the y-axis is in degrees. The colours in Figure 6-5 represent the signal intensity from the ultrasonic transducer at a given scan position. In theory, the graphical output should illustrate that the higher the signal intensity, the higher the likelihood of a leak path being present.

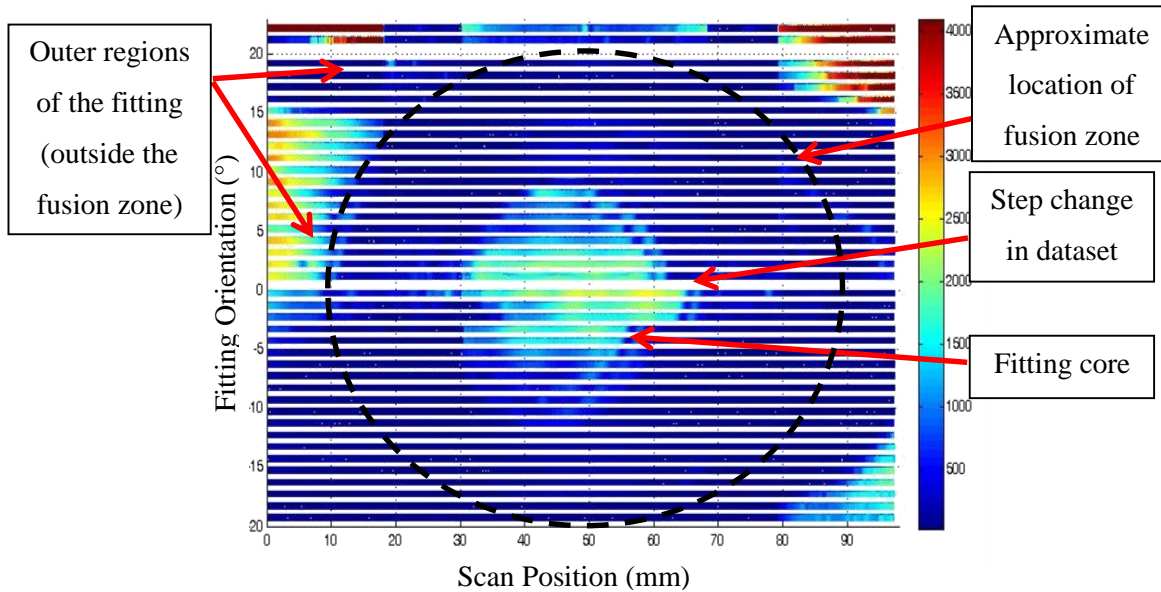


Figure 6-5 Static ultrasonic scan of perfect joint [67]

Highlighted in Figure 6-5 is a step change within the dataset that may indicate a manual discrepancy; most likely from rotating the probe by hand to compensate for the bump on the bore's internal surface of the PE pipe as discussed in Section 6.2.1. In hindsight, this may have been overcome if the rig were fully automated; however this was out of the scope for the MEng project.

The following gives testament to some of the work carried out by the MEng student. As depicted in Table 5-1, a total of six joints were analysed. For explanatory purposes, only three joints will be discussed hereafter (see Table 6-1):

<i>Joint Reference</i>	<i>Pressure range</i>	<i>No. of cycles to failure</i>
H	90% $P_{MAT, MAX}$ (22.5 bar)	1
BW	70% $P_{MAT, MAX}$ (17.5 bar)	3
AP	50% $P_{MAT, MAX}$ (12.5 bar)	119

Table 6-1 Joints discussed in this section

The joints highlighted in Table 6-1 have previously been discussed in Section 5.2. It is important to note that the work undertaken in this section was performed prior to the destructive testing of specimens highlighted in the previous section. Therefore the destructive testing undertaken was to confirm the work carried out using non-destructive ultrasound techniques.

After each specimen was scanned, a hand pump was attached to the stem of the tapping tee and water was pumped through to confirm the location of the leak path; as mentioned previously in Section 6.2.2. Once the leak path was known, the tapping tee was then removed from the parent pipe as per results in Section 5.2.

Figure 6-6 to Figure 6-8 illustrates joints H, BW and AP respectively. Each figure indicates the potential leak path(s) (in **purple**) that are a result of the analyses as well as the actual leak path(s) (in **red**) as a result of the hand pump tests (work previously mentioned in Section 5.2). The approximate location of the circumference of the fusion zone is indicated in **black**.

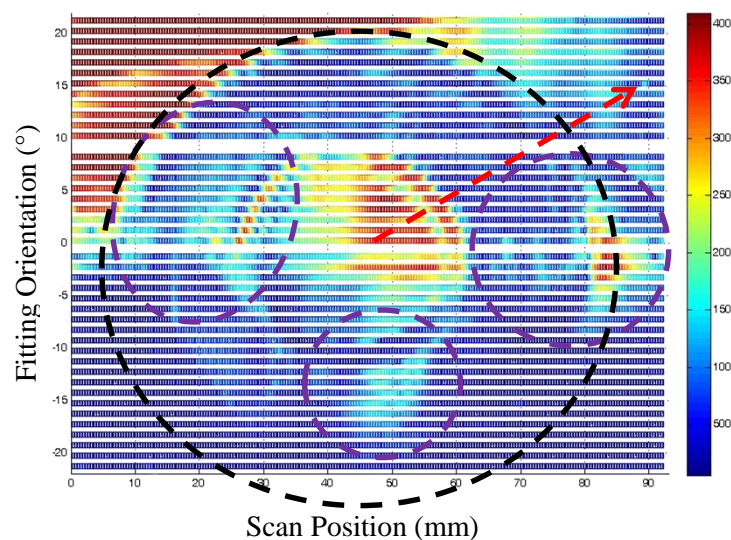


Figure 6-6 Ultrasonic scan of Joint H [67]

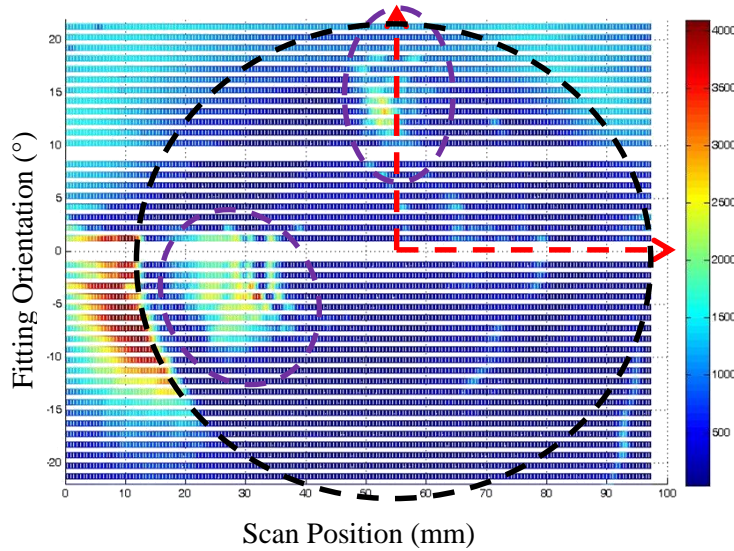


Figure 6-7 Ultrasonic scan of Joint BW [67]

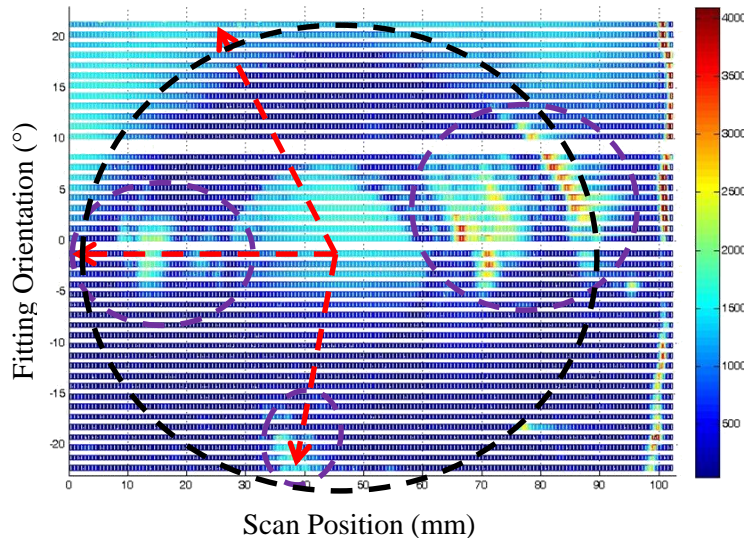


Figure 6-8 Ultrasonic analysis of Joint AP [67]

The ultrasonic scans performed in these instances do not conclusively observe all leak paths in all fittings. There were some instances where the scans completely missed some delaminated areas. However, in some instances, the scans were successful in that the leaking area was observed.

6.3. Real-time analysis

An experiment was developed purely for proof of concept; to observe the failure mechanism of a contaminated electrofusion tapping tee during a live fatigue test using non-destructive

ultrasonic methods – or, if it is at all possible to do so. This experiment ran parallel to the aforementioned MEng project using static methods of ultrasonic analysis.

To reduce the length of long fatigue tests, a specific pressure range and mean was decided whereby the number of cycles to failure could be predicted to a degree of confidence. From the results of the fixed mean approach to the fatigue performance of contaminated electrofusion tapping tees (see Section 4.1, Figure 4-2), the testing parameters were fixed to $P_{MEAN} = 12.5 \text{ bar}$ (1.25 MPa) and $P_{RANGE} = 17.5 \text{ bar}$ (1.75 MPa) - as per $70\% \times P_{MAT,MAX}$. By using these test parameters, the predictability of failure with the 95% confidence limits of the statistical analysis conducted in Section 4.1 was between 3 and 23 cycles.

6.3.1. Rig concept – overcoming obstacles

The main aim of the experiment, and of which the main criteria the rig design needed to satisfy, was to observe crack growth about the fusion interface of a contaminated electrofusion tapping tee under dynamic load using ultrasonic techniques; thus proving the failure mechanism. This would need to be overcome by the design and development of a sensor array that would be located inside the PE pipe; focussing on the fusion zone.

Due to the compressive force that is applied during the fusion and cooling cycles of the electrofusion welding cycle (see Section 1.2.3) via the top-loading G-clamp, a small amount of local deformation on the bore of the PE pipe was observed (also mentioned in Section 6.2.1). A visual inspection of several welded joints revealed that the deformation was in the same location however the magnitude of deformation varied. It was also noted that the pipes were not perfectly round. These issues would need to be overcome in the design of the rig. In general, both ovality and local deformation are small (maximum couple of millimetres), however, not insignificant enough to ignore during the design process as precision engineered parts will need to be manufactured.

It was decided that the best way to observe a crack growth mechanism was to design an array of sensors in an arrangement that would give an appropriate resolution to observe the failure mode. The alternative methodology would be the use of a single fully automated focussing probe that would scan the entire fusion zone in a short space of time. This was ruled out as the results would not give a fair representation of the fusion interface due to the scanning methodology. With this in mind, two design concepts were debated for the initial design of an array of sensors:

- i. Sensors in a fixed linear arrangement can be placed at a fixed distance from the surface of the bore of the pipe. The arrangement would sweep the bore of the pipe local to the fusion zone to observe the failure mechanism.

Advantages: The sensor holder (that houses the fixed linear arrangement of sensors) will require fewer sensors than the ‘pad’ design as the sweeping motion will increase resolution capacity. The rig can be reused to achieve multiple tests.

Disadvantages: Mechanical parts required to perform a sweep of the fusion zone. This will require manufacture and assembling time and any alterations as required. A bespoke program/script will be required to control and acquire data simultaneously.

- ii. A sensor ‘pad’ that would be large enough to cover the tapping tee’s fusion zone. The pad would be located at a fixed offset from the surface of the bore of the pipe, or, attached directly onto the bore of the PE.

Advantages: A high number of sensors will increase the resolution of the observation area (fusion zone). No moving/mechanical parts.

Disadvantages: A higher number of sensors will increase data acquisition requirements and potentially put more strain on the post-processing of data. The sensor ‘pad’ will need to overcome any local deformation of the bore of the PE pipe. More sensors may mean longer manufacturing times and may drive up cost. If sensors are placed directly onto the pipe, glue may be required which means that the sensors may become damaged if removed from the pipe surface – viz. the sensors can only be used once.

It was considered that the linear sensor arrangement (option (i)) would be the best option as the rig can easily be reused therefore achieving more data through repeating tests. Also, a smaller number of sensors would reduce the size of data files acquired and therefore put less strain on the data acquisition software (program) and hardware (computer). This would inevitably make the post-processing of data acquired after the fatigue test much easier.

For this design, the sensor array would be submerged fully in water in order to transmit and receive signals; as the water acts as the couplant media between the sensor and the surface of the PE pipe. Therefore, it is inevitable that the contaminated electrofusion tapping tee specimen would be submerged in water also.

6.3.2. Ultrasonic sensor array design

Circular piezoelectric transducers with a pulse frequency of 10 MHz were used for the sensor arrangement. The transducers were 7 mm in diameter, silver coated and had a protective ceramic coating on the front surface (see Figure 6-9).

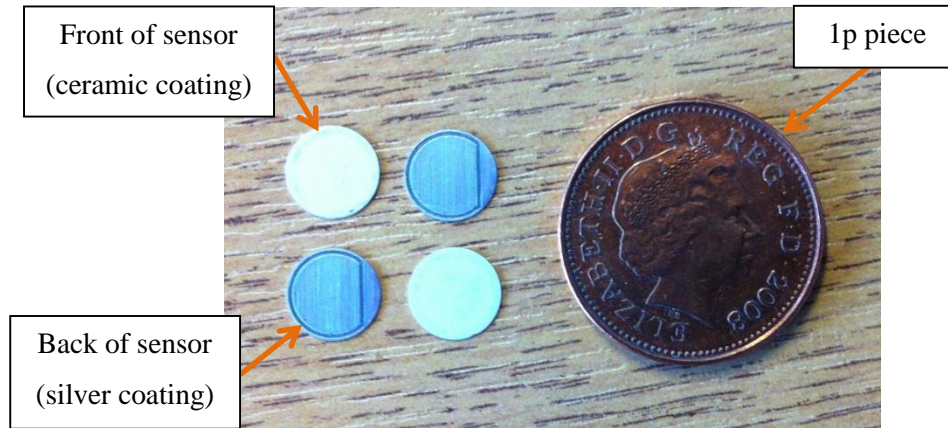


Figure 6-9 Circular piezoelectric transducers

The sensors were modified in size allowing for multiple sensors to be added to a small area to create a bespoke array probe. The circular sensors were cut to a rectangular shape using a custom-built sensor cutting device consisting of a Stanley blade either side of a 0.8 mm feeler gauge blade (see Figure 6-10). The feeler gauge blade was held between the two Stanley blades securely via two ground flat stock bars cut to length, drilled with two M3 nuts and bolts positioned such to hold the assembly together. This gave a cutting width of approximately 1.8 mm for the sensors.

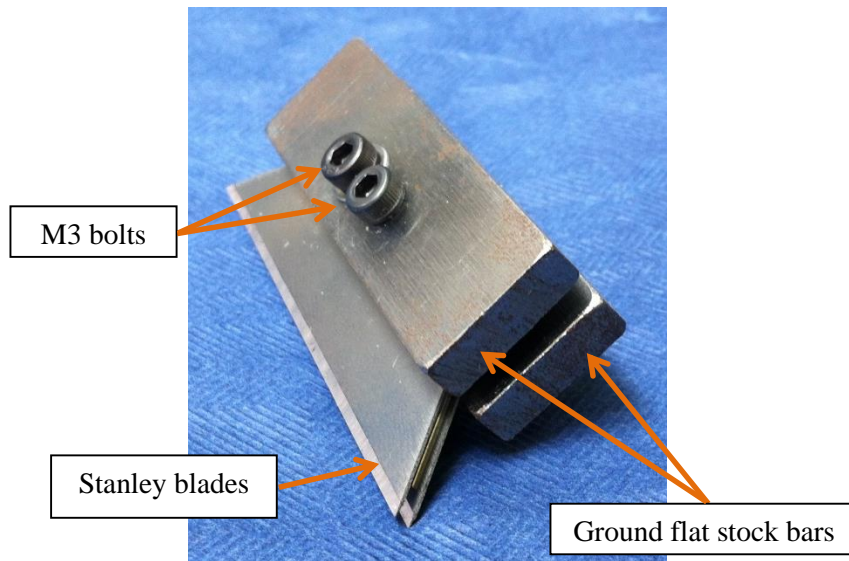


Figure 6-10 Sensor cutting device

The head of a 4 ounce ball-pein hammer was used to gently tap the assembly to cut the sensors to the required width. The sensors were tested after being cut using a basic data acquisition program to ensure they were operating correctly and not damaged as a result of the cutting process.

The area to be scanned was determined by measuring the width of the electrofusion tapping tee's fusion zone. This governed the dimensions for the sensor holder. As the sensor holder was to be submerged in water, aluminium was used as the material of choice as it is corrosion resistant, lighter than steel and arguably more robust than a plastic. A small square bar of aluminium was machined with a keyhole slot (see Figure 6-11) – the sensors would be housed here.

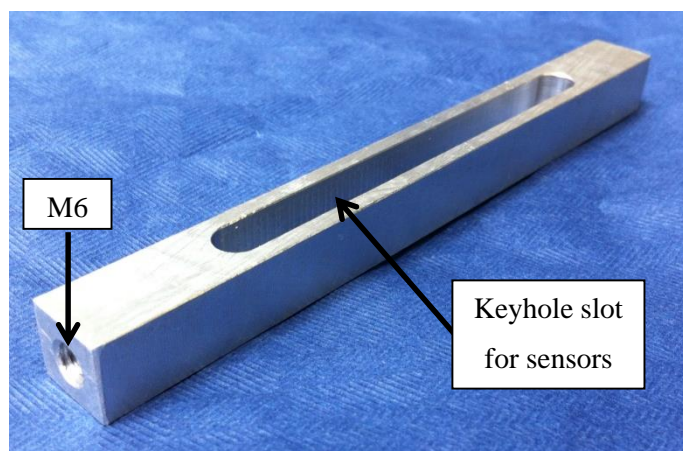


Figure 6-11 Aluminium ultrasound sensor array holder

To ensure the sensors were positioned correctly and evenly, a 2D drawing was created to 1:1 scale using AutoCAD (see Appendix C for all ultrasound rig drawings). The drawing was glued on a smooth, flat surface and double sided tape was placed on the 2D drawing of the sensor arrangement. Sensors were then positioned at 5 mm centres as per the 2D drawing. There were 16 sensors in total to cover the full width of the electrofusion tapping tee's fusion zone. Enamel coated copper wires were carefully soldered to each sensor and then the sensor holder was placed on the double sided tape in such a way that the wires were hanging out of the keyhole slot. It is important to note that the enamel was removed from the copper wire using tin solder and a soldering iron at its highest temperature. A layer of two-part epoxy resin was applied into the keyhole slot to ensure the wires, solder and sensors remain intact for the remainder of the manufacture of the sensor. After the epoxy resin had hardened overnight, coaxial cable was soldered to the copper wires and SMB type connectors were soldered and shrink wrapped on the opposing ends. The keyhole slot was then filled with more epoxy resin and allowed to harden over 24 hours – a 3D representation of the completed array is shown in Figure 6-12.

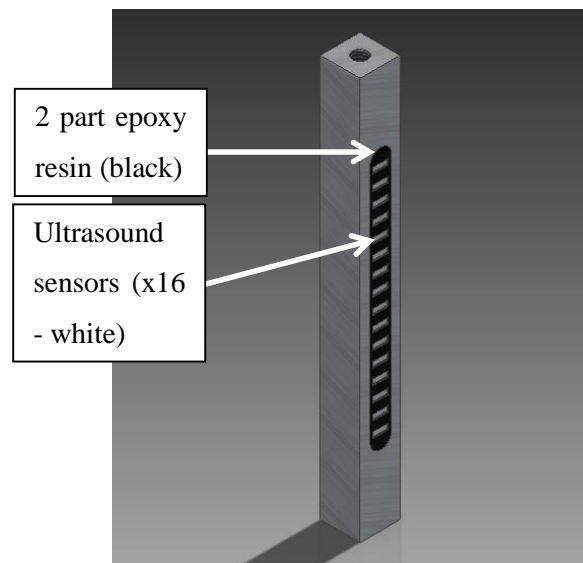


Figure 6-12 Sensor array holder with sensors

The sensor array was then attached to the data acquisition program and all sensors were checked to ensure that no damage had taken place. At this stage it was observed that 3 sensors were not working despite checking the sensors after they had been cut down to size. It can only be assumed that there was a fault in the connection between the copper wires from the sensors and the coaxial cable. Unfortunately, there was limited scope to check the sensors prior to the final casting of epoxy resin. Furthermore, there was no scope to repair the damaged sensors; as an entirely new sensor array would need to be manufactured. In hindsight, this is a

flaw within the design and manufacturing process – in order to rectify the damaged sensors, an entirely new sensor arrangement would need to be recast – i.e. replacing all sensors. Figure 6-13 shows the completed sensor array and indicates the damaged sensors.

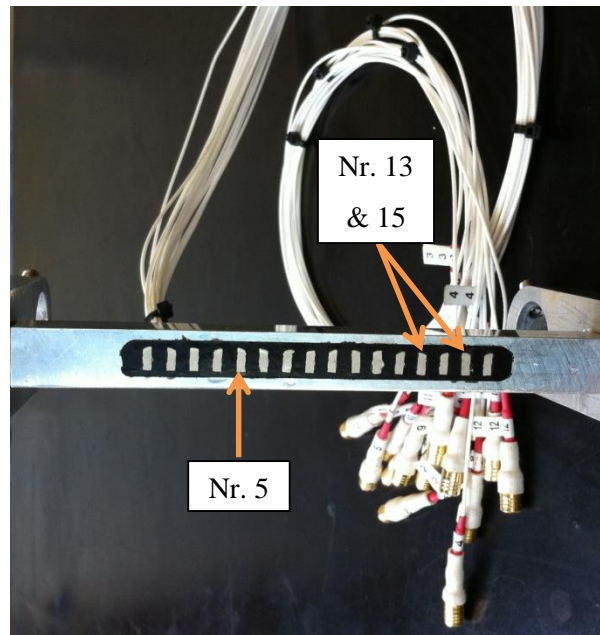


Figure 6-13 Sensor holder showing damaged sensors

6.3.3. Mechanical component design

As mentioned in Section 6.3.1, there was local deformation on the bore of the pipe where the electrofusion tapping tee has been welded. To ensure consistency in signal strength and quality, it is paramount that the distance between the sensor array and the observed element be constant. To overcome this deformation during the live ultrasonic analysis, a fork was designed to go either side of the sensor holder (see Figure 6-14a). The forks were machined from aluminium. The forks would push against a spring and thrust block (Figure 6-14b) which were attached to roller bearings (see Figure 6-16). This in turn, determined a constant offset to the bore of the pipe with respect to the front of the sensor holder.

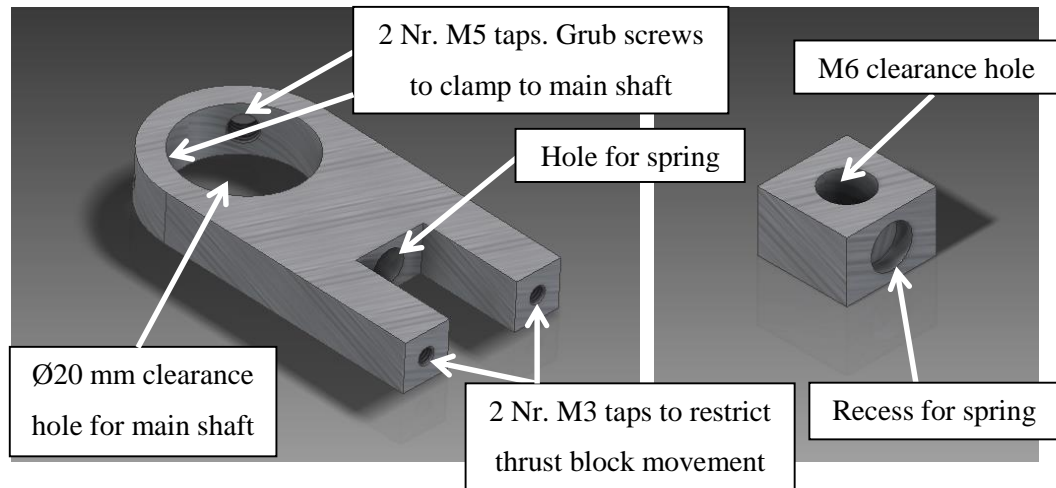


Figure 6-14 Aluminium fork design (a) & aluminium thrust block (b)

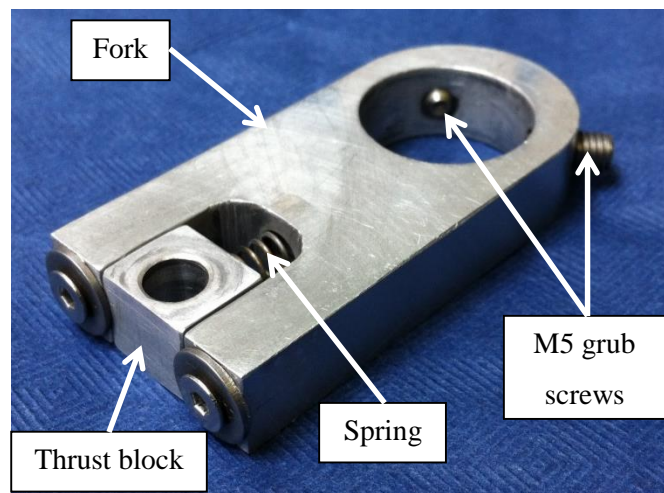


Figure 6-15 Photograph of aluminium fork, spring and thrust block

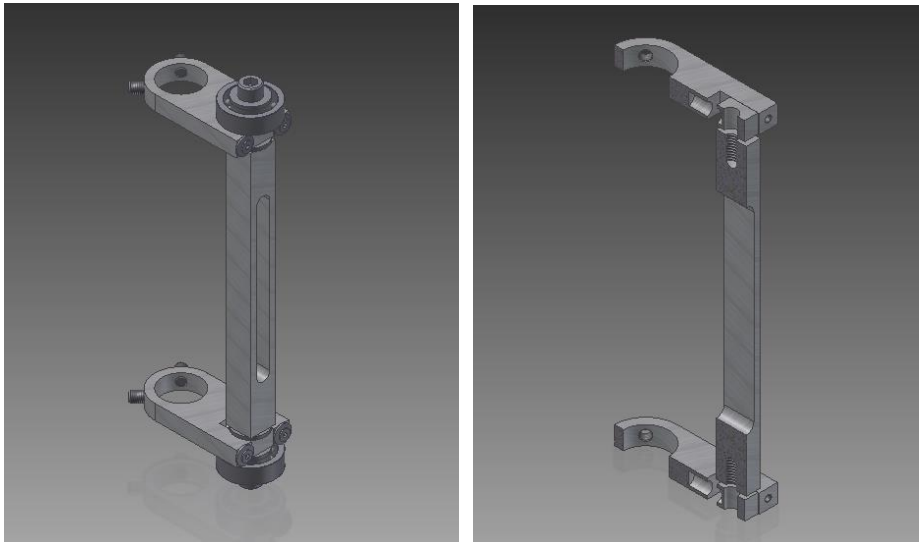


Figure 6-16 Sensor holder, forks roller bearings and fasteners (a) & X-section without fasteners (b)

The forks were designed to feed through a 20 mm diameter solid stainless steel shaft and were held in place using grub screws that would bear onto the surface of the bar once tightened. One end of the bar was drilled to a depth of 9 mm with a 15 mm diameter high strength steel drill bit. A 15 mm diameter ball bearing was crimped into the hole and would act as a pivot point about the centre of the PE pipe. The opposing end of the stainless steel shaft was turned down to 5 mm diameter to a depth of 15 mm to allow the insertion of an aluminium flexible coupler that was purchased off-the-shelf (see Figure 6-17). The coupler eliminates any unwanted lateral forces that may put extra strain on the mechanical components; especially the stepper motor. The drive shaft of a stepper motor was inserted into the opposing end of the flexible coupler and would act as the driving element of the whole rig.

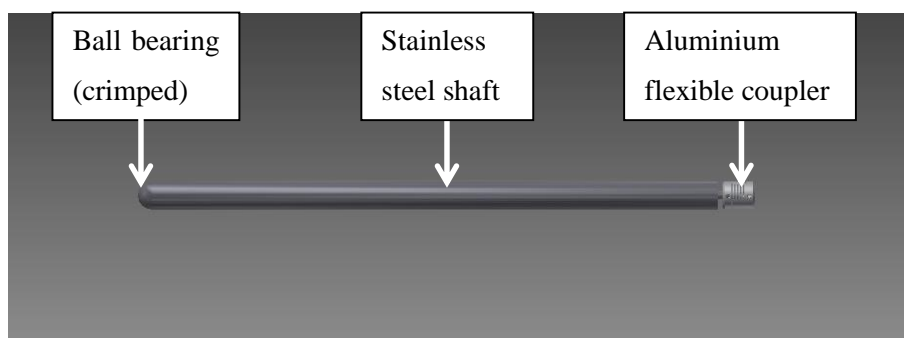


Figure 6-17 Driving shaft and aluminium coupler

A stepper motor was acquired and attached to a secure platform in order to rotate the drive shaft and therefore the sensor holder. In order to eliminate any lateral forces on the stepper

motor, the entire assembly needed to be clamped securely. Therefore, the rig was held using industry standard PE welding clamps. Furthermore, the stepper motor needed to sit securely on a platform that could be held in the PE pipe clamps. A wooden disk was turned to 125 mm diameter and a clearance hole drilled in the centre to allow the 20 mm diameter drive shaft to go through; this would act as a platform for columns that would be fastened to the stepper motor platform. The hole was bored internally so that a bearing could be housed within (see Figure 6-18). The stainless steel drive shaft was pressed onto the inner race of the bearing. The bearing would ensure that the drive shaft ran smoothly during the fatigue test.

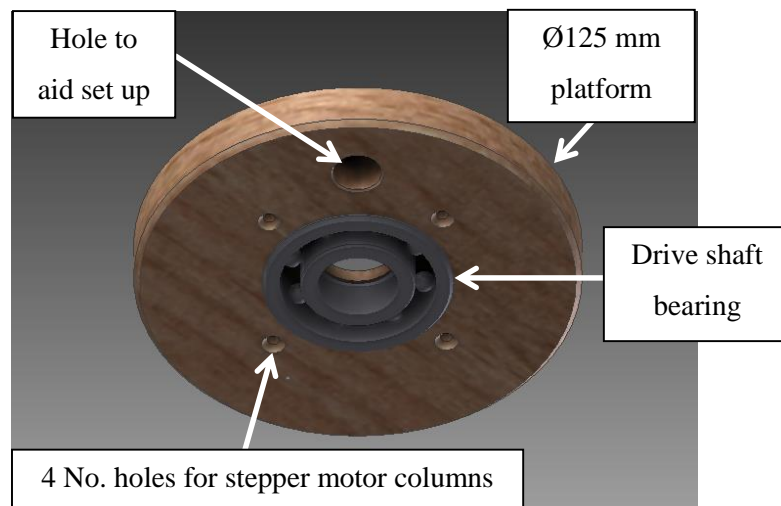


Figure 6-18 Design of column platform and drive shaft bearing

Four plastic columns were machined to identical lengths and tapped so that one end could be fastened to the column platform and the other end fastened to the stepper motor platform. A square was cut from a Perspex sheet and drilled locally to secure the stepper motor. The stepper motor platform assembly is illustrated in Figure 6-19.

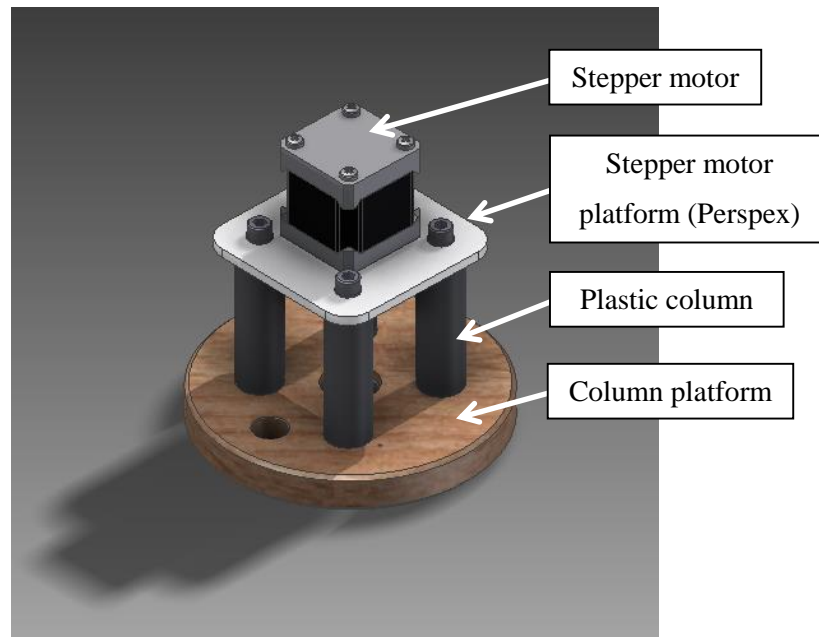


Figure 6-19 Stepper motor, platforms and columns

To ensure that the drive shaft always rotated about the centre point of the pipe, an end cap was designed and machined from stainless steel that would be pressed into one end of the PE pipe. The end cap was drilled and tapped in the centre for an M16 bolt to go through. The M16 bolt was also drilled at the thread end using an 18 mm diameter high strength steel drill bit. The aim of this was to create a conical shape so that the ball bearing of the drive shaft can locate the centre of the end cap and thus the centre of the pipe (see Figure 6-20). An O-ring was housed in a pre-cut groove located at the circumference of the end cap. This ensured that the end cap sat well with the bore of the pipe.

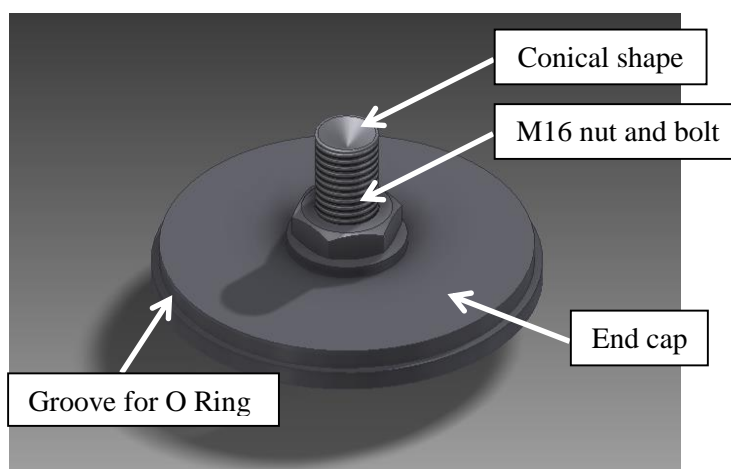


Figure 6-20 Stainless steel end cap

All assembled components are illustrated in Figure 6-21.

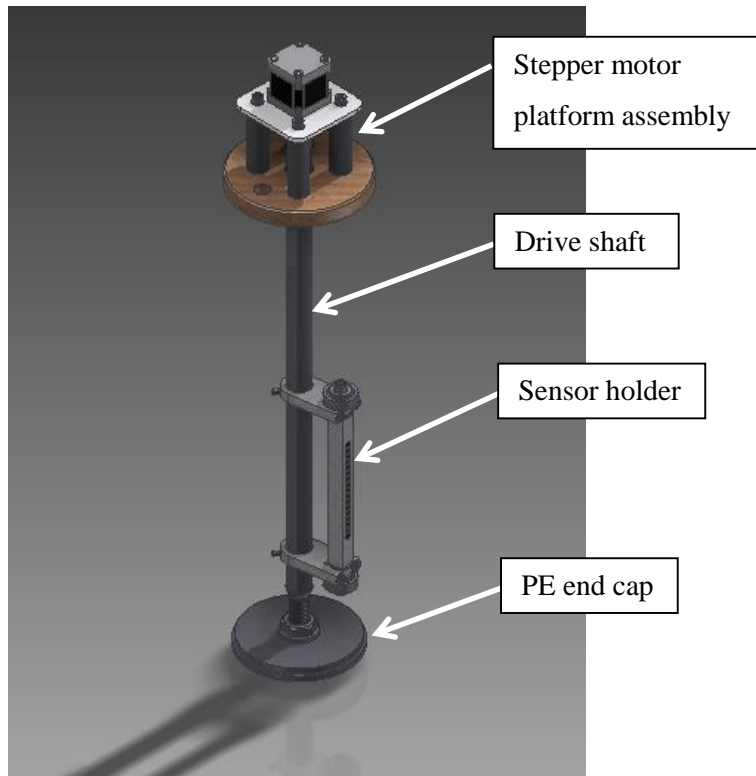


Figure 6-21 Live ultrasound testing rig assembly (model)

The real-time ultrasonic analysis rig can be seen in Figure 6-22. It was noted that the stepper motor would get hot during the test. Therefore a computer fan was retrofitted to the top of the stepper motor in an attempt to keep it cool. The probable reason for the stepper motor getting hot was likely to be due to an increased voltage being passed as a result of the manual alteration of the potentiometer on the stepper motor driver. This ensured the motor outputted maximum torque to rotate the drive shaft. In hindsight, a larger stepper motor (i.e. higher torque rating) would have been more suitable for this set up.

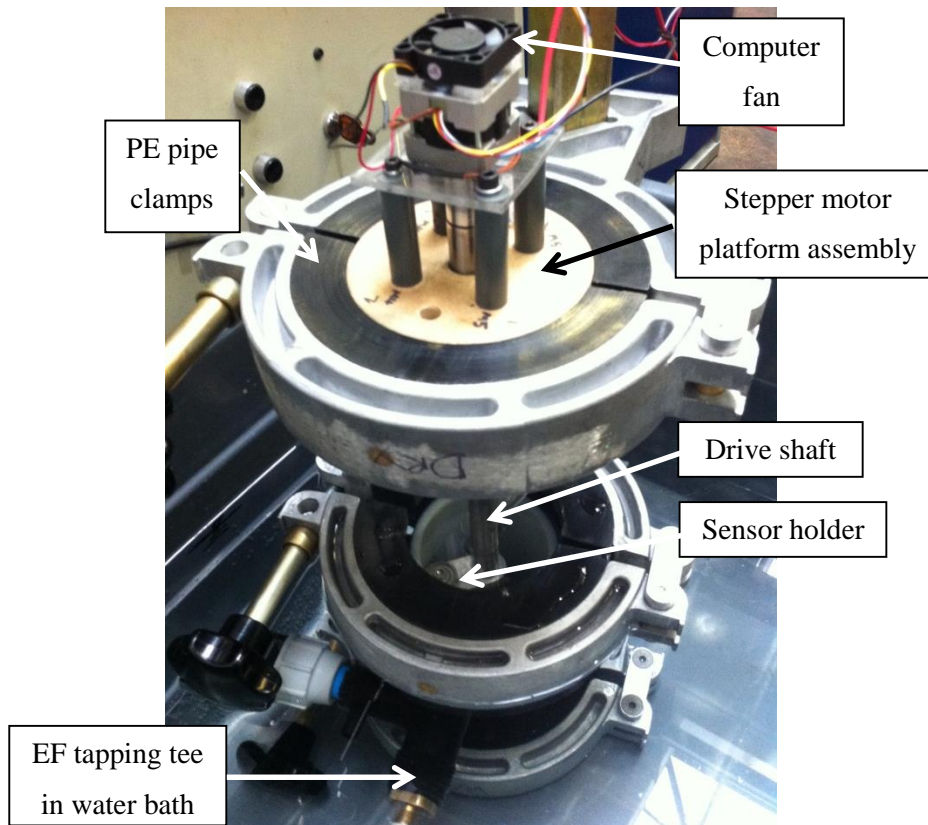


Figure 6-22 Live Ultrasound rig in PE pipe clamps

6.3.4. Controlling and automating the processes

In order to ensure that the data acquired was reliable and consistent, automation of many aspects of the rig were required. A bespoke program was created using LabVIEW to control, automate and collect data during the live fatigue tests.

The stepper motor was driven by a stepper driver, the 'Big Easy Driver' (BED) board. The BED was given a 12 V power supply which powered the stepper motor sequentially. The BED was wired to a micro-processing unit, the Arduino UNO (see Figure 6-23), which gave the required commands to the stepper motor. The Arduino UNO was powered by a USB cable which was linked to the PC containing the LabVIEW program. All commands were delivered through the host program in LabVIEW.

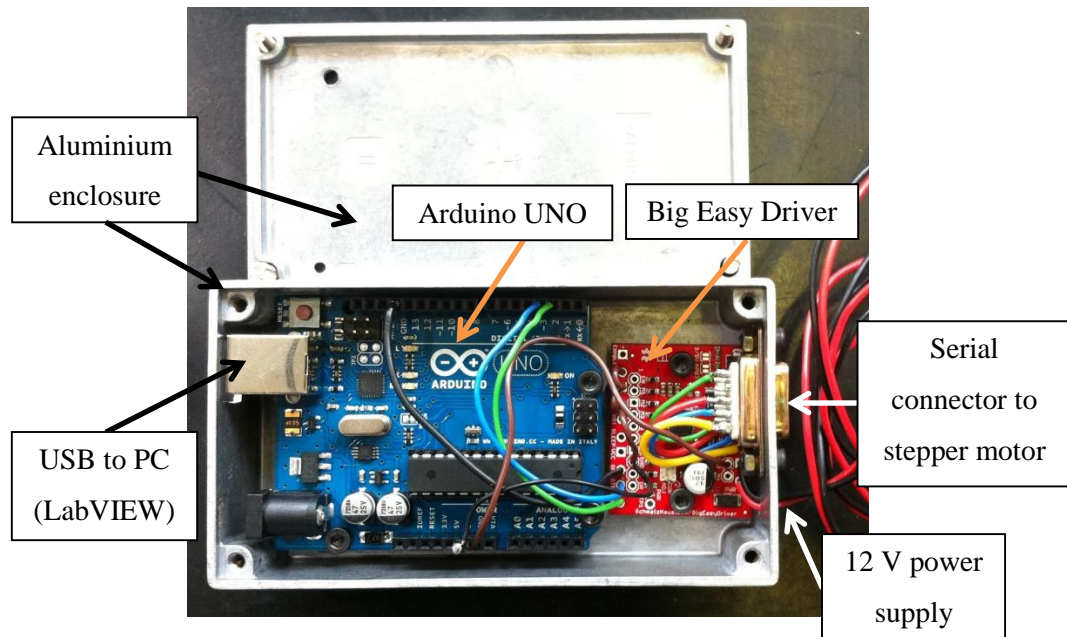


Figure 6-23 Micro-processing unit and stepper motor driver (unwired)

The stepper motor was manufactured to produce 200 steps per revolution (i.e. 1.8° per step). The LabVIEW program was coded such that data would be recorded at each step from all sensors in the ultrasonic array. It shall be noted that the sensor array would not be required to do a full revolution of the pipe as the fitting is only present for approximately 90° of the pipe with respect to the centre of the pipe (see Figure 6-24). Therefore, the stepper motor performs 50 steps from 0° to 90° and thus 50 lines of ultrasonic data.

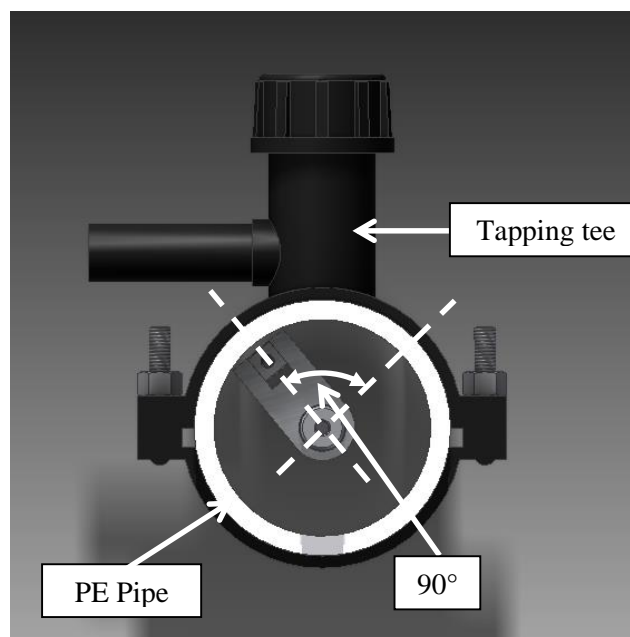


Figure 6-24 Computer representation of pipe, fitting and probe (aerial view)

The computer hardware used for the acquisition of data was manufactured and supplied by Tribosonics Ltd. A multiplexer was designed and built in-house (by another University of Sheffield PhD student) and installed to the existing hardware to increase the acquisition capacity enabling the observation of up to 64 individual sensors. However, due to the nature of a multiplexer, the hardware/software interface only allowed the acquisition of 8 sensors at any one time; although, the switch from sensors 1-to-8 to 9-to-16 to 17-to-24 etc. is almost instantaneous. Creating a 64 sensor array would be time consuming and excessive for the aim of this experiment.

The 16 sensors in the linear sensor array in this experiment were numbered 1 to 16 from top to bottom. With regards to the actual acquisition of the data, the stepper motor was programmed to rotate clockwise (CW) through the 90° fusion zone area but only data from odd numbered sensors would be acquired (i.e. 1, 3, 5... 15). Then the stepper motor would rotate anticlockwise (A-CW) and take readings of all the even numbered sensors (i.e. 2, 4, 6... 16) - returning to the 'home' position (0°). This was collectively known as one 'pass'. Two passes were completed per scan using the ultrasonic array. Figure 6-25 depicts the sequence of events for an individual ultrasonic scan, highlighting the sensor position in degrees.

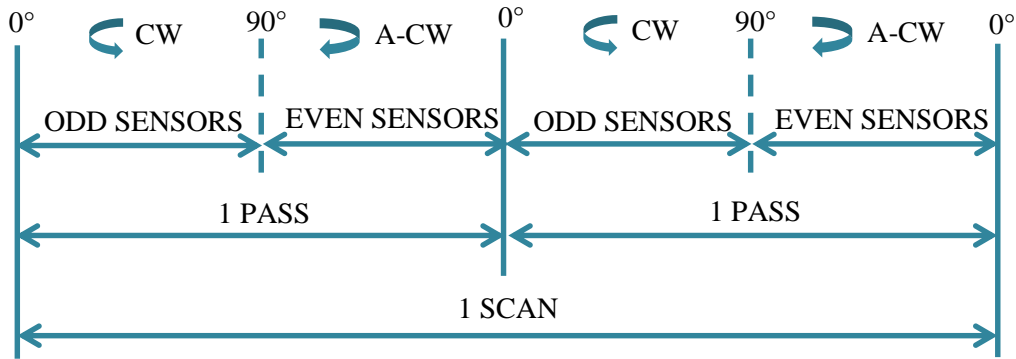


Figure 6-25 Diagram showing 1 scan of ultrasonic rig

A scan was performed at each cycle during the live fatigue test and was approximately 12 seconds in duration (i.e. $t_{SCAN} = 12$ seconds). As the failure mechanism was assumed to be crack propagation about the jointing interface, any crack was assumed to be most evident at the highest pressure in the fatigue cycle (i.e. at $P_{CYCLE\ MAX}$). Therefore, scans were only performed at the maximum pressure of each cycle; hence the ultrasonic array did not scan continuously until failure during the live fatigue test as the amount of data needed to be processed would be gargantuan. The program was coded to perform a scan when a user-defined trigger pressure ($P_{TRIGGER}$) was reached. The trigger pressure was predefined as the maximum pressure expected in the cycle; i.e. $P_{TRIGGER} = P_{CYCLE\ MAX}$. As mentioned in the

introduction of Section 6.3, the fatigue test parameters were fixed to coincide with the $70\% \times P_{MAT,MAX}$ pressure range as explained in the fixed mean pressure approach in Section 3.3.1, thus; $P_{TRIGGER} = P_{CYCLE\ MAX} = 21.25\text{ bar}$ (2.13 MPa). Each scan was approximately 12 seconds in duration. The rest time (at top and bottom of each cycle) associate with $70\% \times P_{MAT,MAX}$ was; $t_{REST} = 14\text{ seconds}$.

As $t_{SCAN} < t_{REST}$, it was assumed that the data captured in this time frame would be likely to illustrate the crack propagation about the welding interface.

Figure 6-26 below shows the expected pressure for the fatigue cycle during the experiment, highlighting the trigger pressures and rest times.

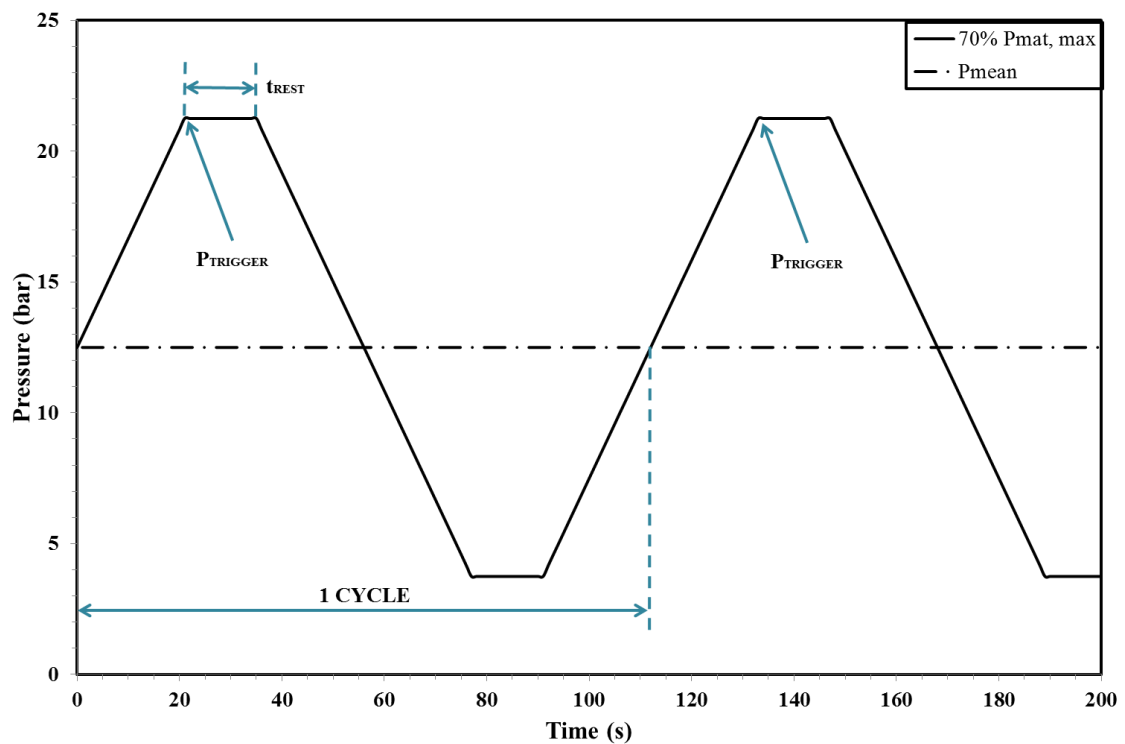


Figure 6-26 Graph showing cycle with trigger and cycle rest period

The trigger pressure was obtained by taking a live analogue signal from the MOOG test controller which has been explained previously in Section 3.2.5. The signal was fed into an external data acquisition (DAQ) device (Model: National Instruments USB-6008) which was connected to the LabVIEW program via a USB cable to the PC. Once the trigger pressure was reached, the stepper motor began to move and thus the acquisition of data. A schematic highlighting the key components and processes can be found in Figure 6-27.

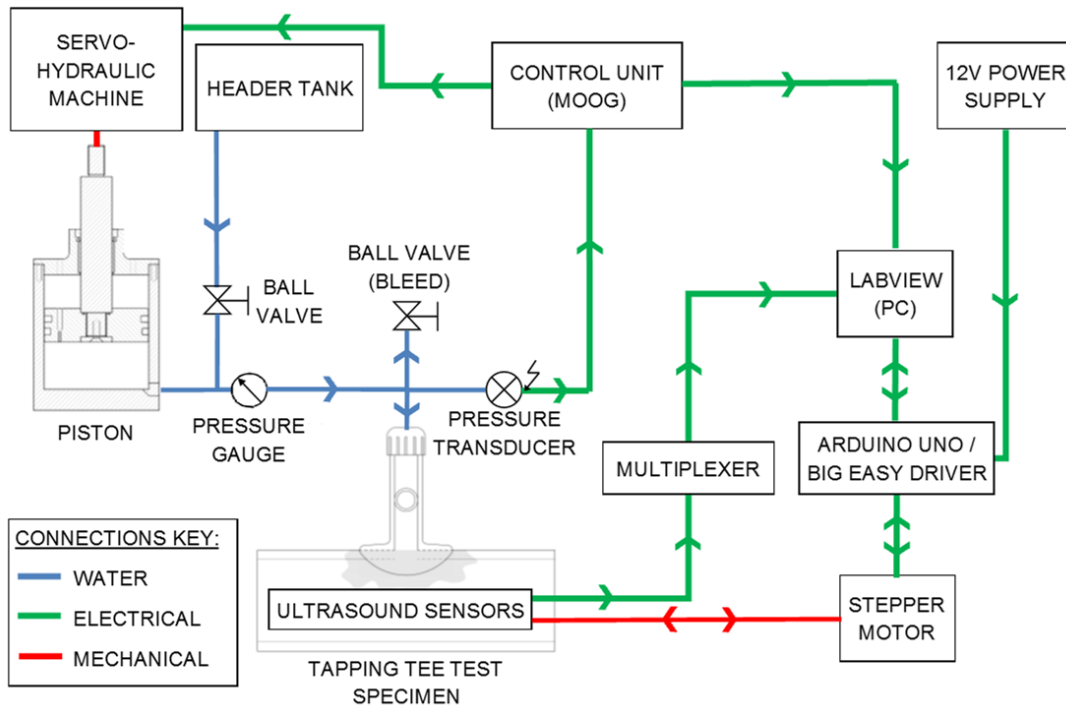


Figure 6-27 Schematic of real-time ultrasound testing rig

6.3.5. Signal acquisition and data processing

Once the mechanical rig has been retrofitted to a contaminated electrofusion tapping tee and the entire rig has been placed into the water bath, the data acquisition program can be loaded and the signals received from the sensors observed. The visual output of the data is represented as a dimensionless amplitude plotted against time (see Figure 6-28); accessible through the LabVIEW program.

For the initial set up, the sensor holder is aligned with the parent pipe so that there is no fitting on the opposing side of the pipe. This allows for individual ‘tuning’ of the sensors by adjusting the gain setting (amplification of signal) to ensure the received signal is strong enough for processing. The ‘delay’ and ‘range’ of the signal was also altered to ensure that the optimum amount of data is acquired. As a benchmark, the reflection of the opposing side of the pipe is used to gauge the signal strength of each sensor.

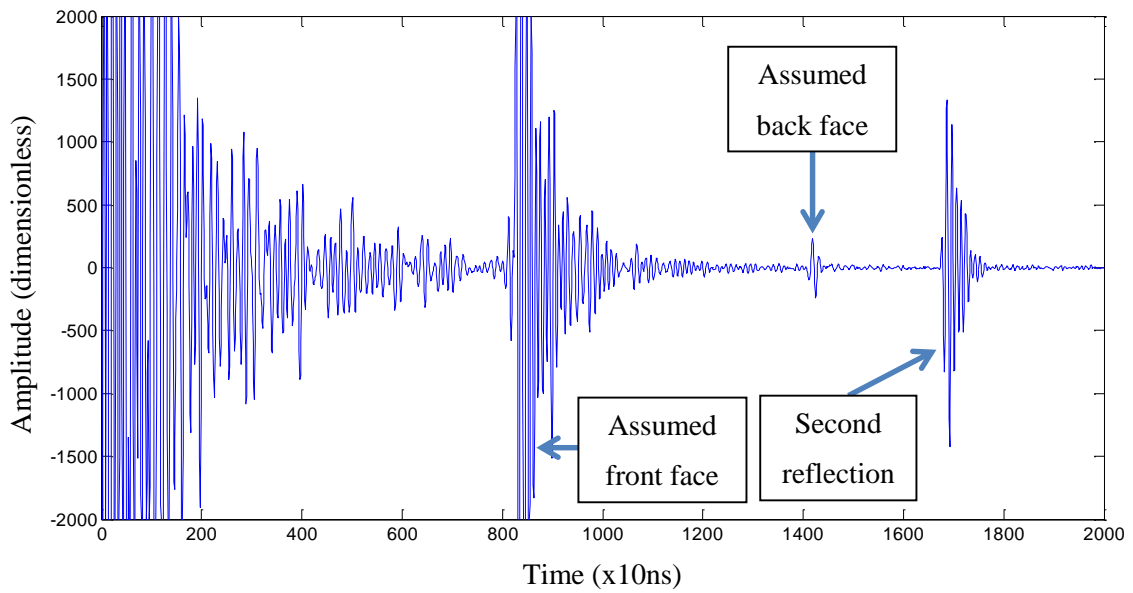


Figure 6-28 Typical initial reading of a single sensor on parent PE pipe

As the thickness of the PE pipe can be measured physically, the time of flight can be calculated to ensure that data analysis occurs in the correct place and ensures the sensor is working properly. The thickness of the pipe was measured as 6.60 mm using a Vernier Caliper,

To confirm the location of the reflection for the back face of the PE pipe, the speed of sound through the PE100 material was assumed to be 2.39×10^3 m/s, as per research by Hagglund *et al.* [76]. Therefore the time of flight is calculated as 5.53×10^{-6} seconds. The approximate time of flight from Figure 6-28 was 5.70×10^{-6} seconds. As these figures are approximately equal and given that there inevitably is some minor variation to the pipe thickness, it can be assumed that the signals received are that of the PE pipe.

It was believed that as this location is known with respect to the x-axis (time) of Figure 6-28, when the sensor rotates through the fusion zone, the signal at this point will disappear as the effective thickness at this point has increased due the tapping tee weld. However, it was believed that as delamination occurs (i.e. crack propagation) the signal observed at this point will appear as the effective distance at the point of delamination will be the same as the initial reading from the opposing side of the pipe. It is on this basis that crack propagation could be monitored and geared the basis of the post-processing of data.

As can be seen in Figure 6-28, the signal observed from the external wall of the pipe was somewhat smaller in comparison to the signal from the front face of the pipe. In order to boost the magnitude of the signal, the gain was increased. Subsequently, this increased the amplitude of any noise present. Each of the 16 sensors was modified manually using the gain function to ensure a strong signal of the external wall of the pipe could be observed.

Each scan was stored as a separate file for processing. All data output was analysed using MATLAB due to its powerful capacity to process vast amounts of data efficiently.

6.3.6. Benchmarking the apparatus

Preliminary tests were conducted to ensure the apparatus was capable of fulfilling the experimental brief of confirming the failure mechanism. The apparatus was benchmarked initially by scanning a PE pipe that had holes drilled in various locations. An area approximately the same size as the underside of an electrofusion tapping tee was drawn on the surface of the pipe. A total of 11 holes were drilled in random locations using a cordless drill. The sizes of the holes ranged from 2 to 10 mm in diameter and are illustrated in Figure 6-29 below.



Figure 6-29 Ø110 mm pipe with holes drilled

The section of pipe was placed in the PE pipe clamp arrangement and placed in the water bath in order to be scanned using the sensor array. As mentioned previously, the sensors were tuned on an individual basis to ensure the signal strength was adequate to observe the external wall of the pipe.

Figure 6-30 shows the results from the ultrasonic data which observed the holes in the pipe. The colour map is created using arbitrary units based on the signal intensity during the scan.

The results are successful in that they show the accurate locations of the holes in the pipe. However, it was noted that the sensors only picked up the holes that were directly opposite the sensor. Although this seems obvious, sensor 3 failed to accurately pick up the top three holes as the sensor must not have been directly over the centre of the holes. This may explain why the data is inconsistent at this point. The bottom holes shown in Figure 6-29 are not shown in Figure 6-30 as sensor 15 was dead, as mentioned in Section 6.3.2.

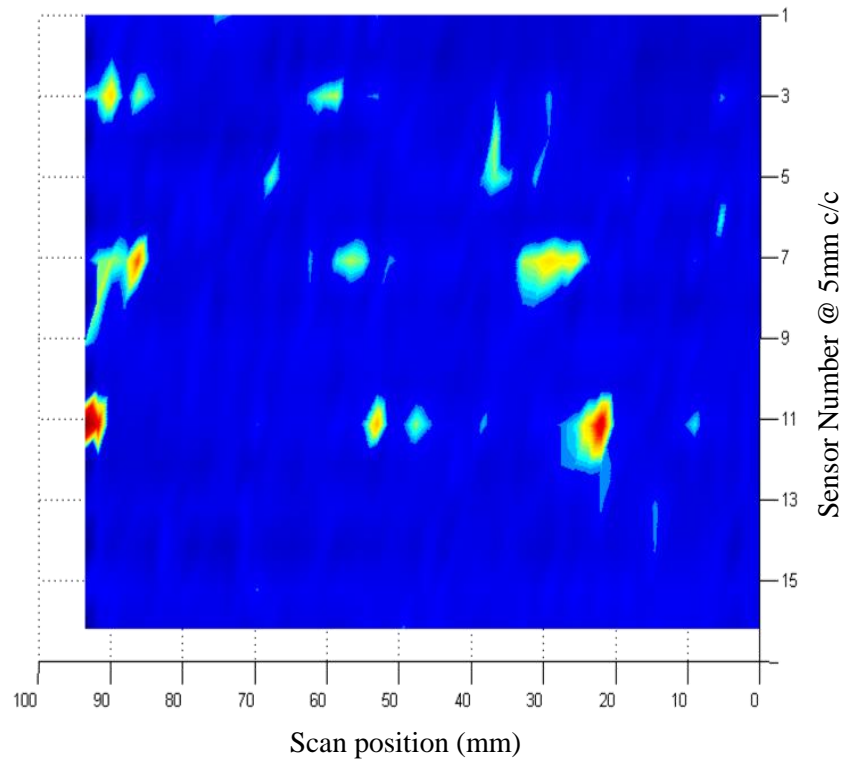


Figure 6-30 Data from ultrasound scan of holes in pipe

To further benchmark the apparatus, a joint was created to best practice principles and scanned using the equipment when it was subject to dynamic load to the regime mentioned in Section 6.3. The experiment aimed to observe the welded fusion zone as an outline but more importantly observe the centre of the fitting where a hole is present. Therefore the signal strength would be at its greatest at the centre of the fitting as there is no fitting present to disturb the reflection of the signal.

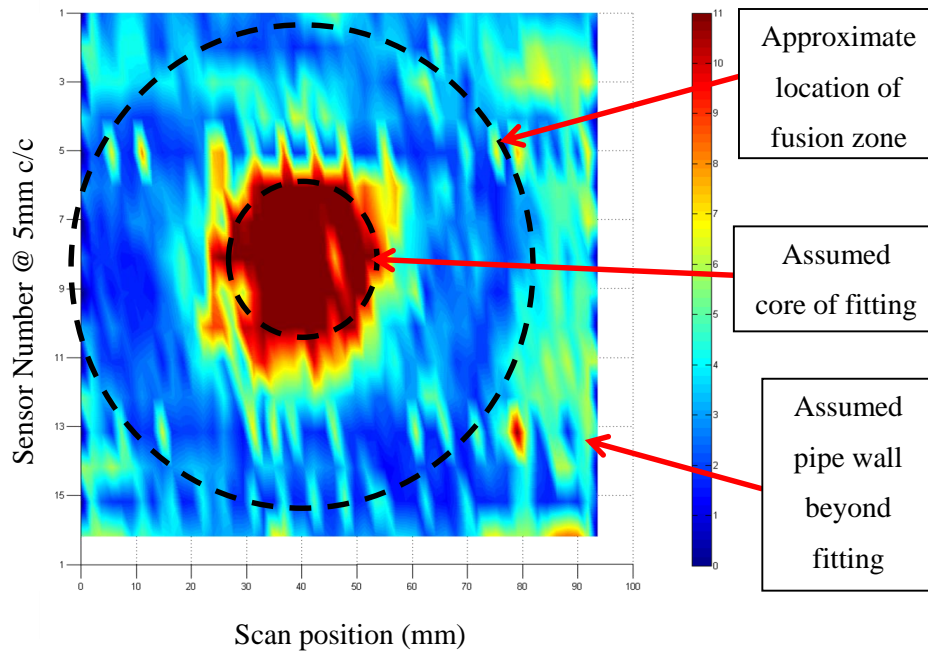


Figure 6-31 Scan of a perfect joint

Figure 6-31 shows the 82nd scan of the perfect joint. The fatigue test was performed for 192 cycles of which no failure occurred. The 82nd scan was selected to represent the approximate middle in the number of cycles conducted. The results depicted clearly show the centre of the fitting. The circumference of the fusion zone can almost be fully observed as well as pipe wall beyond the fitting. However, the results are arguably subjective as they may be seen as ‘open to interpretation’. Accurately positioning the probe before commencing a test to ensure the apparatus effectively scanned the entire fusion zone proved difficult. It was noted that the probe may scan beyond the fitting. Therefore it was expected to observe the pipe beyond the fitting but potentially only on one side of the results.

Despite lessons learned, the rig was assumed to be fit for purpose as it successfully observed holes in pipe as well as a large void in the centre of the tapping tee. The array also appeared to pick up the outline of the fusion zone of the tapping tee. The rig should therefore be able to observe the crack growth or at least any changes to the jointing interface during a live fatigue test.

The limitations of the rig however are evident in that 16 sensors only provide a limited resolution as the sensors are spaced at 5 mm centres. It was also clear that having 3 faulty sensors may skew the results. Despite the 3 sensors being faulty, it was decided to proceed with the experiment with the current array to attempt to fulfil the aims of the experiment. If successful, the sensor array could be remade, ensuring that all 16 sensors are operational, and several tests completed to further verify the hypothesis.

6.3.7. Results from real-time ultrasound analysis

A test was performed on a contaminated electrofusion tapping tee that was subject to dynamic load to the regime previous mentioned in Section 6.3. The specimen, labelled ES, had a fatigue-life of 6 cycles and failed when the pressure was at its maximum on the 7th cycle.

Prior to commencing the fatigue test, an initial scan was performed when no pressure was present in the system. The results of this scan are illustrated in Figure 6-32 where the centre of the tapping tee fitting is easily observed. However, it is clear that for reason unknown by the author, no results were obtained by sensor 9. Here, an outline of the tapping tee can also almost be seen.

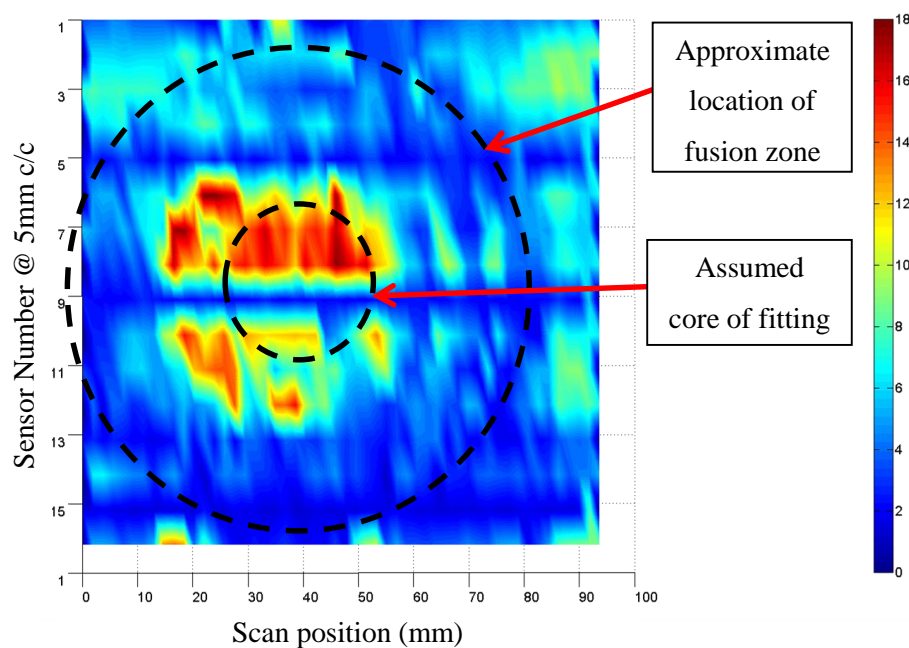


Figure 6-32 Initial scan – No pressure – specimen ES

The specimen was then pressurised to the starting pressure (P_{MEAN}) of 12.5 bar (1.25 MPa) and scanned again to observe any change in results if pressure is present in the system.

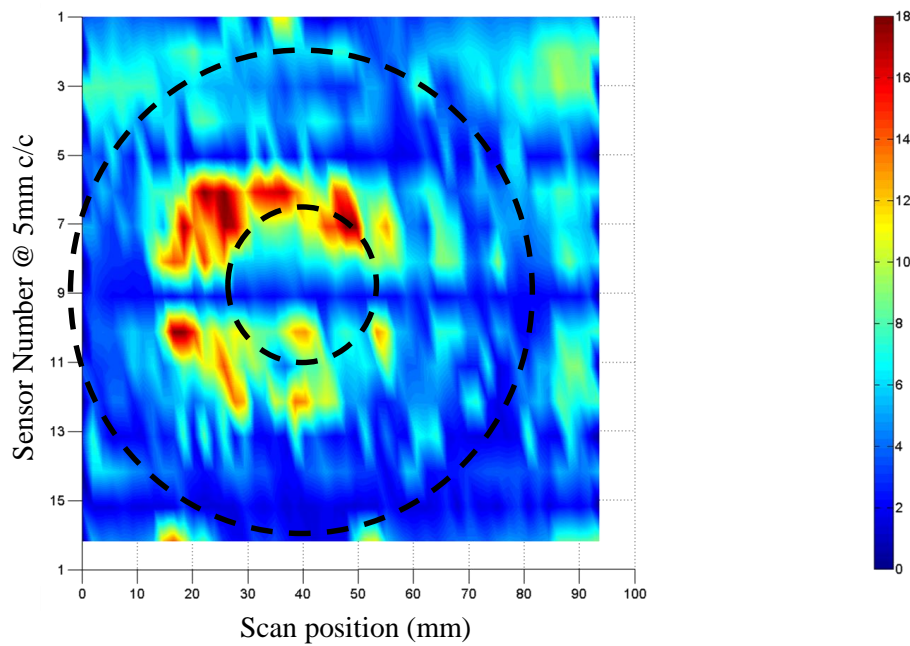


Figure 6-33 Initial scan – 12.5 bar pressure – specimen ES

The results were then compared by subtracting the signal amplitude at the location of each sensor to give the difference between no pressure and 12.5 bar (1.25 MPa) pressure in the system. This was purely to give an indication if any significant changes had taken place as a result of pressurisation of the system. Note that the intensity scale was changed to ensure that minimal changes in signal amplitude were observed.

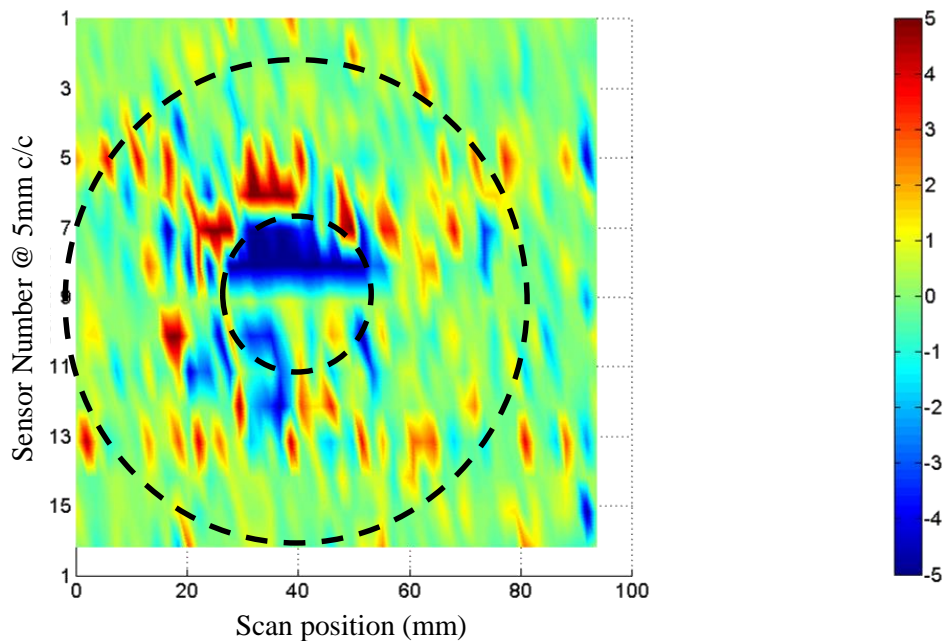


Figure 6-34 Difference in results with respect to starting pressure – specimen ES

As can be seen in Figure 6-34, there is little change in magnitude of signal received about the fusion zone. However, there appears to be a slight change around the centre of the fitting where the signal has intensified. This may be due to pressurisation of the tapping tee potentially initiating a crack mechanism.

Note that after the initial scan was performed, the data acquisition program was deactivated and reactivated once pressure was present in the system. As a consequence, the default settings are implemented upon shutdown and start-up of the program; thus each sensor would need to be retuned with respect to its gain setting. Therefore the results in Figure 6-34 may be exaggerated as a consequence. However, the position of the sensors with respect to the scanning position will remain consistent.

Figure 6-35 shows the results obtained from the first cycle of the fatigue test. It is important to note that further results hereafter are expressed as the difference in signal amplitude with respect to this first scan. Therefore the results expressed in Figure 6-35 are the benchmark of the data analysis.

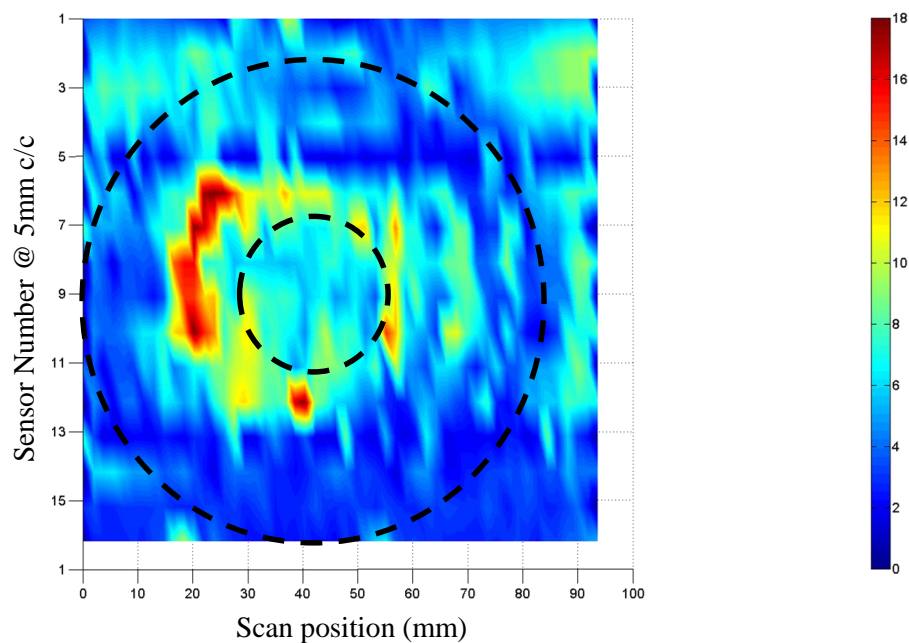


Figure 6-35 First cycle of fatigue test – specimen ES

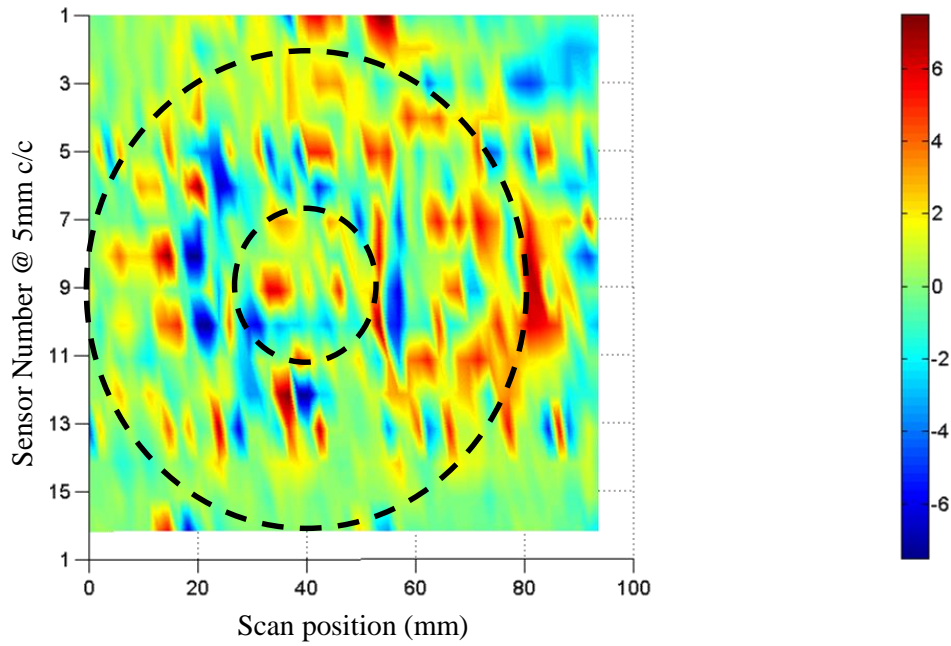


Figure 6-36 Cycle 2 – showing difference from first cycle – specimen ES

The second scan shows a change in signal amplitude between approximate scan positions 60 mm to 90 mm.

During the third cycle, the probe unexpectedly stopped midway through the scan. The cause of this was most likely due to the stepper motor not producing enough torque to rotate the drive shaft. However, as the fatigue test continued to run, the probe was manually located to its original position and reinstated for the remainder of the test. Consequently, scans were not obtained for the third and fourth cycles in the fatigue test. Figure 6-37 (below) shows the fifth cycle of the fatigue test. Like the previous observations, the results hereafter are expressed as the difference in signal intensity with respect to the first cycle of the fatigue test.

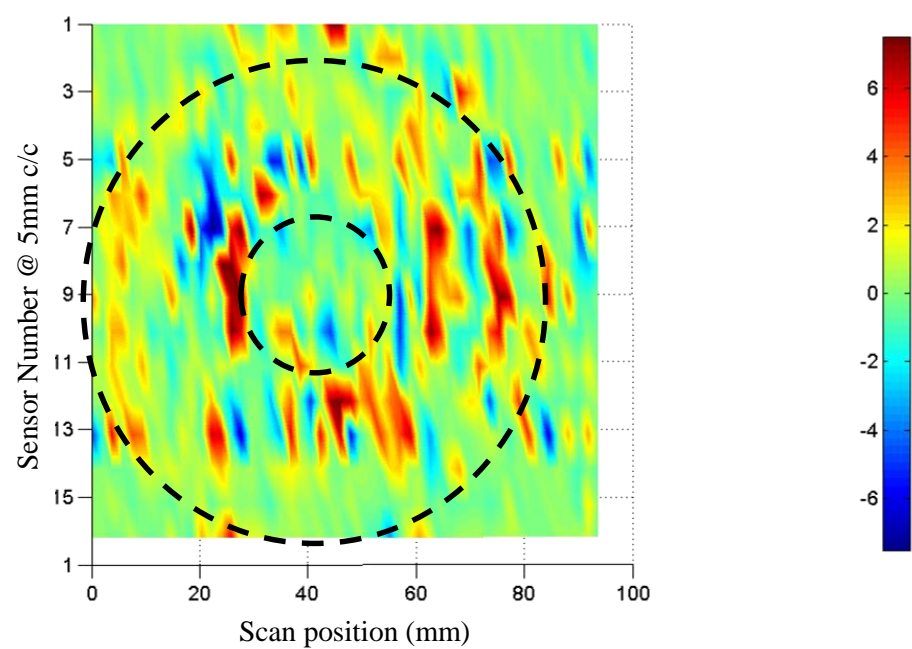


Figure 6-37 Cycle 5 – showing difference from first cycle – specimen ES

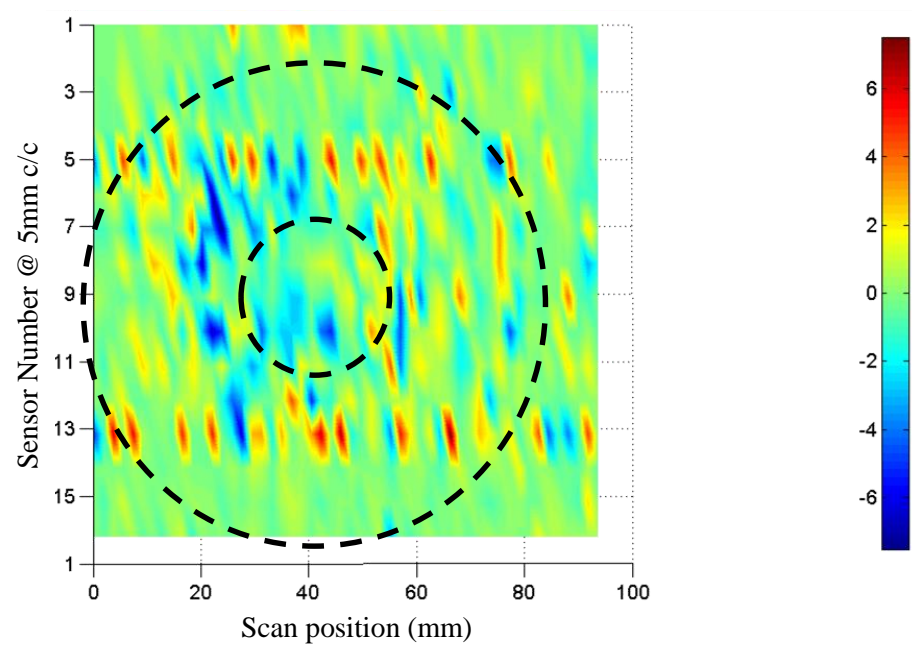


Figure 6-38 Cycle 6 – showing difference from first cycle – specimen ES

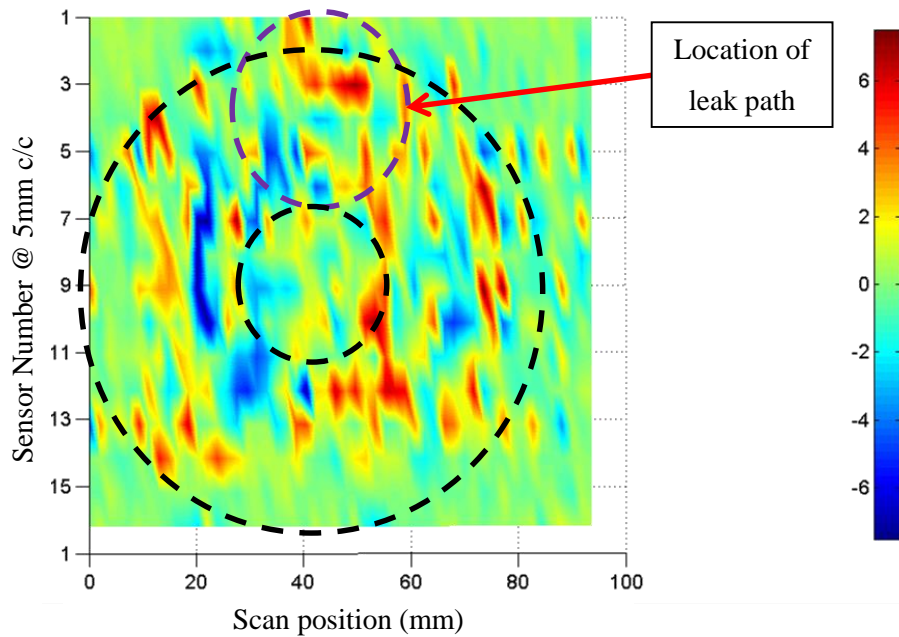


Figure 6-39 Final (7th) cycle – showing difference from first cycle and approximate leak path – specimen ES

It would appear that there was a noticeable change in the signal amplitude between positions 50 mm and 80 mm which suggests that some delamination may have taken place. However, as the scanning probe mechanically failed during the 3rd cycle and required resetting, the results may not give an accurate representation of the failure mechanism. Figure 6-40 shows the major leak path of specimen ES. With respect to the location of failure on the final scan (Figure 6-39), the area of the fusion zone (scanned) that corresponds to the major leak path has been highlighted in Figure 6-39.

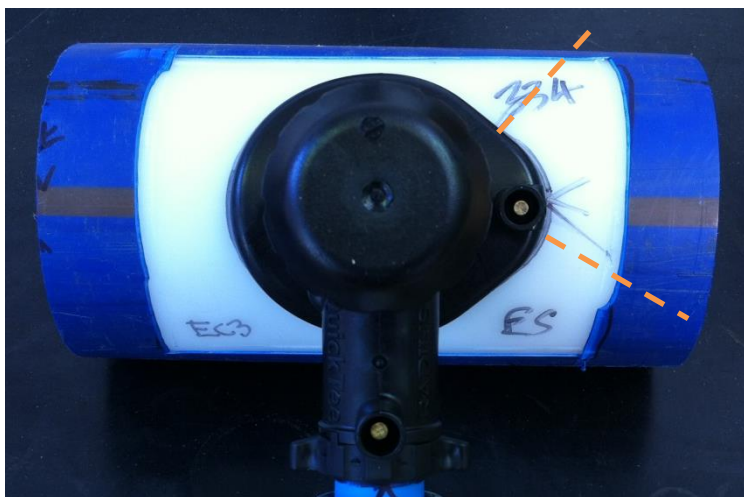


Figure 6-40 Specimen ES showing major leak path

A second test was performed on a specimen labelled ET. Like the previous specimen, ET held a fatigue-life of 6 cycles and also failed at the maximum pressure on the 7th cycle.

Like the previous experiment, the results are expressed as the difference in signal amplitude with respect to the first scan taken on the first cycle of the fatigue test. The first scan is illustrated in Figure 6-41.

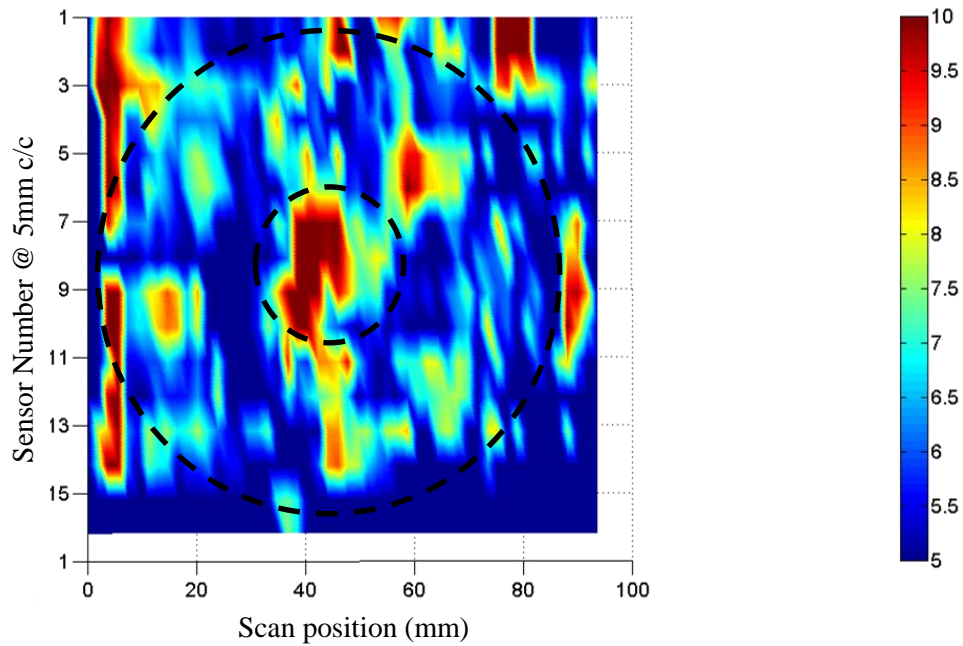


Figure 6-41 First cycle – specimen ET

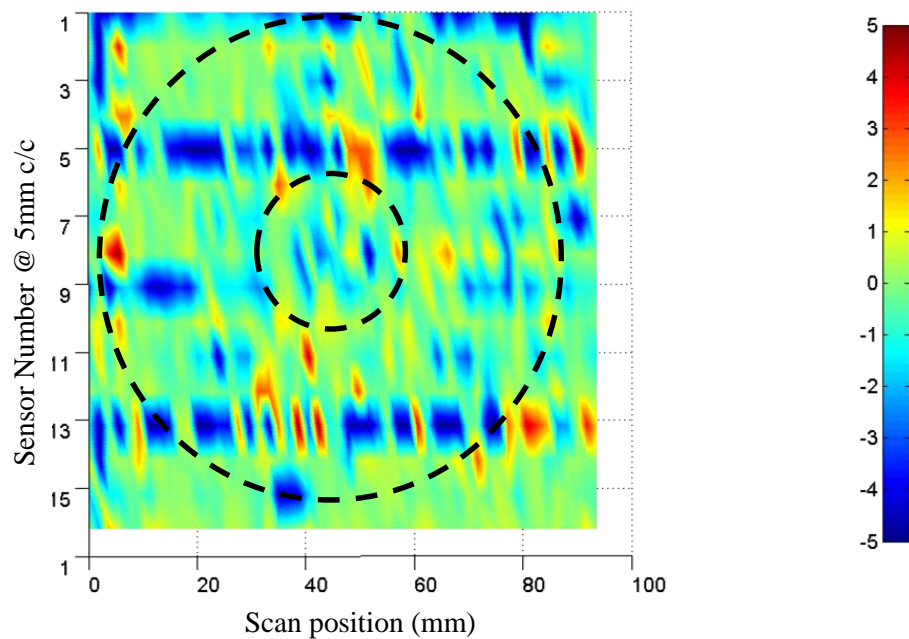


Figure 6-42 Cycle 2 – showing difference from first cycle – specimen ET

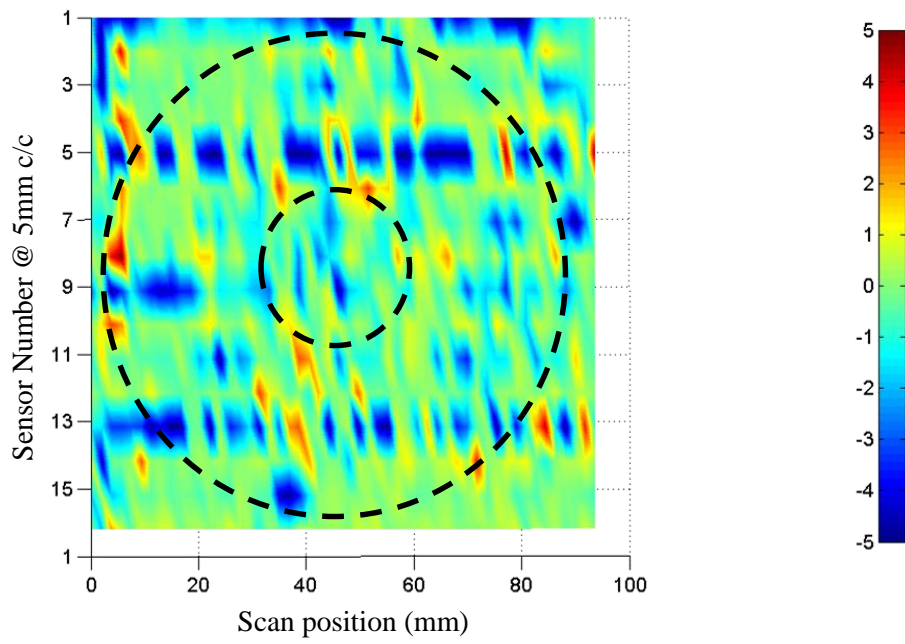


Figure 6-43 Cycle 3 – showing difference from first cycle – specimen ET

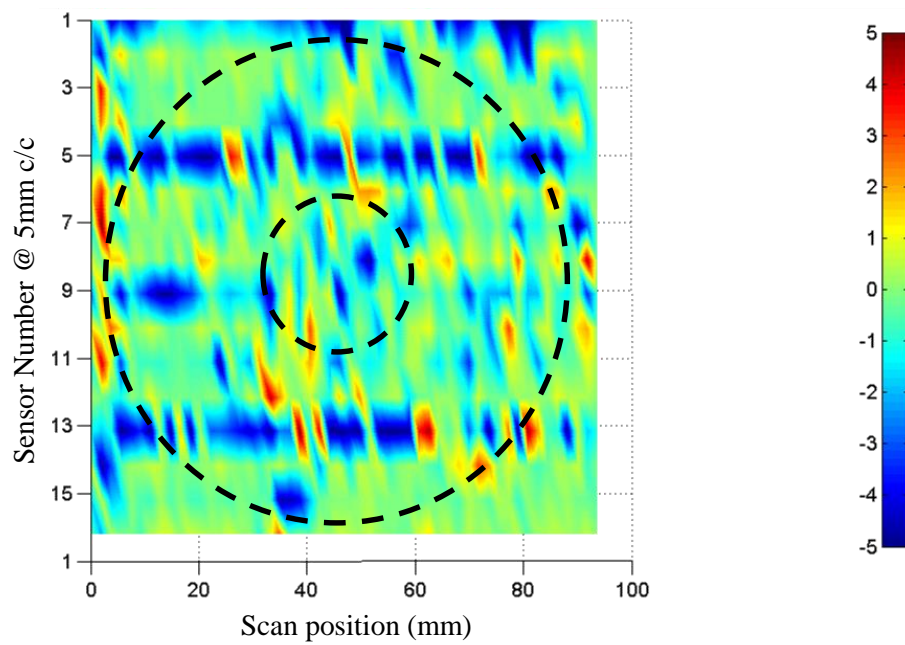


Figure 6-44 Cycle 4 – showing difference from first cycle – specimen ET

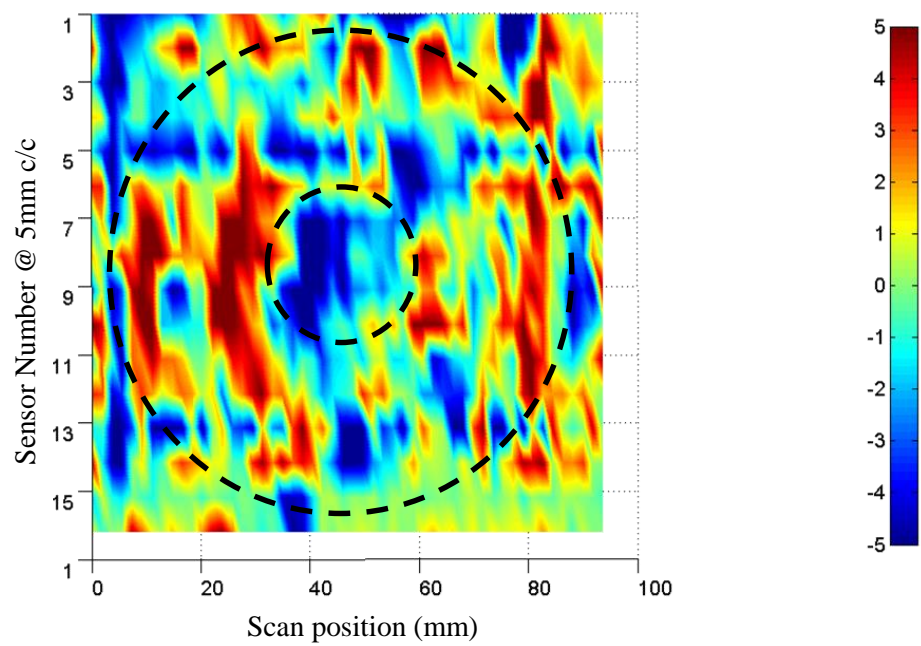


Figure 6-45 Cycle 5 – showing difference from first cycle – specimen ET

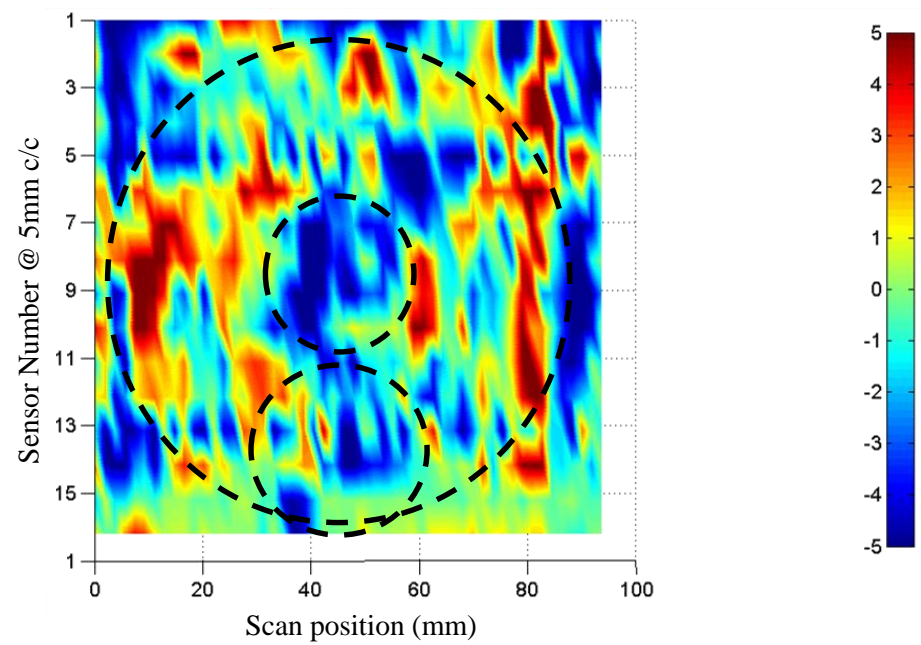


Figure 6-46 Cycle 6 – showing difference from first cycle and approximate leak path – specimen ET

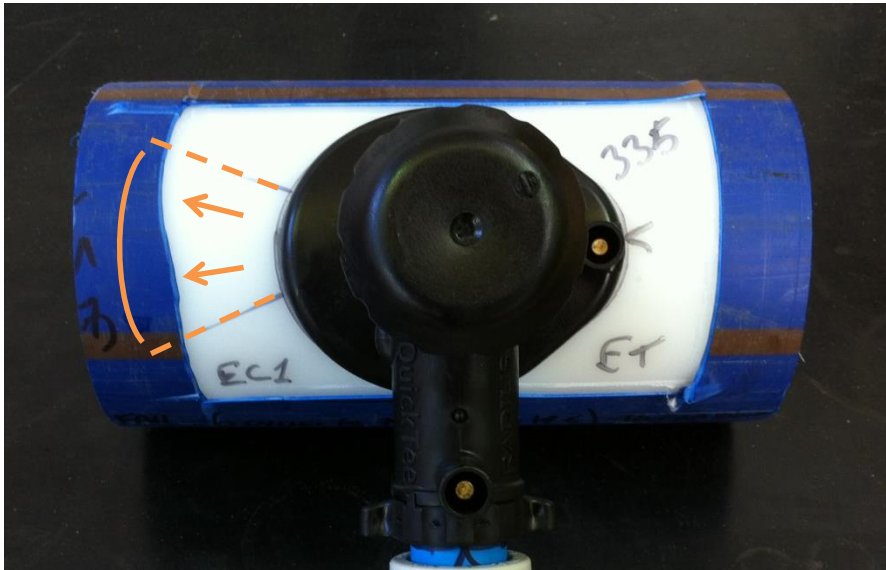


Figure 6-47 Specimen ET showing major leak path

The results suggest the difference in amplitude of the signal increases around the approximate location of the centre of the tapping tee in the final two cycles in the fatigue test. This could be the propagation of a crack(s) about the jointing interface. In contrast, the first three cycles of the test show an abundance of 'green' which represents no change in the difference in signal amplitude in comparison to the first scan of the fatigue test.

Figure 6-47 shows the major leak path of specimen ET; this has also been highlighted in Figure 6-46 at the approximate location in the fusion zone. It becomes clear that the results obtained for specimen ET may not show the failure mechanism of a contaminated electrofusion tapping tee. Interestingly, the signal amplitude appears to increase in the last two cycles which may indicate rapid crack growth. However, it was later discovered by analysing a video of the mechanical scanning of the tapping tee - taken using a static webcam - that the entire probe rotated its 'home' position very slightly after each scan. Thus the home position was not consistent throughout the fatigue test. Although, there was very little difference from the home position on the first scan compared to the last scan; the results obtained from the fatigue test are arguably flawed in that the scan position was not consistent. Therefore the difference in signal amplitudes with respect to the first scan of the fatigue test are also inconsistent, giving an incorrect representation of data.

It would appear that the mechanical ultrasonic data acquisition approach may be too ambitious to prove the failure mechanism as there are too many variables to control in order to ensure that the results that are obtained are accurate and consistent. It was apparent after these tests

that a redesign of the rig may be required with an aim to control the aforementioned variables, or, an entirely new method may need to be adopted in order to confirm the failure mechanism.

6.3.8. Redesigning the apparatus

As the results from the linear sensor array experiment were inconclusive, the ultrasonic rig was redesigned with the aim of further confirming the failure mechanism. Following the design options stipulated in Section 6.3.1 whereby option (i) was selected – sensors in a linear arrangement; the second design option was also pursued further on the basis that the first option was not as successful as expected.

A total of 16 individual sensors were manufactured using 5 MHz sensors. As PE is a very attenuating material, lower frequency sensors were used as the attenuation in PE is frequency dependent; offering lower attenuation at lower frequencies [76]. This will inevitably be an improvement from the previous sensor data which used 10 MHz. Furthermore, BS EN 13100-3 [69] recommends transducers in the range 1 MHz to 5 MHz for inspection of thermoplastics. Each sensor was made to the method highlighted in Section 6.3.2; using a 2D drawing, double sided sticky tape and two part epoxy resin. The only major difference being that instead of casting 16 sensors at once in an array, they were cast individually (see Figure 6-48). The advantage here being that if a sensor were to become damaged, it can be disposed of and another one made to replace it – giving the design redundancy.



Figure 6-48 Individual ultrasound sensors

A pad was created in order to house all 16 sensors in a polar configuration. The sensors were glued directly to the bore of the PE pipe using glue designed specifically for attaching

piezoelectric sensors to surfaces. The sensors were placed local to the fusion zone in a circular arrangement.

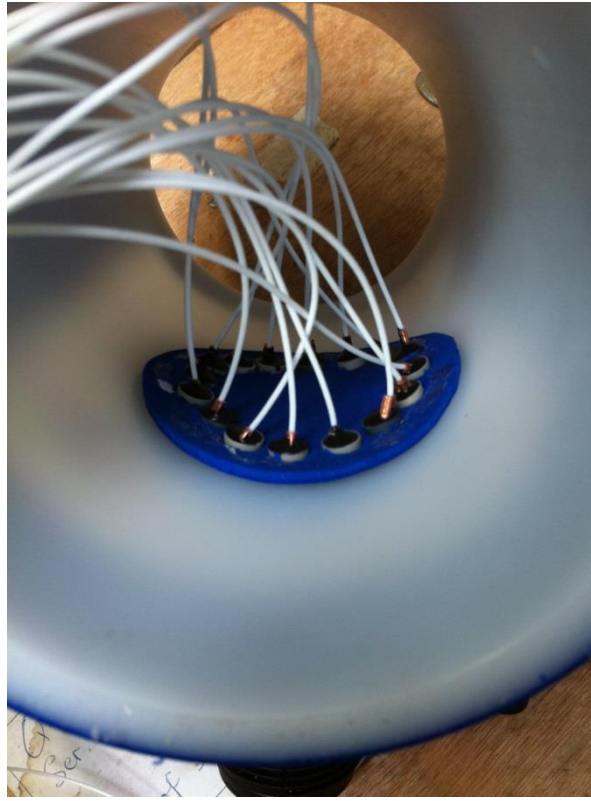


Figure 6-49 Individual sensors in circular arrangement on bore of PE pipe

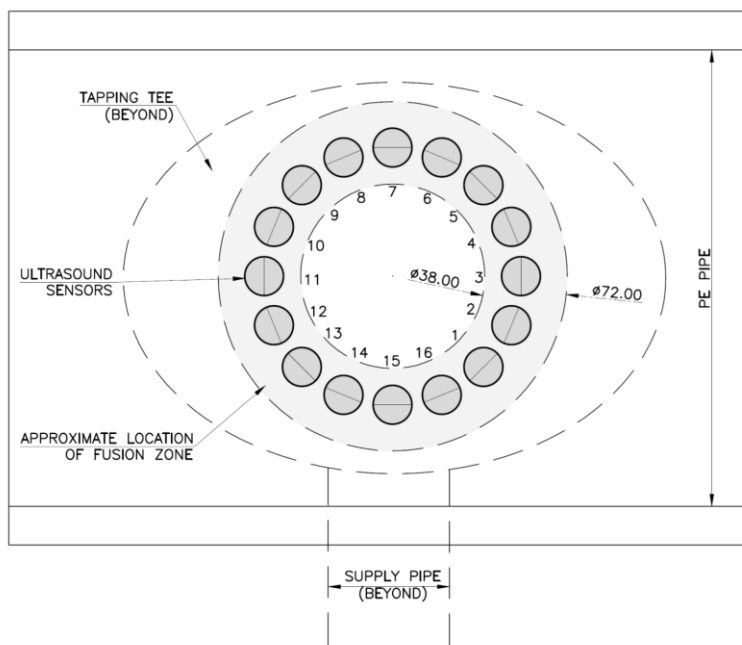


Figure 6-50 Sketch showing sensor numbers with respect to pipe and fusion zone

Like the previous experiment with the linear sensor array, once the rig was ready for testing to commence, each sensor was tuned manually to ensure the magnitude of signal being received was adequate for data processing. The gain was altered for each sensor to ensure maximum signal output. This was aided by gluing a single sensor to a virgin piece of pipe that was not being used for electrofusion welding. By calculating the time it would take for a pulse to return to the sensor from the opposing face of the pipe, an area could be honed as the focal point of the test. This area was then observed for all sensors in the analysis of the data post-test.

6.3.9. Results as a consequence of the redesigned rig

Once the gain settings were altered for each sensor to suit the test, an initial scan was performed on the contaminated electrofusion tapping tee to ensure that the data received by the sensors was sound. Figure 6-51 shows the results from the initial scan performed when no pressure was present in the system; also highlighting the location (number) of each sensor. Much like the data representation of the linear sensor array in Section 6.3.7, the colour map here depicts the signal intensity in arbitrary units obtained by each sensor. The data is illustrated in a circle shape to correspond to the arrangement of the sensor on the pipe; note that the sensor numbers are at a slightly different orientation to the sensors depicted in Figure 6-50.

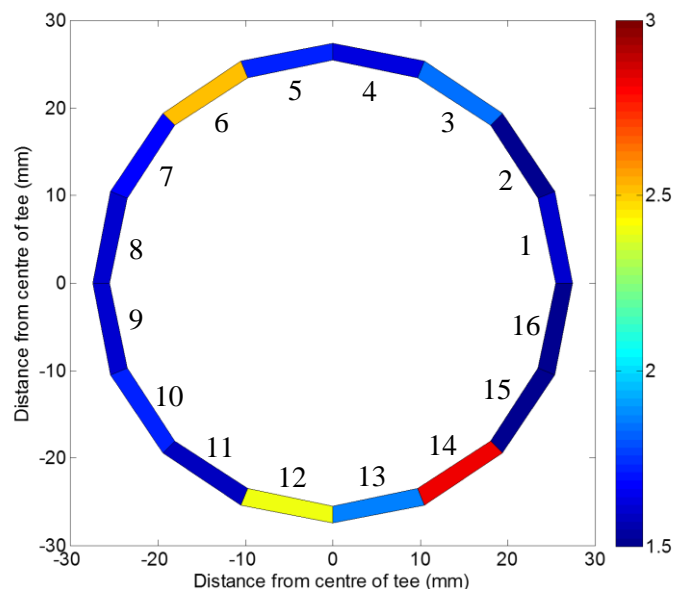


Figure 6-51 Initial scan – no pressure present

After the initial scan was conducted and the data processed, the specimen was pressurised to the fatigue test starting pressure ($P_{\text{MEAN}} = 12.5 \text{ bar}$ [1.25 MPa]) and scanned again to observe any difference in results as a result of the pressurisation of the specimen. It is key to note that it was required to retune the sensors before scanning at the starting pressure. This is due to the design of the data acquisition program whereby all settings are returned to 'default' upon opening and closing the program. Therefore the gain settings may be slightly different to when the initial scan was conducted. Figure 6-52 shows the results from the scan performed when the specimen was pressurised.

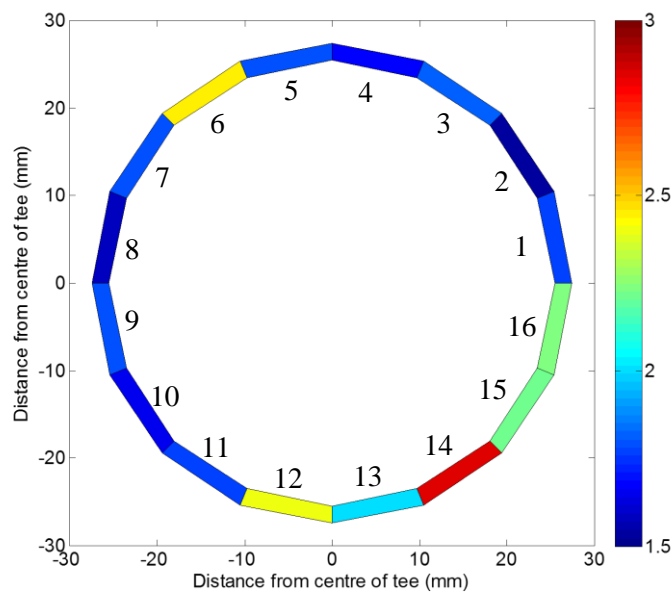


Figure 6-52 Pre-test scan: Pressure = 12.5 bar

Figure 6-53 shows the difference in results from the initial scan – taking the difference in signal magnitude between the two sets of data. It is important to note that the colour grading is a different scale in Figure 6-53 - the original scale being from 1.5 to 3; the new scale being from 0 to 1. This is to ensure that any minor changes of signal intensity are easily identified.

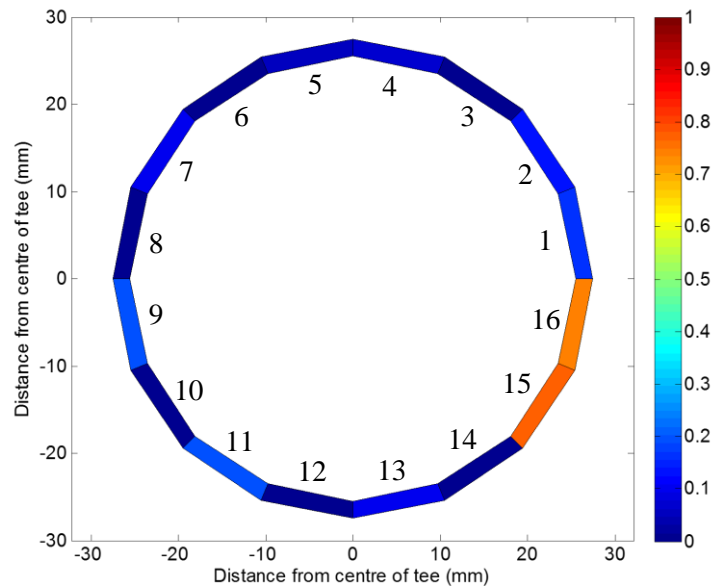


Figure 6-53 Difference at starting pressure – 12.5 bar

The results highlighted in Figure 6-53 suggest there has been an increase in signal strength about sensors 15 and 16. This may indicate that a crack may have developed as a result of pressurising the contaminated electrofusion tapping tee.

To give an indication of the potential crack growth during a live fatigue test, the results are expressed as the change in signal intensity at each sensor with respect to the first scan of the fatigue test. In other words, the initial scans were only performed for reference and will not be used to determine crack propagation about the jointing interface. This should give a strong indication of any difference in the fusion zone local to the ultrasound sensors with respect to dynamic load. Figure 6-54 shows the results from the scan performed at the maximum pressure of the first cycle in the fatigue test. Note how the results correspond to the scan performed when the specimen was initially pressurised to 12.5 bar (1.25 MPa) in Figure 6-53.

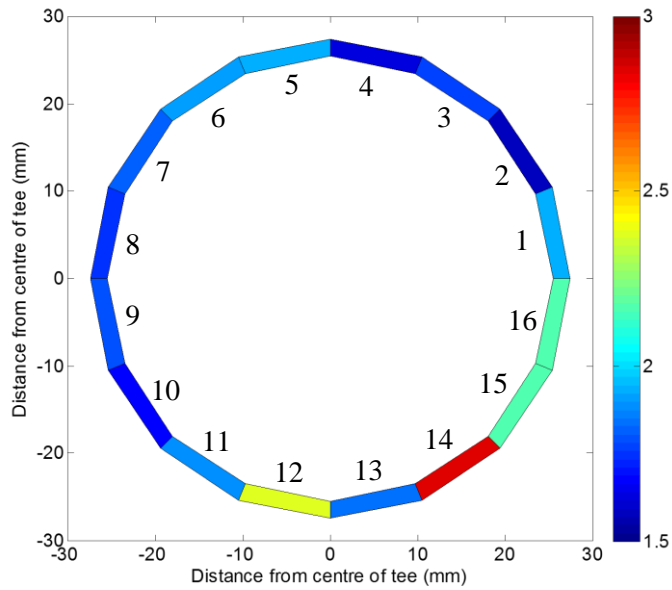


Figure 6-54 First cycle scan (benchmark scan)

Scans were performed at the maximum pressure of each cycle. The results from each scan are displayed in Figure 6-55 to Figure 6-60; each result being the difference in signal intensity from the first scan of the fatigue test. The specimen survived a fatigue-life of 12 cycles.

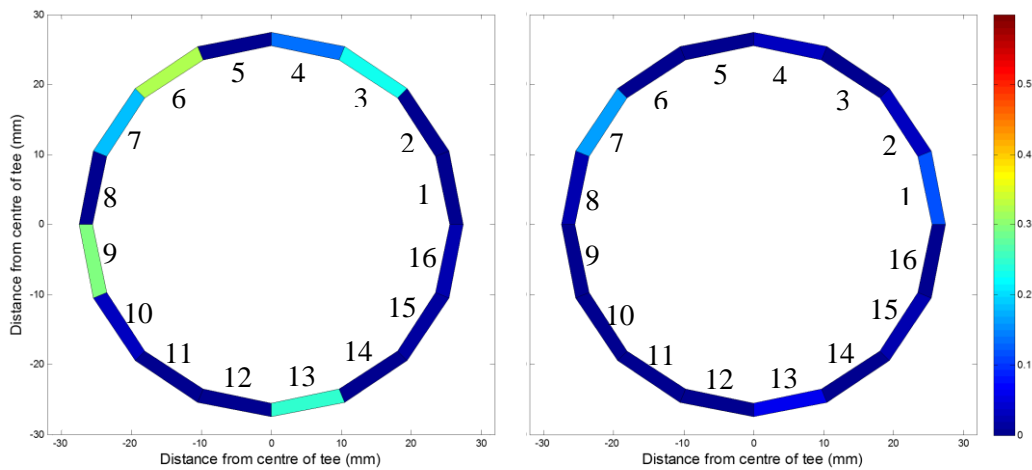


Figure 6-55 Cycle 2 (a) and cycle 3 (b)

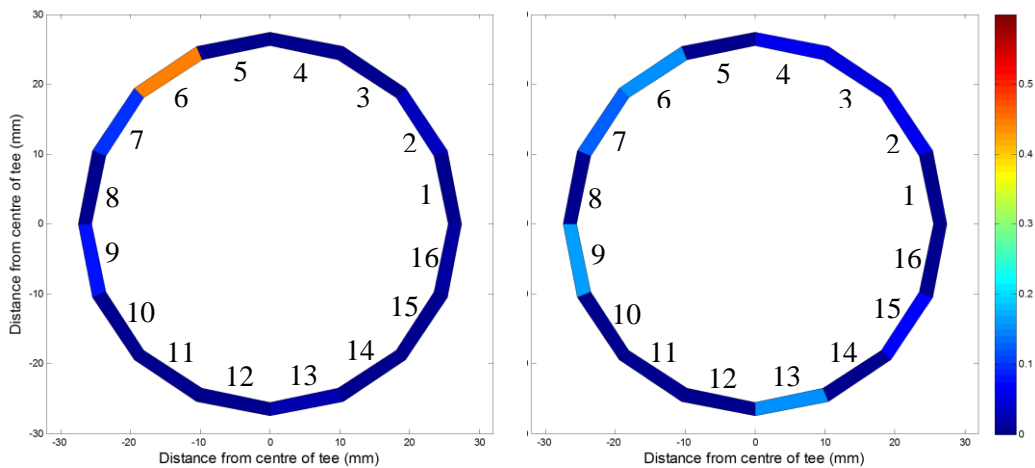


Figure 6-56 Cycle 4 (a) and cycle 5 (b)

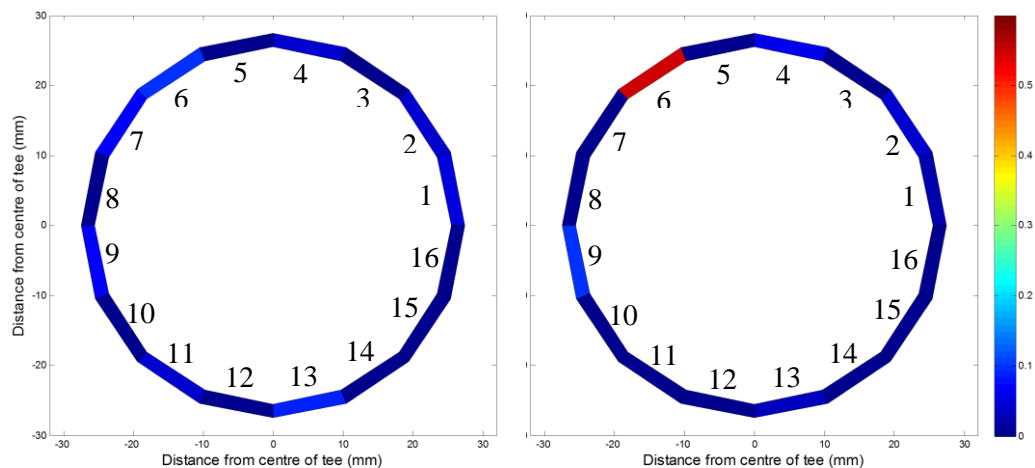


Figure 6-57 Cycle 6 (a) and cycle 7 (b)

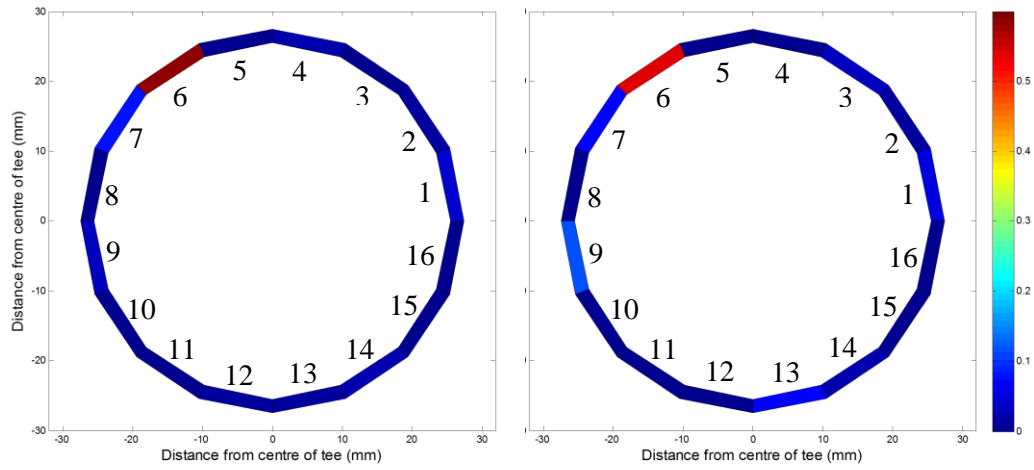


Figure 6-58 Cycle 8 (a) and cycle 9 (b)

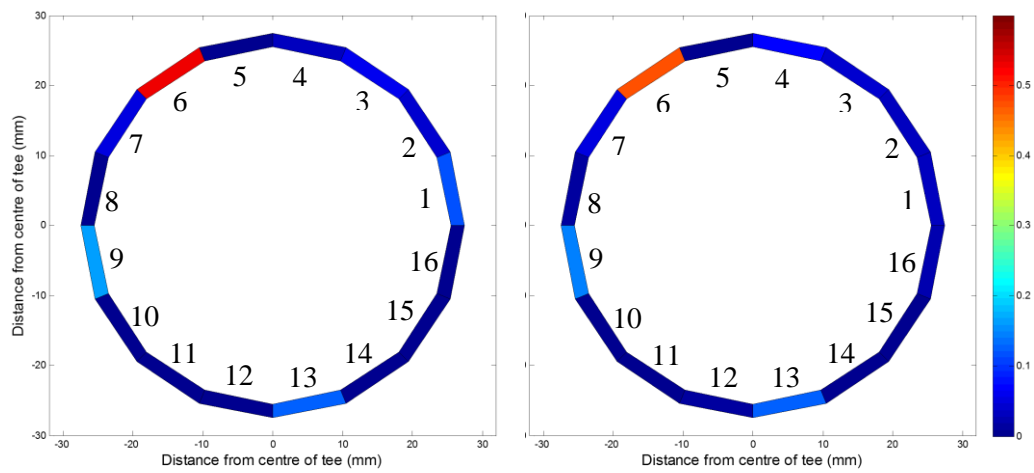


Figure 6-59 Cycles 10 (a) and cycle 11 (b)

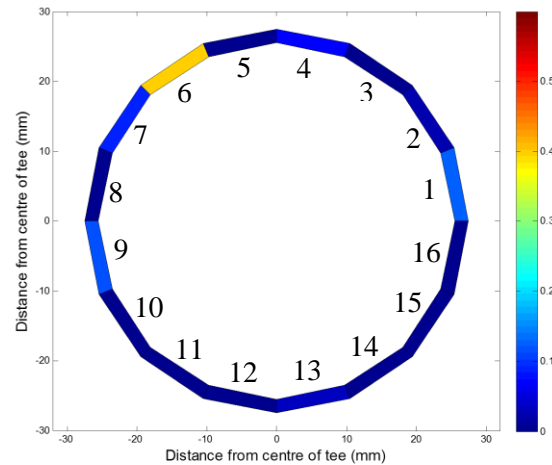


Figure 6-60 Cycle 12 (failure cycle)

The specimen failed on the 12th cycle during the rest time at the top of the cycle, i.e. at maximum pressure. It was also here where the scan commenced as the trigger pressure was active at the top of each cycle. Therefore, it is assumed that the sensors captured the failure as it occurred. Post-experiment, water was pumped through the failed specimen in order to observe the leak path. Figure 6-61 shows the leak path of the failed specimen; a major leak path was observed over sensors 1 to 6.



Figure 6-61 Specimen EU showing leak path area and direction

(Note: Photograph orientated to suit the sensor arrangement in Figure 6-60)

6.4. Conclusion

The general findings of the non-destructive testing of contaminated electrofusion tapping tees are summarised in this section. However, the experiments are discussed in more detail in Chapter 7 and Chapter 8

6.4.1. Static analysis

The design and implementation of a rig capable of performing line scans on joints that have already failed previously under fatigue was successful. However, the design showed limitations with regards to the post-processing of data whereby some step changes were apparent. This may have been mitigated through fully automating the rig. As the static analysis of contaminated electrofusion tapping tees using ultrasonic methods was part of two

consecutive MEng final year projects, it was considered beyond the scope of the students to fully automate such a system.

In general, the results noted the major leak paths of several joints but not all. In some cases sections of the fusion zone appeared to show delamination however no leak path was present at the location when the specimen was pumped with water post-scan. In contrast, some areas of the fusion showed no delamination but then appeared to leak when pumped with water. However, this was not apparent in all cases and therefore may warrant further investigation.

It would appear that the single transducer method for the purpose of observing delamination, and therefore leak paths in already failed contaminated electrofusion tapping tees, may not be the best approach.

6.4.2. Real-time analysis

The initial design concept using a linear arrangement of sensors failed to successfully confirm the failure mechanism of a contaminated electrofusion tapping tee during a live fatigue test. This was mainly due to mechanical issues, i.e. the probe pausing midway through a scan. The issues were most likely due to size (and torque rating) of the stepper motor and in hindsight, may have been overcome by the implementation of a large (more powerful) stepper motor. However, the quality of data was also questionable in that the centre of the tapping tee was not always captured at the start of the first test. As this area should be the most obvious part to observe, how can one guarantee that the data is sound if this area is clear to the interpreter.

The linear sensor arrangement was also manufactured with 3 sensors that did not work which meant that any conclusions made as a result of any testing may need to be redone using an array where all sensors were working; therefore confirming the original conclusions.

The pad sensor arrangement seemed promising in showing the development of cracks through the jointing interface but again limitations within its design meant that solid conclusions could not be drawn. The position of the sensors with respect to the fusion zone meant that delamination would only be observed local to where the sensors were placed. Therefore, an analysis of crack initiation and propagation would be near impossible to observe. The analysis did show some change in the signal amplitude but on most sensors. The most obvious and largest amplitude change was at sensor 6. However, the specimen showed a predominant leak path between sensors 1 to 5; therefore again, the analysis being inconclusive.

Chapter 7

Discussion

This chapter aims to discuss the outcomes of the research project through results obtained via destructive and non-destructive testing. The limitations of the experiments are also discussed to give a thorough perspective of the research with regards to its potential impacts.

Fundamentally, only one size of pipe and fitting were tested in this project. Therefore, in order to gauge a broader understanding of the effects of contaminated electrofusion tapping tees, further testing may be required; using different pipe and fitting products that are available. The observations made in this project are not necessarily representative of all available electrofusion tapping tee products as there will be variation in design and performance potentially. Additionally, the principles of electrofusion jointing with regards to polymer adhesion during the welding process remain the same which gives credibility to this research.

For all the tests conducted in this project on electrofusion tapping tees it is important to note that only the welding interface was subject to testing. The tapping tees were not ‘tapped through’ to the pipe to create a vessel; thus only the welding interface between fitting and pipe were subject to testing.

In this discussion, ‘pressure’ will be discussed in context to water distribution systems. Although this is required to introduce the practical benefits of this research, it is important to note that contaminated electrofusion tapping tees may perform differently if they were tested as a vessel (i.e. tapped through to the host pipe). This method would arguably be more representative of the performance of a contaminated tapping tee in service. However, only the welding interface was tested to eliminate any undesired variables which may cause variations in results. Furthermore, a better understanding of failure mechanics is achievable if the welding interface is assessed only.

7.1. Joint preparation

It is important to understand how joints were created for testing in this project in order to appreciate the benefits of the outcomes of this research. For typical PE pipe products, prior to the assembly of an electrofusion fitting, the oxidised layer on the outside of the PE pipe needs

to be removed. This is usually achieved by the use of a mechanical or hand scraper. Mechanical scrapers are generally preferred where possible as they leave a more consistent surface for jointing. Previously mentioned in Chapter 3, the PE pipe product used for this experiment had a protective polypropylene skin that needed to be removed prior to assembly of the fitting and welding. Once removed it revealed the PE pipe with a smooth extruded external surface of which no additional scraping preparation was required. Therefore, brushing the talc contamination on the pipe surface is arguably more uniform than if it were to be brushed on the scraped surface. No comparative tests were performed between skinned and scraped pipe to observe the difference in distribution of talc therefore no solid conclusions can be made. However, using this product reduced a test variable as the surface of the pipe was consistent throughout the project.

In general, the method in which a contaminant is applied onto the surface of a pipe is important for consistency and repetition. Applying a substance onto a surface using dissimilar methods may give different particulate size and distribution. With regards to the distribution of talc on the surface of the pipe in this project, an experiment was conducted to observe the difference in distribution if the talc were to be applied by brush compared to the recommended WIS method (see Appendix A). WIS 4-32-08 [14] recommends a machine which applies automation to the procedure. However, specialist machines such as this are hard to come by in the industry. Furthermore, if the test is required to be performed in industry, application of the talc using a brush may be acceptable, specifically if there is limited application area such as those for tapping tees [61]. The outcomes of the talc application experiment showed that applying the talc using a brush gave greater coverage on the pipe surface with smaller particulate sizes. This indicates that the contact between pipe and fitting may be considerably reduced – suggesting a worst case scenario. Furthermore, in this project, talc contaminant was applied to the surface of a PE pipe using a soft bristle paint brush. It may seem that application using a brush can be seen as subjective; however, it is believed that this is common practice in the industry.

With regards to the assembly of the fitting onto the pipe prior to welding a point must be raised: hypothetically, if a uniform size and distribution of contaminant were to be achieved consistently and repetitively for the preparation process, the surface of the pipe will be disturbed to some degree once the electrofusion fitting is assembled onto the pipe. To automate the entire process (contaminating and assembling) would take time and may prove costly – especially if very little difference in performance were found. Furthermore, there is no guarantee or test of the distribution of the contamination once the fitting is assembled. From an experimental point of view, there is an argument that more data can reduce uncertainty in some cases. The short term burst tests performed prior to the fatigue tests showed less than 0.8

bar (80 kPa) (<5%) difference in the average and median failure pressures in 4 tests. It can therefore be assumed that the application of talc and the assembly of the fitting were consistent.

Only the jointing interface was tested in this research. Therefore the fitting was not tapped into the pipe in order to create a vessel for testing. This was to mitigate the addition of hoop stress effects within the pipe; focussing the research on the fusion interface alone. With regards to tapping into the pipe, a cutting tool (housed within the tapping tee) is screwed to penetrate the pipe and thus allowing water to flow from the pipe through the fitting in service. There is an argument that if the jointing interface were to be contaminated prior to welding, tapping into the pipe could cause a localised stress that may initiate a crack – reducing the fatigue-life potentially.

7.2. Fatigue performance of contaminated electrofusion tapping tees

In general, the results from extensive testing have shown that failure is possible for contaminated electrofusion tapping tees using a low-cycle fatigue testing regime. However, specific aspects of the research need to be discussed in detail to offer perspective to the previous statement.

7.2.1. The experimental hydraulic rig

An experimental hydraulic rig was designed and built to house two tests: a short term burst test and a long term (low-cycle) fatigue test. The fatigue tests used two approaches: a fixed mean pressure and a variable mean pressure. Both regimes and their outcomes will be discussed separately in Sections 7.2.2 and 7.2.3 respectively.

The hydraulic rig design held certain limitations with regards to the fatigue testing regime. In essence, the rig that was designed to host the aforementioned tests was a hydraulic piston. The piston was housed in a servo-hydraulic fatigue testing machine, typically used to destructively test specimens in tension-tension or compression-tension tests at various frequencies and loading. The bore of the piston was rather large and therefore only small displacements of the piston head were required to create large variations of pressure. As only small displacements were required, this restricted the potential use of the servo-hydraulic machine as the test would appear ‘static’ (at a glance) rather than dynamic when live – this may have a mechanical influence on the machine’s servo-valve that governs the flow of hydraulic oil through the

system. In hindsight, the bore of the piston could have been designed smaller to offer larger stroke lengths. This may have improved the response of the servo-hydraulic testing machine, thus making efficient use of the servo-valve. Furthermore, this may increase the potential for more versatile testing programmes using higher frequencies of 1 Hz for example.

Commenting on the original piston design and set up, this may have been better suited to be retrofitted to an electrically driven machine as opposed to servo-hydraulic machine. Electronic machines can be less responsive than servo-hydraulic machines; this may have eliminated some of the initial ‘teething problems’ associated with tuning the servo-hydraulic rig using the PID control-loop system. However, the servo-hydraulic set up had the potential to increase the frequency of loading – this was not explored in this project.

A failure of a contaminated electrofusion tapping tee was previously described in Chapter 4 as a leak path great enough such that the specimen was unable to maintain pressure. When a specimen failed, the piston head would drop instantaneously to maintain the required (target) pressure. This inevitably forces the water that was housed in the piston cylinder, through the recently made leak path. It cannot be ignored that force exerted by the water passing through may increase the overall size of the leak path; therefore giving an exaggerated indication of the extent of the failure. Footage taken using a high-speed camera at 25 frames/second showed the leak path slightly increase in size upon failure during a ramp to burst test on a contaminated electrofusion tapping tee which supports this theory.

7.2.2. The fixed mean approach

The fixed mean approach showed that fatigue-life is dramatically reduced if the pressure range is increased. However, this is logical considering how the loading patterns (pressure ranges) were developed. A series of short term burst tests were conducted (see Section 3.3.1) to obtain an average failure pressure of a contaminated electrofusion tapping tee. Percentage decrements of the average failure pressure were then taken to create the pressure ranges for fatigue testing. Therefore, logic would suggest that the larger the pressure range – thus closer to the average failure pressure of a contaminated electrofusion tapping tee – the quicker the failure (i.e. reduced fatigue-life). This proved to be the case.

The pressure gradient (rate of increase/decrease) was fixed at 25 bar/min (41.67 kPa/s). The fatigue test was designed to maintain some relation to the current contamination test specified in WIS 4-32-08 [14] – i.e. the short term burst test. Therefore, the pressure was increased from 5 bar/min (8.33 kPa/s) (as per the WIS) to 25 bar/min (41.67 kPa/s) simply to reduce test times and aid in the generation of data worthy for discussion. Burst tests were performed at both

pressure rates and little difference was found. However, this may not be the same for different tapping tee products available in the market.

As the pressure gradient was fixed to 25 bar/min (41.67 kPa/s) for all loading patterns, this inevitably varied the cycle times (frequencies) for each pressure range. This may seem unorthodox for fatigue tests however, as mentioned previously, the regime wished to maintain some relation to current standard testing – specifically, the short term burst test highlighted in WIS 4-32-08 [14].

It is important to note that surge is mentioned in Chapter 1 and examples of variations in pressure are presented. A surge is described as a sudden change in pressure. With regards to this testing programme, the rate of pressure increase/decrease - fixed at 25 bar/min (41.67 kPa/s) – equating to 0.417 bar/sec. The pressure used in this regime can by no means be regarded as a ‘sudden’ change in pressure as literature and high frequency logging data show large increases in pressure over very short spaces of time (<8 bar/sec [48]); thus much faster than 0.417 bar/sec. It can therefore be assumed that this testing regime does not aim to replicate surge events expected in water distribution systems.

As mentioned previously, the loading patterns (pressure ranges) were developed by taking percentage decrements of the average failure pressure of contaminated tapping tees subject to the short term burst test. With regards to the pressure range that may be observed in surge events, the largest loading patterns (such as 90% $P_{MAT, MAX}$) may be seen as too large or not realistic. It is arguable that the lower pressure ranges may appear to be more realistic thus comparable to pressures expected in surge events. However, as the rate of increase in pressure used in this testing programme was relatively slow; this reinforces that relating this testing regime to surge events in water distribution networks directly is not realistic. Importantly, this work has demonstrated that even at low pressure ranges, fatigue failure can occur for contaminated electrofusion tapping tees.

It is important to note the significance of the mean pressure that was selected for this testing regime: 12.5 bar (1.25 MPa). This was calculated as half of the average failure pressure of contaminated electrofusion tapping tees; as mentioned previously. If one were to attempt to relate these results to common operating pressures, this value would arguably be too ‘high’ for distribution mains of 110 mm diameter. For this reason, a second testing regime was developed to observe fatigue-life at nominal operating pressures; this will be discussed further in Section 7.2.3.

It was in the remit of the fatigue experiment to accelerate the time to failure. It is not uncommon in fatigue tests to use an 80 °C bath to house specimens to decrease the time to

failure [37]. However, in this experiment it was decided to test at ambient temperature and use an increased pressure as the failure accelerant. Furthermore, this testing programme has shown that fatigue failures can occur on contaminated electrofusion joints in relatively short spaces of time but at higher than expected pressures – with regards to the operational pressures of water distribution networks.

The loading patterns for the fatigue test were trapezoidal; research by Joseph & Leever [77] and Bowman [49] used these loading patterns on uPVC pipes and PE pipe joints made with electrofusion fittings respectively. There is inevitably a rest period associated with a trapezoidal loading pattern. The rest time for each pressure range was determined as: $t_{REST} = \frac{2}{3} \times t_{RAMP}$, although this meant that the rest time would change consistently between pressure ranges, choosing a consistent rest time may have given slightly different results as this may have affected the creep response of any bonded areas. As the fracture surface of the joint was brittle and the relative tests times are short [low-cycle fatigue], the creep response of contaminated electrofusion joints was not explored in any detail. Static pressure (creep) tests may be required to discuss creep with regards to this testing regime.

The data observed from surge events showed a sinusoidal decrease in pressure range until a steady state pressure was achieved. Therefore there is an argument that the trapezoidal loading pattern is better suited to represent diurnal pressure variation at frequencies less than 0.02 Hz (1 cycle every 50 seconds).

The results illustrated in Figure 4-1 show that for lower pressure ranges, it would appear that the predictability of failure becomes more difficult. With regards to fatigue testing, generally speaking, there will always be an element of scatter in testing results – Dowling [34] explains that if multiple fatigue tests are run at one stress level, there is always statistical scatter in the fatigue-life. Bowman [49] explains with regards to fatigue testing of electrofusion fittings, the fatigue life can vary by a factor of ten if different material is used in the manufacture of electrofusion couplers. It was noted in Section 3.2.1 that the fittings were purchased off-the-shelf, therefore it is possible that the fittings came from multiple batches. This may have contributed to the wide scatter in the results from this experiment, however this seems unlikely as the same product of PE100 grade was used throughout the project.

It is important to note that typical fatigue tests on PE pipe usually indicate a high number of cycles until failure ($>10^5$ cycles); as this testing regime was developed by using pressure ranges that are percentages of the average failure pressure of contaminated electrofusion tapping tees, it can therefore be expected that fatigue-life would be considerably lower than

that of typical fatigue testing programmes. Furthermore this testing regime should be classed a low-cycle fatigue test.

When testing at lower pressure ranges, some joints did not fail after 1000 cycles. The logarithmic trend in Figure 4-1 suggests that there is an increase in fatigue-life as the pressure range decreases. It is possible that failures may have occurred beyond the 1000 cycle limit however, further testing may be required at an increased cycle limit (beyond 1000 cycles) to explore this further. Testing at lower pressure ranges than those used in this fatigue testing regime may also improve the trend-line further, however this will prove costly due to the increase in test times.

7.2.3. The variable mean approach

The variable mean approach sought to observe the fatigue-life of contaminated electrofusion tapping tees at mean pressures that may be observed in the water distribution networks. For this regime, the pressure range remained constant at 15 bar (1.5 MPa). From observing the results from the fixed mean approach, this range was selected as it was assumed that realistic tests times would be achievable if this pressure range were selected and the mean pressure varied.

Tests were performed with mean pressures exceeding and under the original mean pressure defined in the fixed mean approach testing method (i.e. variable pressure range). General observations showed that much like the previous testing method with regards to pressure, as the (mean) pressure increased, the fatigue-life decreased. As the pressure was lowered, the fatigue-life increased – up to the point where some specimens did not fail at 3 different mean pressures. Again, a cycle limit was implemented to improve the momentum of data generation; this was set to 1500 cycles. This was increased from 1000 cycles from the fixed mean testing regime as there appeared to be more scatter in the results than expected. Therefore increasing the cycle limit aided in investigating this.

On the basis that some specimens did not fail and much like the previous testing regime, it can be said that lower mean pressures push the boundaries of obtaining results (failures) for the specific testing parameters set for this regime.

Again, much like the previous testing programme, as the pressure reduced, the breadth of scatter increased. Furthermore, the predictability of failure becomes more difficult to predict as pressure is decreased.

From the results depicted in Figure 4-7, the existence of a bimodal distribution was discussed. Here two gaps were consistent with the lower 3 mean pressures tested. These mean pressures also had several joints that did not fail after 1500 cycles. There is an argument that both gaps would be filled through further testing, however, it is interesting to note the shift in performance in the largest gap. As mentioned in Section 7.2.2, it is possible that the breadth of scatter may have been influenced by the joints being purchased off-the-shelf and therefore are likely to have come from different batches. This may contribute to the explanation of the small shift in performance; or increased scatter.

This testing regime aimed to observe the performance of contaminated electrofusion tapping tees if the mean pressure were to be reduced to pressures that may resemble steady-state pressures in water distribution networks. The lowest mean pressure tested in this regime was 9.5 bar (0.95 MPa). This is arguably quite high for a water distribution mains pressure that may operate between 2 - 6 bar (0.2 – 0.6 MPa), therefore the results cannot be directly comparative. As the pressure range was fixed at 15 bar, the lowest target pressure achieved at the lowest mean pressure tested was 2 bar (0.2 MPa). Test could have been performed at lower mean pressures up to 7.5 bar (0.75 MPa), however, lowering the pressure beyond this would result in negative pressures which was not desirable. Even testing at 7.5 bar (0.75 MPa) may be seen as high for distribution mains; using a lower pressure range will allow for lower mean pressures to be tested. However, based on this methodology of testing, this would increase the test times as the time to failure would be expected to increase – which would make tests unfeasibly long.

7.2.4. Influencing factors

A small number of observations, discussed in Section 4.3, indicated that if a joint were to shift laterally during the welding process of a contaminated electrofusion tapping tee, this may improve the joint's fatigue-life under the fixed mean testing regime. From the research performed, there is some evidence that suggests that lateral shift less than 1.3 mm has no effect on the fatigue performance of contaminated electrofusion tapping tees. However, shifts greater or equal to 1.3 mm but below 2.5 mm ($1.3 \text{ mm} \leq \text{lateral shift} \leq 2.5 \text{ mm}$) appear to have a positive impact on the fatigue performance subject to the fixed mean testing parameters specific to this project. However, one result held a fatigue-life of 514 cycles but only shifted 0.8 mm.

The observations held a potential flaw in that the measurement of lateral shift was not consistent for all joints. Some joints were measured using a Vernier Caliper (accurate to 0.02 mm) post-weld, whereas others were measure using an LVDT and monitored during the

welding the process. The position of the tapping tee with respect to the pipe was marked prior to each weld; the displacement of the tapping tee was measured using the Vernier Caliper post-weld using the mark as a reference. Whereas those observations measured using the LVDT used the tapping tee welding terminal (close to the pipe) as a reference. There is no argument in the accuracy of the LVDT measurements but the Vernier Caliper measurements may be questionable as a thick permanent marker was used as a reference.

The SEM analysis of the failure surface of one contaminated electrofusion tapping tee highlighted in Section 5.4 and further discussed in Section 7.3.1.3, revealed that a small amount of bonding took place about the top of U-valleys that were created as a result of filament wires embedding themselves into the parent pipe. This observation was interesting as a small amount of ductility appeared to be present at a microscopic level. With regards to the influence of a lateral shift on fatigue performance, it is possible that the shift increases the ductile welded area that is local to the aforementioned U-valleys. Further destructive testing and SEM analysis of laterally shifted joints may confirm or disprove this hypothesis.

7.3. Assessing the failure mechanism

To better understand the failure mechanism of contaminated electrofusion tapping tees, destructive and non-destructive testing methods were implemented. These methodologies, outcomes and limitations are discussed in this section – separated into *destructive testing* and *non-destructive testing*.

7.3.1. Destructive testing

Analyses were conducted to better understand the failure mechanism of contaminated electrofusion tapping tees. In general, this was achieved through destructive testing; implementing the crushing decohesion test to ISO 13955 [60].

Initially, using the crushing decohesion test, a comparison was made between a contaminated specimen and a specimen created to best practice principles. A sample set of specimens from the fixed mean approach testing regime were then taken to be analysed post-failure. Water was initially pumped through the specimens to observe their leak paths, then the specimens were subject to the crush decohesion test to visually inspect any differences in adhesion with respect to the welding interface.

A single specimen from the fixed mean approach testing programme was selected, pumped with water to observe the leak path, subject to the crush decohesion test, then an SEM analysis was also performed on four samples that were carefully cut from the parent pipe of the specimen.

7.3.1.1 Perfect vs. imperfect joints

To gauge an understanding of the severity that contamination has on joint integrity, a comparison was made between a contaminated electrofusion tapping tee and a tapping tee made to best practice principles. In brief, there was a clear difference in joint strength between the two specimens; the perfect joint being significantly stronger. However, due to the nature of the test, strength was not quantified and therefore the findings are descriptive.

The perfect joint appeared to show a small amount of stress whitening about the outer circumference of the jointing interface but it was clear that the tapping tee would struggle to be removed from the parent pipe without causing significant damage. It was therefore assumed that a fully ductile failure would occur for this joint.

It shall be noted that ISO 13955 [60] prevents the use of striking forces to aid the removal of a fitting. However, a lever can be used to ‘persuade’ the fitting away from the pipe. For this particular tapping tee - due to its design - there was insufficient purchase to insert a lever to remove the fitting from the parent pipe. Using a lever would assist the fitting to peel away from the pipe, thus ensuring a mode I failure with respect to fracture mechanics.

The contaminated joint mostly peeled away from the parent pipe during the crush test whereas the ‘perfect’ joint did not peel away whatsoever. This illustrated the influence that contamination has on joint strength and that the test was able to differentiate between welds containing talc and those without – an observation also shared by Troughton *et al.* [66]. Furthermore, the contaminated tapping tee showed some of the filament wires still embedded into the parent pipe which was believed may have been offered the joint minor structural strength.

It was noted that a small amount of ductility was observed on the surface of the pipe on the outer circumference of the fusion zone once the fitting was removed. These areas were scattered but visible to the naked eye on closer inspection. It was noted that these areas were consistent with where the fusion wires were embedded into the parent pipe. It was also noted that some of the fusion wires were embedded into the fitting on the inner circumference of the fusion zone. Here, it appeared that a small amount of bonding had taken place.

7.3.1.2 Adhesion with respect to fatigue

Destructive tests were performed on contaminated electrofusion tapping tees that had already failed in the fixed mean fatigue testing regime. The destructive testing was undertaken by the second Masters student. A total of six joints were selected to represent the average number of cycles to failure for each pressure range tested to the fixed mean fatigue testing regime. Firstly, the joints were analysed using ultrasonic techniques in an attempt to observe the leak path(s) post-failure. Water was then passed through the fitting to confirm/disprove the hypotheses. Bonding about the jointing interface was then observed after the specimens were subject to the crushing decohesion test to ISO 13955 [60].

In general, when water was passed through the specimens there were no obvious patterns in the location of the major leak path with respect to all six specimens. This may suggest that the specimens were created without bias. Furthermore, minor leak paths became more predominant in the specimens with the lower pressure ranges. For example, there were no minor leak paths in the specimen that failed at the highest pressure range (90% $P_{MAT\ MAX}$), whereas the specimen at the lowest pressure range (40% $P_{MAT\ MAX}$) showed 2 minor leak paths as well as a major leak path. This may suggest that cracks may propagate in a circular manner – following the direction of the filament wires - about the jointing interface during dynamic loading. As the specimen at the highest pressure range failed within one cycle, there was technically no dynamic load thus circumferential crack propagation about the jointing interface would be less predominant. In this case, as the pressure increases the load will be concentrated to the weakest part of the jointing interface until a leak path is formed (viz. failure occurs).

Once the electrofusion tapping tee was removed from the parent pipe via the crush decohesion test, it became clear that the talc contamination acts almost as a barrier – to put simplistically – denying the polymers of the pipe and fitting to mix. This further enforces research discussed by Marshall *et al.* [24]. However, all specimens showed very small amounts of ductility about the outer circumference of the fusion zone. This was visible on close inspection by the naked eye. This may be due to the small amount of deformation that occurs during the welding process; as the clamping device houses a spring that applies a compressive force between the pipe and fitting. As the fittings coil (filament wire) begins to heat during the fusion process, combined with the compressive force from the spring, this causes a small amount of deformation of the pipe – creating a temporary and local ovality with respect to the clamping device. As a result, the movement at the outer circumference of the fitting may move the talc to allow a limited amount of bonding to take place.

Research by UKWIR [78] observed that the force applied by the spring is reduced due to the deformation of the pipe under compression; this in turn reduces the amount of melt mixing during fusion. This is also true for observations made in this project; however, it is likely that the shape (i.e. design) of the tapping tee gave some degree of melt mixing about the outer circumference due to the deformation of the pipe during the fusion process.

Another explanation for small amount of ductility on the circumference would be due to the placement of the tapping tee onto the surface of the pipe prior to welding. The pipe is initially contaminated using talcum powder; the fitting is then carefully placed onto the surface of the pipe – held in place using the compressive clamp. It is possible that uniformly distributed talc is disturbed on the pipe local to the outer circumference of the fusion zone – potentially exposing virgin pipe; allowing a small amount of localised bonding to take place.

It is interesting to note that the areas that show a small amount of ductility are not necessarily the strongest part of the joint with respect to leak paths. Two joints showed major leak paths that appeared to run through areas that showed little ductility on the circumference of the jointing interface. This was the same for minor leak paths in that they appeared at random and did not correspond to areas that showed ductility.

Once the fitting was removed from the parent pipe, there were some signs of adhesion; this was shown as remains of black polymer on the surface of the pipe about the fusion zone - the black polymer coming from the tapping tee fitting. Again, there appeared to be no clear links between this small amount of adhesion and leak paths. However, the lower pressure range samples: 60%, 50% and 40% $P_{MAT\ MAX}$, showed a major leak path through areas that had very little black remains on the pipe. However, for the specimen at the lowest pressure range, there were other areas that had no adhesion and failed to illustrate a leak path.

Only six specimens were used as the basis of this investigation. Although the specimens were selected to represent the average fatigue-life of each pressure range, a thorough investigation of more specimens would further enforce the hypotheses stated above.

With regards to the discussion above, it was generally assumed that any leak path would propagate radially starting from the centre of the tapping tee; as this is the origin of stress concentration when the test commences. However, the electrofusion filament wire that is heated during the fusion cycle may promote radial development of crack propagation. Therefore, leak paths may not necessarily propagate linearly about the centre of the tapping tee.

It is important to discuss the crush decohesion test in light of the investigation above. The crush decohesion test is used to observe the nature of failure as well as determining the percentage of decohesion between the pipe and fitting (measuring the pipe only). The test was specifically not designed for contaminated assemblies of which have shown to have a brittle surface if contaminated. As this is the case, the percentage of decohesion was not calculated as it would not offer any significant benefit to the research. With regards to the test methodology, a crushing device is used which can promote the fitting to peel away from the pipe. As the pipe is deformed during the test there is an argument that the test does not assess the long term performance of the joint. However, an idea of the amount (percentage) of decohesion of an assembly may give an indication of the quality of the welding parameters.

As the specimens used in this section had already failed during a live fatigue test, it is important to note that the decohesion test is not a suited destructive test to assess the failure mechanism of a contaminated electrofusion tapping tee. Observations of the parent pipe showed that the areas with small amounts of black polymer (from the fitting) were not necessarily the strong points of the joint as major and minor leak paths were predominant over these areas. However, areas such as these as well as the small limited ductile areas about the circumference of the jointing interface, are only predominant due to crushing decohesion test. In general, when a joint fails during a fatigue test, a leak path is created; the fitting is still adhered to the pipe, however, the joint is unable to maintain pressure due to the newly formed leak path – thus not fit for purpose and deemed a ‘failure’. As the fitting is still adhered to the pipe post-failure, it is difficult to assess the failure mechanism using destructive techniques, therefore the crushing decohesion test is not suited to assess the failure mechanism of a contaminated electrofusion tapping tee.

7.3.1.3 Specimen X – SEM analysis

Specimen X was chosen to be analysed using SEM. The specimen had also previously failed under fatigue loading using the fixed mean approach. The specimen held a fatigue-life of 2 cycles at 80% $P_{MAT\ MAX}$. When water was passed through the joint post-failure, two major and two minor leak paths were witnessed. The specimen was subject to the crushing decohesion test. In general, observations did not differ from those discussed in the previous section (7.3.1.1). There were four square areas approximately 15 x 15 mm that were selected to be further analysed using SEM. These were decided as two of the areas appeared to show a small amount of ductility about the outer circumference of the jointing interface. One was selected as there were black polymer remains on the pipe and the last was chosen as the pipe appeared to be all white – i.e. no black polymer remains.

In previous observations on other specimens with the naked eye, all the small amounts of ductility witnessed appeared to be either side of indentations caused by the filament wires during the heating cycle of the welding process. This was further confirmed by the SEM analysis on Specimen X. It appears that the filament wires embed themselves into the parent pipe during the heating cycle of the welding process. Once embedded and cooled, this may offer the assembly additional strength. The depth of the wire with respect to pipe across the fusion zone was not explored due to the complexity of the analysis with respect to the project's timescale. However, it is possible that the depth may be a function of the compressive force exerted by the top-loading G-clamp; fusion time and the melt flow of the materials.

The filament wires created U-shaped valleys that looked like tramlines under the microscope. On closer inspection using SEM, at the brink of the U-valleys elongations of the polymer can be seen on most of the samples. This suggests that the polymers of pipe and fitting have begun to bond at these points and began to craze when subject to the crush test. Some of the elongations were observed with the naked eye in previous experiments; however, using the SEM, it became clear that this occurred on a microscopic scale also. This localised bonding about the brink of the U-valleys is likely to be caused by the displacement of the pipe's polymer when the filament wire is heated and the compressive force of the top-loading G-clamp is present. Here, the contaminated surface is likely to be displaced allowing virgin polymer to bond to the fitting – potentially increasing joint strength.

Closer inspection of the U-valley revealed small white particles that relate to the size and distribution of talc on the surface of the pipe. This may be the talc pressed into the polymer of the pipe during the welding process. Unfortunately, this could not be confirmed during the SEM analysis and would require a further chemical analysis to prove the hypothesis.

In general, between the U-valleys very little bonding took place. The surface looked mainly brittle with very short elongations of polymer at high magnifications. These elongations could be fibrils as a result of crazing (as discussed by Hertzberg and Manson [36]) from the fatigue test. However, this is difficult to confirm as the tapping tee needed to be physically removed from the parent pipe which may have introduced the fibrils.

It can be said that the area between the U-valleys is the weak part of the joint. If this is the case, it is possible that during a dynamic test, water may circumferentially propagate between the valleys as they are the weakest element. Once propagation has reached its maximum, the microscopic bonding about the filament wires may offer the joint its strength. Bonds may slowly unravel under dynamic loading until a clear leak path is presented. However, this hypothesis is difficult to prove using post-failure methods of analysis.

7.3.2. Non-destructive testing

Post-failure analysis was also conducted using non-destructive methods; specifically using ultrasonic techniques. Two Masters level projects, running over consecutive years, were conducted with the aim to develop a rig to observe leak paths in already failed tapping tees. This was achieved by performing line scans on the bore of the pipe local to the fitting. Scans were performed using a single transducer focussing probe.

In tandem with the latter Masters project, two rigs were designed and built to monitor the tapping tee's fusion interface with an aim to confirm the failure mechanism during a live fatigue test. In brief, the first rig held too many variables within its mechanical design which may have given inconsistent results; therefore the rig was redesigned with no moving parts. The second rig failed to confirm the failure mechanism potentially due to the simplicity of the design.

To generalise, in this project non-destructive tests were performed in two scenarios: static and real-time analysis. Both are broken down and discussed in this section.

7.3.2.1 *Static analysis*

The first Masters level project designed and built a rig capable of performing line scans on the bore of the parent pipe local to the welding interface. The analysis hoped to observe delamination at the fusion interface (between pipe and fitting) which would then be confirmed by pumping water through the specimen using a basic hand pump to observe the leak path. The project was successful in that the rig was capable of obtaining data from line scans. However, only some major leak paths were observed and the results appeared misleading in places. This may have been due to the way the data was processed using MATLAB. Regardless, the results did show some promise and warranted further investigation.

It is important to note that the specimens used in the project had already failed from a ramp to burst test. Therefore, the specimens analysed were not from the fatigue testing regimes. From the previous discussion in Section 7.3.1.2, minor leak paths are less predominant in specimens subject to higher pressure ranges with regards to post-failure analysis of fatigue tested joints. Therefore it may be unlikely that any minor leak paths are present and therefore may not be observed using the ultrasonic analysis. However, this is not to say that delamination has taken place in these areas without causing a clear leak path.

Only one of three results is shown in this thesis for the purpose of explanation. The result highlighted in Section 6.2.2 clearly show delamination about the surface that corresponds to the major leak path when water was passed through the specimen. One of the remaining two

results also successfully highlighted a major leak path but there were step changes in the data when graphically illustrated. This was also the case for the final scanned specimen that failed to observe convincingly the major leak path. The step changes in data may have been the manual alteration of the position of the probe in order to perform the line scans. Furthermore, the probe was required to be rotated to compensate the local deformation about the centre of the tapping tee fitting local to the pipe. This may have led to inaccuracies post-analysis of the data. Although the results were inconclusive, the research warranted further investigation.

The second Masters level project aimed to observe trends in leak paths from joints previously tested under dynamic load. This was accomplished by using the rig previously developed for the first Masters level project. In general, the observations made using single focussing probe ultrasonic techniques were not conclusive. In some instances, the leak paths were observed, however, in others the scans completely missed some delaminated areas.

As the failure mechanism of the joints is yet to be confirmed, the failure mechanism was assumed to be crack propagation about the jointing interface. It is fully possible that crack propagation may be random and in more than one location as a result of dynamic loading. Thus multiple potential leak paths may have been observed in non-destructive analyses of the jointing interface and therefore may be misleading with regards to assessing the area in which it failed.

When a specimen fails (see Figure 5-4) and a major leak path is formed, it is important to consider that the piston head of the experimental hydraulic rig (previously mentioned in Section 3.2.3) drops instantaneously in an effort to maintain the target pressure of the cycle. In this effort, the water held within the piston cylinder is forced through the leak path until empty. During this process, it is possible that a local force is exhibited as the volume of water dissipates via the leak path. Therefore it is possible that the leak path opens further (increases in size) during this time. As the flow of water stops, the leak path (gap) may close up again; thus making it difficult to observe the leak path post-failure.

All pipes were cut in half prior to the scan. As the PE pipes method of manufacture is extrusion, when the pipe is cut in half, the pipe begins to revert (close in on itself). This may cause a very small amount of localised stress around the fusion zone – potentially closing any leakage gaps. This may be mitigated by performing analyses on whole pipes, however, the current rig design did not have the capacity to perform scans on whole pipes.

It cannot be ignored that the filament wires at the jointing interface may be heavily influencing the scans of the fusion zone and creating an element of scatter within the dataset. As the transducer receives its strongest signal from surfaces perpendicular to its source, the wires may

create a degree of scatter where the signal is diffracted by the wires. It is also possible that some of the reflections witnessed in the intensity maps may be from the filament wires themselves and not from the delaminated surface of the parent pipe; potentially giving a false reading.

It was required to manually orientate the probe in order to observe the area around the localised bump on the surface of the pipe; this in turn was able to achieve a full dataset of the fusion zone. As this process was not automated, there is an element of risk with regards to operator error and/or inconsistency within datasets. This is likely to be the cause of the step change in some of the dataset. Automating this process would undoubtedly reduce the risk of data inconsistency, however, this was deemed out of scope for the Masters level project.

MATLAB was used to post-process the data. As can be observed in the figures in Section 6.2.3, gaps are evident between each line scan. This is due to the offset caused by the rotation of the pipe in order to perform another line scan. This could have been mitigated by interpolating between points with respect to each line using MATLAB. However, this may be misleading if there are step changes within the dataset. There are entire lines of data missing from each scan. This was believed to be due to the conversion of data in the LabVIEW acquisition software; viz. a bug in the data acquisition program.

No clear conclusions could be drawn from the ultrasonic analyses as observing the delamination in the jointing interface seemed too challenging for a single focussing transducer probe. However, the specimens were further tested using destructive techniques to help to understand the failure mechanism. The outcomes of which are illustrated in Section 5.2.

7.3.2.2 Real-time analysis

The aim of the real-time analysis was to confirm the failure mechanism of contaminated electrofusion tapping tees when they are subject to dynamic loading. In brief, two different rigs were built to accomplish this. The first held variables within its mechanical design which resulted in inconsistent data. The second design was successful in obtaining worthy data but proved too simplistic in design to confirm the failure mechanism.

The first design encompassed a linear arrangement of piezoelectric sensors housed in a bespoke sensor holder. The sensor holder was mechanically fastened to a drive shaft and stepper motor. Although the design and manufacture of the apparatus were sound, the rig failed to obtain conclusive results to confirm the failure mechanism. One of the problems was insufficient power (torque) provided by the stepper motor to drive the main shaft – causing the probe to stop in the middle of a scan in one test; and unwillingly rotating the ‘home’ position

in another scan. In hindsight, both problems could have been resolved by introducing a higher torque rated stepper motor.

Upon reflection, the implementation of the linear sensor rig was necessary in this project as initially there was enough time remaining in the project to repeat the experiment on multiple test specimens to provide enough data to make a strong conclusion. However, as the initial results failed to be conclusive, it became clear that a redesign of the rig would be necessary to confirm the failure mechanism.

The linear sensor arrangement was also limited by only having 13 out of 16 sensors working in the array. Initially, a plan was sought to remake the array with an aim to obtain 16 fully working sensors in a new array. However, the flaw within the design of the linear array was that there would be some element of risk in ‘losing’ sensors every time an arrangement is manufactured. In general, the risk could be reduced through practice, repetition and strong quality control procedures throughout the manufacture process; all of which are time consuming as this is undoubtedly the development of a niche skill (i.e. sensor making) if accomplished in-house. Therefore, this was deemed out of the timeframe of this project and warranted a new plan to confirm the failure mechanism. This provoked the redesign of the rig which aimed to remove as many of the problems encountered from the first design. A modular design offered resilience which ensured that if sensors did not work, they could be replaced/removed thus not jeopardise the results from the experiment. Removing mechanical aspects of the rig may ensure that the data obtained is sound as sensors would be in a fixed position throughout the experiment. However, positioning the sensors was an issue with this design. The sensors could have been arranged so they were at a constant offset to the bore of the pipe – this may require the design and development of a sensor holder with enough ‘flex’ to compensate any irregular shape on the bore. The advantage of this is that the sensors can be used on multiple tests. This arrangement would also require the use of a couplant between the sensor and bore of the pipe. This was decided against as designing and manufacturing a flexible holder seemed too risky in comparison to gluing the sensors directly to the bore of the pipe. However, gluing the sensors directly to the pipe meant that there is an increased risk of damaging the sensors in an attempt to remove them from the bore of the pipe post-scan; thus the sensors being a ‘one use’ entity.

Not previously discussed in Chapter 6 upon the manufacture of the individual sensors which were used to create a pad array, a single sensor was tested on a random piece of PE pipe. The aim of the brief test was to ensure that the sensor design was able to see the back face of the PE pipe. This brief test was successful, however, a piece of pipe was used which was previously mentioned in Section 5.2; i.e. the pipe previously hosted a contaminated

electrofusion tapping tee but was then subject to the crushing decohesion test. The external surface of the pipe, local to the previous location of the electrofusion tapping tee, was uneven and consisted of some black polymer remains from the tapping tee (as per Figure 5-5). The test sensor was placed on the bore of the pipe local to the aforementioned fusion zone on the opposing side. The signal amplitude representing the reflection of the external of the pipe dropped considerably in comparison to the brief test conducted on the (smooth) piece of pipe. This is most likely because the external surface of the pipe is now uneven due to the removal of the tapping which causes the signal to become distorted – i.e. a true perpendicular reflection was not accomplished. It can therefore also be assumed that if a crack were to propagate through the jointing interface during a live fatigue test, the delamination caused as a result of crack growth may distort the signal of the ultrasound sensor thus not being able to accurately observe the crack growth.

The location of the sensors for the pad arrangement were determined by drawing the location of the fusion zone in AutoCAD and selecting a suitable radius that allowed the sensors to be grouped tightly together (see Figure 6-50). Although this is a logical approach for a limited number of sensors, only a small area of the fusion zone was observed by the sensors thus not giving a true representation of the influence dynamic load has on the fusion zone. However, the aim of the experiment was to (hopefully) illustrate the failure mechanism which was assumed to be crack propagation about the jointing interface. If the sensors were successful in observing this, the results may have shown clear areas where delamination was present in the jointing interface. However, this would need to be confirmed by using a secondary set of sensors beyond the existing circular set up to observe the crack propagate as the dynamic test is live. This was considered outside the timeframe of this project.

It cannot be ignored that the filament wires that are likely to be embedded into the parent pipe, as discussed in Chapter 5, may have affected the signal that is being received by the sensors. There are two potential likely scenarios if a sensor pulses directly at the filament wire. The first assumes that there is a loss of signal as it may scatter when it hits the filament wire; the second is where the signal that is received from the sensor is directly reflected from the filament wire which is most likely embedded into the surface of the parent pipe during the welding process. The latter will give a false result in the scan but still may seem like there is activity of a crack which has formed locally to the sensor. This can be overcome by using different methods of ultrasonic analysis such as ‘phased array’ which has proved effective in detecting voids in electrofusion joints [73].

Chapter 8

Conclusions

The main conclusions of this project are summarised below and then explored in greater detail in this chapter.

- Previous research as well as testing conducted to industry standards in this project has shown that contamination of the jointing interface has a negative influence on the mechanical performance of electrofusion joints. Current literature fails to link failures associated with fatigue with poor site practice. No [published] knowledge exists on the fatigue performance of electrofusion tapping tees.
- A bespoke hydraulic piston retrofitted to an existing servo-hydraulic testing machine was used successfully to dynamically test contaminated and uncontaminated electrofusion tapping tees.
- Low-cycle fatigue can be used to destructively test electrofusion tapping tees subject to talc contaminant in a relatively short space of time under high loading conditions; pressure ranges tested between 12.5 bar (1.25 MPa) and 22.5 bar (2.25 MPa) failed in less than 500 cycles with a mean pressure of 12.5 bar (1.25 MPa).
- Joints made to best practice principles and tested under fatigue in this project, did not fail when subjected to 1000 cycles at 22.5 bar (2.25 MPa) pressure range and 12.5 bar (1.25 MPa) mean pressure. Whereas contaminated electrofusion tapping tees failed to reach 1 cycle under these parameters.
- The predictability of failure under fatigue loading decreased as the mean pressure or pressure range is decreased.
- Lower pressure ranges used in the fatigue tests correspond to ranges expected during surge events. However, the rate of increase/decrease in pressure used in the fatigue tests were far slower than those experienced in such events; the loading rate used aimed to maintain consistency with current Water Industry Specifications. Due to this, it is difficult to relate field data to this work in order to predict in service lifetimes.
- SEM analysis of a specimen's fusion interface was observed which showed small amounts of ductility at the threshold of U-valleys which previously housed the filament wires – indicating that localised bonding occurs at these locations.

- Non-destructive post-fatigue failure analysis using a single ultrasonic focussing probe showed promise for observing leak paths. However, further investigation showed limitations in the technique due to the complexity of the fusion interface.
- Two bespoke ultrasonic instrumentation rigs were created to confirm the failure mechanism during a live fatigue test. In essence, both rigs failed to confirm the failure mechanism. However, a change in signal intensity was observed in the initial pressurisation of the specimen (prior to dynamic loading) which may be an influencing factor on the of the fatigue-life of contaminated tapping tees.

This thesis has presented work that relates to the fatigue of contaminated electrofusion tapping tees. It has also aimed to better understand the performance and failure mechanism of contaminated electrofusion tapping tees under dynamic load through the use of industry standard and new experimental testing techniques. Experimental methodologies and apparatus were designed and built to accommodate the research conducted in this project. Drawing on the outcomes of this project, this chapter is dedicated to the conclusions of all experimental work undertaken.

In comparison to PE pipe, very little published work exists on the assessment of electrofusion joints with respect to fatigue loading. Furthermore, there are only a handful of publications that make reference to electrofusion tapping tees – none of these make reference to fatigue. Due to the limited size of the fusion zone, tapping tees can be easier to work with and understand mechanically. However, these products are typically used to link costumers with the distribution main, whereas the coupler is used to join pipes of all sizes. Therefore couplers may be held in higher regard with respect to performance.

Contamination of the jointing interface is an undesired entity of electrofusion jointing. Quantifying the risk of contamination with regards to electrofusion jointing has not been explored in this project, however, the significant difference in performance between contaminated joints and joints made to best practice principles has been presented. There is distinctive reduction in performance and joint strength if the jointing interface is contaminated with fine china talc prior to welding. Furthermore, it is fundamental to note that joints welded to best practice principles and tested in this project did not fail.

All work carried out in this project has been performed using one type and size of fitting and pipe from the same manufacturer. The discussion and conclusions still carry weight and validity as the welding process and procedure are standard. However, to gauge a broader understanding of the performance of all products available in the market, the tests outlined in this project may need to be repeated on other products.

8.1. Current literature

The literature survey revealed that PE pipe has significant long term properties, potentially exceeding its 50 year design life by another 50 years [13]. Furthermore, PE pipe has excellent resistance to sudden increases in pressure and performing well when subject to surge loading [29].

Electrofusion jointing holds advantages over buttfusion and mechanical jointing and can leave a homogenous joint (disregarding the fusion wires) once complete. Literature revealed that contamination at the jointing interface can significantly reduce joint strength with regards to electrofusion joints.

Current literature fails to link failures associated with fatigue with poor site practice. Although there may be good reason for this – high frequency logging infrastructure is required local to the failure – water distribution networks experience variations in pressure which cannot be (and are not) ignored in the design process.

8.2. The fatigue performance of electrofusion tapping tees

Two low-cycle fatigue testing regimes were created to assess the performance of contaminated electrofusion tapping tees: a fixed mean and a variable mean approach. In general for both testing regimes, the results showed that fatigue-failure occurs in a relatively short space of time under high loading conditions. An exponential increase in fatigue performance was seen as the pressure range or mean pressure was decreased - respective to the aforementioned testing regimes. For both testing regimes, the predictability of failure also became more difficult as the pressure range or mean pressure decreased – this was mainly due to increase in scatter within the results. Although scatter is expected in fatigue testing, it was believed that the joints may have slight variations in performance due to different batches of manufacture – however, this cannot be verified.

Two joints made to best practice principles were tested under the fixed mean testing regime at the largest pressure range, of which no failures were observed. Contaminated joints tested under the same loading conditions barely held a fatigue-life of one cycle, further illustrating the detrimental effect that contamination has on joint integrity.

Some pressure ranges used in the fatigue testing regimes aimed to replicate ranges that may be experienced in water distribution systems during surge events. However, the larger pressure

ranges used in the fixed mean testing regime were an unrealistic representation of the pressure ranges expected. It is believed that the lower pressure ranges may be more consistent with pressure ranges experienced in surge events. However, the cycle frequencies used in both fatigue testing approaches were by no means short in duration therefore there is limited support to link the results obtained from this project with surge data that may be experienced in service. The pressure gradient used in both testing regimes was based on current standards to the short term burst test highlighted in WIS 4-32-08 [14].

To conclude, the experimental data shows that joint failures associated with fatigue are possible on talc contaminated joints under the proposed testing parameters. Although PE pipe has good short term resistance to increases in pressure (i.e. surge) in a nominal working scenario, this research suggests that if a product were to be installed incorrectly, the asset may fail prematurely.

8.3. Destructive tests

Destructive tests were carried out using the crushing decohesion testing methodology highlighted in ISO 13955 [60]. The comparison between a joint contaminated with fine china talc and a joint made to best practice principles showed the distinct decrease in joint strength if it were to be contaminated prior to the welding process. Notably, the joint made to best practice principles remained fully adhered to the parent pipe after the maximum crushing distance was achieved.

The crushing decohesion test was repeated on specimens that had previously failed by leaking after the fixed mean fatigue testing approach. Comparisons were made between specimens that failed in different pressure ranges with respect to the fixed mean. It appeared that major leak paths were created at random (i.e. no obvious common failure locations), however, minor leak paths become more frequent as the pressure range was decreased. This suggests that a crack growth mechanism may be more predominant in the lower pressure ranges whereas the higher pressure ranges only create a (major) leak path through the weakest point.

Specimen X was a contaminated joint that previously failed in the fixed mean fatigue testing regime. The specimen was subject to the crushing decohesion test and 4 samples were selected via a visual observation of the pipe's failure surface for further investigation using SEM techniques. U-valleys were observed whereby the filament wires had embedded themselves into the parent pipe during the welding process. The U-valleys were created using a combination of heat from the fusion wires and the compressive force from the top-loading G-

clamp. Small amounts of ductility were observed at the thresholds of the U-valleys which appeared to be the joint's source of strength. Under SEM analysis, the failure surface between U-valleys showed no ductility proving that little bonding took place. Interestingly, there appeared to be speckles of a substance (different to the parent material) embedded onto the surface of the pipe; distinctively in the U-valleys. It is believed that this is the talc contamination embedded onto the pipe but this was unable to be confirmed at the time of the analysis.

With regards to the fatigue performance of contaminated electrofusion tapping tees previously concluded in Section 8.2, a small number of observations in results were witnessed as there appeared to be a noticeable increase in performance that was believed to be due to a lateral shift in the electrofusion tapping tee during the welding process. This was overcome and therefore did not influence the fatigue results in the main body of the project. With regards to the SEM analysis, it is possible that the aforementioned ductility at the thresholds of the U-valleys may increase when a lateral shift occurs during the welding cycle showing a noticeable increase in contaminated joint performance when subject to the low-cycle fatigue testing regimes.

8.4. Non-destructive tests

Non-destructive tests were conducted using ultrasonic techniques post-failure to observe leak paths and during live fatigue tests to confirm the failure mechanism.

Initial investigations using a single focussing transducer probe to observe leak paths showed promise and warranted further investigation using the same technique to observe leak path trends with respect to fatigue failures through the fixed mean testing approach.

The leak path observations showed limitations in that data inconsistency prevailed in all specimen scans. It is believed that this can be mitigated through automation of the scanning procedure. However, even through automation of the procedure, there is no guarantee that the data presented would actually illustrate the leak path due to the complexity of the fusion interface – containing fusion wires and an inconsistent surface due to delamination. Therefore, any data collected would need to be confirmed using trialled and tested non-destructive techniques such as phased array ultrasonic testing [72] or microwave imaging [79].

Bespoke ultrasonic instrumentation was created in an attempt to confirm the failure mechanism of a contaminated electrofusion tapping tee during live fatigue tests. The linear

sensor array gave a good resolution of results, however, not all sensors were operational therefore the array would need to be remade to confirm the results. The data acquisition aspects of the design were reliable in that data was presented consistently; however, mechanical aspects of the rig required further improvements in order to strengthen the confidence in results. The aforementioned downfalls led to the redesign of the apparatus to a modular approach to increase resilience. However, single transducer elements meant that the resolution of the fusion zone was dramatically reduced in comparison to the original design. In essence, the modular design failed to confirm the failure mechanism during the live fatigue test. However, the results did show an increase in signal intensity in the initial pressurisation of the contaminated tapping tee which suggests that the majority of delamination may have occurred at this time. Even through further testing, this hypothesis may not be confirmed unless the resolution of the fusion zone thus the welding interface is increased. Furthermore, the filament wires may have been influencing the signal strength and quality – therefore it would be recommended to adopt the phased array ultrasonic approach to confirm the failure mechanism during the live fatigue test.

8.5. Application to industry

8.5.1. Operation and installation

The operation of large water distribution systems can be difficult to understand due to their complexity. Linking fatigue failures with the contamination of electrofusion joints has proven to be an extremely difficult task. It shall be noted that to the author's knowledge, there is no published work linking contaminated electrofusion joints and fatigue failure. However, this work has illustrated that even in laboratory conditions, the prediction of failure of contaminated tapping tees can be difficult. It is noted that the risk of contamination occurring on-site is deemed out of the scope of this project.

Failures associated with fatigue in water distribution networks are potentially difficult to track as high frequency pressure loggers are likely to be required to observe unsteady conditions of a given area. Permanently installing high frequency pressure loggers is not seen as a financially viable solution for asset owners. The reality is that any given failure may have had multiple influences on the outcome. For example, the environment in which an asset is buried can inherit undesired loading conditions, such as: point loads or imposed loads caused by highway traffic above. Such examples may contribute to a failure and they may be additive in that there will be a number of causes that may have influenced the failure. Therefore, it is arguable that

a single root cause of a given failure could be difficult to ascribe due to the complex nature of distribution systems and the endless variables that can contribute to failure. It is therefore logical to consider each failure on an individual basis.

Joint integrity systems can be used to aid in maintaining the standard of on-site workmanship. For the purpose of this project, these systems were not discussed. Tighter training standards may improve site practice; which may mitigate the use of joint integrity systems. However, joint integrity systems hold other advantages in that they can also be used to improve the traceability of assets.

This research illustrates that contamination has a detrimental effect on joint integrity. In general, contamination of the jointing interface must be avoided at all costs on-site; although it was noted that installation conditions can be far from ideal – however, a clean jointing surface should be achievable.

8.5.2. Experimental research approach

The fixed mean low-cycle fatigue results showed an exponential increase in fatigue-life as the pressure range is decreased but the predictability of failure also becomes evidently more difficult – as noted previously, large pressure ranges were used in this testing regime. This may illustrate that as the failure of contaminated joints in a controlled environment is difficult to predict, they will be even harder to predict in-service in distribution systems.

Joints made to best practice principles were tested under the fixed mean testing regime whereby no failures occurred; signifying the integrity of good joints in comparison to contaminated ones.

From the general trend in results of the variable mean low-cycle fatigue approach, there is an argument that smoothing variations in pressure may increase the fatigue-life of a contaminated tapping tee. However, it is important to note that as the mean pressure was reduced, the predictability of failure also became more difficult. Therefore, the advantage may not be obvious if this were to be adopted.

For the welding of electrofusion tapping tees, WIS 4-32-08 [14] states that a 2 minute pressure test at least 1.5 times the lower of the nominal pressure rating of the pipe or fitting be applied prior to tapping into the host main. For example, for a 10 bar pipe (or fitting), a hydraulic pressure of 15 bar (1.5 MPa) will be applied for the duration. The test is used to ensure that the fitting is leak-tight prior to tapping into the host main. The results from this project also revealed that a joint contaminated with talc may pass this pressure test. Electrofusion tapping

tees tested to this standard will also undergo the (contamination) short term burst test of which failures above 18 bar (1.8 MPa) pressure is deemed a pass. Therefore it would seem logical that contaminated joint may pass the short 2 minute pressure test. It is therefore recommended that the on-site test may need updating based on this research; a suggestion is given in Section 8.6.1.

8.6. Future directions

As a result of the research conducted in combination with industry experience, observations and results obtained from several testing programmes, the following paragraphs will give an insight into the potential directions that further research can pursue with regards to this project. Each suggested direction will be given an estimated timescale for completion of the works; these estimates are based upon the researcher having a basic knowledge in the field respect to the outlined project. The major risk(s), according to the author, with respect to the completion timescale are also presented.

8.6.1. On-site testing methodology

Failure in contaminated electrofusion tapping tees has been proven through a low-cycle fatigue testing regime. The research holds value in that an on-site testing methodology could be adopted based on the fixed mean testing regime. This can potentially improve asset integrity by promoting failure in contaminated joints prior to commissioning without compromising the long term strength of joints made to best practice principles.

The current WIS requirement is that a back-pressure test be conducted on an electrofusion tapping tee post-weld to check for leaks. The pressure is increased to 1.5 the nominal pressure rating of the pipe or fitting (whichever is lowest) and held for 2 minutes. For the product tested in this project, the research suggests that a contaminated joint is likely to pass the back-pressure test. An on-site testing methodology could be developed to use a short cycle programme at elevated pressure to promote failure of contaminated tapping tees. A full testing programme will need to be developed and implemented on all available tapping tee and pipe products. This is undoubtedly a large testing programme but not necessarily a long one (in duration). Furthermore, a consistent and pragmatic cyclic loading device could be developed that can be used by operatives on-site. For quality control purposes, the device should be automated and carry some method of data acquisition for evidence and maintaining records.

However, issues may arise as this research has solely been conducted using a fine china talc as a contaminant as this has the greatest effect on the fracture toughness of electrofusion joints. In reality, talc is not found on site therefore there is no guarantee that joints containing other contaminants will fail prematurely using the test methodology. Furthermore, there is no guarantee that low-cycle fatigue testing on tapping tee products does not compromise the longevity of assets welded to best practice. Only further research will confirm/disprove this.

Estimated timescale for this project: between 6 and 12 months for testing and interpretation of results. This is heavily dependent on the availability of testing machines and the acquisition of products to test from willing manufacturers. If successful, further time will be required to develop the testing methodology for on-site applications – this may include the development of on-site test equipment.

8.6.2. Confirm the failure mechanism – non-destructive testing

This research project failed to confirm the failure mechanism using non-destructive methods of analysis during a live-fatigue test. It was discussed that the ‘pad sensor’ arrangement provided good results but the resolution with respect to the entire fusion zone was insufficient to offer a clear perspective of the failure mechanism. Signal acquisition with respect to the results also discussed that there was no guarantee that the sensors were observing delamination about the jointing interface. It was thereby proposed that the phased array method of ultrasonic analysis would be recommended as this has a proven record within the industry. As the experimental hydraulic rig (i.e. the fatigue rig) has proven to be effective at the University of Sheffield, it would make sense to hire/loan the phased array equipment for analysis of the failure mechanism during a live fatigue test. To speed up the interpretation of results, it may be worthwhile allowing the results to be analysed by an expert user of the equipment – this may have financial implications.

Estimated timescale for project: 2 months from obtaining the ultrasound equipment. Further time may be required depending on the quality of results obtained; i.e. further testing may be required.

8.6.3. Influencing welding parameters

This thesis commented on several results that appeared to have an increase in performance due to a lateral shift of the joint during the welding process. It was further discussed that the measurement of lateral shift was not consistent; however, the observations may warrant further

investigation. Hypotheses were discussed which may be proven/disproven through further testing and analysis.

Estimated timescale for project: difficult to estimate. This project has a lot of aspects to consider and therefore cannot be given a predicted timescale. An understanding of the welding parameters required to achieve specific quantities of shift will be required. Further fatigue testing may also be required. SEM analyses may be required post-failure to observe and compare fracture surfaces of joints with and without lateral shift – the crush decohesion test may be required here. Furthermore, an investigation can take place whereby the performance of joints made to best practice that include a lateral shift may be compared.

8.6.4. Further investigation of specimens that did not fail

It was noted in the results of Chapter 4, that there were several joints that did not fail under fatigue loading. In general, these joints were tested using low pressure ranges. Although these joints are included as results in this research and have been previously discussed, no further work was carried out destructively or non-destructively. It is therefore a suggestion that further work can be carried out on these joints to further investigate the reasons why they did not fail during dynamic loading. Non-destructive testing can be implemented to observe the current condition of the jointing interfaces and if any delamination has occurred. Specimens can then either be subject to further dynamic loading or tested destructively using such tests as the crushing decohesion test.

Estimated timescale for project: between 2 to 6 months. This is dependent on the direction in which this research is taken. If further dynamic testing is required at lower pressure ranges, this may increase the duration of the project depending times to failure (i.e. fatigue-life).

8.6.5. Development of quantitative destructive test methodology for electrofusion tapping tees

Although the crushing decohesion test requires a calculation of the amount of decohesion about the jointing interface defined as a percentage, to the author's knowledge, there is no quantitative destructive test for electrofusion tapping tees. On deeper thought, this seems logical as the shape of the tapping tee varies from product to product - not to mention the potential difference in the size of the fusion zone. Ensuring a consistent geometry for the purpose of linear elastic fracture mechanics analysis is essential and may prove difficult for smaller products. This is also fundamental for repetition of tests across all products allowing for a comparative observation to be made. The basic modes of failure with regards to fracture

mechanics would need to be addressed to ensure the joint failed appropriately and quantitative data produced. It is paramount to ensure that repetition of the test is plausible across all available products, besides obtaining a final figure/measure post-test, and whether or not the industry would benefit from such a test.

Estimated timescale for project: difficult to predict. This project would need to seek support from the industry to see if there is a demand for such a test. If so, this project would require a further literature survey and an overview of the types of tapping tee design that is available to ensure the proposed test is universal to all products.

References

- [1] OfWAT, “History of the water and sewerage sectors,” 17 March 2014. [Online]. Available: <http://www.ofwat.gov.uk/industryoverview/history>.
- [2] A. C. Twort, F. M. Law and F. W. Crowley, Water Supply, Sevenoaks, Kent: Edward Arnold, 1985.
- [3] Plastics Pipe Institute, Handbook of Polyethylene Pipe, 2nd ed., Irving, Texas: Plastics Pipe Institute, 2008.
- [4] Plastic Pipes Group, “History,” 23 April 2014. [Online]. Available: <http://www.plasticpipesgroup.com/about/history/>.
- [5] E. Grann-Meyer, Polyethylene Pipes in applied Engineering, Brussels: Total, 2005.
- [6] J. Rotheiser, Joining of Plastics, 3rd ed., Munich: Hanser Publications, 2009.
- [7] UKWIR, “Leakage from PE pipe systems,” UK Water Industry Research Limited, London, 2011.
- [8] British Plastics Federation, “A history of plastics,” 23 January 2014. [Online]. Available: http://www.bpf.co.uk/Plastipedia/Plastics_History/Default.aspx.
- [9] ISO 12162, “thermoplastics materials for pipes and fittings for pressure applications - Classification, designation and design coefficient,” British Standards Institute, London, 2009.
- [10] ISO 9080, “Plastic piping and ducting systems - Determination of the long-term hydrostatic strength of thermoplastics materials in pipe form by extrapolation,” International Organization for Standardisation, London, 2012.
- [11] C. O'Connor, “The Nature of Polyethylene Pipe Failure,” *Pipeline & Gas Journal*, vol. 239, no. 12, December 2012.

-
- [12] S. MacKellar, D. Lowe, E. Ingham, D. Carey and C. Ashdown, "Solutions to installation difficulties with PE pipelines," in *Plastic Pipes XIII*, Washington, 2006.
- [13] E. Hoang and D. Lowe, "Lifetime predictions of a Blue PE100 Water Pipe," *Polymer Degradation and Stability*, pp. 1496-1503, 2008.
- [14] WIS 4-32-08, "Specification for fusion jointing of polyethylene pressure pipeline systems using PE 80 and PE 100 materials," WRc PLC, Swindon, 2002.
- [15] WRc PLC, Manual for the repair of distribution trunk mains, 1st ed., J. Burlton and S. Blois, Eds., Swindon: WRc PLC, 1994.
- [16] J. Bowman, "A review of the electrofusion joining process for polyethylene pipe systems," *Polymer Engineering and Science*, vol. 37, no. 4, pp. 674-691, April 1997.
- [17] Plastics Design Library, Handbook of Plastics Joining, Norwich. NY: Plastics Design Library (a division of William Andrew Inc.), 1997.
- [18] R. S. R. Parker and P. Taylor, Adhesion and Adhesives, 1st ed., Oxford: Pergamon Press Ltd, 1966.
- [19] B. Cosgrove, The Toughness Characteristics of Butt Fusion and Electrofusion Joints in Polyethylene Water Pipe, Manchester: PhD Thesis, Manchester Metropolitan University, 1994.
- [20] E. M. Petrie, "Plastics and Elastomers as Adhesives," in *Handbook of Plastics and Elastomers*, C. A. Harper, Ed., USA, McGraw-Hill, 1975, pp. 6-7.
- [21] G. P. Marshall, D. S. Hepburn, D. Pearson and S. MacKellar, "Factors Affecting the Toughness of Electrofusion Joints in PE Pipe Systems for the Water Industry," *Progress in Rubber & Plastic Technology*, pp. 211-233, 1995.
- [22] OfWAT, "OfWAT Glossary of terms," 20 January 2014. [Online]. Available: http://www.ofwat.gov.uk/aboutofwat/gud_pro_ofwatglossary.pdf.
- [23] J. E. Van Zyl and C. R. I. Clayton, "The effect of pressure on leakage in water distribution systems," *Proceedings of the Institute of Civil Engineers - Water Management* 160, pp. 109-114, 2007.

-
- [24] G. P. Marshall, D. S. Hepburn and N. Netherwood, "Improvements in Electrofusion Welding in the UK Water Industry," in *Plastic Pipes IX*, Edinburgh, 1995.
- [25] UKWIR, "Plastic Pipeline System - Analysis of system failures," UK Water Industry Research Limited, London, 1997.
- [26] UKWIR, "Evaluation of welding and jointing of plastic pressure pipes," UK Water Industry Research Limited, London, 2000.
- [27] C. O'Connor, "Polyethylene pipeline systems - Avoiding the pitfalls of Fusion Welding," in *7th Pipeline Technology Conference*, Hannover, Germany, 2012.
- [28] E. B. Wylie, V. L. Streeter and L. Suo, *Fluid Transients in Systems*, Prentice Hall, 1993.
- [29] S. H. Beech, A. Headford, S. Hunt and G. Sandilands, "The Resistance of polyethylene water pipeline systems to surge pressure," in *Plastic Pipes IX*, Edinburgh, 1995.
- [30] A. L. Headford, D. J. Hill and K. A. Wilson, "20+ Years Experience with PE Pipe for Water in the UK," in *Plastic Pipes XII*, Milan, Italy, 2004.
- [31] H. Rezaei, *Personal Communication*, Coventry, 2013.
- [32] D. Lowe, P. Starkey and E. Ingham, "Lifetime of PE Electrofusion Joints," in *Plastic Pipes XIV*, Budapest, Hungary, 2008.
- [33] R. J. Young and P. A. Lovell, *Introduction to polymers*, 3rd ed., Manchester: CRC Press, 2011.
- [34] N. E. Dowling, *Mechanical Behavior of materials*, 2nd ed., New Jersey: Prentice Hall, 1999.
- [35] L. H. Gabriel, *Corrugated Polyethylene pipe design manual and installation guide*, Plastics Pipe Institute, 2003.
- [36] R. W. Hertzberg and J. A. Manson, *Fatigue of engineering plastics*, London: Academic Press INC. (London) LTD, 1980.
- [37] J. Bowman, "The Fatigue response for Polyvinyl Chloride and Polyethylene Pipe Systems," *ASTM Special Technical Publication Issue*, no. 1093, pp. 101-121, 1990.

-
- [38] R. Ayer, A. Hiltner and E. Baer, "A fatigue-to-creep correlation in air for application to environmental stress cracking of polyethylene," *Journal of Materials Science*, no. 42, pp. 7004-7015, 2007.
- [39] J. J. Strebel and A. Moet, "Accelerated fatigue fracture mechanism of medium density polyethylene pipe material," *Journal of Materials Science*, no. 26, pp. 5671-5680, 1991.
- [40] M. Parsons, E. V. Stepanov, A. Hiltner and E. Baer, "Correlation of fatigue and creep slow crack growth in a medium density polyethylene pipe material," *Journal of Materials Science*, vol. 35, pp. 2659-2674, 2000.
- [41] P. T. Reynolds and C. C. Lawrence, "Deformation and failure in polyethylene: correlation between mechanisms of creep and fatigue," *Journal of Materials Science*, vol. 26, pp. 6197-6202, 1991.
- [42] H. Nishimura and I. Narisawa, "Fatigue Behaviour of Medium-Density Polyethylene Pipes," *Polymer Engineering and Science*, no. 31, pp. 399-403, 1991.
- [43] C. B. Bucknall and P. Dumbleton, "Factors affecting fatigue crack growth in HDPE," *Plastics and Rubber Processing and Applications*, no. 5, pp. 343-347, 1985.
- [44] Y. Q. Zhou and N. Brown, "The fatigue behaviour of notched polyethylene as a function of R," *Journal of Materials Science*, no. 24, pp. 1458-1466, 1989.
- [45] S. K. Phua, C. C. Lawrence and R. Potter, "Fractographic study of high-density polyethylene pipe," *Journal of Materials Science*, vol. 33, pp. 1699-1702, 1998.
- [46] G. J. Sandilands and J. Bowman, "An examination of the role of flaw size and material toughness in the brittle fracture of polyethylene pipes," *Journal of Material Science*, vol. 21, pp. 2881-2888, 1986.
- [47] G. P. Marshall, S. Brogden and M. Shepherd, "Evaluation of the Surge and Fatigue Resistance of PVC and PE Pipeline Materials for tuse in the UK Water Industry," in *Plastic Pipes X*, Gothenburg, 1998.
- [48] IGN 4-37-02, "Design against surge and fatigue conditions for thermoplastic pipes," WRc PLC, Swindon, 1999.

- [49] J. Bowman, "The fatigue performance of polyethylene pipe joints made with electrofusion fittings," *Plastics and Rubber Processing and Applications*, vol. 9, pp. 147-153, 1988.
- [50] American Water Works Association, PE Pipe - Design and Installation, American Water Works Association, 2006.
- [51] J. G. Williams, *Fracture Mechanics of Polymers*, Chichester, West Sussex: Ellis Horwood Ltd, 1984.
- [52] H. L. Ewalds and R. J. H. Wanhill, *Fracture Mechanics*, London: Edward Arnold, 1991.
- [53] UKWIR, "Pipeline Innovation Final Report," UK Water Industry Research Limited, London, 1996.
- [54] WRc PLC, "Civil Engineering Specification for the Water Industry (7th Edition)," WRc PLC, Swindon, 2011.
- [55] BS EN 12201-1, "Plastic Piping Systems for water supply, and for drainage and sewerage under pressure - Polyethylene (PE) - Part 1: General," British Standards Institute, London, 2011.
- [56] BS EN 12201-2, "Plastics piping systems for water supply, and for drainage and sewerage under pressure - Polyethylene (PE). Part 2: Pipes," British Standards Institute, London, 2011.
- [57] BS EN 12201-3, "Plastics piping systems for water supply, and for drainage and sewerage under pressure - Polyethylene (PE) - Part 3: Fittings," British Standards Institute, London, 2011.
- [58] BS EN 12201-5, "Plastics piping systems for water supply, and for drainage and sewerage under pressure - Polyethylene (PE). Part 5: Fitness for purpose of the system," British Standards Institute, London, 2011.
- [59] PD CEN/TS 12201-7, "Plastic Piping Systems for water supply, and for drainage and sewerage under pressure - Polyethylene (PE) - Part 7: Guidance for the assessment of conformity," British Standards Institute, London, 2014.

-
- [60] ISO 13955, "Plastic pipes and fittings - Crushing decohesion test for polyethylene (PE) electrofusion assemblies," International Organisation for Standardization, London, 1997.
- [61] UKWIR, "Plastic Pipeline Systems - Pipeline Innovation," UK Water Industry Research Limited, London, 1997.
- [62] D. Blockley, *New Dictionary of Civil Engineering*, London: Penguin Books, 2005.
- [63] F. Scholten, "Energy-to-failure to assess the quality of electrofusion joints in PE pipes," in *Plastic Pipes XVII*, Chicago, 2014.
- [64] ISO 13954, "Plastic pipes and fittings - Peel decohesion test for polyethylene (PE) electrofusion assemblies of nominal outside diameter greater than or equal to 90 mm," International Organization for Standardization, London, 1997.
- [65] H. Nishimura, "Evaluation of Electrofusion Joint Strength of Polyethylene Pipes for Gas Distribution," in *Plastic Pipes XV*, Vancouver, 2010.
- [66] M. Troughton, C. Brown, J. Hessel and M. Piovano, "Comparison of long-term and short-term tests for electrofusion joints in PE pipe," in *Plastic Pipes XIII*, Washington, 2006.
- [67] N. Shipway, "Understanding leak path trends in polyethylene joints using non-destructive testing for the water industry," MEng Thesis: Department of Mechanical Engineering, University of Sheffield, Sheffield, 2014.
- [68] P. T. Reynolds and C. C. Lawrence, "Mechanisms of deformation in the fatigue of polyethylene pipe," *Journal of Materials Science*, vol. 28, pp. 2277-2282, 1993.
- [69] BS EN 13100-3, "Non-destructive testing of welded joints in thermoplastics semi-finished products - Part 3: ultrasonic testing," British Standards Institute, London, 2004.
- [70] J. Szilard, "Physical principles of ultrasonic testing," in *Ultrasonic Testing - Non-conventional testing techniques*, Binghampton, N.Y., John Wiley & Sons, 1982, pp. 1-5.

- [71] R. Mills, "Ultrasonic measurement of lubricant films generated at the piston-cylinder interface of internal combustion engines," PhD Thesis: Department of Mechanical Engineering, University of Sheffield, Sheffield, 2012.
- [72] F. Hagglund, M. A. Spicer and M. Troughton, "Development of Phased Array Ultrasonic Inspection Techniques for testing welded joints in plastic (PE) pipes," in *18th World Conference on Nondestructive Testing*, Durban, South Africa, 2012.
- [73] M. Troughton, M. Spicer and F. Hagglund, "Development of an automated phased array ultrasonic inspection system and flaw acceptance criteria for welded joints in polyethylene pipes," in *Plastic Pipes XVI*, Barcelona, Spain, 2012.
- [74] K. Y. Siaw, "Leakage path investigation for electrofusion joint," MEng Thesis: Department of Mechanical Engineering, University of Sheffield, Sheffield, 2013.
- [75] T. Howard, *Personal communication*, Sheffield: University of Sheffield, 2014.
- [76] F. Hagglund, M. A. Spicer and M. J. Troughton, "Phased array Ultrasonic Testing of Welded Joints in Plastic (PE) Pipes," in *6th Middle East Non-destructive Testing Conference*, Kingdom of Bahrain, 2012.
- [77] S. H. Joseph and P. S. Leever, "Failure mechanics of uPVC cyclically pressurized water pipelines," *Journal of material science*, vol. 20, pp. 237-345, 1985.
- [78] UKWIR, "Performance of Electrofusion joints for PE pipes," UK Water Industry Research Limited, London, 1998.
- [79] K. Murphy and D. Lowe, "Evaluation of a novel Microwave based NDT inspection method for Polyethylene joints," in *Plastic Pipes XV*, Vancouver, 2010.

Appendix A Contamination Experiment

Background

WIS 4-32-08 [14] – *Appendix A: Method of assessing tolerance of electrofusion welds to contamination – short term burst test*; requires a machine/device to create an even distribution of talc contaminant on the pipe prior to creating an electrofusion joint. This is to ensure a consistent application of contaminant is applied and that it is repetitive and transferable in the industry; i.e. test specimens created by different manufacturers are made in a consistent manner. However, to the author's knowledge, there is only one machine in the UK that can achieve this and common practice for manufacturers is to apply the contaminant to the pipe using a soft bristle brush. It was believed that applying the talc contaminant by brush may have a worsening effect to joint integrity than application by machine. However, application by brush is a manual procedure and will therefore vary from person to person.

With regards to the creation of test specimens for this project, an experiment took place to observe the difference in application methods of talc contaminated joints. Furthermore, the aims of the experiment were as follows:

- Observe the average particle size of the talc contaminant;
- Observe an average distribution of contaminant comparing two methods of application: (i) applied by brush – common practice for manufacturers, (ii) applied via a fine mesh specified in WIS 4-32-08 [14].

To achieve these aims a rig was developed to replicate the method specified in WIS 4-32-08 [14]. Furthermore, a digital microscope was used to observe the distribution and particle size.

Methodology

A 110 mm diameter ‘skinned’ SDR 11 PE pipe was cut longitudinally to approximate dimensions 60 x 50 mm. It is key to note that the dimensions specified are only a guideline due to the curved nature of the pipe. As a microscope is to be used to observe a very small area, thus the exact dimensions of the cut pipe are not critical. However, the cut section needs to be large enough to offer a realistic area to brush as if it were to be used for contaminating a pipe for the short term burst test.

The skin was removed from the outside of the pipe using the appropriate peelable skin removal tool. The exposed pipe was cleaned using an alcohol based welding wipe.

For applying the talc to the PE sample using a mesh, a fine printing mesh¹ was obtained from a UK manufacturer and was restrained between two fixed points; parallel aluminium cylindrical bars. A small pile of talc was placed on the mesh and was pushed through with a straight edge fixed to 45° to the surface of the mesh. It shall be noted that the mesh assembly was offset from the PE sample by approximately 8 mm.

A 25 mm wide clean soft bristled paint brush was obtained to apply the talc onto the PE samples. UKWIR [62] recommend the use of a 2 inch (≈51 mm) soft paint brush, however, it was found that the 25 mm (≈1 inch) was more controlled; therefore it was used in preference.

The technique for applying the talc was as follows:

- i) Ensure there is no foreign objects on the brush or in the talc container
- ii) Carefully dip the paint brush in talc container – talc will grip to the bristle ends of the brush
- iii) Gently tap the brush with the index finger to remove any excess talc back into the container
- iv) Dap the brush perpendicular to the sample on the left hand side of the sample – clumps of talc should appear on the pipe
- v) Angle the brush at an approximate 45° angle from the PE pipe and make brushing strokes from left to right only; rotating the brush if and when required
- vi) Make a visual observation to ensure there is an even distribution of talc on the surface of the sample.

Note: it should be clear to see the talc on the surface of the pipe on close inspection.

¹ Mesh opening = $53 \pm 6 \mu\text{m}$, nominal wire diameter = $43 \mu\text{m}$

A portable digital microscope, Dino-lite, was manually calibrated to the following magnifications in order to observe the particle size and distribution: x250 (x248.3), x200 (x195.3), x50 (x50.5).

Results

The digital microscope was calibrated and the printer mesh was observed at x248.3 magnification (see Figure A-1).

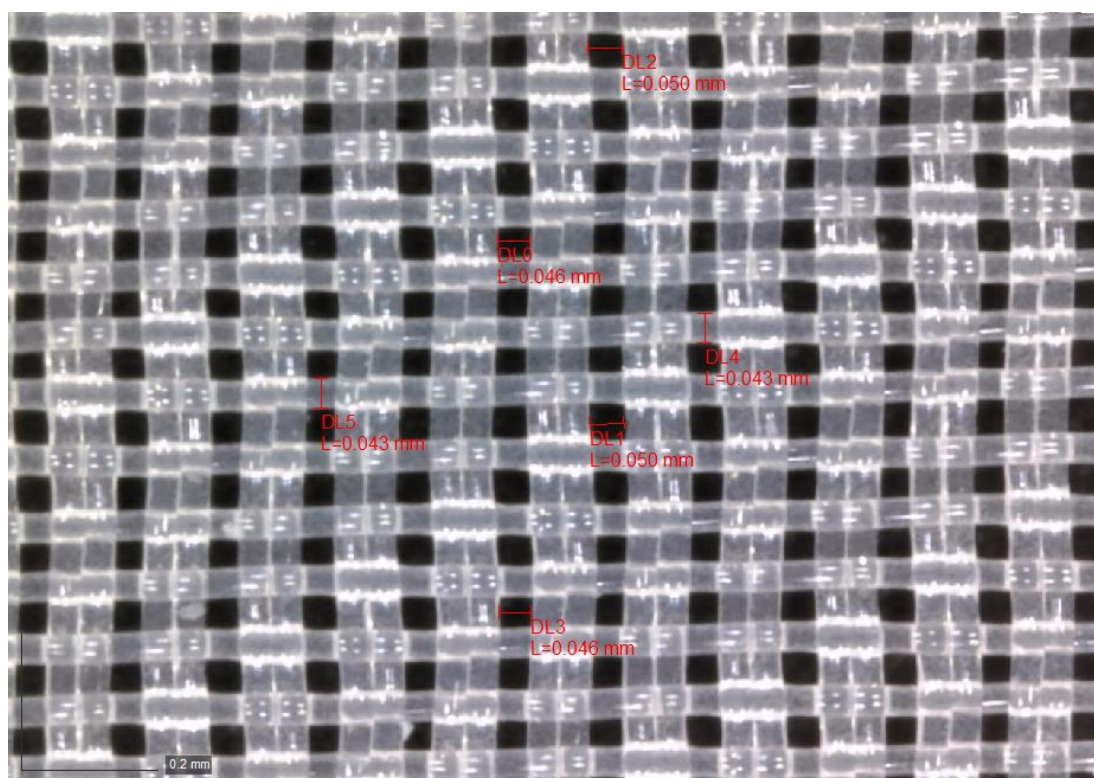


Figure A-1 Mesh at magnification x248.3

Talc contamination was distributed on a PE sample using the printer mesh. The sample was observed at two magnifications, x50.5 (Figure A-2) and x195.3 (Figure A-3). Furthermore, a sample was prepared using a brush using the aforementioned technique and was observed using the same scales.

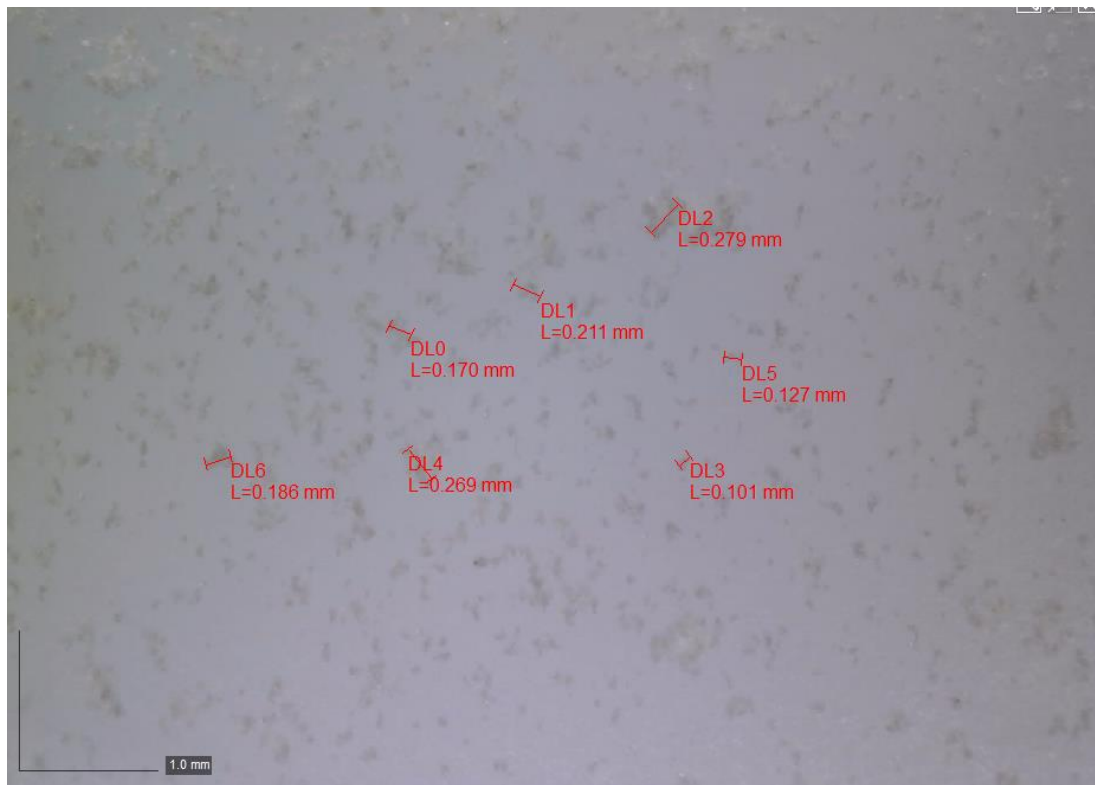


Figure A-2 Mesh - contamination on pipe surface at x50.5

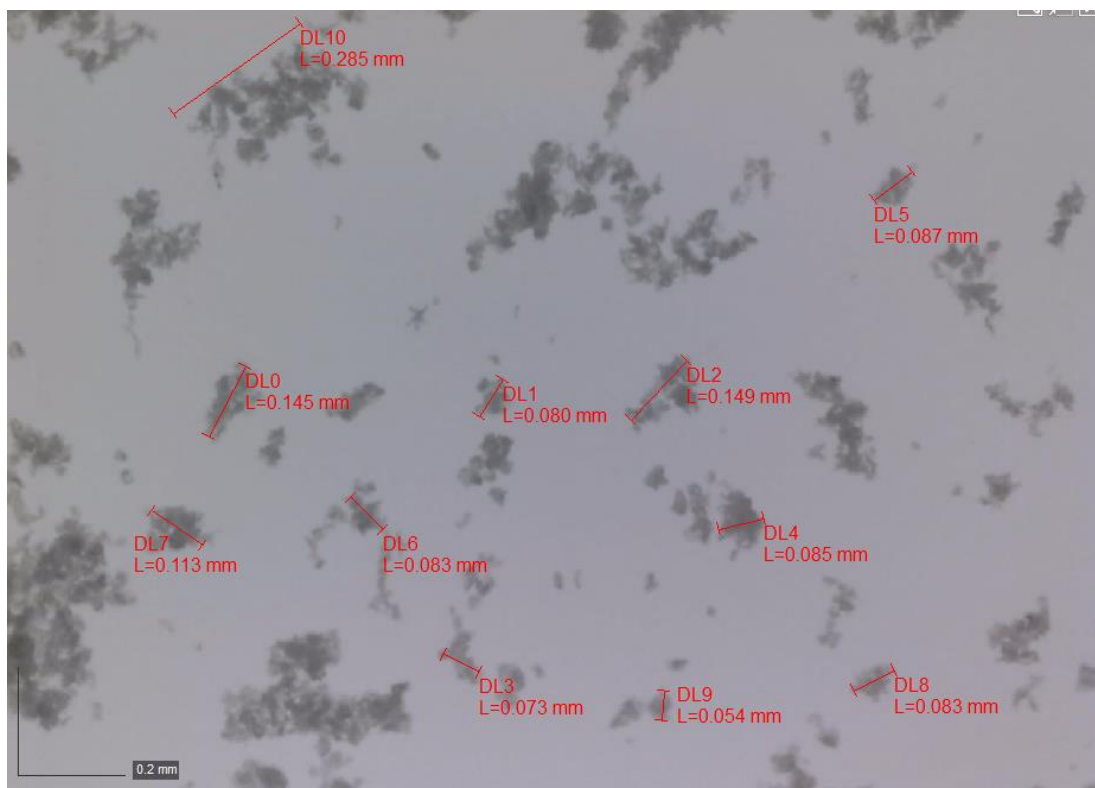


Figure A-3 Mesh - contamination on pipe surface at x195.3

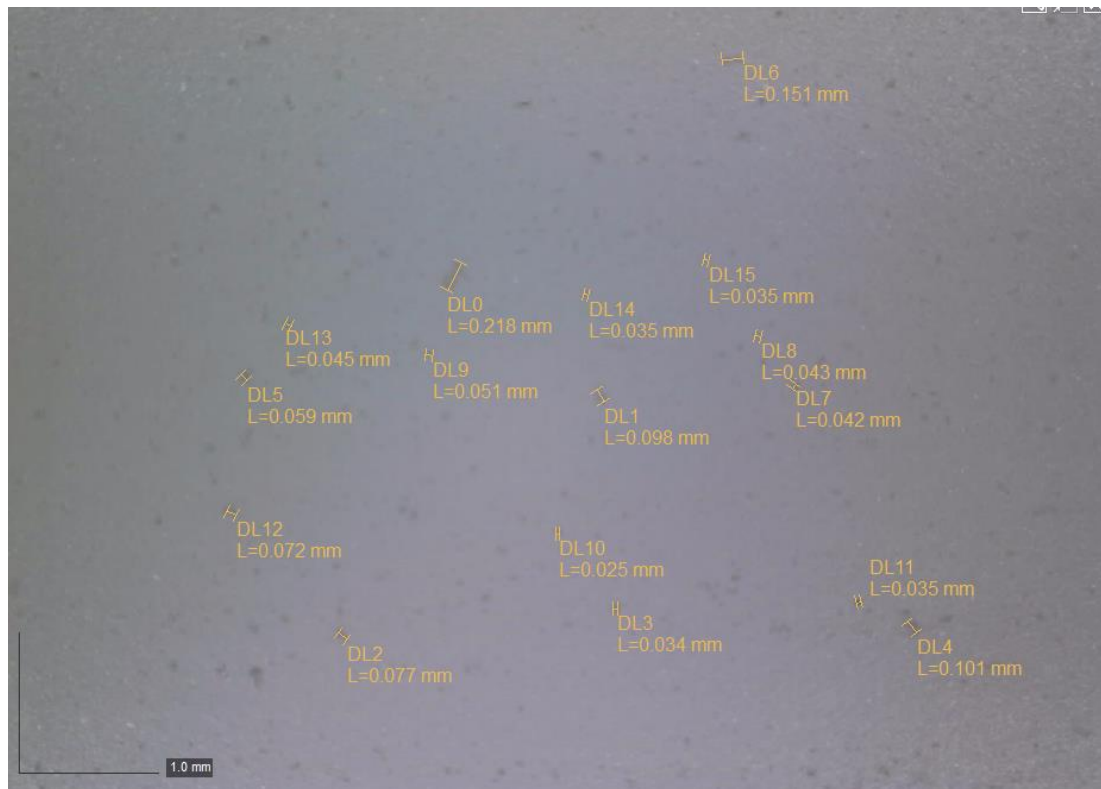


Figure A-4 Brush - contamination on pipe at x50.5

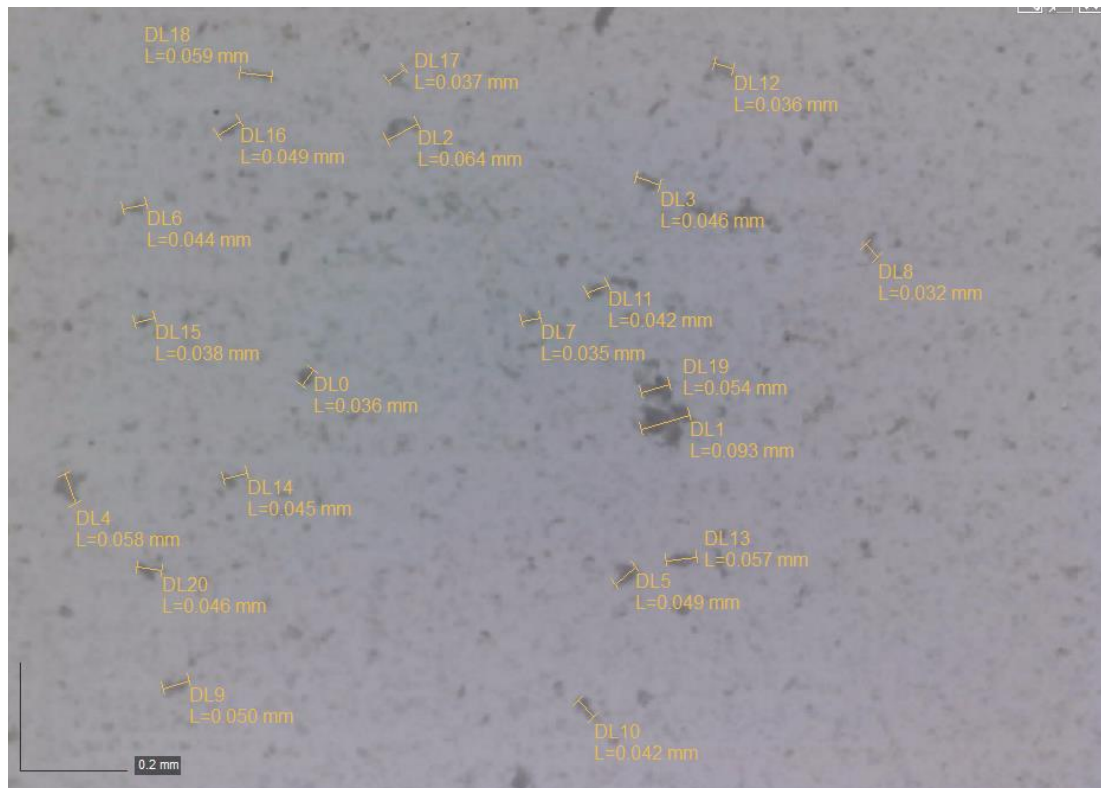


Figure A-5 Brush – contamination on pipe at x195.3

Discussion and Conclusions

It is key to note that a machine was not created to evenly distribute the talc via the printing mesh and onto the pipe. This was deemed impractical with regards to the timescale of the project. The focus of the experiment was to observe the difference in grouping and distribution if the contaminant is applied by different methodologies.

This experiment was crucial in order to aid the understanding for joints created in this project. Furthermore, it clearly shows the expected distribution if the pipe were to be brushed with the talc contamination.

With regards to the rig that was created to replicate the recommended WIS 4-32-08 [14] device, the key design components were highlighted from the specification and implemented in the design of the rig. This was inclusive to the aperture size of the mesh and the type of talc used (fine China talc with particle size 0.63 μm to 6.3 μm).

The results show that the range of particle sizing is greater when the talc is applied using the mesh arrangement. However, the distances between the particle groupings of talc appeared to be greater than if the particles were to be brushed on. This suggests that there is a higher distribution of particulate contamination as well as a greater range in size when using the brush. As this was the case, it was assumed that proceeding to use a brush to apply the talc contamination would be suitable for the project as long as all the specimens were created using the same technique (stated in this methodology) and the same operative to reduce the risk of diversifying results.

To further compare the performance of the talc application a detailed experiment could have been conducted whereby electrofusion joints could have been created using both application techniques. The specimens could then have been subject to the short term burst test as highlight in WIS 4-32-08 [14] to see if there is a difference in burst pressure. However, the need for further experimentation was not necessary for this project as the microscopy work was deemed satisfactory.

Appendix B Equipment used

Tool description	Manufacturer/type
Electrofusion Control Unit	Fusion Provida QBox – 110 v
Pipe cutter	Caldervale Technology – 42 mm
Rotary scraper	Caldervale Technology – Ø25 mm
Peelable skin removal tool	Caldervale Technology - Profuse exposure tool (plastic)
Hand scraper	Harris scraper – 63 mm
Large pipe clamps	Caldervale Technology – mains restraining clamp – Ø63-180 mm
Small pipe clamps	Caldervale Technology – Straight, 45°, 90° - Ø25-32 mm
Top-loading G-clamp	Caldervale Technology – top loading clamp
Hand Saw	Hand Saw - 600 mm

Table B-1 Welding Equipment

Description	Manufacturer/type
Servo-hydraulic testing machine	ESH - Max. load 50 kN
Test Controller	MOOG – Portable test controller (Part No. STO03014-205)
Pressure Transducer	Transamerica Instruments BHL-4250-00 (0 – 160 bar)
Pressure gauge	0 – 60 bar

Table B-2 Fatigue Testing equipment

Appendix C Experimental hydraulic rig & Ultrasonic rig Drawings

See attached CD for the following CAD drawings:

Drawing No.	Title	Revision	Paper size
T/SK2	Hydraulic rig – general arrangement drawing	A	A4
T/SK3	Piston rod – General Arrangement and Section	B	A4
T/SK4	Cylinder cap – General Arrangement and Sections	C	A4
T/SK5	Hydraulic piston head General Arrangement, Section and Details	B	A3
T/SK6	Cylinder – General Arrangement and Sections	B	A4
T/SK9	Rig to piston rod connector General Arrangement and Sections	-	A4
T/SK10	Rig Baseplate Alterations – General Arrangement and Sections	-	A4
T/SK11	Brass fitting – Top-tee to 3/8” BSP	A	A4
T/SK17	End caps for PE pipe	-	A4
T/SK18	Ultrasound probe holder – General Arrangement and Sections	A	A4
T/SK19	Tapping tee, coupler and Heat Affected Zone (HAZ) diagrams	-	A4
T/SK20	Fork and thrust block - General Arrangement and Sections	-	A4

-	Brass Bush (cylinder cap)	-	A4
-	Cylinder cap	-	A3
-	Piston Cylinder	-	A3
-	Piston Head [2 sheets]	-	A3
-	Piston Rod	-	A4
-	Base plate modifications	-	A3

-	Ultrasound probe holder	-	A3
-	Column platform	-	A3
-	Drive Shaft	-	A4

-	Probe fork	-	A3
-	Thrust block	-	A4
-	Ultrasound rig assembly	-	A3